(12) INTERNATIONAL APPLICATION PUBLISHED UNDER THE PATENT COOPERATION TREATY (PCT)

(19) World Intellectual Property Organization
International Bureau

(43) International Publication Date
27 October 2022 (27.10.2022)

WIPO | PCT

(10) International Publication Number
WO 2022/224203 A1

(51) International Patent Classification:
*C07K 16/10* (2006.01) *A61K 49/00* (2006.01)
*A61K 9/72* (2006.01) *A61P 31/14* (2006.01)
*A61K 39/42* (2006.01) *C12N 15/13* (2006.01)
*A61K 39/44* (2006.01) *G01N 33/569* (2006.01)
*A61K 47/68* (2017.01)

(21) International Application Number:
PCT/IB2022/053756

(22) International Filing Date:
22 April 2022 (22.04.2022)

(25) Filing Language: English

(26) Publication Language: English

(30) Priority Data:
3,115,877 22 April 2021 (22.04.2021) CA

(71) Applicant: **NATIONAL RESEARCH COUNCIL OF CANADA** [CA/CA]; 1200 Montreal Road, Ottawa, Ontario K1A 0R6 (CA).

(72) Inventors: **TANHA, Jamshid**; 2162 Valin Street, Orleans, Ontario K4A 4T2 (CA). **ROSSOTTI, Martin A.**; 197 Guigues Avenue, Ottawa, Ontario K1N 5J1 (CA).

(74) Agent: **SMITH, Jessica** et al.; 1200 Montreal Road, Ottawa, Ontario K1A 0R6 (CA).

(81) Designated States *(unless otherwise indicated, for every kind of national protection available)*: AE, AG, AL, AM, AO, AT, AU, AZ, BA, BB, BG, BH, BN, BR, BW, BY, BZ, CA, CH, CL, CN, CO, CR, CU, CZ, DE, DJ, DK, DM, DO, DZ, EC, EE, EG, ES, FI, GB, GD, GE, GH, GM, GT, HN, HR, HU, ID, IL, IN, IR, IS, IT, JM, JO, JP, KE, KG, KH, KN, KP, KR, KW, KZ, LA, LC, LK, LR, LS, LU, LY, MA, MD, ME, MG, MK, MN, MW, MX, MY, MZ, NA, NG, NI, NO, NZ, OM, PA, PE, PG, PH, PL, PT, QA, RO, RS, RU, RW, SA, SC, SD, SE, SG, SK, SL, ST, SV, SY, TH, TJ, TM, TN, TR, TT, TZ, UA, UG, US, UZ, VC, VN, WS, ZA, ZM, ZW.

(84) Designated States *(unless otherwise indicated, for every kind of regional protection available)*: ARIPO (BW, GH, GM, KE, LR, LS, MW, MZ, NA, RW, SD, SL, ST, SZ, TZ,

(54) Title: ANTIBODIES THAT BIND SARS-COV-2 SPIKE PROTEIN

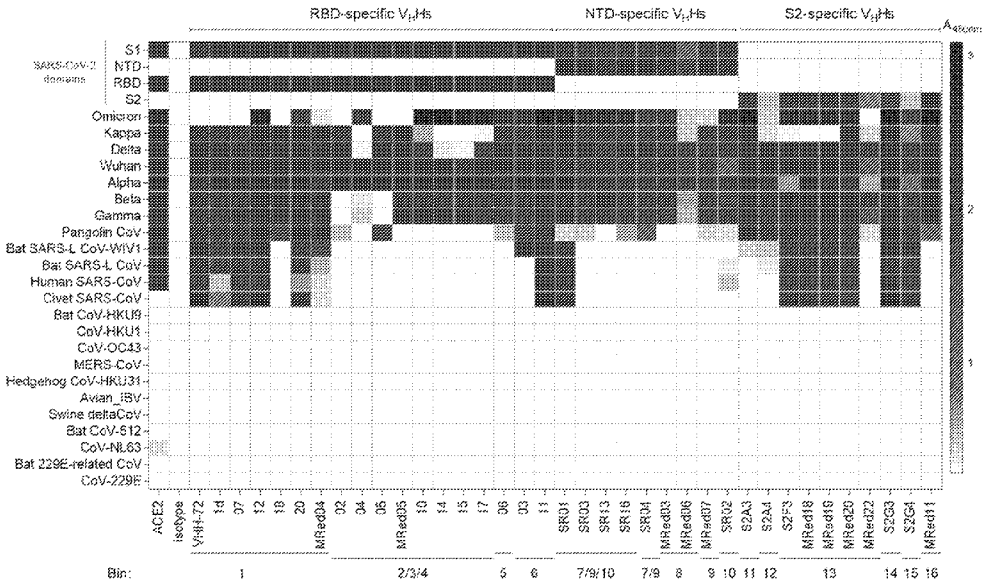


FIG. 6B

(57) Abstract: Described herein are antibodies that specifically recognize the SARS-CoV-2 spike (S) polypeptide,compositions comprising said antibodies, uses thereof, and methods employing said antibodies. Eachantibody specifically recognizes the S1-RBD domain, S1-NTD domain, or S2 subunit of the SARS-CoV-2 spike polypeptide. Some antibodies are cross-reactive with variants of SARS-CoV-2 and othercoronavirus spike polypeptides, such as SARS-CoV S, pangolin CoV S, bat SARS-like CoV S, andcivet SARS-CoV S.

*[Continued on next page]*

WO 2022/224203 A1

UG, ZM, ZW), Eurasian (AM, AZ, BY, KG, KZ, RU, TJ, TM), European (AL, AT, BE, BG, CH, CY, CZ, DE, DK, EE, ES, FI, FR, GB, GR, HR, HU, IE, IS, IT, LT, LU, LV, MC, MK, MT, NL, NO, PL, PT, RO, RS, SE, SI, SK, SM, TR), OAPI (BF, BJ, CF, CG, CI, CM, GA, GN, GQ, GW, KM, ML, MR, NE, SN, TD, TG).

**Declarations under Rule 4.17:**

— *as to applicant's entitlement to apply for and be granted a patent (Rule 4.17(ii))*
— *of inventorship (Rule 4.17(iv))*

**Published:**

— *with international search report (Art. 21(3))*
— *with sequence listing part of description (Rule 5.2(a))*
— *in black and white; the international application as filed contained color or greyscale and is available for download from PATENTSCOPE*

# ANTIBODIES THAT BIND SARS-COV-2 SPIKE PROTEIN

## FIELD

**[0001]** The present disclosure relates to antibodies that specifically bind a coronavirus spike polypeptide, particularly the spike polypeptide of SARS-CoV-2 and variants thereof, and to the use of such antibodies for various applications including the detection of a coronavirus and/or treatment or prevention of a coronavirus infection.

## BACKGROUND

**[0002]** Coronavirus is a single-stranded enveloped RNA virus belonging to the subfamily Coronavirinae in the order *Nidovirales*. Based on genomic structure, coronaviruses have been classified into four genera; *Alphacoronavirus*, *Betacoronavirus*, *Gammacoronavirus*, and *Deltacoronavirus*; two of which (alphacoronaviruses and betacoronaviruses) infect mammals. Seven coronaviruses are known to cause human disease: HCoV 229E, HCov OC43, HCoVNL63, HCoVHKU1, SARS-CoV, MERS-CoV, and SARS-CoV-2. Three coronaviruses, SARS-CoV, MERS-CoV, and SARS-CoV-2, cause serious illness in humans, whereas the remaining four human coronaviruses are associated with mild illness.

**[0003]** Since 2002, there have been three coronavirus outbreaks causing serious human illness. The first outbreak, caused by SARS-CoV, originated in China with the first case reported in November 2002. By July 2003, there were 8098 cases and 774 deaths in 29 countries (Arora et al., 2020). The second outbreak, caused by MERS-CoV, originated in Saudi Arabia, with the first case reported in June 2012. The disease was ultimately identified in 26 countries, with 1621 confirmed cases and 584 deaths (Arora et al., 2020). The third outbreak, caused by SARS-CoV-2, originated in China with the first case reported in December 2019. On March 11, 2020, the World Health Organization (WHO) declared the outbreak a pandemic. According to information provided by the Johns Hopkins Coronavirus Resource Center, as of April 22, 2021, the global case count was 144 million and there had been 3.06 million deaths worldwide.

**[0004]** Coronavirus entry into host cells is mediated by the coronavirus spike protein (S), which is a homotrimeric glycoprotein. The spike polypeptide includes three segments, an ectodomain, a single-pass transmembrane anchor, and an intracellular tail. The spike ectodomain is made up of

a receptor-binding subunit (S1) and a membrane-fusion subunit (S2). S1 includes two major domains, an N-terminal domain (NTD) and a C-terminal domain (CTD), which is also known as the receptor binding domain (RBD). Following the RBD, S1 contains two subdomains (SD1 and S1-SD2) as described in Lan et al., 2020.

**[0005]** During virus entry, S1 binds to a host cell surface receptor and S2 fuses the host and viral membranes (Li, 2016). The host cell surface receptor bound by both SARS-CoV and SARS-CoV-2 is a zinc peptidase angiotensin-converting enzyme 2 (ACE2), whereas MERS-CoV recognizes a serine peptidase (DPP4) (Li, 2016; Zhou et al, 2020). The receptor binding domain (RBD) of SARS-CoV-2 has been characterized and the binding mode of the SARS-CoV-2 RBD to ACE2 has been found to be nearly identical to that observed for SARS-CoV (Lan et al., 2020).

**[0006]** There are currently few treatments available for SARS-CoV-2 infection or other coronavirus infections and, while vaccines for SARS-CoV-2 are now coming onto the market, vaccine distribution is far from complete. Additionally, the duration and breadth of protection offered by SARS-CoV-2 vaccines is not yet known, meaning that vaccinated individuals may become increasingly susceptible to subsequent infection with time. Further, vaccination may be ineffective for immunocompromised individuals, leaving them susceptible to life-threatening coronavirus infections. Antibodies that neutralize coronaviruses, such as SARS-CoV-2, have significant potential as therapeutic agents. Further antibodies with high affinity for coronaviruses, such as SARS-CoV-2, may allow for detection, quantification, or capture of coronaviruses with high sensitivity and specificity.

## SUMMARY

**[0007]** Provided is an isolated or purified antibody that specifically recognizes at least one coronavirus spike polypeptide, wherein the antibody comprises an antigen binding portion of an antibody heavy chain, wherein the antigen binding portion comprises a first complementarity determining region (CDR1), a second complementarity determining region (CDR2), and a third complementarity determining region (CDR3), and wherein CDR1, CDR2, and CDR3, respectively, comprise the amino acid sequence set forth in:

SEQ ID NO: 1, SEQ ID NO: 45, and SEQ ID NO: 90;

SEQ ID NO: 2, SEQ ID NO: 45, and SEQ ID NO: 91;

SEQ ID NO: 1, SEQ ID NO: 46, and SEQ ID NO: 92;
SEQ ID NO: 3, SEQ ID NO: 47, and SEQ ID NO: 93;
SEQ ID NO: 4, SEQ ID NO: 48, and SEQ ID NO: 94;
SEQ ID NO: 5, SEQ ID NO: 49, and SEQ ID NO: 95;
SEQ ID NO: 6, SEQ ID NO: 50, and SEQ ID NO: 96;
SEQ ID NO: 7, SEQ ID NO: 51, and SEQ ID NO: 97;
SEQ ID NO: 8, SEQ ID NO: 52, and SEQ ID NO: 98;
SEQ ID NO: 9, SEQ ID NO: 53, and SEQ ID NO: 99;
SEQ ID NO: 10, SEQ ID NO: 54, and SEQ ID NO: 100;
SEQ ID NO: 11, SEQ ID NO: 55, and SEQ ID NO: 101;
SEQ ID NO: 12, SEQ ID NO: 56, and SEQ ID NO: 102;
SEQ ID NO: 13, SEQ ID NO: 57, and SEQ ID NO: 103;
SEQ ID NO: 14, SEQ ID NO: 58, and SEQ ID NO: 104;
SEQ ID NO: 15, SEQ ID NO: 59, and SEQ ID NO: 105;
SEQ ID NO: 16, SEQ ID NO: 60, and SEQ ID NO: 106;
SEQ ID NO: 17, SEQ ID NO: 61, and SEQ ID NO: 107;
SEQ ID NO: 18, SEQ ID NO: 62, and SEQ ID NO: 108;
SEQ ID NO: 19, SEQ ID NO: 63, and SEQ ID NO: 109;
SEQ ID NO: 20, SEQ ID NO: 64, and SEQ ID NO: 110;
SEQ ID NO: 21, SEQ ID NO: 65, and SEQ ID NO: 111;
SEQ ID NO: 22, SEQ ID NO: 66, and SEQ ID NO: 112;
SEQ ID NO: 23, SEQ ID NO: 67, and SEQ ID NO: 113;
SEQ ID NO: 24, SEQ ID NO: 68, and SEQ ID NO: 114;
SEQ ID NO: 25, SEQ ID NO: 69, and SEQ ID NO: 115;
SEQ ID NO: 26, SEQ ID NO: 70, and SEQ ID NO: 116;
SEQ ID NO: 27, SEQ ID NO: 71, and SEQ ID NO: 117;
SEQ ID NO: 28, SEQ ID NO: 72, and SEQ ID NO: 118;
SEQ ID NO: 29, SEQ ID NO: 73, and SEQ ID NO: 119;
SEQ ID NO: 30, SEQ ID NO: 74, and SEQ ID NO: 120;
SEQ ID NO: 31, SEQ ID NO: 75, and SEQ ID NO: 121;
SEQ ID NO: 32, SEQ ID NO: 76, and SEQ ID NO: 122;

SEQ ID NO: 33, SEQ ID NO: 77, and SEQ ID NO: 123;
SEQ ID NO: 34, SEQ ID NO: 78, and SEQ ID NO: 124;
SEQ ID NO: 35, SEQ ID NO: 79, and SEQ ID NO: 125;
SEQ ID NO: 36, SEQ ID NO: 80, and SEQ ID NO: 125;
SEQ ID NO: 20, SEQ ID NO: 81, and SEQ ID NO: 126;
SEQ ID NO: 20, SEQ ID NO: 81, and SEQ ID NO: 127;
SEQ ID NO: 37, SEQ ID NO: 82, and SEQ ID NO: 128;
SEQ ID NO: 38, SEQ ID NO: 83, and SEQ ID NO: 129;
SEQ ID NO: 39, SEQ ID NO: 84, and SEQ ID NO: 130;
SEQ ID NO: 40, SEQ ID NO: 85, and SEQ ID NO: 131;
SEQ ID NO: 41, SEQ ID NO: 86, and SEQ ID NO: 132;
SEQ ID NO: 42, SEQ ID NO: 87, and SEQ ID NO: 133;
SEQ ID NO: 43, SEQ ID NO: 88, and SEQ ID NO: 134; or
SEQ ID NO: 44, SEQ ID NO: 89, and SEQ ID NO: 135.

**[0008]** In an embodiment, the antibody is a neutralizing antibody and CDR1, CDR2, and CDR3, respectively, comprise the amino acid sequence set forth in:

SEQ ID NO: 1, SEQ ID NO: 45, and SEQ ID NO: 90;
SEQ ID NO: 1, SEQ ID NO: 46, and SEQ ID NO: 92;
SEQ ID NO: 2, SEQ ID NO: 45, and SEQ ID NO: 91;
SEQ ID NO: 3, SEQ ID NO: 47, and SEQ ID NO: 93;
SEQ ID NO: 4, SEQ ID NO: 48, and SEQ ID NO: 94;
SEQ ID NO: 5, SEQ ID NO: 49, and SEQ ID NO: 95;
SEQ ID NO: 6, SEQ ID NO: 50, and SEQ ID NO: 96;
SEQ ID NO: 7, SEQ ID NO: 51, and SEQ ID NO: 97;
SEQ ID NO: 8, SEQ ID NO: 52, and SEQ ID NO: 98;
SEQ ID NO: 10, SEQ ID NO: 54, and SEQ ID NO: 100;
SEQ ID NO: 11, SEQ ID NO: 55, and SEQ ID NO: 101;
SEQ ID NO: 13, SEQ ID NO: 57, and SEQ ID NO: 103;
SEQ ID NO: 14, SEQ ID NO: 58, and SEQ ID NO: 104;
SEQ ID NO: 15, SEQ ID NO: 59, and SEQ ID NO: 105;
SEQ ID NO: 16, SEQ ID NO: 60, and SEQ ID NO: 106;

SEQ ID NO: 17, SEQ ID NO: 61, and SEQ ID NO: 107;
SEQ ID NO: 19, SEQ ID NO: 63, and SEQ ID NO: 109;
SEQ ID NO: 20, SEQ ID NO: 81, and SEQ ID NO: 127;
SEQ ID NO: 21, SEQ ID NO: 65, and SEQ ID NO: 111;
SEQ ID NO: 22, SEQ ID NO: 66, and SEQ ID NO: 112;
SEQ ID NO: 23, SEQ ID NO: 67, and SEQ ID NO: 113;
SEQ ID NO: 25, SEQ ID NO: 69, and SEQ ID NO: 115;
SEQ ID NO: 26, SEQ ID NO: 70, and SEQ ID NO: 116;
SEQ ID NO: 27, SEQ ID NO: 71, and SEQ ID NO: 117;
SEQ ID NO: 32, SEQ ID NO: 76, and SEQ ID NO: 122;
SEQ ID NO: 33, SEQ ID NO: 77, and SEQ ID NO: 123; or
SEQ ID NO: 36, SEQ ID NO: 80, and SEQ ID NO: 125.

**[0009]** In an embodiment, the antibody specifically binds the S1-NTD domain of the coronavirus spike polypeptide and CDR1, CDR2, and CDR3, respectively, comprise the amino acid sequence set forth in:

SEQ ID NO: 21, SEQ ID NO: 65, and SEQ ID NO: 111;
SEQ ID NO: 22, SEQ ID NO: 66, and SEQ ID NO: 112;
SEQ ID NO: 23, SEQ ID NO: 67, and SEQ ID NO: 113;
SEQ ID NO: 24, SEQ ID NO: 68, and SEQ ID NO: 114;
SEQ ID NO: 25, SEQ ID NO: 69, and SEQ ID NO: 115;
SEQ ID NO: 26, SEQ ID NO: 70, and SEQ ID NO: 116;
SEQ ID NO: 20, SEQ ID NO: 81, and SEQ ID NO: 126;
SEQ ID NO: 37, SEQ ID NO: 82, and SEQ ID NO: 128; or
SEQ ID NO: 38, SEQ ID NO: 83, and SEQ ID NO: 129.

**[0010]** In an embodiment, the antibody specifically binds the S2 subunit of the coronavirus spike polypeptide and CDR1, CDR2, and CDR3, respectively, comprise the amino acid sequence set forth in:

SEQ ID NO: 27, SEQ ID NO: 71, and SEQ ID NO: 117;
SEQ ID NO: 28, SEQ ID NO: 72, and SEQ ID NO: 118;
SEQ ID NO: 29, SEQ ID NO: 73, and SEQ ID NO: 119;

SEQ ID NO: 30, SEQ ID NO: 74, and SEQ ID NO: 120;
SEQ ID NO: 31, SEQ ID NO: 75, and SEQ ID NO: 121;
SEQ ID NO: 32, SEQ ID NO: 76, and SEQ ID NO: 122;
SEQ ID NO: 33, SEQ ID NO: 77, and SEQ ID NO: 123;
SEQ ID NO: 34, SEQ ID NO: 78, and SEQ ID NO: 124;
SEQ ID NO: 39, SEQ ID NO: 84, and SEQ ID NO: 130;
SEQ ID NO: 40, SEQ ID NO: 85, and SEQ ID NO: 131;
SEQ ID NO: 41, SEQ ID NO: 86, and SEQ ID NO: 132;
SEQ ID NO: 42, SEQ ID NO: 87, and SEQ ID NO: 133;
SEQ ID NO: 43, SEQ ID NO: 88, and SEQ ID NO: 134; or
SEQ ID NO: 44, SEQ ID NO: 89, and SEQ ID NO: 135.

**[0011]** In an embodiment, the antibody specifically binds the S1-RBD domain of the coronavirus spike polypeptide and CDR1, CDR2, and CDR3, respectively, comprise the amino acid sequence set forth in:

SEQ ID NO: 1, SEQ ID NO: 45, and SEQ ID NO: 90;
SEQ ID NO: 2, SEQ ID NO: 45, and SEQ ID NO: 91;
SEQ ID NO: 1, SEQ ID NO: 46, and SEQ ID NO: 92;
SEQ ID NO: 3, SEQ ID NO: 47, and SEQ ID NO: 93;
SEQ ID NO: 4, SEQ ID NO: 48, and SEQ ID NO: 94;
SEQ ID NO: 5, SEQ ID NO: 49, and SEQ ID NO: 95;
SEQ ID NO: 6, SEQ ID NO: 50, and SEQ ID NO: 96;
SEQ ID NO: 7, SEQ ID NO: 51, and SEQ ID NO: 97;
SEQ ID NO: 8, SEQ ID NO: 52, and SEQ ID NO: 98;
SEQ ID NO: 9, SEQ ID NO: 53, and SEQ ID NO: 99;
SEQ ID NO: 10, SEQ ID NO: 54, and SEQ ID NO: 100;
SEQ ID NO: 11, SEQ ID NO: 55, and SEQ ID NO: 101;
SEQ ID NO: 12, SEQ ID NO: 56, and SEQ ID NO: 102;
SEQ ID NO: 13, SEQ ID NO: 57, and SEQ ID NO: 103;
SEQ ID NO: 14, SEQ ID NO: 58, and SEQ ID NO: 104;
SEQ ID NO: 15, SEQ ID NO: 59, and SEQ ID NO: 105;
SEQ ID NO: 16, SEQ ID NO: 60, and SEQ ID NO: 106;

SEQ ID NO: 17, SEQ ID NO: 61, and SEQ ID NO: 107;
SEQ ID NO: 18, SEQ ID NO: 62, and SEQ ID NO: 108;
SEQ ID NO: 19, SEQ ID NO: 63, and SEQ ID NO: 109;
SEQ ID NO: 20, SEQ ID NO: 64, and SEQ ID NO: 110;
SEQ ID NO: 35, SEQ ID NO: 79, and SEQ ID NO: 125;
SEQ ID NO: 36, SEQ ID NO: 80, and SEQ ID NO: 125; or
SEQ ID NO: 20, SEQ ID NO: 81, and SEQ ID NO: 127.

**[0012]** In an embodiment, the antibody is cross-reactive with the spike polypeptide of SARS-CoV-2 and SARS-CoV, and CDR1, CDR2, and CDR3, respectively, comprise the amino acid sequence set forth in:

SEQ ID NO: 1, SEQ ID NO: 45, and SEQ ID NO: 92;
SEQ ID NO: 9, SEQ ID NO: 53, and SEQ ID NO: 99;
SEQ ID NO: 21, SEQ ID NO: 65, and SEQ ID NO: 111;
SEQ ID NO: 22, SEQ ID NO: 66, and SEQ ID NO: 112;
SEQ ID NO: 8, SEQ ID NO: 52, and SEQ ID NO: 98;
SEQ ID NO: 11, SEQ ID NO: 55, and SEQ ID NO: 101;
SEQ ID NO: 13, SEQ ID NO: 57, and SEQ ID NO: 103;
SEQ ID NO: 18, SEQ ID NO: 62, and SEQ ID NO: 108;
SEQ ID NO: 19, SEQ ID NO: 63, and SEQ ID NO: 109;
SEQ ID NO: 36, SEQ ID NO: 80, and SEQ ID NO: 125;
SEQ ID NO: 28, SEQ ID NO: 72, and SEQ ID NO: 118;
SEQ ID NO: 30, SEQ ID NO: 74, and SEQ ID NO: 120;
SEQ ID NO: 31, SEQ ID NO: 75, and SEQ ID NO: 121;
SEQ ID NO: 32, SEQ ID NO: 76, and SEQ ID NO: 122;
SEQ ID NO: 33, SEQ ID NO: 77, and SEQ ID NO: 123;
SEQ ID NO: 40, SEQ ID NO: 85, and SEQ ID NO: 131;
SEQ ID NO: 41, SEQ ID NO: 86, and SEQ ID NO: 132; or
SEQ ID NO: 42, SEQ ID NO: 87, and SEQ ID NO: 133.

**[0013]** In an embodiment, the antibody recognizes a linear epitope, and CDR1, CDR2, and CDR3, respectively, comprise the amino acid sequence set forth in:

SEQ ID NO: 21, SEQ ID NO: 65, and SEQ ID NO: 111;
SEQ ID NO: 24, SEQ ID NO: 68, and SEQ ID NO: 114;
SEQ ID NO: 27, SEQ ID NO: 71, and SEQ ID NO: 117;
SEQ ID NO: 28, SEQ ID NO: 72, and SEQ ID NO: 118;
SEQ ID NO: 29, SEQ ID NO: 73, and SEQ ID NO: 119;
SEQ ID NO: 31, SEQ ID NO: 75, and SEQ ID NO: 121;
SEQ ID NO: 32, SEQ ID NO: 76, and SEQ ID NO: 122;
SEQ ID NO: 30, SEQ ID NO: 74, and SEQ ID NO: 120;
SEQ ID NO: 39, SEQ ID NO: 84, and SEQ ID NO: 130;
SEQ ID NO: 40, SEQ ID NO: 85, and SEQ ID NO: 131; or
SEQ ID NO: 41, SEQ ID NO: 86, and SEQ ID NO: 132.

**[0014]** In an embodiment, the antibody comprises the amino acid sequence set forth in SEQ ID NO: 183.

**[0015]** In an embodiment of the antibody, CDR1, CDR2, and CDR3, respectively, comprise the amino acid sequence set forth in:

SEQ ID NO: 21, SEQ ID NO: 65, and SEQ ID NO: 111;
SEQ ID NO: 23, SEQ ID NO: 67, and SEQ ID NO: 113; or
SEQ ID NO: 24, SEQ ID NO: 68, and SEQ ID NO: 114.

**[0016]** In an embodiment of the antibody, CDR1, CDR2, and CDR3, respectively, comprise the amino acid sequence set forth in: SEQ ID NO: 38, SEQ ID NO: 83, and SEQ ID NO: 129.

**[0017]** In an embodiment of the antibody, CDR1, CDR2, and CDR3, respectively, comprise the amino acid sequence set forth in:

SEQ ID NO: 20, SEQ ID NO: 81, and SEQ ID NO: 126 or
SEQ ID NO: 37, SEQ ID NO: 82, and SEQ ID NO: 128.

**[0018]** In an embodiment, the antibody comprises the amino acid sequence set forth in SEQ ID NO: 184.

**[0019]** In an embodiment, the antibody comprises the amino acid sequence set forth in SEQ ID NO: 158, SEQ ID NO: 157, SEQ ID NO: 172, SEQ ID NO: 175, SEQ ID NO: 176, SEQ ID NO:

160, SEQ ID NO: 161, SEQ ID NO: 159, or SEQ ID NO: 162, or an amino acid sequence having at least 75%, at least 80%, at least 85%, at least 90%, at least 95%, at least 96%, at least 97%, at least 98%, or at least 99% sequence identity to the full length of the amino acid sequence set forth in SEQ ID NO: 158, SEQ ID NO: 157, SEQ ID NO: 172, SEQ ID NO: 175, SEQ ID NO: 176, SEQ ID NO: 160, SEQ ID NO: 161, SEQ ID NO: 159, and/or SEQ ID NO: 162.

**[0020]** In an embodiment of the antibody, CDR1, CDR2, and CDR3, respectively, comprise the amino acid sequence set forth in:

SEQ ID NO: 31, SEQ ID NO: 75, and SEQ ID NO: 121;
SEQ ID NO: 40, SEQ ID NO: 85, and SEQ ID NO: 131;
SEQ ID NO: 41, SEQ ID NO: 86, and SEQ ID NO: 132;
SEQ ID NO: 42, SEQ ID NO: 87, and SEQ ID NO: 133;
SEQ ID NO: 43, SEQ ID NO: 88, and SEQ ID NO: 134; or
SEQ ID NO: 44, SEQ ID NO: 89, and SEQ ID NO: 135.

**[0021]** In an embodiment of the antibody, CDR1, CDR2, and CDR3, respectively, comprise the amino acid sequence set forth in SEQ ID NO: 33, SEQ ID NO: 77, and SEQ ID NO: 123.

**[0022]** In an embodiment of the antibody, CDR1, CDR2, and CDR3, respectively, comprise the amino acid sequence set forth in SEQ ID NO: 32, SEQ ID NO: 76, and SEQ ID NO: 122.

**[0023]** In an embodiment of the antibody, CDR1, CDR2, and CDR3, respectively, comprise the amino acid sequence set forth in SEQ ID NO: 27, SEQ ID NO: 71, and SEQ ID NO: 117.

**[0024]** In an embodiment of the antibody, CDR1, CDR2, and CDR3, respectively, comprise the amino acid sequence set forth in SEQ ID NO: 28, SEQ ID NO: 72, and SEQ ID NO: 118.

**[0025]** In an embodiment, the antibody comprises the amino acid sequence set forth in SEQ ID NO: 185.

**[0026]** In an embodiment, the antibody comprises the amino acid sequence set forth in SEQ ID NO: 180, SEQ ID NO: 182, SEQ ID NO: 166, SEQ ID NO: 177, SEQ ID NO: 179, SEQ ID NO: 163, SEQ ID NO: 164, SEQ ID NO: 167, SEQ ID NO: 170, SEQ ID NO: 168, SEQ ID NO: 169, SEQ ID NO: 181, SEQ ID NO: 165, or SEQ ID NO: 178, or an amino acid sequence having at

least 75%, at least 80%, at least 85%, at least 90%, at least 95%, at least 96%, at least 97%, at least 98%, or at least 99% sequence identity to the full length of the amino acid sequence set forth in SEQ ID NO: 180, SEQ ID NO: 182, SEQ ID NO: 166, SEQ ID NO: 177, SEQ ID NO: 179, SEQ ID NO: 163, SEQ ID NO: 164, SEQ ID NO: 167, SEQ ID NO: 170, SEQ ID NO: 168, SEQ ID NO: 169, SEQ ID NO: 181, SEQ ID NO: 165, and/or SEQ ID NO: 178.

**[0027]** In an embodiment of the antibody, CDR1, CDR2, and CDR3, respectively, comprise the amino acid sequence set forth in:

SEQ ID NO: 5, SEQ ID NO: 49, and SEQ ID NO: 95;
SEQ ID NO: 14, SEQ ID NO: 58, and SEQ ID NO: 104;
SEQ ID NO: 16, SEQ ID NO: 60, and SEQ ID NO: 106;
SEQ ID NO: 10, SEQ ID NO: 54, and SEQ ID NO: 100;
SEQ ID NO: 15, SEQ ID NO: 59, and SEQ ID NO: 105; or
SEQ ID NO: 20, SEQ ID NO: 81, and SEQ ID NO: 127.

**[0028]** In an embodiment of the antibody, CDR1, CDR2, and CDR3, respectively, comprise the amino acid sequence set forth in:

SEQ ID NO: 3, SEQ ID NO: 47, and SEQ ID NO: 93;
SEQ ID NO: 6, SEQ ID NO: 50, and SEQ ID NO: 96;
SEQ ID NO: 14, SEQ ID NO: 58, and SEQ ID NO: 104;
SEQ ID NO: 10, SEQ ID NO: 54, and SEQ ID NO: 100;
SEQ ID NO: 15, SEQ ID NO: 59, and SEQ ID NO: 105; or
SEQ ID NO: 20, SEQ ID NO: 81, and SEQ ID NO: 127.

**[0029]** In an embodiment of the antibody, CDR1, CDR2, and CDR3, respectively, comprise the amino acid sequence set forth in:

SEQ ID NO: 3, SEQ ID NO: 47, and SEQ ID NO: 93;
SEQ ID NO: 6, SEQ ID NO: 50, and SEQ ID NO: 96;
SEQ ID NO: 16, SEQ ID NO: 60, and SEQ ID NO: 106;
SEQ ID NO: 10, SEQ ID NO: 54, and SEQ ID NO: 100;
SEQ ID NO: 15, SEQ ID NO: 59, and SEQ ID NO: 105; or
SEQ ID NO: 20, SEQ ID NO: 81, and SEQ ID NO: 127.

**[0030]** In an embodiment of the antibody, CDR1, CDR2, and CDR3, respectively, comprise the amino acid sequence set forth in SEQ ID NO: 7, SEQ ID NO: 51, and SEQ ID NO: 97.

**[0031]** In an embodiment of the antibody, CDR1, CDR2, and CDR3, respectively, comprise the amino acid sequence set forth in:

SEQ ID NO: 4, SEQ ID NO: 48, and SEQ ID NO: 94;

SEQ ID NO: 9, SEQ ID NO: 53, and SEQ ID NO: 99;

SEQ ID NO: 11, SEQ ID NO: 55, and SEQ ID NO: 101; or

SEQ ID NO: 12, SEQ ID NO: 56, and SEQ ID NO: 102.

**[0032]** In an embodiment of the antibody, CDR1, CDR2, and CDR3, respectively, comprise the amino acid sequence set forth in:

SEQ ID NO: 3, SEQ ID NO: 47, and SEQ ID NO: 93;

SEQ ID NO: 6, SEQ ID NO: 50, and SEQ ID NO: 96;

SEQ ID NO: 10, SEQ ID NO: 54, and SEQ ID NO: 100;

SEQ ID NO: 15, SEQ ID NO: 59, and SEQ ID NO: 105; or

SEQ ID NO: 20, SEQ ID NO: 81, and SEQ ID NO: 127.

**[0033]** In an embodiment of the antibody, CDR1, CDR2, and CDR3, respectively, comprise the amino acid sequence set forth in:

SEQ ID NO: 10, SEQ ID NO: 54, and SEQ ID NO: 100;

SEQ ID NO: 15, SEQ ID NO: 59, and SEQ ID NO: 105; or

SEQ ID NO: 20, SEQ ID NO: 81, and SEQ ID NO: 127.

**[0034]** In an embodiment of the antibody, CDR1, CDR2, and CDR3, respectively, comprise the amino acid sequence set forth in:

SEQ ID NO: 14, SEQ ID NO: 58, and SEQ ID NO: 104;

SEQ ID NO: 10, SEQ ID NO: 54, and SEQ ID NO: 100;

SEQ ID NO: 15, SEQ ID NO: 59, and SEQ ID NO: 105; or

SEQ ID NO: 20, SEQ ID NO: 81, and SEQ ID NO: 127.

**[0035]** In an embodiment of the antibody, CDR1, CDR2, and CDR3, respectively, comprise the amino acid sequence set forth in:

SEQ ID NO: 16, SEQ ID NO: 60, and SEQ ID NO: 106;
SEQ ID NO: 10, SEQ ID NO: 54, and SEQ ID NO: 100;
SEQ ID NO: 15, SEQ ID NO: 59, and SEQ ID NO: 105; or
SEQ ID NO: 20, SEQ ID NO: 81, and SEQ ID NO: 127.

**[0036]** In an embodiment of the antibody, CDR1, CDR2, and CDR3, respectively, comprise the amino acid sequence set forth in:

SEQ ID NO: 1, SEQ ID NO: 45, and SEQ ID NO: 90;
SEQ ID NO: 1, SEQ ID NO: 46, and SEQ ID NO: 92;
SEQ ID NO: 2, SEQ ID NO: 45, and SEQ ID NO: 91;
SEQ ID NO: 8, SEQ ID NO: 52, and SEQ ID NO: 98;
SEQ ID NO: 13, SEQ ID NO: 57, and SEQ ID NO: 103;
SEQ ID NO: 17, SEQ ID NO: 61, and SEQ ID NO: 107;
SEQ ID NO: 19, SEQ ID NO: 63, and SEQ ID NO: 109;
SEQ ID NO: 35, SEQ ID NO: 79, and SEQ ID NO: 125; or
SEQ ID NO: 36, SEQ ID NO: 80, and SEQ ID NO: 125.

**[0037]** In an embodiment, the antibody comprises the amino acid sequence set forth in SEQ ID NO: 186.

**[0038]** In an embodiment, the antibody comprises the amino acid sequence set forth in SEQ ID NO: 171, SEQ ID NO: 173, SEQ ID NO: 149, SEQ ID NO: 155, SEQ ID NO: 147, SEQ ID NO: 148, SEQ ID NO: 139, SEQ ID NO: 142, SEQ ID NO: 154, SEQ ID NO: 144, SEQ ID NO: 145, SEQ ID NO: 156, SEQ ID NO: 174, SEQ ID NO: 137, SEQ ID NO: 136, SEQ ID NO: 138, SEQ ID NO: 152, SEQ ID NO: 153, SEQ ID NO: 140, SEQ ID NO: 143, SEQ ID NO: 141, SEQ ID NO: 146, SEQ ID NO: 150, or SEQ ID NO: 151, or an amino acid sequence having at least 75%, at least 80%, at least 85%, at least 90%, at least 95%, at least 96%, at least 97%, at least 98%, or at least 99% sequence identity to the full length of the amino acid sequence set forth in SEQ ID NO: 171, SEQ ID NO: 173, SEQ ID NO: 149, SEQ ID NO: 155, SEQ ID NO: 147, SEQ ID NO: 148, SEQ ID NO: 139, SEQ ID NO: 142, SEQ ID NO: 154, SEQ ID NO: 144, SEQ ID NO: 145, SEQ ID NO: 156, SEQ ID NO: 174, SEQ ID NO: 137, SEQ ID NO: 136, SEQ ID NO: 138, SEQ ID NO: 152, SEQ ID NO: 153, SEQ ID NO: 140, SEQ ID NO: 143, SEQ ID NO: 141, SEQ ID NO: 146, SEQ ID NO: 150, and/or SEQ ID NO: 151.

**[0039]** In an embodiment, the antibody is a single domain antibody. In a further embodiment, the antibody is a $V_HH$.

**[0040]** In an embodiment the antibody is of camelid origin.

**[0041]** In an embodiment, the antibody is in a multivalent display format. In a further embodiment, the antibody is linked to an Fc fragment. In a further embodiment, the Fc-linked antibody is in a bivalent display format.

**[0042]** In an embodiment of the antibody, the at least one coronavirus spike polypeptide specifically binds an ACE2 receptor.

**[0043]** In an embodiment of the antibody, the at least one coronavirus spike polypeptide comprises a SARS-CoV-2 spike polypeptide.

**[0044]** In an embodiment of the antibody, the at least one coronavirus spike polypeptide is comprised within a homotrimer.

**[0045]** Another embodiment is an antibody cocktail composition comprising two or more of the antibodies as described herein. The composition may comprise two, three, four, five, or more different antibodies as described herein. The antibody cocktail composition may further comprise a pharmaceutically acceptable carrier and/or diluent.

**[0046]** Another embodiment is a nucleic acid molecule encoding an antibody as described herein. A further embodiment is a vector comprising the nucleic acid molecule. In an embodiment of the vector, the nucleic acid molecule is operably linked to at least one promoter and/or regulatory element to enable expression in a host cell. An additional embodiment is a host cell comprising the vector.

**[0047]** Another embodiment is a pharmaceutical composition comprising at least one antibody as defined herein and a pharmaceutically acceptable carrier and/or diluent. In an embodiment, the pharmaceutical composition is for delivery by inhalation or nebulization.

**[0048]** Another embodiment is a composition comprising at least one antibody as defined herein, linked to another molecule. In an embodiment, the other molecule is a label or polypeptide. In an embodiment, the other molecule is an ACE2 polypeptide or a fragment thereof.

**[0049]** Another embodiment is a composition or apparatus comprising at least one antibody as defined herein immobilized on a substrate. A further embodiment is a method for capturing a coronavirus or a coronavirus spike polypeptide or fragment thereof from a sample, the method comprising exposing the sample to the composition or apparatus. In an embodiment, the coronavirus is a coronavirus that specifically binds an ACE2 receptor or the coronavirus spike polypeptide is a coronavirus spike polypeptide that specifically binds an ACE2 receptor. In an embodiment, the coronavirus is SARS-CoV-2 or SARS-CoV.

**[0050]** Another embodiment is use of an antibody as described herein to treat or detect a coronavirus infection. In an embodiment, the coronavirus infection is caused by at least one coronavirus that specifically binds an ACE2 receptor. In an embodiment, the coronavirus infection is caused by SARS-CoV-2 and/or SARS-CoV.

**[0051]** Another embodiment is use of an antibody or composition as described herein to detect, quantify and/or capture a coronavirus; or to detect, quantify and/or capture a coronavirus spike polypeptide or fragment thereof. In an embodiment, the coronavirus is a coronavirus that specifically binds an ACE2 receptor or the coronavirus spike polypeptide is a coronavirus spike polypeptide that specifically binds an ACE2 receptor. In an embodiment, the coronavirus is SARS-CoV-2 or SARS-CoV.

**[0052]** Another embodiment is a method for treating or preventing a coronavirus infection, the method comprising administering at least one antibody or composition as described herein to a subject in need thereof. In an embodiment, the coronavirus infection is caused by at least one coronavirus that specifically binds an ACE2 receptor. In an embodiment, the coronavirus infection is caused by SARS-CoV-2 and/or SARS-CoV. In an embodiment, the administration is by inhalation or nebulization.

**[0053]** Another embodiment is a method for detecting the presence of a coronavirus or a coronavirus spike polypeptide or fragment thereof in a sample, the method comprising exposing the sample to at least one antibody or composition as described herein and assaying for specific binding between the at least one antibody and the sample, wherein specific binding indicates a presence of the at least one coronavirus or coronavirus spike polypeptide or fragment thereof in the sample.

**[0054]** In an embodiment of the methods described in the preceding paragraphs, the coronavirus is a coronavirus that specifically binds an ACE2 receptor or the coronavirus spike polypeptide is a coronavirus spike polypeptide that specifically binds an ACE2 receptor. In an embodiment, coronavirus is SARS-CoV-2 or SARS-CoV, or the coronavirus spike polypeptide or fragment thereof is a SARS-CoV-2 or SARS-CoV coronavirus spike polypeptide or fragment thereof.

**[0055]** Another embodiment is an antibody or composition as described herein for use to detect or treat a coronavirus infection. In an embodiment, the coronavirus infection is caused by at least one coronavirus that specifically binds an ACE2 receptor. In an embodiment, the at least one coronavirus is SARS-CoV-2 and/or SARS-CoV.

**[0056]** Another embodiment is an antibody composition as described herein for use to detect, quantify and/or capture a coronavirus; or to detect, quantify and/or capture a coronavirus spike polypeptide or fragment thereof. In an embodiment, the coronavirus is a coronavirus that specifically binds an ACE2 receptor, or the coronavirus spike polypeptide is a coronavirus spike polypeptide that specifically binds an ACE2 receptor. In an embodiment, the coronavirus is SARS-CoV-2 or SARS-CoV or the coronavirus spike polypeptide or fragment thereof is a SARS-CoV-2 or SARS-CoV spike polypeptide or fragment thereof.

**[0057]** Another embodiment is use of an antibody as described herein in the manufacture of a medicament for prevention or treatment of a coronavirus infection. In an embodiment, the coronavirus infection is caused by at least one coronavirus that specifically binds an ACE2 receptor. In an embodiment, the at least one coronavirus is SARS-CoV-2 and/or SARS-CoV. In an embodiment, the medicament is for delivery by inhalation or nebulization.

## BRIEF DESCRIPTION OF THE DRAWINGS

**[0058]** Throughout the present disclosure, including in the drawings, antibodies may be referred to by their full name, e.g. NRCoV2-1d, NRCoV2-02, NRCoV2-SR03, or NRCoV2-MRed02, or by an abbreviation in which the "NRCoV2-" portion of the antibody name is omitted, e.g. 1d, 02, SR03, or MRed02. Further, "RBD" and "S1-RBD" are used interchangeably, as are "NTD" and "S1-NTD".

**[0059]** **Figures 1A** and **1B** describe antigen validation by ELISA. **Fig. 1A** shows the results of an ELISA assessing the binding of microtiter-well-adsorbed (S, S1, S2, S1-RBD) and microtiter-

well-captured (AviTag-S1, AviTag-S1-RBD) SARS-CoV-2 spike protein fragments to cognate ACE2 receptor (ACE2-hFc). AviTag-S1 and AviTag-S1-RBD were captured on streptavidin-coated microtiter wells through their C-terminal biotins. **Fig. 1B** shows the results of an ELISA confirming the binding of microtiter-well-adsorbed SARS-CoV-2 spike protein fragments S, S1, S2 and S1-RBD to a commercial rabbit anti-SARS-CoV-2 S polyclonal antibody (pAb).

**[0060]** **Figures 2A** and **2B** show the results of llama serology. **Fig. 2A** shows the results of an ELISA performed with pre-immune (day 0) and immune (day 21 and 28) sera, demonstrating that spike protein-immunized Maple Red and Eva Green llamas generated a strong immune response against target antigens S, S1, S2 and S1-RBD. ELISA performed with day 0, 21 and 28 sera showed spike protein-immunized llamas did not react with non-target antigens (casein and dipeptidase 1 [DPEP1]), demonstrating specificity of the immune response. **Fig. 2B** shows flow cytometry surrogate neutralization assays performed with pre-immune (day 0) and immune (day 21 and 28) sera demonstrating that the Eva Green llama mounted a polyclonal immune response that was more potent in inhibiting the binding of SARS-CoV-2 S to ACE2 than Maple Red's. Due to a lack of complete curves, inhibitory serum titers for Maple Red sera were estimated assuming similar upper plateaus as those for Eva Green sera.

**[0061]** **Figure 3** provides a schematic representation of three different antibody formats: monomeric $V_HH$, bivalent $V_HH$-Fc and monovalent $V_HH$-Fc.

**[0062]** **Figures 4A** and **4B** show size-exclusion chromatogram (SEC) profiles of anti-SARS-CoV-2 spike protein $V_HH$s. **Fig. 4A** shows SEC profiles of Eva Green $V_HH$s. **Fig. 4B** shows SEC profiles of Maple Red $V_HH$s. $V_e$, elution volume: mAU, milliabsorbance unit.

**[0063]** **Figures 5A** and **5B** show data on the thermostability of anti-SARS-CoV-2 spike protein $V_HH$s. **Fig. 5A** provides representative examples showing the thermal unfolding of NRCoV2-1d, NRCoV2-02, NRCoV2-07 and NRCoV2-11, as determined using CD spectroscopy. **Fig. 5B** provides a summary of $V_HH$ $T_m$s. The dotted line across the graph in **Fig. 5B** represents the median $T_m$ (70.4°C).

**[0064]** **Figures 6A, 6B, 6C, 6D** and **6E** show SPR/ELISA binding affinity, specificity and cross-reactivity data for anti-SARS-CoV-2 $V_HH$s and $V_HH$-Fcs. **Figs. 6A** and **6B** show the results of

ELISA assessing the cross-reactivity of anti-SARS-CoV-2 $V_HH$-Fcs against to a collection of spike glycoproteins from various coronavirus genera and SARS-CoV-2 variants. Assays were performed at a fixed $V_HH$-Fc concentration (13 nM). The $V_HH$-72 (Wrapp et al., 2020) benchmark and human ACE-2 were included for comparison. The epitope bin numbers provided along the bottom of **Fig. 6B** correspond to the bins shown in **Fig. 9G**. **Fig. 6C** shows representative SPR sensorgrams showing single-cycle kinetic analysis of NRCoV2-02, NRCoV2-07, NRCoV2-SR03 and NRCoV2-S2A4 $V_HH$ binding to SARS-CoV S and SARS-CoV-2 S, S1, S2 and S1-RBD. Spike proteins were captured on CM5 sensorchip surfaces, followed by flowing $V_HH$s over the sensorchip surfaces at the concentration ranges shown in each panel. "NRCoV2-02/NRCoV2-07", "SR03" and "S2A4" represent SPR binding profiles for $V_HH$s specific to SARS-CoV-2 S1-RBD, S1-NTD and S2, respectively. "NRCoV2-07" also represents binding profiles for $V_HH$s that cross-react with SARS-CoV. **Figs. 6D** and **6E** show the results of ELISA assessing the domain specificity of a set of anti-SARS-CoV-2 $V_HH$-Fcs. Assays were performed against SARS-CoV-2 S, S1, S1-NTD and S1-RBD at a fixed concentration (13 nM) (**Fig. 6D**) or varying concentrations (**Fig. 6E**) of $V_HH$-Fcs. In the graphs shown in **Fig. 6E**, NRCoV2-02 is included as an internal control (dashed line).

**[0065]** **Figures 7A** and **7B** show on-/off-rate maps summarizing $V_HH$ kinetic rate constants, $k_a$s and $k_d$s. Diagonal lines represent equilibrium dissociation constants, $K_D$s. Maps were constructed using the $V_HH$ binding data against SARS-CoV-2 S (**Fig. 7A**) and SARS-CoV S (**Fig. 7B**). In **Fig. 7A**, $V_HH$s are clustered based on subunit/domain specificity determined in **Example 5**. Anti-SARS-CoV $V_HH$-72, which cross-reacts with SARS-CoV-2 S1-RBD (Wrapp et al., 2020), and the monomeric ACE2 (ACE2-$H_6$) are included as benchmark/reference binders.

**[0066]** **Figures 8A** and **8B** show the results of flow cytometry assessing the binding of $V_HH$-Fcs to SARS-CoV-2 S-expressing CHO-S cells. **Fig. 8A** shows representative examples. **Fig. 8B** summarizes affinity values, i.e., $EC_{50}$s, determined from graphs in **Fig. 8A**. $V_HH$-72 (Wrapp et al., 2020; open circle) is included for comparison. The line through the data points is the median.

**[0067]** **Figures 9A**, **9B**, **9C**, **9D**, **9E, 9F,** and **9G** show epitope typing and binning data obtained by SDS-PAGE/WB, sandwich ELISA and SPR. **Fig. 9A** and **9B** show the results of epitope typing of anti-SARS-CoV-2 $V_HH$s by SDS-PAGE/WB. Binding of biotinylated $V_HH$s or $V_HH$-Fcs to

denatured SARS-CoV-2 S was detected using streptavidin-peroxidase conjugate (**Fig. 9A**) or anti-human Ig Fc antibody-peroxidase conjugate (**Fig. 9B**), respectively. Presence of binding signals indicates $V_HH$ recognizing a linear epitope. The absence of binding signals is an indirect indication of $V_HHs$ recognizing conformational epitopes. Toxin A-specific A20.1 $V_HH$ (Hussack et al., 2011) was used as a negative antibody control. "PBS" and "A20.1" represent experiments where $V_HH$ test articles were replaced with PBS and *C. difficile* toxin A-specific $V_HH$ A20.1. **Fig. 9C** shows representative sensorgrams showing SPR epitope binning on SARS-CoV-2 S-immobilized surfaces. **Figs. 9D** and **9E** show epitope binning of S1-RBD-specific $V_HHs$ by competitive sandwich ELISA. ELISA binding results for pair-wise combinations of $V_HHs$ against S1 are presented as a heat map. Binding pairs giving binding signal (shaded) were considered as recognizing non-overlapping epitopes hence belonging to different epitope bins or $V_HH$ clusters, while those giving no/week binding signals (colorless/pale shading) were considered to be recognizing overlapping epitopes belonging to the same epitope bins. ACE2-Fc and $V_HH$-72 $V_HH/V_HH$-Fc benchmark (Wrapp et al., 2020) were also included in assays. Wells captured with *C. difficile* toxin A-specific $V_HH$ negative control, A20.1 (Hussack et al., 2011), did not give any binding. **Fig. 9F** provides a schematic summary of the initial epitope binning results. NRCoV2-1c and NRCoV2-MRed02 were assigned to bin 1 since their CDRs were essentially the same as to those of NRCoV2-1a/1d and NRCoV2-MRed04, respectively, with experimentally defined bins. **Fig. 9G** provides a schematic summary of binning results after further characterization. Unless specified otherwise, references to epitope bin numbers throughout the present disclosure refer to the bins identified in **Fig. 9F**. The bin numbers provided in **Fig. 9E** correspond to the bins shown in **Fig. 9G**.

**[0068]** **Figure 10** shows the results of ELISA assessing the ability of monomeric $V_HHs$ in blocking ("neutralizing") the binding of human ACE2 receptor (ACE2-Fc) to its SARS-CoV-2 S1-RBD ligand (i.e., S). $A_{450\ nm}$ is a measure of blocking. $V_HH$-72 $V_HH$ (Wrapp et al., 2020) and monomeric ACE2-$H_6$ served as positive antibody controls, while toxin A-specific A20.1 $V_HH$ (Hussack et al., 2011) was a negative antibody control. "PBS" represents assays in which $V_HH$ was substituted with PBS and, similar to the A20.1 control, provides a reference binding signal for lack of any blocking ("min inhibition"). The "-ACE2-Fc" control represents an assay in which ACE2-Fc is omitted and provides a reference binding signal for 100% blocking ("max inhibition").

**[0069]** **Figure 11** shows sensorgrams showing the ability of monomeric $V_HHs$ in blocking ("neutralizing") the binding of ACE2 receptor to its ligand SARS-CoV-2 S. A tandem SPR in two different orientation formats were performed where injection of $V_HH$ (orientation #1) or ACE2 (orientation #2) at 20 – 40 × $K_D$ concentration ($V_HH$) or 1 μM (ACE2) over sensor chip-immobilized S was followed by injection of $V_HH$ + ACE2 mix at the same $V_HH$ and ACE2 concentrations. Solid and dashed profiles represent binding results with the two orientation formats. "NRCoV2-02:ACE2" represents profiles for blocking (neutralizing) $V_HHs$ where the addition of the $V_HH$ or ACE2 results in no significant increase in binding over that achieved by the injection of the ACE2 or $V_HH$ over the antigen surface. "NRCoV2-11:ACE2" represents profiles for non-blocking (non-neutralizing $V_HHs$ where the addition of the $V_HH$ or ACE2 results in significant increase in binding over that achieved by the injection of the ACE2 or $V_HH$ over the antigen surface. ΔRUs, representing binding differences between the first and second injection, were calculated from the sensorgrams and used to identify $V_HHs$ that block (neutralize) the binding of ACE2 receptor to its ligand S1-RBD. ACE2 is provided as an abbreviation for monomeric ACE2-$H_6$.

**[0070]** **Figures 12A** and **12B** show the results of flow cytometry assessing the ability of monomeric $V_HHs$ in blocking ("neutralizing") the binding of SARS-CoV-2 S to ACE2-expressing Vero E6 cells at 100 nM (**Fig. 12A**) or increasing (**Fig. 12B**) $V_HH$ concentrations. **Fig. 12B** provides plots showing inhibition of SARS-CoV-2 S binding to Vero E6 cells as a function of $V_HH$ concentration. The NRCoV2-1d, NRCoV2-02, NRCoV2-05, and NRCoV2-11 $V_HHs$ are S1-RBD, SR13, S1-NTD-specific. Monomeric ACE2 (ACE2-$H_6$) serves as positive "antibody" control and reference, and $V_HH$-72 $V_HH$ (Wrapp et al., 2020) is included as benchmark. "A20.1" and "PBS" represent negative control assays in which $V_HHs$ were replaced with *C. difficile* toxin A-specific A20.1 $V_HH$ (Hussack et al., 2011) and PBS, respectively.

**[0071]** **Figures 13A** and **13B** show virus-neutralizing potential of $V_HH$-Fcs in flow cytometry-based surrogate virus neutralization assays. **Fig. 13A** shows flow cytometry assessing the ability of bivalent $V_HH$-Fcs in blocking ("neutralizing") the binding of SARS-CoV-2 S to ACE2-expressing Vero E6 cells at 250 nM $V_HH$-Fc concentrations. **Fig. 13B** shows flow cytometry assessing the ability of bivalent $V_HH$-Fcs in blocking ("neutralizing") the binding of SARS-CoV-2 S to ACE2-expressing Vero E6 cells at increasing $V_HH$-Fc concentrations. NRCoV2-1d,

NRCoV2-02, NRCoV2-04, NRCoV2-05, NRCoV2-11, and NRCoV2-20 $V_HH$-Fcs are S1-RBD-specific, while NRCoV2-SR01 and NRCoV2-SR13 $V_HH$-Fcs are S1-NTD-specific. $V_HH$-72 $V_HH$-Fc (Wrapp et al., 2020) is included as a benchmark. "A20.1" and "PBS" represent negative control assays in which $V_HH$s were replaced with *C. difficile* toxin A-specific A20.1 $V_HH$ (Hussack et al., 2011) and PBS, respectively.

**[0072]** **Figures 14A** and **14B** show the results of a $V_HH$-Fc *in vitro* live-virus micro-neutralization assay. Antibody concentrations that gave 100% neutralization, i.e., $MN_{100}$s, were used to rank the neutralizing potency of $V_HH$-Fcs. A lower $MN_{100}$ means a higher neutralization potency. $V_HH$-72 (Wrapp et al., 2020) is included as benchmark. **Fig. 14A** provides a plot showing the $MN_{100}$s of bivalent $V_HH$-Fcs. The inset shows $MN_{100}$s of monomeric NRCoV2-02 and $V_HH$-72 $V_HH$s. *The $MN_{100}$ of NRCoV2-02 bivalent $V_HH$-Fc is $\leq$0.01 nM, since its potency was not tested below the 0.01 nM concentration. **Fig. 14B** provides a plot comparing the $MN_{100}$s of bivalent $V_HH$-Fcs to monovalent $V_HH$-Fcs. Monovalent $V_HH$-72-Fc did not show $MN_{100}$ at the highest concentration tested (350 nM). In monovalent $V_HH$-Fc constructs, one heavy chain displays an S-specific $V_HH$, while the other displays a *C. difficile* toxin A-specific, mock $V_HH$ (A26.8) (Hussack et al., 2011).

**[0073]** **Figures 15A**, **15B, 15C, 15D,** and **15E** show the results of $V_HH$-Fc *in vitro* live-virus neutralization assay. **Fig. 15A** shows inhibition capability of S1-RBD-specific $V_HH$-Fcs at high (312.5 nM) and low (2.5 nM) $V_HH$-Fc concentrations. As expected, NRCoV2-08, NRCoV2-19 and NRCoV2-21 which showed no binding to spike protein-expressing CHO cells (CHO-S), do not neutralize either. $V_HH$-72 (Wrapp et al., 2020) and *C. difficile* toxin A-specific $V_HH$ A20.1 (Hussack et al., 2011) are included as benchmark and negative control, respectively. **Figs. 15B-D** provide representative examples showing inhibition capability of $V_HH$-Fcs as a function of $V_HH$-Fc concentration, for select S-RBD specific antibodies (**Fig. 15B**), S1-NTD-specific antibodies (**Fig. 15C**), and S2-specific antibodies (**Fig. 15D**). Antibody concentrations that gave 50% neutralization, i.e., $IC_{50}$s, were calculated from graphs and used to rank the neutralizing potency of $V_HH$-Fcs. Bin ud, epitope bin undetermined. **Fig. 15E** shows a summary of $IC_{50}$ categorized based on subunit/domain specificity and epitope bin. A lower $IC_{50}$ means a higher neutralization potency. $V_HH$-72 is shown as open circle in bin 1. Bin ud, epitope bin undetermined. The line through the data points is the median.

**[0074]** **Figures 16A, 16B, 16C,** and **16D** show data on the stability of $V_HHs$ against aerosolization treatment. **Fig. 16A** shows SEC profiles of pre- *vs* post-aerosolized $V_HHs$, for representative $V_HHs$. NRCoV2-1d, NRCoV2-02 and NRCoV2-07 represent the vast majority of $V_HHs$ which were resistant to aerosolization-induced aggregation, showing a homogenously monomeric peak. In contrast, the $V_HH$-72 benchmark forms a significant amount of soluble aggregates following aerosolization. NRCoV2-11 on the other hand represents the few $V_HHs$ that formed visible, precipitating aggregates reflected in significant reduction of their monomeric peak areas (compare monomeric peak for pre- vs post-aeosolized NRCoV2-11). $V_e$, elution volume. **Fig. 16B** summarizes the % recovery of all $V_HHs$ and **Fig. 16C** summarizes the % recovery of a subset of $V_HHs$. % recovery represents the proportion of a $V_HH$ that remained monomerically soluble following aerosolization. The open circle in **Fig. 16B** represents benchmark $V_HH$-72. The line through the data points is the median. **Fig. 16D** shows the results of ELISA assessing the effect of aerosolization on the functionality of $V_HHs$ by comparing the binding activity of pre- *vs* post-aerosolized $V_HHs$ against SARS-CoV-2 S. Essentially identical $EC_{50}$s for pre- *vs* post-aerosolized $V_HHs$ clearly indicate aerosolization had no effect on the functional activity of $V_HHs$. Pre, pre-aerosolized $V_HH$; post, post-aerosolized $V_HH$.

**[0075]** **Figure 17** provides the results of sandwich ELISA demonstrating the potential utility of $V_HHs$ in detecting/capturing SARS-CoV-2, SARS-CoV and related viruses, as well as their spike proteins. SARS-CoV-2 S, S1 and S1-RBD antigens were used as surrogates for viruses. Specific detection of S, S1 and S1-RBD was achieved using NRCoV2-02 $V_HH$ as the capture antibody and NRCoV2-1d, NRCoV2-02, NRCoV2-04, NRCoV2-07, or NRCoV2-11 $V_HH$-Fcs as detecting antibodies. $SC_{50}$ is the concentration of antigen that gives 50% binding and were calculated from graphs.

**[0076]** **Figure 18** shows an alignment of amino acid sequences of S-specific $V_HH$ antibodies described herein.

**[0077]** **Figure 19** shows an alignment of amino acid sequences of S1-NTD-specific $V_HH$ antibodies described herein.

**[0078]** **Figure 20** shows an alignment of amino acid sequences of S2-specific $V_HH$ antibodies described herein.

**[0079]** **Figure 21** shows an alignment of amino acid sequences of S1-RBD-specific $V_HH$ antibodies described herein.

**[0080]** **Figures 22A, 22B, 22C,** and **22D** show the results of efficacy tests of $V_HH$-Fcs in hamsters challenged with SARS-CoV-2. **Fig. 22A** shows lung viral load in $V_HH$-Fc-treated ($V_HH$-72 benchmark, 1d, 05, MRed05, SR01, S2A3, 1d/MRed05, 1d/SR01) and control groups treated with PBS or isotype A20.1 $V_HH$-Fc at 5 dpi. PFU, plaque-forming unit. **Fig. 22B** shows the percent body weight change for antibody-treated and control groups. **Fig. 22C** shows the percent body weight change at 5 dpi. In **Fig. 22A** and **Fig. 22C**, treatment effects, assessed by one-way ANOVA with Dunnett's multiple comparison post hoc test, were significant (*$p<0.05$, **$p<0.01$, ***$p<0.001$ or ****$p<0.0001$). Dunnett's test was performed by comparing treatment groups against the isotype control. ns, not significant. **Fig. 22D** shows a correlation curve of body weight change vs viral titer at 5 dpi. A strong negative correlation ($r = -0.9436$, $p<0.0001$) between body weight change and lung viral titer was observed.

**[0081]** **Figure 23** shows immunohistochemical demonstration of SARS-CoV-2 nucleocapsid (N) protein in the lungs of $V_HH$-Fcs-treated animals. Untreated (PBS) and A20.1 isotype-treated animals showed strong viral N protein immunoreactivity which was mainly found in large multifocal patches of consolidated areas. Black arrow indicates the presence of viral N protein in bronchiolar epithelial cells. Omission of anti-nucleocapsid antibody eliminated the staining (Negative). Shown also is the absence of staining in healthy animals (Naïve). A marked reduction in viral N protein staining was seen in all lung tissues examined from $V_HH$-Fc-treated animals (middle and bottom panels). While no staining was observed in 05, MRed05, 1d/SR01 and 1d/MRed05, small foci of viral N protein was detected in $V_HH$-72, 1d, SR01 and S2A3. Representative images are shown from a single experiment.

**[0082]** **Figure 24** shows immunohistochemical detection of infiltrating macrophages in the lungs of $V_HH$-Fc-treated animals. Untreated (PBS) and A20.1 isotype-treated animals showed an intense immune reaction to anti-Iba-1 antibody and an increased number of Iba-1-positive macrophagesin the consolidated areas. A substantial reduction in the number of Iba-1-positive macrophages was seen in the perivascular areas and pulmonary interstitium in the lungs of $V_HH$-Fc-treated animals. Representative images are shown from a single experiment.

**[0083]** **Figure 25** shows immunohistochemical detection of T lymphocytes in the lungs of $V_HH$-Fc-treated animals. Untreated (PBS) and A20.1 isotype-treated animals showed an increased number of T lymphocytes in the pulmonary interstitium. A dramatic decrease in the number of T lymphocytes was seen in the lungs of $V_HH$-Fc-treated animals. Representative images are shown from a single experiment.

**[0084]** **Figure 26** shows immunohistochemical detection of apoptotic cells in the lungs of $V_HH$-Fc-treated animals. Untreated (PBS) and A20.1 isotype-treated animals showed an increase in the number of TUNEL-positive cells with classical features of apoptotic cells in the pulmonary interstitium. The large grey frame in the corner of PBS panel shows the magnification of the region (small grey frame) in the lung parenchyma, scale bar = 50 µm. A marked reduction in the TUNEL-positive cells was seen in the lungs of NRCoV2-05- and NRCoV2-MRed05-treated animals. Black arrows indicate occasional TUNEL-positive cells. Representative images are shown from a single experiment.

**[0085]** **Figure 27** shows on-/off-rate maps summarizing $V_HH$ kinetic rate constants, kas and kds determined by SPR for the binding of $V_HH$s to SARS-CoV S.

**[0086]** **Figures 28A** and **28B** show on-/off-rate maps summarizing $V_HH$ kinetic rate constants, kas and kds determined by SPR for the binding of $V_HH$s to SARS-CoV-2 Alpha S (**Fig. 28A**) and SARS-CoV-2 Beta S (**Fig. 28B**).

**[0087]** **Figure 29** shows representative SPR sensorgrams showing single-cycle kinetics analysis of NRCoV2-02, NRCoV2-15 and NRCoV2-MRed05 binding to Wuhan, Alpha and Beta S (NRCoV2-02, NRCoV2-15) and RBD (NRCoV2-MRed05).

**[0088]** **Figure 30** shows a summary of $IC_{50}$s obtained by live virus neutralization assays (LVNAs) for $V_HH$-Fcs against Wuhan, Alpha, and Beta SARS-CoV-2 variants. The epitope bin numbers provided in **Fig. 30** correspond to the bins shown in **Fig. 9G**.

**[0089]** **Figures 31A, 31B, 31C,** and **31D** show results from live virus neutralization assays assessing the ability of SARS-CoV-2 $V_HH$-Fcs in blocking the infection of ACE2-expressing Vero E6 cells by SARS-CoV-2 Alpha (**Fig. 31A** and **Fig. 31C**) and Beta (**Fig. 31B** and **Fig. 31D**) variants at fixed (**Fig. 31A** and **Fig. 31B**) or varying (**Fig. 31C** and **Fig. 31D**) $V_HH$-Fc

concentrations. Inhibition assays shown in **Fig. 31A** and **Fig. 31B** were performed at 312, 12.5 or 0.5 nM $V_HH$-Fc concentrations. $IC_{50}$s calculated from graphs in **Fig. 31C** and **Fig. 31D** are recorded in Table 19. $V_HH$-72 and *C. difficile* toxin A-specific $V_HH$ A20.1 are included as a benchmark and negative antibody control, respectively. The epitope bin numbers provided in **Figs. 31C** and **31D** correspond to the bins shown in **Fig. 9G**.

**[0090]** **Figure 32** shows in vivo stability and persistence of $V_HH$s. Stability and persistence were determined by monitoring the concentration of a representative $V_HH$-Fc (NRCoV2-1d) in hamster blood at various days post-injection by ELISA. $V_HH$-72 $V_HH$-Fc was used as the benchmark.

DETAILED DESCRIPTION

**[0091]** The following is a detailed description provided to aid those skilled in the art in practicing the present disclosure. Unless otherwise defined, all technical and scientific terms used herein have the same meaning as commonly understood by one of ordinary skill in the art to which this disclosure belongs. The terminology used in the description herein is for describing particular embodiments only and is not intended to be limiting of the disclosure.

**[0092]** Terms defined below may have the meanings ascribed to them, unless specified otherwise. However, it should be understood that other meanings that are known or understood by those having ordinary skill in the art are also possible, and within the scope of the present disclosure. In the case of conflict, the present specification, including definitions, will control. In addition, the materials, methods, and examples are illustrative only and not intended to be limiting.

**Definitions**

**[0093]** The "coronavirus spike polypeptide" or "coronavirus spike protein" (S) is the major coronavirus surface protein, and is a glycosylated homotrimer that binds to a host cell receptor and mediates coronavirus entry into a host cell. The coronavirus may be SARS-CoV-2, SARS-CoV, or another coronavirus. "SARS-CoV-2" may be used herein to refer to any strain or variant of the SARS-CoV-2 virus. Similarly, "SARS-CoV" may be used to refer to any strain or variant of the SARS-CoV virus. A SARS-CoV-2 variant is a strain of SARS-CoV-2 that comprises one or more mutations relative to the Wuhan strain of SARS-CoV-2. A variant may be, but need not be, a

variant that has been designated as a variant of concern or a variant of interest by the World Health Organization.

**[0094]** As used herein, the term "polypeptide" refers to a molecule comprising two or more amino acid residues linked by peptide bonds. A polypeptide may have primary, secondary, and/or tertiary structure. A "protein" comprises at least one polypeptide and may have primary, secondary, tertiary, and/or quaternary structure. The terms "polypeptide" and "protein" are often used interchangeably, and a polypeptide may be comprised by a protein. For example, a protein may be a homo- or hetero-multimer that comprises two or more polypeptides, or a protein may comprise a single polypeptide. A polypeptide or protein may include one or more post-translational modifications, such as, but not limited to, glycosylation, phosphorylation, lipidation, S-nitrosylation, N-acetylation, or methylation.

**[0095]** As used herein, the term "fragment", in the context of a polypeptide, refers to a portion of a polypeptide comprising a series of consecutive amino acid residues from a parent polypeptide. In a specific embodiment, the term "fragment" refers to an amino acid sequence of at least 5, at least 10, at least 15, at least 20, at least 25, at least 30, at least 35, at least 40, at least 45, or at least 50 consecutive amino acid residues from a parent polypeptide. In embodiments, a fragment may comprise an epitope or binding domain from a parent polypeptide. In embodiments, a fragment may be a biologically active fragment that retains one or more functional characteristics of a parent polypeptide.

**[0096]** The term "antibody", as used herein, refers to an antigen binding protein comprising at least a heavy chain variable region ($V_H$) that binds a target epitope. The term antibody includes monoclonal antibodies comprising immunoglobulin heavy and light chain molecules, single heavy chain variable domain antibodies, and variants and derivatives thereof, including chimeric variants of monoclonal and single heavy chain variable domain antibodies. The antibody may be a naturally-occurring antibody, it may be obtained by manipulation of a naturally-occurring antibody, or it may be produced using recombinant methods. For example, an antibody may include, but is not limited to a Fv, single-chain Fv (scFv; a molecule consisting of $V_L$ and $V_H$ connected with a peptide linker), Fab, F(ab')2, single domain antibody (sdAb; an antibody composed of a single $V_L$ or $V_H$), or a multivalent presentation of any of these. Antibodies such as

those just described may require linker sequences, disulfide bonds, or other types of covalent bond to link different portions of the antibody. Those of skill in the art will be familiar with the requirements of the different types of antibodies and various approaches for their construction.

**[0097]** In a non-limiting example, the antibody may be a single domain antibody derived from a naturally- occurring source. Heavy chain antibodies of camelid origin (Hamers-Casterman et al, 1993) lack light chains and thus their antigen binding sites consist of one domain, termed $V_HH$. sdAbs have also been observed in shark and are termed VNAR (Nuttall et al, 2003). Other sdAbs may be engineered based on human Ig heavy and light chain sequences (Jespers et al, 2004; To et al, 2005). As used herein, the term "single domain antibody" includes single domain antibodies directly isolated from $V_H$, $V_HH$, $V_L$, or VNAR reservoir of any origin through phage display or other technologies, single domain antibodies derived from the aforementioned single domain antibodies, recombinantly produced single domain antibodies, as well as single domain antibodies generated through further modification of such single domain antibodies by humanization, affinity maturation, stabilization, solubilization, camelization, or other methods of antibody engineering. Also encompassed by the disclosure are homologues, derivatives, or fragments that retain the antigen-binding function and specificity of the single domain antibody.

**[0098]** Single domain antibodies possess desirable properties for antibody molecules, such as high thermostability, high detergent resistance, relatively high resistance to proteases (Dumoulin et al, 2002) and high production yield (Arbabi-Ghahroudi et al, 1997). They can also be engineered to have very high affinity by isolation from an immune library (Li et al, 2009) or by in vitro affinity maturation (Davies & Riechmann, 1996). Further modifications to increase stability, such as the introduction of non-canonical disulfide bonds (Hussack et al, 2011; Kim et al, 2012), may also be brought to a single domain antibody.

**[0099]** A person of skill in the art would be well-acquainted with the structure of a single-domain antibody. A single domain antibody comprises a single immunoglobulin domain that retains the immunoglobulin fold; most notably, only three CDR/hypervariable loops form the antigen-binding site. However, and as would be understood by one of skill in the art, not all CDRs may be required for binding the antigen. For example, and without wishing to be limiting, one, two, or three of the CDRs may contribute to binding and recognition of the antigen by a single domain antibody. The

CDRs of the single domain antibody or variable domain are referred to herein as CDR1, CDR2, and CDR3, and numbered as defined by Lefranc et al., 2003.

**[00100]** As described herein, the amino acid sequence and structure of a heavy chain variable domain, including a $V_HH$, can be considered—without however being limited thereto—to be comprised of four framework regions or 'FR', which are referred to in the art and herein as 'Framework region 1' or 'FR1'; as 'Framework region 2' or 'FR2'; as 'Framework region 3' or 'FR3'; and as 'Framework region 4' or 'FR4', respectively; which framework regions are interrupted by three complementarity determining regions or 'CDR's', which are referred to in the art as 'Complementarity Determining Region 1' or 'CDR1'; as 'Complementarity Determining Region 2' or 'CDR2'; and as 'Complementarity Determining Region 3' or 'CDR3', respectively. CDRs described in the present disclosure have been defined using the IMGT numbering system (Lefranc et al, 2003).

**[00101]** The term "binding" as used herein in the context of binding between an antibody, such as a $V_HH$, and a coronavirus spike protein epitope as a target, refers to the process of a non-covalent interaction between molecules. Preferably, said binding is specific. The terms 'specific' or 'specificity' or grammatical variations thereof refer to the number of different types of antigens or their epitopes to which a particular antibody such as a $V_HH$ can bind. The specificity of an antibody, also referred to as "specific binding", can be determined based on affinity. A specific antibody preferably has a binding affinity (Kd) for its epitope of less than $10^{-7}$ M, preferably less than $10^{-8}$ M.

**[00102]** The term "affinity", as used herein, refers to the strength of a binding reaction between a binding domain of an antibody and an epitope. It is the sum of the attractive and repulsive forces operating between the binding domain and the epitope. The term "affinity", as used herein, refers to the equilibrium dissociation constant, Kd.

**[00103]** The term "epitope" or "antigenic determinant", as used herein, refers to a part of an antigen that is recognized by an antibody. The term epitope includes linear epitopes and conformational epitopes. A linear epitope is an epitope that is recognized by an antibody based on its primary structure, and a stretch of contiguous amino acids is sufficient for binding. A

conformational epitope is based on 3-D surface features and shape and/or tertiary structure of the antigen.

**[00104]** The term “neutralizing antibody”, as used herein, refers to an antibody that, when bound to an epitope, interferes with at least one of the steps leading to the release of a virus genome, such as a coronavirus genome, into a host cell.

**[00105]** The term “subject”, as used herein, refers to an animal that is susceptible to infection by a coronavirus. The subject may be an animal that is susceptible to infection by a coronavirus that binds an ACE2 receptor, such as SARS-CoV-2 or SARS-CoV. The subject may be a human or non-human animal. Preferably the subject is a human or non-human mammal. Correspondingly, the ACE2 receptor may be a human ACE2 receptor or an animal ACE2 receptor.

**[00106]** The term “administering”, as used herein, refers to the introduction into a subject of a therapeutic agent. Many administration routes are known in the art, and include, but are not limited to, parenteral (intravenous, intramuscular, and subcutaneous), oral, nasal, ocular, transmucosal (buccal, vaginal, and rectal), transdermal, and pulmonary administration.

**[00107]** The terms “strong interaction” and “strong binding”, as used herein, refer to the presence of salt bridges and cation-pi interactions between amino acid residues, as is known to the skilled person.

**[00108]** The terms “weak interaction” and “weak binding”, as used herein, refer to the presence of hydrogen bonds and non-bonded/hydrophobic interactions, as is known to the skilled person.

**[00109]** The term "purified," as used herein, refers to a molecule, e.g. a polypeptide or protein that has been identified and substantially separated and/or recovered from the components of its natural environment. The term “isolated antibody”, as used herein, refers to an antibody that is substantially freed from other antibody molecules having different antigenic specificities. Further, a purified or isolated antibody may be substantially free of one or more other cellular and/or chemical substances. Absolute purity is not required for a molecule to be considered purified or isolated.

**[00110]** The term "pharmaceutically acceptable", as used herein, means generally regarded as safe when administered to humans. Preferably, as used herein, the term "pharmaceutically acceptable" is approved by a federal or state government regulatory agency for use in animals, more preferably in humans. The term "carrier" means a diluent, adjuvant, excipient, or vehicle with which a compound is formulated and/or administered. Such pharmaceutical carriers can be water and sterile liquids, such as petroleum, animal, vegetable or synthetically derived oils such as peanut oil, soybean oil, mineral oil, sesame oil. Water or saline solutions and aqueous dextrose and glycerol solutions are preferably used as carriers for injectable solutions. Suitable pharmaceutical carriers are, for example, described in "Remington (23rd edition), The Science and Practice of Pharmacy".

**[00111]** As used herein the term "linked" or "linkage" includes covalent and non-covalent linkage (bonding). As used herein, the term "linker" refers to a chemical group or molecule that can be used to join one molecule to another. An antibody may be linked to another molecule by a linker or an antibody may be directly linked (aka joined, fused, or bonded) to another molecule, without the use of a linker. Suitable linkers are known in the art and may be selected based on the chemical nature of the molecules being joined. Examples of linkers include peptide linkers and chemical cross-linkers. Peptide linkers may comprise a single amino acid residue or a plurality of amino acid residues. An antibody and a polypeptide may, for example, be linked by chemical conjugation, with or without the use of a linker, or produced as a fusion, for example by recombinant protein expression.

**[00112]** As used herein the term "label" refers to a molecule or compound that can be used to label a molecule, such as an antibody, to allow detection of the molecule. Suitable labels will be known to one skilled in the art and include, but are not limited to, radioisotopes; enzymes, such as horse radish peroxidase (HRP) or calf intestinal alkaline phosphate (AP); fluorophores; antigen binding fragments from cleaved antibodies (Fabs); and colloidal gold. Covalent linkage is commonly used to link a label to a molecule of interest, however, non-covalent linkage is also possible, for example, when the label is a Fab.

**[00113]** As used herein, the term "nucleic acid molecule" refers to any nucleic acid-containing molecule including, but not limited to, DNA, RNA, and DNA/RNA hybrids, in any form and/or

conformation. The term encompasses nucleic acids that include any of the known base analogs of DNA and RNA. For example, single-stranded, double-stranded, nuclear, extranuclear, extracellular, and isolated nucleic acids are all contemplated.

**[00114]** As used herein, the term "vector" refers to a synthetic nucleotide sequence used for manipulation of genetic material, including but not limited to cloning, subcloning, sequencing, or introduction of exogenous genetic material into cells, tissues or organisms. It is understood by one skilled in the art that vectors may contain synthetic DNA sequences, naturally occurring DNA sequences, or both. Examples of commonly used vectors include plasmids, viral vectors, cosmids, and artificial chromosomes.

**[00115]** As used herein, the term "regulatory sequence" includes promoters, enhancers and other expression control elements, such as polyadenylation sequences, matrix attachment sites, insulator regions for expression of multiple genes on a single construct, ribosome entry/attachment sites, introns that are able to enhance expression, and silencers. Promoters may be cell-specific or tissue-specific to facilitate expression in a desired target.

**[00116]** When referring to two nucleotide sequences, one being a regulatory sequence, the term "operably linked" is used herein to mean that the two sequences are associated in a manner that allows the regulatory sequence to affect expression of the other nucleotide sequence. It is not required that the operably-linked sequences be directly adjacent to one another with no intervening sequence(s).

**[00117]** As used herein, the term "host cell" refers to a cell into which a nucleic acid molecule or vector may be introduced, for example to allow for replication of the nucleic acid molecule or vector by the host cell and/or to allow for expression of the nucleic acid molecule, or of a nucleic acid molecule comprised by the vector, by the host cell to produce a product of interest, such as an RNA or protein. In a specific embodiment, the nucleic acid molecule may encode an antibody as described herein, and introduction of the nucleic acid molecule into the host cell may allow the antibody to be expressed by the host cell. A host cell may be any suitable cell, such as a bacterial cell or eukaryotic cell. Commonly used host cells include *E. coli*, yeast, and mammalian cells, such as, but not limited to, Chinese hamster ovary (CHO) cells, mouse myeloma cells, and human embryonic kidney (HEK) cells.

**[00118]** The term “treatment” and variations thereof, such as “treat” or “treating”, as used herein, refer to the administration of a therapeutic molecule or composition to a subject to reduce or eliminate one or more symptoms of an illness or disease in the subject and/or to reduce the duration of the illness or disease in the subject.

**[00119]** The term “prevention” and variations thereof, such as “prevent” or “preventing”, as used herein, refer to the prophylactic administration of a therapeutic molecule or composition to a subject to prevent the occurrence of, or to reduce the severity of, an illness or disease in the subject.

**[00120]** The term “sample” as used herein, refers to a sample in which a coronavirus presence is suspected or expected. For example, the sample may be a biological sample from a subject, such as, but not limited to, blood or a fraction thereof, saliva, cellular material, urine, or feces; a sample from a bioreactor; or an environmental sample.

**[00121]** The term "sequence identity" as used herein refers to the percentage of sequence identity between two amino acid sequences or two nucleic acid sequences. To determine the percent identity of two amino acid sequences or of two nucleic acid sequences, the sequences are aligned for optimal comparison purposes (e.g. gaps can be introduced in the sequence of a first amino acid or nucleic acid sequence for optimal alignment with a second amino acid or nucleic acid sequence). The amino acid residues or nucleotides at corresponding amino acid positions or nucleotide positions are then compared. When a position in the first sequence is occupied by the same amino acid residue or nucleotide as the corresponding position in the second sequence, then the molecules are identical at that position. The percent identity between the two sequences is a function of the number of identical positions shared by the sequences (i.e. % identity = (number of identical overlapping positions/total number of positions) x 100). In one embodiment, the two sequences are the same length. The determination of percent identity between two sequences can also be accomplished using a mathematical algorithm. One non-limiting example of a mathematical algorithm utilized for the comparison of two sequences is the algorithm of Karlin and Altschul, 1990, modified as in Karlin and Altschul, 1993. Such an algorithm is incorporated into the NBLAST and XBLAST programs of Altschul et al., 1990. BLAST nucleotide searches can be performed with the NBLAST nucleotide program parameters set, e.g. for score=100, wordlength=12 to obtain nucleotide sequences homologous to a nucleic acid molecules of the

present disclosure. BLAST protein searches can be performed with the XBLAST program parameters set, e.g. to score-50, wordlength=3 to obtain amino acid sequences homologous to a protein molecule of the present invention. To obtain gapped alignments for comparison purposes, Gapped BLAST can be utilized as described in Altschul et al., 1997. Alternatively, PSI-BLAST can be used to perform an iterated search which detects distant relationships between molecules. When utilizing BLAST, Gapped BLAST, and PSI-Blast programs, the default parameters of the respective programs (e.g. of XBLAST and NBLAST) can be used (see, e.g. the NCBI website). Another non-limiting example of a mathematical algorithm utilized for the comparison of sequences is the algorithm of Myers and Miller, 1988. Such an algorithm is incorporated in the ALIGN program (version 2.0) which is part of the GCG sequence alignment software package. When utilizing the ALIGN program for comparing amino acid sequences, a PAM120 weight residue table, a gap length penalty of 12, and a gap penalty of 4 can be used. The percent identity between two sequences can be determined using techniques similar to those described above, with or without allowing gaps. In calculating percent identity, typically only exact matches are counted.

**[00122]** As used herein the singular forms "a", "an", and "the" include plural references unless the context clearly dictates otherwise.

**[00123]** The phrase "and/or", as used herein, should be understood to mean "either or both" of the elements so conjoined, i.e., elements that are conjunctively present in some cases and disjunctively present in other cases. Multiple elements listed with "and/or" should be construed in the same fashion, i.e., "one or more" of the elements so conjoined. Other elements may optionally be present other than the elements specifically identified by the "and/or" clause, whether related or unrelated to those elements specifically identified.

**[00124]** As used herein in the specification and in the claims, "or" should be understood to have the same meaning as "and/or" as defined above. For example, when separating items in a list, "or" or "and/or" shall be interpreted as being inclusive, i.e., the inclusion of at least one, but also including more than one, of a number or list of elements, and, optionally, additional unlisted items. Only terms clearly indicated to the contrary, such as "only one of' or "exactly one of" or, when used in the claims, "consisting of" will refer to the inclusion of exactly one element of a number or list of elements. In general, the term "or" as used herein shall only be interpreted as indicating

exclusive alternatives (i.e., "one or the other but not both") when preceded by terms of exclusivity, such as "either," "one of," "only one of," or "exactly one of."

**[00125]** As used herein, all transitional phrases such as "comprising," "including," "carrying," "having," "containing," "involving," "holding," "composed of," and the like are to be understood to be open-ended, i.e., to mean including but not limited to. Only the transitional phrases "consisting of" and "consisting essentially of" shall be closed or semi-closed transitional phrases, respectively.

**[00126]** As used herein, the phrase "at least one," in reference to a list of one or more elements, should be understood to mean at least one element selected from any one or more of the elements in the list of elements, but not necessarily including at least one of each and every element specifically listed within the list of elements and not excluding any combinations of elements in the list of elements. This definition also allows that elements may optionally be present other than the elements specifically identified within the list of elements to which the phrase "at least one" refers, whether related or unrelated to those elements specifically identified.

**Description**

**[00127]** The present disclosure relates to SARS-CoV-2 spike protein-specific antibodies and uses thereof. Provided are isolated or purified antibodies comprising complementarity determining region (CDR) 1, CDR2, and CDR3 sequences as outlined in **Table 6**. The antibodies described herein recognize a variety of spike protein epitopes in different subunit and domains of the coronavirus spike protein, specifically S2, the N-terminal domain of S1 (S1-NTD), and the receptor binding domain of S1 (S1-RBD). Within these subunits/domains, antibodies described herein recognize several different epitopes. Because of this epitopic diversity, antibodies described herein may be used in combination, for example for combination therapy, or as bi-specific or multi-specific antibodies.

**[00128]** An antibody as described herein comprises an antigen binding portion of an antibody heavy chain, wherein the antigen binding portion comprises a first complementarity determining region (CDR1), a second complementarity determining region (CDR2), and a third complementarity determining region (CDR3), and wherein CDR1, CDR2, and CDR3,

respectively, comprise the amino acid sequence set forth in: SEQ ID NO: 1, SEQ ID NO: 45, and SEQ ID NO: 90; SEQ ID NO: 2, SEQ ID NO: 45, and SEQ ID NO: 91; SEQ ID NO: 1, SEQ ID NO: 46, and SEQ ID NO: 92; SEQ ID NO: 3, SEQ ID NO: 47, and SEQ ID NO: 93; SEQ ID NO: 4, SEQ ID NO: 48, and SEQ ID NO: 94; SEQ ID NO: 5, SEQ ID NO: 49, and SEQ ID NO: 95; SEQ ID NO: 6, SEQ ID NO: 50, and SEQ ID NO: 96; SEQ ID NO: 7, SEQ ID NO: 51, and SEQ ID NO: 97; SEQ ID NO: 8, SEQ ID NO: 52, and SEQ ID NO: 98; SEQ ID NO: 9, SEQ ID NO: 53, and SEQ ID NO: 99; SEQ ID NO: 10, SEQ ID NO: 54, and SEQ ID NO: 100; SEQ ID NO: 11, SEQ ID NO: 55, and SEQ ID NO: 101; SEQ ID NO: 12, SEQ ID NO: 56, and SEQ ID NO: 102; SEQ ID NO: 13, SEQ ID NO: 57, and SEQ ID NO: 103; SEQ ID NO: 14, SEQ ID NO: 58, and SEQ ID NO: 104; SEQ ID NO: 15, SEQ ID NO: 59, and SEQ ID NO: 105; SEQ ID NO: 16, SEQ ID NO: 60, and SEQ ID NO: 106; SEQ ID NO: 17, SEQ ID NO: 61, and SEQ ID NO: 107; SEQ ID NO: 18, SEQ ID NO: 62, and SEQ ID NO: 108; SEQ ID NO: 19, SEQ ID NO: 63, and SEQ ID NO: 109; SEQ ID NO: 20, SEQ ID NO: 64, and SEQ ID NO: 110; SEQ ID NO: 21, SEQ ID NO: 65, and SEQ ID NO: 111; SEQ ID NO: 22, SEQ ID NO: 66, and SEQ ID NO: 112; SEQ ID NO: 23, SEQ ID NO: 67, and SEQ ID NO: 113; SEQ ID NO: 24, SEQ ID NO: 68, and SEQ ID NO: 114; SEQ ID NO: 25, SEQ ID NO: 69, and SEQ ID NO: 115; SEQ ID NO: 26, SEQ ID NO: 70, and SEQ ID NO: 116; SEQ ID NO: 27, SEQ ID NO: 71, and SEQ ID NO: 117; SEQ ID NO: 28, SEQ ID NO: 72, and SEQ ID NO: 118; SEQ ID NO: 29, SEQ ID NO: 73, and SEQ ID NO: 119; SEQ ID NO: 30, SEQ ID NO: 74, and SEQ ID NO: 120; SEQ ID NO: 31, SEQ ID NO: 75, and SEQ ID NO: 121; SEQ ID NO: 32, SEQ ID NO: 76, and SEQ ID NO: 122; SEQ ID NO: 33, SEQ ID NO: 77, and SEQ ID NO: 123; SEQ ID NO: 34, SEQ ID NO: 78, and SEQ ID NO: 124; SEQ ID NO: 35, SEQ ID NO: 79, and SEQ ID NO: 125; SEQ ID NO: 36, SEQ ID NO: 80, and SEQ ID NO: 125; SEQ ID NO: 20, SEQ ID NO: 81, and SEQ ID NO: 126; SEQ ID NO: 20, SEQ ID NO: 81, and SEQ ID NO: 127; SEQ ID NO: 37, SEQ ID NO: 82, and SEQ ID NO: 128; SEQ ID NO: 38, SEQ ID NO: 83, and SEQ ID NO: 129; SEQ ID NO: 39, SEQ ID NO: 84, and SEQ ID NO: 130; SEQ ID NO: 40, SEQ ID NO: 85, and SEQ ID NO: 131; SEQ ID NO: 41, SEQ ID NO: 86, and SEQ ID NO: 132; SEQ ID NO: 42, SEQ ID NO: 87, and SEQ ID NO: 133; SEQ ID NO: 43, SEQ ID NO: 88, and SEQ ID NO: 134; or SEQ ID NO: 44, SEQ ID NO: 89, and SEQ ID NO: 135. In an embodiment, the antibody comprises the amino acid sequence set forth in SEQ ID NO: 183, 184, 185, or 186.

**[00129]** In an embodiment, an antibody as described herein comprises the amino acid sequence set forth in SEQ ID NO: 136, SEQ ID NO: 137, SEQ ID NO: 138, SEQ ID NO: 139, SEQ ID NO: 140, SEQ ID NO: 141, SEQ ID NO: 142, SEQ ID NO: 143, SEQ ID NO: 144, SEQ ID NO: 145, SEQ ID NO: 146, SEQ ID NO: 147, SEQ ID NO: 148, SEQ ID NO: 149, SEQ ID NO: 150, SEQ ID NO: 151, SEQ ID NO: 152, SEQ ID NO: 153, SEQ ID NO: 154, SEQ ID NO: 155, SEQ ID NO: 156, SEQ ID NO: 157, SEQ ID NO: 158, SEQ ID NO: 159, SEQ ID NO: 160, SEQ ID NO: 161, SEQ ID NO: 162, SEQ ID NO: 163, SEQ ID NO: 164, SEQ ID NO: 165, SEQ ID NO: 166, SEQ ID NO: 167, SEQ ID NO: 168, SEQ ID NO: 169, SEQ ID NO: 170, SEQ ID NO: 171, SEQ ID NO: 172, SEQ ID NO: 173, SEQ ID NO: 174, SEQ ID NO: 175, SEQ ID NO: 176, SEQ ID NO: 177, SEQ ID NO: 178, SEQ ID NO: 179, SEQ ID NO: 180, SEQ ID NO: 181, or SEQ ID NO: 182. In another embodiment, the antibody comprises an amino acid sequence having at least 75%, at least 80%, at least 85%, at least 90%, at least 95%, at least 96%, at least 97%, at least 98%, or at least 99% sequence identity to the full length of the amino acid sequence set forth in SEQ ID NO: 136, SEQ ID NO: 137, SEQ ID NO: 138, SEQ ID NO: 139, SEQ ID NO: 140, SEQ ID NO: 141, SEQ ID NO: 142, SEQ ID NO: 143, SEQ ID NO: 144, SEQ ID NO: 145, SEQ ID NO: 146, SEQ ID NO: 147, SEQ ID NO: 148, SEQ ID NO: 149, SEQ ID NO: 150, SEQ ID NO: 151, SEQ ID NO: 152, SEQ ID NO: 153, SEQ ID NO: 154, SEQ ID NO: 155, SEQ ID NO: 156, SEQ ID NO: 157, SEQ ID NO: 158, SEQ ID NO: 159, SEQ ID NO: 160, SEQ ID NO: 161, SEQ ID NO: 162, SEQ ID NO: 163, SEQ ID NO: 164, SEQ ID NO: 165, SEQ ID NO: 166, SEQ ID NO: 167, SEQ ID NO: 168, SEQ ID NO: 169, SEQ ID NO: 170, SEQ ID NO: 171, SEQ ID NO: 172, SEQ ID NO: 173, SEQ ID NO: 174, SEQ ID NO: 175, SEQ ID NO: 176, SEQ ID NO: 177, SEQ ID NO: 178, SEQ ID NO: 179, SEQ ID NO: 180, SEQ ID NO: 181, and/or SEQ ID NO: 182 and comprises CDR1, CDR2, and CDR3 sequences that, respectively, comprise the amino acid sequence set forth in: SEQ ID NO: 1, SEQ ID NO: 45, and SEQ ID NO: 90; SEQ ID NO: 2, SEQ ID NO: 45, and SEQ ID NO: 91; SEQ ID NO: 1, SEQ ID NO: 46, and SEQ ID NO: 92; SEQ ID NO: 3, SEQ ID NO: 47, and SEQ ID NO: 93; SEQ ID NO: 4, SEQ ID NO: 48, and SEQ ID NO: 94; SEQ ID NO: 5, SEQ ID NO: 49, and SEQ ID NO: 95; SEQ ID NO: 6, SEQ ID NO: 50, and SEQ ID NO: 96; SEQ ID NO: 7, SEQ ID NO: 51, and SEQ ID NO: 97; SEQ ID NO: 8, SEQ ID NO: 52, and SEQ ID NO: 98; SEQ ID NO: 9, SEQ ID NO: 53, and SEQ ID NO: 99; SEQ ID NO: 10, SEQ ID NO: 54, and SEQ ID NO: 100; SEQ ID NO: 11, SEQ ID NO: 55, and SEQ ID NO: 101; SEQ ID NO: 12, SEQ ID NO: 56, and SEQ ID NO: 102; SEQ ID NO: 13, SEQ ID NO: 57,

and SEQ ID NO: 103; SEQ ID NO: 14, SEQ ID NO: 58, and SEQ ID NO: 104; SEQ ID NO: 15, SEQ ID NO: 59, and SEQ ID NO: 105; SEQ ID NO: 16, SEQ ID NO: 60, and SEQ ID NO: 106; SEQ ID NO: 17, SEQ ID NO: 61, and SEQ ID NO: 107; SEQ ID NO: 18, SEQ ID NO: 62, and SEQ ID NO: 108; SEQ ID NO: 19, SEQ ID NO: 63, and SEQ ID NO: 109; SEQ ID NO: 20, SEQ ID NO: 64, and SEQ ID NO: 110; SEQ ID NO: 21, SEQ ID NO: 65, and SEQ ID NO: 111; SEQ ID NO: 22, SEQ ID NO: 66, and SEQ ID NO: 112; SEQ ID NO: 23, SEQ ID NO: 67, and SEQ ID NO: 113; SEQ ID NO: 24, SEQ ID NO: 68, and SEQ ID NO: 114; SEQ ID NO: 25, SEQ ID NO: 69, and SEQ ID NO: 115; SEQ ID NO: 26, SEQ ID NO: 70, and SEQ ID NO: 116; SEQ ID NO: 27, SEQ ID NO: 71, and SEQ ID NO: 117; SEQ ID NO: 28, SEQ ID NO: 72, and SEQ ID NO: 118; SEQ ID NO: 29, SEQ ID NO: 73, and SEQ ID NO: 119; SEQ ID NO: 30, SEQ ID NO: 74, and SEQ ID NO: 120; SEQ ID NO: 31, SEQ ID NO: 75, and SEQ ID NO: 121; SEQ ID NO: 32, SEQ ID NO: 76, and SEQ ID NO: 122; SEQ ID NO: 33, SEQ ID NO: 77, and SEQ ID NO: 123; SEQ ID NO: 34, SEQ ID NO: 78, and SEQ ID NO: 124; SEQ ID NO: 35, SEQ ID NO: 79, and SEQ ID NO: 125; SEQ ID NO: 36, SEQ ID NO: 80, and SEQ ID NO: 125; SEQ ID NO: 20, SEQ ID NO: 81, and SEQ ID NO: 126; SEQ ID NO: 20, SEQ ID NO: 81, and SEQ ID NO: 127; SEQ ID NO: 37, SEQ ID NO: 82, and SEQ ID NO: 128; SEQ ID NO: 38, SEQ ID NO: 83, and SEQ ID NO: 129; SEQ ID NO: 39, SEQ ID NO: 84, and SEQ ID NO: 130; SEQ ID NO: 40, SEQ ID NO: 85, and SEQ ID NO: 131; SEQ ID NO: 41, SEQ ID NO: 86, and SEQ ID NO: 132; SEQ ID NO: 42, SEQ ID NO: 87, and SEQ ID NO: 133; SEQ ID NO: 43, SEQ ID NO: 88, and SEQ ID NO: 134; or SEQ ID NO: 44, SEQ ID NO: 89, and SEQ ID NO: 135.

**[00130]** Another embodiment is a nucleic acid molecule encoding an antibody as described herein. A further embodiment is a vector comprising the nucleic acid molecule. Optionally, the nucleic acid molecule may be operably linked to at least one promoter and/or regulatory element to enable expression in a host cell. A further embodiment is a host cell comprising the nucleic acid or vector.

**[00131]** An antibody as described herein may be comprised within a composition. For example, the antibody may be comprised within a pharmaceutical composition that comprises a pharmaceutically acceptable carrier and/or diluent, the antibody may be linked to another molecule, or the antibody may be immobilized on a substrate. In an embodiment, the pharmaceutical composition may be for delivery by inhalation or nebulization.

**[00132]** Antibodies and compositions as described herein may be used, or for use, to treat or prevent a coronavirus infection, including an infection caused by at least one coronavirus that specifically binds an ACE2 receptor. Antibodies as described herein may also be used in the manufacture of a medicament for prevention or treatment of a coronavirus infection. In a specific embodiment, the at least one coronavirus is SARS-CoV-2 and/or SARS-CoV. Further provided is a method for prevention or treatment of a coronavirus infection comprising administering an antibody or composition as described herein to a subject in need thereof. In an embodiment, the administration is by inhalation or nebulization.

**[00133]** Antibodies and compositions as described herein may also be used, or for use, to detect, quantify, and/or capture a coronavirus, a coronavirus spike polypeptide or a coronavirus spike polypeptide fragment. Further provided are methods for detecting, quantifying, and/or capturing a coronavirus, a coronavirus spike polypeptide or a coronavirus spike polypeptide fragment using an antibody or composition as described herein. In an embodiment, the coronavirus or spike polypeptide is a coronavirus or spike polypeptide that specifically binds an ACE2 receptor. The ACE2 receptor may be a human ACE2 receptor or an animal ACE2 receptor. In a specific embodiment, the coronavirus is SARS-CoV-2 or SARS-CoV, or the spike polypeptide or fragment thereof is from SARS-CoV-2 or SARS-CoV

**[00134]** Several of the antibodies described herein have the characteristics of neutralizing antibodies, and some have been demonstrated to be cross-reactive with the spike protein of other coronaviruses, such as SARS-CoV and related coronaviruses that infect bats, pangolin, and civet, suggesting that antibodies described herein may be useful for binding the spike protein of more than one coronavirus; including coronaviruses that bind an ACE2 receptor, such as SARS-CoV-2 and SARS-CoV. Antibodies described herein have also been demonstrated to bind various SARS-CoV-2 spike protein variants, such as the Wuhan-Hu-1 variant that was first identified in China; the B.1.1.7 variant that was first identified in the United Kingdom (also referred to herein as the UK variant, or the Alpha variant); the B.1.352 variant that was first identified in South Africa (also referred to herein as the South Africa variant, or the Beta variant), the B.1.617.1 variant that was first detected in India (also referred to herein as Kappa); the B.1.617.2 variant that was first detected in India (also referred to herein as Delta); and the B.1.1.529 variant that was first detected in South Africa (also referred to herein as Omicron).

**[00135]** Antibodies described herein may be linked to another molecule or substrate. For example, they may be linked to a detectable label to allow detection, quantification, and/or visualization; they may be linked to a molecule that extends antibody half-life, such as polyethylene glycol (PEG), Ig Fc, serum albumin, serum-albumin-specific antibody, serum-albumin-specific peptide, or Fc-specific peptides, proteins or antibodies; they may be linked to a therapeutic molecule; they may be immobilized onto a substrate, such as a plastic surface, a magnetic bead or a protein sheet or bead; and/or they may be linked to a polypeptide. In a specific embodiment, antibodies described herein may be linked to an ACE2 polypeptide or a fragment thereof.

**[00136]** Antibodies described herein may also be employed in various formats and combinations. For example, antibodies described herein may be monoparatropic or multiparatropic (including biparatropic), or monospecific or multispecific (including bispecific). Antibodies described herein may be in a monovalent format or in a multivalent format (including a bivalent format). Antibodies described herein that are specific for the same or different epitopes, or for the same or different spike protein subunit or domains, may be linked, for example to produce antibodies with different affinities and/or specificities. Further, antibodies described herein may be linked to one or more other antibodies or antibody fragments. In addition, antibodies described herein may be used individually or in combination. A combination may comprise any two or more antibodies described herein, or it may comprise at least one antibody described herein and another antibody. In some embodiments, the antibodies are $V_HH$ antibodies or $V_HH$-Fc antibodies.

**[00137]** Antibodies described herein may be useful for a variety of applications. For example, they may be useful for detecting the presence of a coronavirus or a coronavirus spike polypeptide or fragment thereof; for capturing a coronavirus or a coronavirus spike polypeptide or fragment thereof; for quantifying the amount of a coronavirus or a coronavirus spike polypeptide or fragment thereof in a sample; for treatment or prevention of a coronavirus infection; for diagnosing a coronavirus infection; for monitoring the production of a coronavirus spike protein or fragment thereof; for purification of a coronavirus spike protein or fragment thereof; for detecting the level of expression of a coronavirus spike protein or fragment thereof, and/or for quantifying the amount of a coronavirus. Antibodies described herein have been shown to be stable against aerosolization, indicating that they may be suitable for delivery to the lungs by inhalation or nebulization. Further,

cross-reactive antibodies may have general applicability for the treatment, prevention, detection, quantification or capture of coronaviruses, in addition to SARS-CoV-2, or coronavirus spike polypeptides or fragments thereof from coronaviruses in addition to SARS-CoV-2. In specific embodiments, cross-reactive antibodies may be used to bind coronaviruses or coronavirus spike polypeptides that bind an ACE2 receptor, including fragments of such coronavirus spike polypeptides.

**[00138]** Antibodies described herein may be classified based on the spike protein subunit or domain to which they bind. Nine antibodies were generated that bind to the S1-NTD domain, 24 antibodies were generated that bind to the S1-RBD domain, and 14 antibodies were generated that bind to the S2 subunit (see Tables 5 and 6). Neutralization assays, as described in the Examples, identified antibodies with neutralizing properties within each of these three groups. To the inventors' knowledge, this is the first known observation of single domain antibodies neutralizing the SARS-CoV-2 virus by targeting a non-S1-RBD region of S, i.e., S1-NTD or S2.

**[00139]** Within the three groups of antibodies identified above, further classification is possible based on epitope specificity, which was determined by epitope binning experiments (see Example 7). Preliminary results showed that antibodies binding to S1-NTD may be grouped into three epitope bins; antibodies binding S1-RBD may be grouped into six epitope bins, with some overlap between bins; and antibodies binding S2 may be grouped into five epitope bins (**Fig. 9F**). Further characterization identified additional epitope bins, so that antibodies binding to S1-NTD may be grouped into four epitope bins; antibodies binding S1-RBD may be grouped into six epitope bins, with some overlap between bins; and antibodies binding S2 may be grouped into seven epitope bins (**Fig. 9G**).

**[00140]** Antibodies described herein may also be classified based on their pattern of cross-reactivity with different coronavirus spike proteins and/or spike protein variants, as shown in **Figures 6A** and **6B**. Antibodies that recognize the same set of spike proteins and/or spike protein variants may be viewed as a single group.

**[00141]** As demonstrated in the Examples, several of the antibodies described herein have substantially increased binding affinity in comparison to a benchmark $V_HH$ spike protein antibody, $V_HH$-72 (Wrapp et al., 2020). Further, many of the antibodies described herein are demonstrated

to outperform $V_HH$-72 in neutralization assays, and some are demonstrated to be more broadly neutralizing than $V_HH$-72. Additionally, some antibodies described herein are demonstrated to be more broadly cross-reactive than $V_HH$-72.

**[00142]** The antibodies described in the following examples may be modified, while still retaining antigen specificity. For example, changes may be introduced into the amino acid sequence of the framework regions, or the antibodies may be humanized. The antibodies may also be linked to other molecule(s). Antibodies and compositions resulting from such modifications are contemplated and encompassed by the present disclosure.

**Examples**

**[00143]** The following non-limiting examples are illustrative of the present disclosure and/or outline studies conducted pertaining to the present disclosure.

**[00144]** Several coronavirus spike protein fragments (spike protein antigens) were used in the Examples described below. **Table 1** provides a list of spike protein fragments used in these studies.

**[00145] Table 1.** Coronavirus spike protein fragments used for library selection, binding and epitope study experiments

| Description | Accession number | Source | Tag | Reference describing expression & purification |
|---|---|---|---|---|
| S1 (aa16-685) (Wuhan) | QHD43416.1[b] | National Research Council of Canada (NRC) | FLAG, 6xHis | Akache et al., 2021 |
| S1 (aa16-685) (Wuhan) | QHD43416.1[b] | ACROBiosystems | AviTag, 6xHis | na |
| S1 (aa16-685) (Wuhan) | QHD43416.1[b] | ACROBiosystems | Human IgG1 Fc | na |
| NTD (aa16-305) (Wuhan) | QHD43416.1[b] | NRC | FLAG, 6xHis | Akache et al., 2021 |
| RBD/SD1 (aa319-591) (Wuhan) | QHD43416.1[b] | NRC | Human IgG1 Fc | Wrapp et al., 2020 |

| | | | | |
|---|---|---|---|---|
| RBD/SD1 (aa319-591) (Wuhan) | QHD43416.1[b] | NRC | 6xHis | Wrapp et al., 2020 |
| RBD_short (aa331-521) (Wuhan) | QHD43416.1[b] | NRC | 6xHis | Akache et al., 2021 |
| RBD (aa319-541) (Wuhan) | QHD43416.1[b] | NRC | FLAG-6xHis (N-term), E5 (C-term) | Akache et al., 2021 |
| RBD_α (aa319-541) (B.1.1.7) | QHD43416.1[b] | NRC | FLAG, 6xHis | Colwill et al., 2021 |
| RBD_β (aa319-541) (B.1.351) | QHD43416.1[b] | NRC | FLAG, 6xHis | Colwill et al., 2021 |
| RBD_Wuhan (aa319-541) | QHD43416.1[b] | ACROBiosystems | AviTag, 6xHis | na |
| RBD_SARS-CoV (aa306-527) | AAP13442.1[b] | NRC | FLAG, 6xHis | Sulea et al., 2022 |
| S2 (aa686-1208) (Wuhan) | QHD43416.1[b] | NRC | FLAG, 6xHis | Akache et al., 2021 |
| Swine deltaCoV S[a] | AIH06857.1[b] | NRC | FLAG-Dual Strep-6xHis | Galipeau et al., 2021 |
| Avian_IBV S[a] | AAP92675.1[b] | NRC | FLAG-Dual Strep-6xHis | Galipeau et al., 2021 |
| Pangolin CoV S[a] | QIA48632.1[b] | NRC | FLAG-Dual Strep-6xHis | Galipeau et al., 2021 |
| Hedgehog CoV HKU31 S[a] | QGA70702.0[b] | NRC | FLAG-Dual Strep-6xHis | Galipeau et al., 2021 |
| Bat CoV HKU9 S[a] | YP_001039971.1[c] | NRC | FLAG-Dual Strep-6xHis | Galipeau et al., 2021 |
| Bat SARS like CoV-WIV1 S[a] | AGZ48828.1[b] | NRC | FLAG-Dual Strep-6xHis | Galipeau et al., 2021 |
| Bat 229E-related CoV S[a] | APD51507.1[b] | NRC | FLAG-Dual Strep-6xHis | Galipeau et al., 2021 |
| Bat CoV 512 S[a] | YP_001351684.1[c] | NRC | FLAG-Dual Strep-6xHis | Galipeau et al., 2021 |
| Bat SARS like CoV[a] | ATO98157.1[b] | NRC | FLAG-Dual Strep-6xHis | Galipeau et al., 2021 |

| | | | | |
|---|---|---|---|---|
| Civet SARS-CoV[1] S[a] | AAU04646.1[b] | NRC | FLAG-Dual Strep-6xHis | Galipeau et al., 2021 |
| Human MERS-CoV S[a] | AGH58717.1[b] | NRC | FLAG-Dual Strep-6xHis | Galipeau et al., 2021 |
| Human CoV-NL63 S | APF29071.1[b] | Sino Biological | 6xHis | na |
| Human CoV-OC43 S[a] | AGT51431.1[b] | NRC | FLAG-Dual Strep-6xHis | Galipeau et al., 2021 |
| Human CoV-HKU1 S | Q0ZME7.1[d] | Sino Biological | 6xHis | na |
| Human CoV-229E S[a] | AAK32191.1[b] | Sino Biological | 6xHis | na |
| Human SARS-CoV S[a] | AAP13442.1[b] | NRC | FLAG-Dual Strep-6xHis | Galipeau et al., 2021 |
| Human SARS-CoV-2_Wuhan S[a] (SmT1) | QHD43416.1[b] | NRC | FLAG, 6xHis | Colwill et al., 2021 |
| Human SARS-CoV-2_α (B.1.351) S[a] | - | NRC | FLAG, 6xHis | Galipeau et al., 2021 |
| Human SARS-CoV-2_β (B. 1.1.7) S[a] | - | NRC | FLAG, 6xHis | Galipeau et al., 2021 |
| Human SARS-CoV-2_γ (P.1) S[a] | - | NRC | none | Galipeau et al., 2021 |
| Human SARS-CoV-2_Δ (B.1.617.2) S[a] | - | NRC | FLAG, 6xHis | Stuible et al., 2021 |
| Human SARS-CoV-2_κ (B.1.617.1) S[a] | - | NRC | FLAG, 6xHis | Stuible et al., 2021 |
| Human SARS-CoV-2_Omicron (B.1.1.529) S[a] | - | NRC | FLAG, 6xHis | Sulea et al., 2022 |
| Human ACE2 (aa18-740) | Q9BYF1-1[d] | ACROBiosystems | Human IgG1 Fc | na |
| Human ACE2 (aa18-615) | Q9BYF1-1[d] | NRC | 6xHis | Wrapp et al., 2020 |

[a]Proteins are C-terminally fused to the resistin trimerization domain. [b]GenBank; [c]NCBI; [d]UniProt. na, not applicable

## Example 1: Antigen Validation

### *Introduction*

**[00146]** Prior to use in library selection (panning) experiments, four SARS-CoV-2 spike protein antigens (S, S1, S1-RBD, and S2, as described in **Table 1**) were validated for structural integrity and functionality in adsorbed/captured states on microtiter wells by standard ELISA. Unless stated otherwise, all spike protein fragments used in the following Examples were produced as described in Stuible et al., 2021.

***Materials and Methods***

**[00147]** *Binding to cognate human angiotensin converting enzyme (ACE2) receptor*

**[00148]** ELISA was performed to determine if spike proteins were able to bind to human ACE2 when passively adsorbed (S, S1, S1-RBD and S2) or captured (S1, S1-RBD) on microtiter wells. For passive adsorption, wells of NUNC® Immulon 4 HBX MaxiSorp™ microtiter plates (Thermo Fisher, Cat#3855) were coated with 50 ng of SARS-CoV-2 spike proteins (S, S1, S2, S1-RBD) in 100 µL PBS overnight at 4°C. Following removal of protein solutions and three washes with PBST (PBS supplemented with 0.05% [v/v] Tween® 20), wells were blocked with PBSC (1% [w/v] casein [SIGMA, Cat#E3414] in PBS) at room temperature for 1 h. For capturing, *in vivo* biotinylated fragments harboring the AviTag™ (AviTag-S1, AviTag-S1-RBD) were diluted in PBS and added at 50 ng/well (100 µL) to pre-blocked Streptavidin Coated High Capacity Strip wells (Thermo Fisher, Cat#15501). After 1 h incubation at room temperature, wells were washed five times with PBST and incubated for an additional hour with 100 µL/well of 2-fold serially diluted ACE2-Fc (human ACE2 fused to human IgG1 Fc domain; ACROBiosystems, Cat#AC2-H5257) in PBSTC (PBS/0.2% casein/0.1% Tween® 20). Wells were washed five times and incubated for 1 h with 1 µg/mL HRP-conjugated goat anti-human IgG (SIGMA, Cat#A0170). Wells were washed 10 times and incubated with 100 µL peroxidase substrate solution (SeraCare, Cat#50-76-00) at room temperature for 15 min. Reactions were stopped by adding 50 µL 1 M $H_2SO_4$ to wells, and absorbance were subsequently measured at 450 nm using a Multiskan™ FC photometer (Thermo Fisher).

**[00149]** *Binding to cognate anti-spike protein polyclonal antibody*

**[00150]** The four spike antigens were passively adsorbed as described above. After blocking with PBSC, wells were emptied, washed five times and incubated at room temperature for 1 h with 100

µL of 1 µg/mL anti-SARS-CoV-2 spike rabbit polyclonal antibody (Sino Biologicals, Cat#40589-T62) in PBSCT. Following 10 washes with PBST, wells were incubated with 100 µL 1/2500 dilution (320 ng/mL) of goat anti-rabbit:HRP (Jackson Immunoresearch, Cat#111-035-144) in PBSCT for 1 h at room temperature. After 1 h incubation and final five washes with PBST, the peroxidase activity was determined as described above.

***Results and Discussion***

**[00151]** The passively adsorbed spike fragments, S, S1, S1-RBD, as well as the streptavidin-captured fragments, AviTag-S1-RBD and AviTag-S1, were found to bind to ACE2 with similarly high affinities ($EC_{50}$ = 0.10 – 0.32 nM; **Fig. 1A, Table 2**). As expected, the S2 subunit of the spike protein did not bind to ACE2. Additionally, as shown in **Fig. 1B** and **Table 3**, all four spike fragments in passively-adsorbed states (S, S1, S2, and S1-RBD), bound with high affinity ($EC_{50}$ = 0.34 – 0.65 nM) to a polyclonal antibody known to be specific for SARS-CoV-2 spike protein; confirming the structural integrity/identity of the spike protein fragments. The ELISA data demonstrate that the various spike fragments tested should maintain their natural and intact structures in passively-adsorbed and captured states during panning experiments.

**[00152] Table 2:** Binding affinity ($EC_{50}$) of passively absorbed spike fragments and streptavidin-captured spike fragments to ACE2

| **Antigen** | **S** | **S1** | **S2** | **S1-RBD** | **AviTag-S1-RBD** | **AviTag-S1** |
|---|---|---|---|---|---|---|
| ***EC*$_{50}$ (nM)** | 0.26 | 0.28 | nb | 0.32 | 0.10 | 0.28 |

"nb" indicates lack or no binding.

**[00153] Table 3:** Binding affinity ($EC_{50}$) of passively absorbed spike fragments to a polyclonal antibody known to be specific for SARS-CoV-2 spike protein

| **Antigen** | **S** | **S1** | **S2** | **S1-RBD** |
|---|---|---|---|---|
| ***EC*$_{50}$ (nM)** | 0.34 | 0.59 | 0.6 | 0.65 |

**Example 2: Llama Immunization and Serum Analyses**

***Introduction***

**[00154]** As described below, two llamas were immunized with SARS-CoV-2 S or S/S1-RBD to trigger the generation of a diverse pool of antibodies targeting manifold sites over the surface of S, and targeting the S1-RBD sub-domain of S which is used by the virus to start the process of host cell infection through interaction with the ACE2 receptor. Llama sera were assessed by ELISAs for generation of immune responses against SARS-CoV-2 spike proteins, and by flow cytometry surrogate neutralization assays for generation of neutralizing antibodies.

***Materials and Methods***

**[00155]** *Llama immunization*

**[00156]** Immunizations were performed at Cedarlane Laboratories (Burlington, ON, Canada) and essentially as described (Hussack et al., 2011). One llama (Eva Green) was immunized with 100 μg of S in 500 μL PBS combined with 500 μL of Freund's complete adjuvant on day 0, followed by immunization with 70 μg of S1-RBD (ACROBiosystems, Cat#SPD-S52H6) in Freund's incomplete adjuvant on each of days 7, 14, and 21. Bleeds were taken at days 0, 21, and 28. A second llama (Maple Red) was immunized with 100 μg of S in 500 μL PBS combined with 500 μL of Freund's complete adjuvant on day 0, followed by immunization with 100 μg of S mixed with Freund's incomplete adjuvant on day 7, and immunization with 50 μg of S mixed with Freund's incomplete adjuvant on each of days 14 and 21.

**[00157]** *Serum ELISA*

**[00158]** Llama sera were tested for antigen-specific immune response by ELISA essentially as described (Hussack et al., 2011; Henry et al., 2016). Briefly, dilutions of sera in PBST were added to wells pre-coated with S, S1, S2 or S1-RBD. Negative antigen control wells were pre-coated with casein (100 μL of 1% v/w) or recombinant human dipeptidase 1 ectodomain, DPEP1 (50 ng/well; Sino Biological, Cat#13543-H08H). Following 1 h incubation at room temperature, wells were washed 10 times with PBST and incubated with HRP-conjugated polyclonal goat anti-llama IgG heavy and light chain antibody (Bethyl, Cat#A160-100P) for 1 h at room temperature. After 10 washes, the peroxidase activity was determined as described above.

**[00159]** *Serum surrogate neutralization assay by flow cytometry*

**[00160]** Trimeric SARS-CoV-2 S was chemically biotinylated using EZ-Link™ NHS-LC-LC-Biotin following manufacturer's instructions (Thermo Fisher, Cat#21343). Vero E6 cells (ATCC, Cat#CRL-1586) were maintained according to ATCC protocols. Briefly, cells were grown to confluency in DMEM medium (Thermo Fisher, Cat#11965084) supplemented with 10% heat inactivated FBS (Thermo Fisher, Cat#10438034) and 2 mM Glutamax™ (Thermofisher, Cat#35050061) at 37°C in a humidified 5% $CO_2$ atmosphere in T75 flasks. For flow cytometry experiments, cells were harvested by Accutase™ (Thermo Fisher, Cat#A111050) treatment, washed once by centrifugation, and resuspended at $1 \times 10^6$ cells/mL in PBSB (PBS containing 1% BSA) and 0.05% [v/v] sodium azide [SIGMA, Cat#S2002]). Cells were kept on ice until use. To determine the presence of neutralizing antibodies in the immune sera of llamas, 400 ng of chemically biotinylated trimeric SARS-CoV-2 S was mixed with $5 \times 10^4$ Vero E6 cells in the presence of 2-fold dilutions of sera (pre immune, day 21 and day 28 serum) in a final volume of 150 µL. Following 1 h of incubation on ice, cells were washed twice with PBSB by centrifugation for 5 min at 1200 rpm and then incubated for an additional hour with 50 µL of Streptavidin, R-Phycoerythrin Conjugate (SAPE, ThermoFisher, Cat# S866) at 250 ng/mL diluted in PBSB. After a final wash, cells were resuspended in 100 µL PBSB and data were acquired on a CytoFLEX® S flow cytometer (Beckman Coulter, Brea, CA) and analyzed by FlowJo™ software (FlowJo LLC, v10.6.2, Ashland, OR). Percent inhibition (neutralization) was calculated according to the following formula: % inhibition = 100 x [1 - ($F_n$ - $F_{min}$) / ($F_{max}$ - $F_{min}$)], where, $F_n$ is the measured fluorescence at any given competitor serum dilution, $F_{min}$ is the baseline fluorescence measured in the presence of cells and SAPE only, and $F_{max}$ is the maximum fluorescence, measured in the absence of competitor serum.

***Results and Discussion***

**[00161]** The results of ELISAs performed with pre-immune (day 0) and immune (day 21 and 28) sera demonstrate that both llamas generated a strong immune response against target immunogens S, S1, S2 and S1-RBD (**Fig. 2A**). Based on $EC_{50}$ values, which indicate the strength of immune responses, Eva Green generated a stronger immune response, up to 10-fold stronger, than Maple Red consistently across all four spike fragments (**Fig. 2A**; **Table 4**). Further, the immune responses were specific for SARS-CoV-2 antigens, as sera from day 0, 21 and 28 did not react with casein or DPEP1. Interestingly, one initial injection of S was enough to develop a strong, maximum

immune response against S2 by Eva Green. Llama sera were also assessed by flow cytometry surrogate neutralization assays for generation of neutralizing antibodies, i.e., antibodies that block the interaction between the trimeric SARS-CoV-2 S and ACE2 displayed on the surface of Vero E6 cells. As shown in **Fig. 2B** and **Table 5**, inhibition serum titers of 3300 (Day 21) and 6200 (Day 28) reciprocal serum dilution (RSD) were obtained in the case of Eva Green sera whereas weaker inhibition serum titers, <200 (Day 21) and <400 RSD (Day 28), were obtained for Maple Red.

**[00162] Table 4.** ELISA results summarizing day 0, 21 and 28 binding serum titers ($EC_{50}$s) of Eva Green and Maple Red llamas against spike protein fragments S, S1, S2 and S1-RBD

| **Llama** | **Day** | **Binding serum titer, $EC_{50}$ (reciprocal serum dilution)** | | | |
|---|---|---|---|---|---|
| | | **S** | **S1** | **S2** | **S1-RBD** |
| **Eva Green** | 0 | - | - | - | - |
| | 21 | $1.0x10^6$ | $1.8x10^6$ | $0.3x10^6$ | $2.2x10^6$ |
| | 28 | $1.2x10^6$ | $1.8x10^6$ | $0.4x10^6$ | $2.0x10^6$ |
| **Maple Red** | 0 | - | - | - | - |
| | 21 | $0.2x10^6$ | $0.3x10^6$ | $0.1x10^6$ | $0.2x10^6$ |
| | 28 | $0.3x10^6$ | $0.3x10^6$ | $0.2x10^6$ | $0.3x10^6$ |

Dashes indicate lack of binding.

**[00163] Table 5.** Flow cytometry-based surrogate virus neutralization assay results summarizing day 21 and 28 inhibition serum titers ($IC_{50}$s) of Eva Green and Maple Red llamas using spike protein S as surrogate for the virus

| **Llama** | **Inhibition serum titer, $IC_{50}$ (reciprocal serum dilution)** | |
|---|---|---|
| | **Day 21** | **Day 28** |
| **Eva Green** | 3300 | 6200 |
| **Maple Red** | <200 | <400 |

**Example 3: Phage Display Library Construction, Selection and Screening**

***Introduction***

**[00164]** Two libraries (Eva Green and Maple Red) were constructed and subjected to selection against spike protein fragments. Selection and screening efforts were aimed at isolating not only S1-RBD binders, but also S1-NTD and S2 binders, as recent findings indicate that in addition to S1-RBD binders, S1-NTD and S2 binders could also be neutralizing (Rogers et al., 2020; Ravichandran et al., 2020). To this end, two libraries were generated and were selected under six different conditions to maximize the number and epitopic diversity of hits against S1-RBD, S1-NTD and S2. After two rounds of selection, monoclonal phages ELISA and DNA sequencing were performed to identify antigen-specific hits.

***Materials and Methods***

**[00165]** *Phage display library construction*

**[00166]** On day 28, 100 mL of blood from each of the two llamas was drawn and peripheral blood mononuclear cells (PBMCs) were purified by Ficoll® gradient at Cedarlane Laboratories (Burlington, ON, Canada). Two independent phage-displayed $V_H/V_HH$ libraries were constructed from ~$5 \times 10^7$ PBMCs as described previously (Henry et al., 2016; Rossotti et al., 2015; Henry et al., 2015). Total RNA was extracted from PBMCs using TRIzol™ Plus RNA Purification Kit (Thermo Fisher, Cat#12183555) following manufacturer's instructions and used to reverse transcribe cDNA with SuperScript™ IV VILO™ Master Mix supplemented with random hexamer (Thermofisher, Cat#SO142) and oligo (dT) (Thermofisher, Cat#AM5730G) primers. $V_H/V_HH$ genes were amplified using semi-nested PCR and cloned into the phagemid vector pMED1, followed by transformation of *E. coli* TG1 to construct two libraries with sizes of $1 \times 10^7$ and $2 \times 10^7$ independent transformants for Eva Green and Maple Red, respectively. Both libraries showed an insert rate of ~95%, as verified by DNA sequencing. Phage particles displaying the $V_HS/V_HHs$ were rescued from *E. coli* cell libraries using M13K07 helper phage (New England Biolabs, Cat#N0315S) as described in Hussack et al., 2011 and used for selection experiments described below.

**[00167]** *Library selection and screening*

**[00168]** Library selections (pannings) and screenings were performed essentially as described (Hussack et al., 2011; Rossotti et al., 2015). Library selections were performed on microtiter wells

under 6 different phage binding/elution conditions designated P1 – P6. Briefly, for the phage binding step, library phages were diluted at $1 \times 10^{11}$ colony-forming units (cfu)/mL in PBSBT [PBS supplemented with 1% [w/v] BSA and 0.05% Tween® 20] and incubated in antigen-coated microtiter wells for 2 h at 4°C. For P1 – P4, phages were added to wells with passively-adsorbed S (10 µg/well; P1), passively-adsorbed S2 (10 µg/well; P2), streptavidin-captured biotinylated S1 (0.5 µg/well; P3) and streptavidin-captured biotinylated S1-RBD (0.5 µg/well; P4). For P5, phages were pre-absorbed on passively-adsorbed S1-RBD wells (10 µg/well) for 1 h at 4°C and then the unbound phage in the solution was transferred to wells with streptavidin-captured biotinylated S1 (0.5 µg/well) in the presence of non-biotinylated S1-RBD competitor in solution (10 µg/well). Following the binding stage (P1 – P5), wells were washed 10 times with PBST and bound phages were eluted by treatment with 100 mM glycine pH 2.2 for 10 min at room temperature, followed by immediate neutralization of phages with 2 M Tris. Similar to P4, in P6, phages were bound on streptavidin-captured biotinylated S1-RBD but elution of bound phages were carried out competitively with 50 nM ACE2-Fc following the washing step. For all pannings, a small aliquot of eluted phage was used to determine their titer on LB-agar/ampicillin plates and the remaining were used for their subsequent amplification in *E.coli* TG1 strain (Hussack et al., 2011). The amplified phages were used as input for the next round of selection as described above.

**[00169]** After two rounds of selection, 16 (Eva Green) or 12 (Maple Red) colonies from each of the P1 – P6 selections were screened for antigen binding by monoclonal phage ELISA against S, S1, S2 and S1-RBD. Individual colonies from eluted-phage titer plates were grown in 96 deep well plates in 0.5 mL 2YT media/100 µg/mL-carbenicillin/1% (w/v) glucose at 37°C and 250 rpm to an $OD_{600}$ of 0.5. Then, $10^{10}$ cfu M13K07 helper phage was added to each well and incubation continued for another 30 min under the same conditions. Cells were subsequently pelleted by centrifugation, the supernatant was discarded and the bacterial pellets were resuspended in 500 µL 2YT/100 µg/mL carbencillin/50 µg/mL kanamycin and incubated overnight at 28°C. Next day, phage supernatants were recovered by centrifugation, diluted 3-fold in PBSTC and used in subsequent screening assays by ELISA. To this end, antigens were coated onto microtiter wells at 50 ng/well overnight at 4°C. Next day, plates were blocked with PBSC, washed five times with PBSTC, and 100 µL of phage supernatants prepared above were added to wells, followed by incubation for 1 h at room temperature in an orbital shaking platform. After 10 washes, binding of

phages was detected by adding 100 µL/well of anti-M13:HRP (Santa Cruz, Cat#SC-53004HRP) at 40 ng/mL in PBSTC and incubating as above. After 10 washes, the peroxidase activity was determined as described previously. Following confirmation of success of library panning as determined by monoclonal phages ELISA, a total of ≈1200 individual clones (≈100 clones per panning strategy; ≈600 clones per library) were colony-PCRed and subsequently sequenced, resulting in the identification of 35 (Eva Green) and 12 (Maple Red) potential spike-specific $V_HH$ antibodies.

***Results and Discussion***

**[00170]** Eva Green and Maple Red libraries were constructed with functional sizes (library sizes corrected for insert rate) of ~1 x $10^7$ and ~2 x $10^7$, respectively. Two rounds of selection under six different panning conditions (P1 – P6) were subsequently performed for both libraries. To confirm the success of selection in enriching for binders, samples of 12-16 clones per panning condition were tested for binding against S, S1, S2 and S1-RBD by phage ELISA. The frequent occurrence of positive clones determined by monoclonal phage ELISA confirmed selections efficiently enriched for binders. Specificity patterns observed, i.e., binding against S vs S1 vs. S2 vs S1-RBD, in sample sets reflected the selection strategy as well as the immunization strategy (Eva Green was immunized with S once but predominantly [three times] with S1-RBD). In P3, P4 and P6, as expected based on the selection strategy, essentially all binders were S1-RBD specific. For Maple Red, the immunization with the whole spike S generated a strong bias against non-S1-RBD-specific antibodies, an observation recently seen with patients recovered from SARS-CoV-2 natural infection (Rogers et al., 2020) and rabbits immunized with SARS-CoV-2 S (Ravichandran et al.. 2020). Panning against S (P1) essentially produced S2 binders as opposed to S1-RBD binders seen in the case of Eva Green library. Additionally, in contrast to what was observed in the case of the Eva Green, for the Maple Red P3 strategy, where panning was performed against S1, half of the binders tested were specific for non-S1-RBD region of S1. Nonetheless when selections were specifically directed towards S1-RBD binders, as in the P4 and P6 selection strategies, all tested binders were S1-RBD specific. Additionally, the P5 strategy almost exclusively selected for $V_HHs$ specific to non-RBD region of the S1 subunit. In summary, the immunization strategy was a key determinant of the outcome of *in vivo* generated $V_HHs$ with respect to spike subunit/domain specificity, and *in vitro* directed selection strategies effectively

yielded intended binding specificities. Subsequently, a larger number of clones, >600 clones per library, were screened by DNA sequencing to obtain a large pool of potential binders. The unique sequences were subjected to binding validation, as described below.

**Example 4: $V_HH$ Cloning/Expression in *E. coli*, Stability/Affinity Validation and Cross-Reactivity Studies**

***Introduction***

**[00171]** Hits identified by monoclonal phage ELISA and DNA sequencing were cloned into the expression vector pMRo.BAP.$H_6$ (Rossotti et al., 2019), produced as $His_6$-tagged $V_HHs$ in the periplasmic space of *E. coli* BL21(DE3) and purified by immobilized metal-ion affinity chromatography (IMAC). $V_HHs$ were subsequently validated for binding and further explored for cross-reactivity soluble ELISA against SARS-CoV-2, SARS-CoV and MERS-CoV spike proteins. Additionally, $V_HHs$ were validated for aggregation resistance by size exclusion chromatography (SEC) and thermostability by circular dichroism $T_m$ measurement assays. Lead $V_HHs$ were produced in mammalian cells in fusion with human IgG1 Fc and were subsequently tested in a comprehensive cross-reactivity ELISA against a collection of various coronavirus spike proteins (S).

***Materials and Methods***

**[00172]** *DNA sequence analysis and $V_HH$ production in E. coli*

**[00173]** Colonies were analyzed by DNA sequencing and identified $V_HH$ sequences were aligned using IMGT system. $V_HHs$ were subsequently cloned into pET expression vector (Novagen, Madison, WI) for their production in BL21(DE3) *E.coli* as monomeric soluble protein (Rosotti et al., 2019). Briefly, individual colonies were cultured overnight in 10 mL of LB supplemented with 50 µg/mL of kanamycin (LB/Kan) at 37°C and 250 rpm. After 16 h, cultures were added to 250 mL LB/Kan and grown to an $OD_{600}$ of 0.6. Expression of $V_HHs$ was induced with 10 µM of IPTG (isopropyl β-D-1-thiogalactopyranoside) overnight at 28°C and 250 rpm. The following day, bacterial pellets were harvested by centrifugation at 6,000 rpm for 15 min at 4°C and $V_H$/$V_HHs$ were extracted by sonication and purified by IMAC as described previously (Rosotti et al., 2019). In addition, for ELISA (see below), a small fraction was biotinylated by incubating 1 mg of

purified $V_HHs$ with 10 µM of ATP (Alfa Aesar, Cat#CAAAJ61125-09), 100 µM of D-(+)-biotin (VWR, Cat#97061-446) and a bacterial cell extract overexpressing *E.coli* BirA as described previously (Rossotti et al., 2015b). The same procedure was followed to produce a biotinylated $V_HH$-72 benchmark $V_HH$ (Wrapp et al., 2020), a SARS-CoV spike protein-specific $V_HH$ that cross-reacts with the SARS-CoV-2 spike protein receptor binding domain.

**[00174]** *$V_HH$ binding validation and preliminary cross-reactivity studies by ELISA*

**[00175]** Binding validation studies were performed with S1-RBD-specific clones. Briefly, microtiter well plates were coated with 50 ng/well SARS-CoV-2 S1-RBD in 100 µL PBS overnight at 4°C. Plates were blocked with PBSC for 1 h at room temperature, then washed five times with PBST and incubated with decreasing concentrations of biotinylated $V_HHs$. After 1 h incubation, plates were washed 10 times with PBST and binding of $V_HHs$ was probed using HRP-streptavidin (Jackson ImmunoResearch, Cat#016-030-084). Finally, plates were washed 10 times with PBST and peroxidase activity was determined as described above.

**[00176]** *Stability determinations by size exclusion chromatography (SEC) and circular dichroism*

**[00177]** Purified $V_HHs$ were subjected to SEC to validate their aggregation resistance. Briefly, 2 mg of each affinity purified $V_HH$ was injected into Superdex™ 75 GL column (Cytiva) connected to an ÄKTA FPLC protein purification system (Cytiva) as previously described (Henry et al., 2017). PBS was used as running buffer at 0.8 mL/min. Fractions corresponding to the monomeric peak were pooled and stored at 4°C until use. To determine thermostability, $V_HH$ $T_m$s were measured by circular dichroism as previously described (Henry et al., 2017). Ellipticity of $V_HHs$ were determined at 200 µg/mL $V_HH$ concentrations and 205 nm wavelength in 100 mM sodium phosphate buffer, pH 7.4. Ellipticity measurements were normalized to percentage scale and $T_m$s were determined from plot of % folded *vs* temperature and fitting the data to a Boltzmann distribution.

**[00178]** *Production of $V_HHs$ in mammalian cells in fusion with human IgG1 Fc*

**[00179]** Codon-optimized genes for bivalent $V_HH$-Fcs were synthesized (GenScript). For heterodimeric monovalent $V_HH$-Fcs, $V_HH$ genes were PCR amplified as described previously and cloned into pTT5-hIgG1Fc between the genes for human $V_H$ leader sequence and the human IgG1

hinge/Fc sequences, using NarI/HindIII restriction sites. Bivalent $V_HH$-Fcs were produced by transient transfection of HEK293-6E cells followed by protein A affinity chromatography as previously described (Rosotti et al., 2019). Heterodimeric monovalent $V_HH$-Fcs were produced by co-transfection of HEK293-6E cells with two pTT5 vectors, one encoding for a 6xHis-tagged heavy chain ($V_HH1$-hinge-$C_H2$-$C_H3$-$His_6$), the other for a non-tagged heavy chain of a different $V_HH$ ($V_HH2$-hinge-$C_H2$-$C_H3$). The heterodimeric antibodies were purified by sequential protein A affinity chromatography and IMAC. For IMAC, antibodies were eluted using a linear 0 - 0.5 M imidazole gradient over 20 column volumes to separate species bearing one 6×His tag (heterodimeric, monovalent) from those bearing two 6×His tags (homodimeric, bivalent). Proteins were buffer exchanged using Amicon® Ultra-15 Centrifugal Filter Units (Millipore, Cat#UFC905024) with phosphate-buffered saline (PBS), pH 7.4. The same procedure was applied for the generation of the reference bio-$V_HH$-72 and $V_HH$-72-Fc using the sequence published by Wrapp et al., 2020. The sequence of the $V_HH$ was ordered as GeneBlock (IDT DNA) flanked by SfiI sites for cloning into pMRo.BAP.H6, and NarI/HindIII for cloning into pTT5-hIgG1Fc. Protein purity was evaluated by SDS-PAGE using 4–20% Mini-PROTEAN® TGX Stain-Free™ Gels (Bio-Rad, Cat#17000435).

**[00180]** *$V_HH$-Fc comprehensive cross-reactivity studies by ELISA*

**[00181]** Recombinant coronavirus spike proteins S (**Table 1**) were coated overnight onto NUNC® MaxiSorp™ 4BX plates (Thermo Fisher) at 50 ng/well in 100 µL of PBS, pH 7.4. The next day, plates were blocked with 200 µL PBSC for 1 h at room temperature, then washed five times with PBST and incubated at room temperature for 1 h on rocking platform at 80 rpm with 1 µg/mL $V_HH$-Fc diluted in PBSTC. Plates were washed five times with PBSTC and binding of $V_HH$-Fcs was detected using 1 µg/mL HRP-conjugated goat anti-human IgG. Finally plates were washed five times and peroxidase (HRP) activity was measured as described above.

***Results and Discussion***

**[00182]** A total of ~1200 colonies were analyzed by DNA sequencing. Forty seven potential $V_HH$ binders were identified from the two libraries (35 from the Eva Green and 12 from the Maple Red library) by phage ELISA and DNA sequencing, with the vast majority (35 $V_HH$s) coming from the Eva Green library (**Tables 6** and **7**). Some $V_HH$s may be clonally related due to their high sequence

identity in their CDRs. Examples include NRCoV2-1a, NRCoV2-1c and NRCoV2-1d from the Eva Green library (**Table 6**) and NRCoV2-MRed02 and NRCoV2-MRed04 from the Maple Red library (**Table 7**). $V_HH$ hits were cloned in *E. coli,* confirmed by DNA sequencing, and expressed and purified by IMAC. Following expression of $V_HHs$, the binding of a sample set of $V_HHs$ was validated by ELISA. Affinities, expressed as $EC_{50}s$, were high, ranging from 0.4 to 7.2 nM (data not shown). $V_HHs$ were also tested for aggregation resistance and stability, and cross-reactivity.

**[00183]** Aggregation resistance and stability are desirable attributes of biotherapeutics, as they affect both efficacy and manufacturability. By size exclusion chromatography, all $V_HHs$ tested were found to be aggregation resistant (**Figs. 4A** and **4B**), except for NRCoV2-08, which showed some degree of aggregation The $V_HHs$ were also tested for thermal stability and found to be highly thermostable. With the exception of NRCoV2-11, which had a relatively lower $T_m$ of 60.4°C, the remaining 25 $V_HHs$ tested had $T_m$s higher than 65°C, with a $T_m$ range and median of 65.5 – 79.8°C and 70.4°C, respectively (**Figs. 5A** and **5B**). Many $V_HHs$ had $T_m$s that were higher than that of the $V_HH$-72 benchmark (73.0°C). $V_HHs$ with antigen binding activity were produced as monomeric and dimeric $V_HH$-Fcs for subsequent binding and neutralization assays. The schematic formats of these fusion molecules are depicted in **Fig. 3**.

**[00184]** The results of cross-reactivity studies using SARS-CoV-2 variants and various coronaviruses are shown in **Fig. 6A** and **6B**. Initial experiments showed that for the UK (Alpha) and South Africa (Beta) variants of SARS-CoV-2, eight out of nine S1-NTD-specific $V_HHs$ tested were cross-reactive to both variants (**Fig. 6A**). In the case of S1-RBD-specific $V_HHs$, 15/20 cross-reacted to both variants and an additional four cross-reacted with the UK variant. Only one (NRCoV2-08) $V_HH$ was not cross-reactive at all. Additionally, one S1-NTD-specific $V_HH$, six S1-RBD-specfic and eight S2-specific $V_HHs$ cross-reacted with SARS-CoV. Many antibodies also cross-reacted with pangolin CoV, with fewer, but still significant, numbers cross-reacting to SARS-like CoV W1V1, bat SARS-like CoV and civet SARS-CoV with similar cross-reactivity patterns. None of the antibodies tested cross-reacted with Swine deltaCoV, Avian IBV, hedgehog CoV HKU31, Bat CoV HKU9, Bat 229E-related CoV, bat CoV 512, human MERS betaCoV Jordan, human CoV-NL63, Human CoV-OC43 or human CoV-HKU1.

**[00185]** In a subsequent experiment (results shown in **Fig. 6B**), $V_HHs$ were examined for cross-reactivity to a collection of spike glycoproteins from various coronavirus genera and SARS-CoV-

2 variants by ELISA (**Fig. 6B**) and SPR (**Tables 11** and **12**), many $V_HH$-Fcs cross-reacted with the S protein from variants Alpha, Beta, Gamma, Delta and Kappa (B.1.617.1; Variant Being Monitored [VBM]). The exceptions were: 1) RBD-specific $V_HHs$ NRCoV2-02/ NRCoV2-05 did not cross-react with Beta and Gamma and NRCoV2-04/ NRCoV2-14/ NRCoV2-15, did not cross-react with Kappa and 2) S2-specific $V_HHs$ NRCoV2-MRed18 and NRCoV2-MRed19 did not cross-react with Kappa. All nine NTD-specific $V_HHs$ cross-reacted with all variants tested. Additionally, many $V_HHs$ cross-reacted with pangolin CoV, with fewer cross-reacting to SARS-CoV, SARS-like CoV WIV1, bat SARS-like CoV and civet SARS CoV. These viruses, including variants, are all of the Betacoronavirus Sarbecovirus subgenus. None of the antibodies tested cross-reacted with the remaining 11 non-Sarbecovirus Betacoronavirus, or with Alphacoronavirus, Deltacoronavirus or Gammacoronavirus. 29 $V_HHs$ cross-reacted with the Omicron variant (**Fig. 6B**). The broadly cross-reactive antibodies included $V_HHs$ targeting all three regions of the S protein (RBD, NTD, S2). The most broadly cross-reactive $V_HHs$ recognizing 10 – 12 viruses, including SARS-CoV-2 variants, were two NTD binders (NRCoV2-SR01, NRCoV2-SR02), six RBD binders (NRCoV2-1d, NRCoV2-07, NRCoV2-11, NRCoV2-12, NRCoV2-20, NRCoV2-MRed04) and six S2 binders (NRCoV2-S2F3, NRCoV2-S2G3, NRCoV2-S2G4, NRCoV2-MRed18, NRCoV2-MRed19, NRCoV2-MRed20). The VHH-72 benchmark was also broadly cross-reactive. The panel of $V_HHs$ had similar cross-reactivity profiles to human ACE2, except that ACE2 did not bind civet SARS-CoV S and, unsurprisingly, bound HCoV-NL63 S.

**[00186]** When tested by SPR against SARS-CoV, 12 out of 14 ELISA-positive $V_HHs$ cross-reacted with SARS-CoV S, most with comparably high affinities (**Table 11**. Seven of these $V_HHs$ were S2-specific, four were RBD-specific and one was NTD-specific. Against the Alpha and Beta variants, the SPR cross-reactivity data, performed with 37 $V_HHs$, were consistent with ELISA, except for NRCoV2-04 and NRCoV2-14, which were negative or very weak for binding to the Beta variant by SPR (**Tables 11** and **12**). All 37 $V_HHs$ tested bound the Alpha variant S protein, and 34 were also cross-reactive to the Beta variant S protein (**Figs. 28A** (Alpha) and **28B** (Beta); **Fig. 29**; **Table 11**; **Table 12**). Thirteen out of 17 RBD-specific $V_HHs$ bound all three variants with similar affinities, except for $V_HHs$ NRCoV2-10, NRCoV2-15 and NRCoV2-17 which bound to the Beta variant with 40 – 50-fold weaker affinity; the remaining four that did not bind the Beta variant showed cross-reactivity with the Alpha variant with similar (NRCoV2-04, NRCoV2-14) or reduced (~5-fold [NRCoV2-05] and ~20-fold [NRCoV2-02]) affinity relative to the Wuhan

variant. All NTD-specific and S2-specific $V_HHs$ cross-reacted with the three variants with essentially the same or similar affinities.

**[00187]** The cross-reactivity of the $V_HHs$ and $V_HH$-Fcs is significant, as it is believed that the progenitor of SARS-CoV was generated by recombination among bat SARS-like coronaviruses that spread to humans via civet cat as an intermediate host (Zheng et al, 2020). Further, most new emerging viruses are derived from strains circulating in zoonotic reservoirs. Antibodies that can cross-react against a variety of animal and human coronaviruses have potential to be used for detection and/or treatment of emerging coronavirus outbreaks.

**[00188] Table 6:** CDR-IMGT sequences of anti-spike protein $V_HHs$ obtained from Eva Green phage display library

| $V_HH$ | CDR 1 | SEQ ID NO: | CDR 2 | SEQ ID NO: | CDR 3 | SEQ ID NO: | Subunit/ domain specificity | Selection strategy |
|---|---|---|---|---|---|---|---|---|
| NRCoV2-1a[2] | GSTLDYYA | 1 | VSSSDGST | 45 | AADYSMRPLWVSRWHRDYEY | 90 | S1-RBD | P1, P3, P4, P6 |
| NRCoV2-1c[2] | GSILDYYA | 2 | VSSSDGST | 45 | AADYSMRRFAVGRWHRDYEY | 91 | S1-RBD | P1, P3, P4, P6 |
| NRCoV2-1d[1] | GSTLDYYA | 1 | VSSSDGNT | 46 | AADYSMRPFAVGRWHRDYEY | 92 | S1-RBD | P1, P3, P4, P6 |
| NRCoV2-02[1] | GFTFSNYA | 3 | ISGRGDDT | 47 | TKGPDLYYFGSGYSD | 93 | S1-RBD | P1, P3, P4, P5, P6 |
| NRCoV2-03[1] | GITFSYYA | 4 | MSNMDST | 48 | NIYGPTYSTRRNEY | 94 | S1-RBD | P4, P6 |
| NRCoV2-04[1] | GSPFSNVV | 5 | ISGGGIA | 49 | WSSYEST | 95 | S1-RBD | P1, P3, P4, P6 |
| NRCoV2-05[1] | GFIFSNYA | 6 | INSGGGDT | 50 | SKGPVSSYYGSGYDY | 96 | S1-RBD | P1, P3, P4, P6 |
| NRCoV2-06[1] | VSTFSSYA | 7 | IGFVGAT | 51 | NARHYGGSEY | 97 | S1-RBD | P4, P6 |
| NRCoV2-07[1] | GVTLDYYA | 8 | ISSNGRRN | 52 | AAVQDVHGDNYYCTSPNEYNV | 98 | S1-RBD | P1, P3, P4, P6 |
| NRCoV2-08[2] | GFTLDDYA | 9 | ISRSGTTT | 53 | AADYQYSTYCLGYDAHYEY | 99 | S1-RBD | P4, P6 |
| NRCoV2-10[1] | GNTFSRSN | 10 | ISSRGIS | 54 | YAADDLGDY | 100 | S1-RBD | P1, P3, P4 |
| NRCoV2-11[1] | GSSLDSYS | 11 | ISRYYSST | 55 | AARSRDFSSPFSATDTYTS | 101 | S1-RBD | P1, P5 |
| NRCoV2-11a[2] | GFTLDSYN | 12 | ISRYYEST | 56 | AARSRDFSSPISATDKYGS | 102 | S1-RBD | P5 |
| NRCoV2-12[2] | GRTFRNYV | 13 | VAAISWGGTEI | 57 | AADRGLSYYYTRTTEYNY | 103 | S1-RBD | P1, P4, P6 |
| NRCoV2-14[1] | GTTFSHYA | 14 | ISVFGST | 58 | HAVNADIGGDY | 104 | S1-RBD | P3 |
| NRCoV2-15[1] | GSTSGRNT | 15 | VSTSGAT | 59 | YAAYGGGGDY | 105 | S1-RBD | P1, P3, P4, P6 |
| NRCoV2-17[1] | GSPFSQLA | 16 | ISPTGNR | 60 | QAANVNGGDY | 106 | S1-RBD | P4 |
| NRCoV2-18[1] | GITISGYN | 17 | INSGGST | 61 | SLHTSHDY | 107 | S1-RBD | P1, P3, P4, P5, P6 |
| NRCoV2-19[2] | GLTLNSYA | 18 | LTSGGTG | 62 | AADRARLRFGCSLNFRREVAYDY | 108 | S1-RBD | P1, P4 |
| NRCoV2-20[1] | GRTFSNYV | 19 | VAVISGSDTET | 63 | AADRGMSYYYTRATEYYY | 109 | S1-RBD | P4 |
| NRCoV2-21[2] | GFTLDYYA | 20 | ISSGGST | 64 | AADHRGRSLRFGCSSSTTDYLY | 110 | S1-RBD | P1, P4, P5 |

| | | | | | | | | |
|---|---|---|---|---|---|---|---|---|
| NRCoV2-SR01[3] | GFTFDNYA | 21 | ISGNGGVT | 65 | AATGIRSTWSVYGCSRLAGPYDY | 111 | S1-NTD | P3, P5 |
| NRCoV2-SR02[3] | EFTLNYYS | 22 | IRYSGGGI | 66 | AADRLYSRACPTAGGRNY | 112 | S1-NTD | P5 |
| NRCoV2-SR03[3] | GSIFSNNH | 23 | ISSGGKT | 67 | NRGGWEYRSSYYIMGPH | 113 | S1-NTD | P3, P5 |
| NRCoV2-SR04[3] | GRTFSSHT | 24 | ISMGGNTNYA | 68 | NTAALVGNRLLPMATIT | 114 | S1-NTD | P5 |
| NRCoV2-SR13[3] | GSRFGSKH | 25 | ISSGGST | 69 | NMGGWDYRSNTYIPGSRSDY | 115 | S1-NTD | P3, P5 |
| NRCoV2-SR16[3] | GTTFSRYH | 26 | ISTSGAV | 70 | NTGGWDYRSSTFIMGLN | 116 | S1-NTD | P3, P5 |
| NRCoV2-S2A3[1] | GRPYSNYA | 27 | KQRELVAAISSGGTT | 71 | NTGSLSYGGSVYYPSYDN | 117 | S2 | P2 |
| NRCoV2-S2A4[1] | GSPFRSNV | 28 | ISTGGSR | 72 | HAAARDSHGIYLLDT | 118 | S2 | P2 |
| NRCoV2-S2B3[2] | ASTFGDSA | 29 | ISTGSNT | 73 | NYRSIYYGQNF | 119 | S2 | P2 |
| NRCoV2-S2H4[2] | GFTFNLYS | 30 | INSGDRDSTT | 74 | ALVFGYTSRDYCLTPKRGNY | 120 | S2 | P2 |
| NRCoV2-S2F3[1] | VRILSVPA | 31 | ITSGGST | 75 | NLRDILSQPF | 121 | S2 | P2 |
| NRCoV2-S2G3[1] | GSTFGIFL | 32 | ITSGGAT | 76 | YTTKRDDASVY | 122 | S2 | P2 |
| NRCoV2-S2G4[1] | GSTFSGYA | 33 | ISSDGDK | 77 | NKHWWTGDW | 123 | S2 | P2 |
| NRCoV2-S202[2] | GITVSRIG | 34 | ISAGGST | 78 | NYGPGYRKAA | 124 | S2 | P2 |

Subunit/domain specificities were determined by [1]SPR, [2]ELISA or [3]both. SPR assays and ELISAs were performed against various spike protein subunit/domains using $V_HHs$ and $V_HH$-Fcs, respectively.

**[00189] Table 7:** CDR-IMGT sequences of anti-spike protein $V_HHs$ obtained from Maple Red $V_HH$ phage display library

| $V_HH$ | CDR 1 | SEQ ID NO: | CDR 2 | SEQ ID NO: | CDR 3 | SEQ ID NO: | Subunit/domain/ specificity | Selection strategy |
|---|---|---|---|---|---|---|---|---|
| NRCoV2-MRed02[2] | GNIFSINS | 35 | IWSDSRT | 79 | AADRGFVVRGQYDY | 125 | S1-RBD | P1, P3, P4, P6 |
| NRCoV2-MRed04[1] | GNSFSINT | 36 | IWSDTTT | 80 | AADRGFVVRGQYDY | 125 | S1-RBD | P4, P6 |
| NRCoV2-MRed03[3] | GFTLDYYA | 20 | ISSSDGST | 81 | ATDAFATCDSWYAQIAQYDF | 126 | S1-NTD | P3, P5 |
| NRCoV2-MRed05[2] | GFTLDYYA | 20 | ISSSDGST | 81 | ATGPQAYYSGSYYFQCPQAGMDY | 127 | S1-RBD | P4, P6 |
| NRCoV2-MRed06[3] | GFTLAYYA | 37 | ISSSDGSA | 82 | ATDSFSSCSDYESGMDF | 128 | S1-NTD | P3 |
| NRCoV2-MRed07[3] | GSIGPFNT | 38 | ITRGGVT | 83 | YANYGWAIPY | 129 | S1-NTD | P3 |
| NRCoV2-MRed11[1] | GFTFSSYA | 39 | INSGGGST | 84 | ATTISDGSSWSTKSY | 130 | S2 | P1, P2 |
| NRCoV2-MRed18[1] | TTVFGRNA | 40 | VSDGGTP | 85 | NYYNYYYGRNF | 131 | S2 | P2 |
| NRCoV2-MRed19[1] | TIIFKGQT | 41 | MTTSGSA | 86 | YMHSVYYGIDY | 132 | S2 | P2 |
| NRCoV2-MRed20[1] | GLSFSSYD | 42 | IRESGSGT | 87 | AAKPPFYGSGTYSTPRAYLY | 133 | S2 | P2 |
| NRCoV2-MRed22[1] | GSVFASNA | 43 | ISSRGST | 88 | NAREFTGFDY | 134 | S2 | P2 |
| NRCoV2-MRed25[1] | GHTFSRYG | 44 | ISWRGDST | 89 | AAEMWGTATIVASRYTY | 135 | S2 | P2 |

Domain/subunit specificities were determined by [1]SPR, [2]ELISA or [3]both. SPR assays and ELISAs were performed against various spike protein domains/subunit using $V_HHs$ and $V_HH$-Fcs, respectively.

**Example 5: Binding characteristics of $V_HHs$ and $V_HH$-Fcs: Surface Plasmon Resonance (SPR) and ELISA Binding Studies**

***Introduction***

**[00190]** Binding of anti-SARS-CoV-2 $V_HHs$ against various SARS-CoV-2 spike protein fragments (Wuhan) was assayed using SPR and ELISA to determine their affinity and domain/sub-domain specificity. Binding of $V_HHs$ against SARS-CoV, SARS-CoV-2 UK (Alpha) variant and SARS-CoV-2 South African (Beta) variant spike protein S was also carried out to determine their virus cross-reactivity patterns.

***Materials and Methods***

**[00191]** *Affinity/specificity determination of $V_HHs$ against SARS-CoV spike (S), SARS-CoV-2 spike (S) and SARS-CoV-2 spike fragments by SPR*

**[00192]** Standard SPR techniques were used for binding studies. All SPR assays were performed on a Biacore™ T200 instrument (Cytiva) at 25°C with HBS-EP running buffer (10 mM HEPES, 150 mM NaCl, 3 mM EDTA, 0.005 % [v/v] Tween® 20, pH 7.4) and CM5 sensor chips (Cytiva). Prior to SPR analyses all analytes in flow ($V_HHs$, ACE2 receptor) were SEC-purified on a Superdex™ 75 Increase 10/300 GL column (Cytiva) in HBS-EP buffer at a flow rate of 0.8 mL/min to obtain monomeric proteins. SARS-CoV spike (S), SARS-CoV-2 spike trimer (S) and various SARS-CoV-2 spike fragments were immobilized on CM5 sensor chips through standard amine coupling (10 mM acetate buffer, pH 4.0; Cytiva). On the first sensor chip, 1983 response units (RUs) of SARS-CoV spike (Sino Biologicals, Cat# 40634-V08B), 843 RUs of SARS-CoV-2 S1-RBD fused to human Fc (S1-RBD-Fc) and 972 RUs of EGFR (irrelevant control surface) were immobilized. On a second sensor chip, 2346 RUs of SARS-CoV-2 S, 1141 RUs of SARS-CoV-2 S1 subunit and 1028 RUs of SARS-CoV-2 S2 subunit were immobilized. The theoretical maximum binding response for $V_HHs$ binding to these surfaces ranged from 224 – 262 RUs. An ethanolamine blocked surface on each sensor chip served as a reference. Single cycle kinetics was used to determine $V_HH$ and ACE2 binding kinetics and affinities. $V_HHs$ at various concentration ranges (from 0.25 – 4 nM to 125 – 2000 nM) were flowed over all surfaces at a flow rate of 40

μL/min with 180 s of contact time and 600 s of dissociation time. Surfaces were regenerated with a 12 s pulse of 10 mM glycine, pH 1.5, at a flow rate of 100 μL/min. Injection of EGFR-specific $V_HH$ EK2 served as a negative control for the SARS-CoV and SARS-CoV-2 surfaces and as a positive control for the EGFR surface. The ACE2 affinity was determined using similar conditions by flowing a range of monomeric ACE2 concentrations (31.53 – 500 nM). All affinities were calculated by fitting reference flow cell-subtracted data to a 1:1 interaction model using BIAevaluation Software v3.0 (Cytiva).

**[00193]** For $V_HH$ 12 and MRed05, $V_HH$-Fc formats were used in SPR experiments. Approximately 200 RUs of $V_HH$-Fcs (2 μg/mL) were captured on goat anti-human IgG surfaces (4000 RUs, Jackson ImmunoResearch, Cat#109-005-098) at a flow rate of 10 μL/min for 30 s. A range of SEC-purified RBD fragments (**Table 1**; SARS-CoV, Wuhan, Alpha and Beta) at 0.62 – 10 nM were flowed over the captured $V_HH$-Fc at a flow rate of 40 μL/min with 180 s of contact time and 300 s of dissociation. Surfaces were regenerated with a 120 s pulse of 10 mM glycine, pH 1.5, at a flow rate of 50 μL/min. Affinities were calculated from reference flow cell subtracted sensorgrams as described above.

**[00194]** *Domain specificity determination of $V_HH$s by ELISA.*

**[00195]** $V_HH$s that bound to the S1 subunit but not its S1-RBD domain in SPR assays, were further examined by ELISA to determine if they were binding to the S1-NTD domain of S1. Briefly, S, S1, S1-NTD and S1-RBD were coated onto NUNC® MaxiSorp™ 4BX plates (Thermo Fisher) at 100 ng/well in 100 μL PBS, pH 7.4. The next day, plates were blocked with 200 μL PBSC for 1 h at room temperature, then washed five times with PBST and incubated with fixed (13 nM) or decreasing concentrations of $V_HH$-Fcs diluted in PBSTC. After 1 h, plates were washed 10 times with PBSTC and binding of $V_HH$-Fc fusions was detected by incubating wells with 100 μL of 1 μg/mL HRP-conjugated goat anti-human IgG. Finally, plates were washed 10 times with PBST and peroxidase activity was determined as described above. $EC_{50}$s for the binding of $V_HH$-Fcs to S and S fragments were obtained from the plot of $A_{450\ nm}$ (binding) *vs* $V_HH$-Fc concentration. S1-NTD covering amino acids 16-305 of SARS-CoV-2 S (GenBank accession number: QHD43416.1) was expressed in CHO cells.

**[00196]** *Affinity/specificity determination of $V_HHs$ against spike protein S from SARS-CoV-2 Wuhan, UK (Alpha) and South African (Beta) variants by SPR*

**[00197]** Affinity and specificity of $V_HHs$ against spike protein S from SARS-CoV-2 Wuhan, UK and South African variants by SPR was determined essentially as described above.

***Results and Discussion***

**[00198]** $V_HHs$ were tested by SPR against SARS-CoV-2 S, S1, S1-RBD and S2 to determine their affinity and domain/sub-domain specificity. Binding data are presented in **Fig. 6C, Figs. 7A-B**, **Table 8** and **Table 9.** In SPR binding assays, NRCoV2-SR01, NRCoV2-SR02, NRCoV2-SR03, NRCoV2-SR04, NRCoV2-SR13, NRCoV2-SR16, NRCoV2-MRed03, NRCoV2-MRed06 and NRCoV2-MRed07 bound to the S1 subunit but not to its S1-RBD domain. Subsequent ELISAs performed against SARS-CoV-2 S, S1, S1-NTD and S1-RBD showed these $V_HHs$ were S1-NTD-specific (**Figs. 6D** and **6E** and **Table 10**). $V_HHs$ displayed high affinity towards their target (i.e., S) with the vast majority having $K_D$s in the range of single-digit-nM to pM. Three clusters of $V_HHs$ based on domain/subdomain specificity were identified: (i) S1-RBD-specific $V_HHs$; (ii) S1-NTD-spepcfic $V_HHs$; and (iii) S2-specific $V_HHs$ (**Fig. 7A**).

**[00199]** As for the S1-RBD-specific $V_HHs$, with the exception of NRCoV2-06, which had an affinity of 223 nM (**Table 11**), the remaining 16 cluster members displayed high affinities ranging from 0.02 - 10 nM, all vastly outperforming the benchmark $V_HH$-72 $V_HH$, which had a $K_D$ of 86.2 nM. Nine $V_HHs$ were S1-NTD-specific and, similar to S1-RBD-specific $V_HHs$, displayed high affinities ($K_D$s) in the range of 0.1 – 5.2 nM. Lastly, 11 $V_HHs$ were S2 subunit-specific, with similarly high affinities ($K_D$s) ranging from 0.09 – 12.8 nM.

**[00200]** $V_HHs$ were tested against SARS-CoV (S) in SPR assays for quantitative determination of cross-reactivity. $V_HHs$ were first screened for cross-reactivity at fixed concentrations. Twelve out of 37 $V_HHs$ screened showed cross-reactivity to SARS-CoV S. These 12 $V_HHs$ were subsequently subjected to comprehensive binding analysis against both SARS-CoV S and SARS-CoV-2 S at multiple $V_HH$ concentrations. The SPR cross-reactivity results, which agreed with those from ELISAs, are presented in **Fig. 27** and **Table 11**. Seven out of the 12 $V_HHs$ tested were

S2-specific, four were S1-RBD-specific and one was S1-NTD-specific. NRCoV2-MRed04 showed weak binding to SARS-CoV S compared to SARS-CoV-2 S (300 nM for SARS-CoV S *vs* 1 nM for SARS-CoV-2 S), but the remaining $V_HHs$ cross-reacted with high/comparable affinities to both SARS-CoV-2 S and SARS-CoV S. NRCoV2-07, NRCoV2-12, NRCoV2-MRed18, NRCoV2-MRed19 and NRCoV2-MRed20 cross-reacted with SARS-CoV S with relatively lower affinities in comparison to SARS-CoV-2 S, but nonetheless with high absolute affinities in the low nanomolar $K_D$ range. The S1-NTD-specific $V_HH$, NRCoV2-SR01, cross-reacted with SARS-CoV S with high affinity (0.15 nM for SARS-CoV S *vs* 0.56 nM for SARS-CoV-2 S); one S1-RBD-specific $V_HH$, NRCoV2-11, cross-reacted with SARS-CoV S with very high affinity (0.014 nM for SARS-CoV S *vs* 0.018 nM for SARS-CoV-2 S); and four S2-specific $V_HHs$ demonstrated high, comparable affinities to SARS-CoV and SARS-CoV-2 S in the single-digit-nM to pM $K_D$ range.

**[00201]** Against the Alpha and Beta variants, SPR cross-reactivity data performed with 37 $V_HHs$, were consistent with ELISA, except for NRCoV2-04 and NRCoV2-14 which were negative or very weak for binding to the Beta variant by SPR. All 37 $V_HHs$ tested bound the Alpha variant S protein, 34 of which were also cross-reactive to the Beta variant S protein (**Fig. 28A, Fig. 28B** and **Table 12**). Thirteen out of 17 RBD-specific $V_HHs$ bound all three variants with similar affinities, except for $V_HHs$ NRCoV2-10, NRCoV2-15 and NRCoV2-17 which bound to the Beta variant with 40 – 50-fold weaker affinity; the remaining four that did not bind the Beta variant showed cross-reactivity with the Alpha variant with similar (NRCoV2-04, NRCoV2-14) or reduced (~5-fold [NRCoV2-05] and ~20-fold [NRCoV2-02]) affinity relative to the Wuhan variant. All NTD-specific and S2-specific $V_HHs$ cross-reacted with the three variants with essentially the same or similar affinities.

**[00202] Table 8:** Kinetic and equilibrium constants for the binding of Eva Green $V_HHs$ to SARS-CoV-2 Wuhan spike protein fragments

| **$V_HH$/ ACE2** | **S1-RBD-Fc[1]** | | | **S[1]** | | | **S1[1]** | | | **S2[1]** | | |
|---|---|---|---|---|---|---|---|---|---|---|---|---|
| | $k_a$ (1/Ms) | $k_d$ (1/s) | $K_D$ (M) | $k_a$ (1/Ms) | $k_d$ (1/s) | $K_D$ (M) | $k_a$ (1/Ms) | $k_d$ (1/s) | $K_D$ (M) | $k_a$ (1/Ms) | $k_d$ (1/s) | $K_D$ (M) |
| NRCoV2-1d | 5.62E+05 | 1.18E-03 | 2.10E-09 | 1.06E+06 | 1.17E-03 | 1.10E-09 | 8.67E+05 | 1.14E-03 | 1.32E-09 | - | - | - |
| NRCoV2-02 | 1.83E+06 | 1.41E-03 | 7.73E-10 | 2.14E+06 | 1.41E-03 | 6.61E-10 | 2.10E+06 | 1.38E-03 | 6.59E-10 | - | - | - |
| NRCoV2-03 | 1.66E+05 | 2.55E-04 | 1.53E-09 | 2.50E+05 | 3.34E-04 | 1.34E-09 | 2.41E+05 | 2.63E-04 | 1.09E-09 | - | - | - |
| NRCoV2-04 | 1.53E+06 | 1.92E-02 | 1.25E-08 | 1.97E+06 | 1.98E-02 | 1.00E-08 | 1.61E+06 | 1.80E-02 | 1.12E-08 | - | - | - |
| NRCoV2-05 | 2.51E+06 | 5.85E-03 | 2.33E-09 | 4.33E+06 | 7.43E-03 | 1.72E-09 | 4.03E+06 | 8.06E-03 | 2.00E-09 | - | - | - |
| NRCoV2-06 | 5.94E+04 | 4.15E-03 | 6.99E-08 | 3.02E+04 | 4.69E-03 | 1.55E-07 | 1.04E+05 | 1.33E-02 | 1.29E-07 | - | - | - |
| NRCoV2-07 | 3.18E+05 | 2.84E-04 | 8.94E-10 | 3.50E+05 | 4.03E-04 | 1.15E-09 | 3.01E+05 | 3.08E-04 | 1.02E-09 | - | - | - |
| NRCoV2-10 | 3.51E+05 | 9.32E-05 | 2.66E-10 | 4.83E+05 | 9.27E-05 | 1.92E-10 | 4.48E+05 | 9.54E-05 | 2.13E-10 | - | - | - |
| NRCoV2-11 | 8.92E+05 | 2.26E-04 | 2.53E-10 | 1.21E+06 | 4.73E-05 | 3.91E-11 | 1.08E+06 | 1.80E-04 | 1.67E-10 | - | - | - |
| NRCoV2-12 | 7.60E+05 | 3.69E-05 | 4.86E-11 | nd | | | | | | - | - | |
| NRCoV2-14 | 2.61E+05 | 9.44E-04 | 3.61E-09 | 5.28E+05 | 1.64E-03 | 3.10E-09 | 3.19E+05 | 1.12E-03 | 3.49E-09 | - | - | - |
| NRCoV2-15 | 6.82E+05 | 2.33E-04 | 3.42E-10 | 7.06E+05 | 2.21E-04 | 3.13E-10 | 6.75E+05 | 2.25E-04 | 3.33E-10 | - | - | - |
| NRCoV2-17 | 5.67E+05 | 2.24E-04 | 3.95E-10 | 6.59E+05 | 9.79E-05 | 1.49E-10 | 6.29E+05 | 9.66E-05 | 1.53E-10 | - | - | - |
| NRCoV2-18 | 2.68E+05 | 1.97E-04 | 7.36E-10 | 3.95E+05 | 1.52E-04 | 3.84E-10 | 3.08E+05 | 1.65E-04 | 5.36E-10 | - | - | - |
| NRCoV2-20 | 1.43E+06 | 1.23E-02 | 8.61E-09 | 2.37E+06 | 1.59E-02 | 6.73E-09 | 1.96E+06 | 1.89E-02 | 9.63E-09 | - | - | - |

| | | | | | | | | | | | | |
|---|---|---|---|---|---|---|---|---|---|---|---|---|
| NRCoV2-SR01 | - | - | - | 2.77E+06 | 1.23E-03 | 4.45E-10 | 3.63E+06 | 1.58E-03 | 4.37E-10 | - | - | - |
| NRCoV2-SR02 | - | - | - | 9.67E+05 | 5.71E-04 | 5.90E-10 | 1.05E+06 | 5.55E-04 | 5.30E-10 | - | - | - |
| NRCoV2-SR03 | - | - | - | 1.01E+06 | 1.02E-03 | 1.01E-09 | 9.05E+05 | 1.03E-03 | 1.13E-09 | - | - | - |
| NRCoV2-SR04 | - | - | - | 2.39E+06 | 3.35E-04 | 1.40E-10 | 2.18E+06 | 4.93E-04 | 2.26E-10 | - | - | - |
| NRCoV2-SR13 | - | - | - | 1.83E+06 | 4.81E-03 | 2.62E-09 | 2.25E+06 | 5.45E-03 | 2.43E-09 | - | - | - |
| NRCoV2-SR16 | - | - | - | 6.57E+05 | 1.20E-03 | 1.82E-09 | 7.39E+05 | 1.15E-03 | 1.55E-09 | - | - | - |
| NRCoV2-S2A3 | - | - | - | 8.40E+04 | 1.30E-04 | 1.55E-09 | - | - | - | 4.60E+04 | 1.03E-04 | 2.23E-09 |
| NRCoV2-S2A4 | - | - | - | 3.49E+04 | 4.46E-04 | 1.28E-08 | - | - | - | 2.81E+04 | 4.14E-04 | 1.47E-08 |
| NRCoV2-S2G3 | - | - | - | 1.62E+05 | 6.07E-04 | 3.74E-09 | - | - | - | 1.47E+05 | 6.27E-04 | 4.28E-09 |
| NRCoV2-S2G4 | - | - | - | 8.93E+05 | 2.07E-04 | 2.32E-10 | - | - | - | 9.25E+05 | 3.82E-04 | 4.13E-10 |
| NRCoV2-S2F3 | - | - | - | 1.56E+05 | 4.73E-04 | 3.03E-09 | - | - | - | 1.01E+05 | 6.29E-04 | 6.22E-09 |
| $V_HH$-72[2] | 6.67E+05 | 1.34E-01 | 2.00E-07 | 1.10E+06 | 1.56E-01 | 1.42E-07 | 9.40E+05 | 1.46E-01 | 1.56E-07 | - | - | - |
| ACE2-H6[2] | 3.71E+04 | 1.18E-02 | 3.17E-07 | 6.02E+04 | 9.96E-03 | 1.65E-07 | 6.21E+04 | 1.24E-02 | 2.00E-07 | - | - | - |
| NRCsdAb022[2] | - | - | - | - | - | - | - | - | - | - | - | - |

[1]For any given $V_HH$, $K_D$ values across different spike fragments, S1-RBD-Fc, S1, S2 and S were in agreement. Lack of $V_HH$ binding for certain spike fragments is consistent with $V_HH$s' subunit/domain specificities. Binding parameters were determined by flowing monomeric $V_HH$s over sensorchip surfaces coated with various spike fragments, except for binding parameters for NRCoV2-12 which were obtained by flowing monomeric RBDs over $V_HH$-Fc-captured surfaces. Dashes indicate lack of binding. "nd", not done, [2]$V_HH$-72 (Wrapp et al., 2020) and ACE2-H6 are positive binder controls, EGFR-specific $V_HH$, NRCsdAb022 (Rossotti et al., 2019) is a negative control.

**[00203] Table 9:** Kinetic and equilibrium dissociation constants for the binding of Maple Red $V_HHs$ to various SARS-CoV-2 Wuhan spike protein fragments

| $V_HH$/ ACE2[1] | **S1-RBD-Fc[1]** | | | **S[1]** | | | **S1[1]** | | | **S2[1]** | | |
|---|---|---|---|---|---|---|---|---|---|---|---|---|
| | *k*a (1/Ms) | *k*d (1/s) | *K*D (M) | *k*a (1/Ms) | *k*d (1/s) | *K*D (M) | *k*a (1/Ms) | *k*d (1/s) | *K*D (M) | *k*a (1/Ms) | *k*d (1/s) | *K*D (M) |
| NRCoV2-MRed03 | - | - | - | 1.57E+05 | 8.14E-05 | 5.20E-10 | 2.76E+05 | 6.15E-05 | 2.23E-10 | - | - | - |
| NRCoV2-MRed04 | 8.55E+05 | 1.76E-03 | 2.06E-09 | 1.39E+06 | 1.50E-03 | 1.09E-09 | 1.09E+06 | 1.83E-03 | 1.68E-09 | - | - | - |
| NRCoV2-MRed05 | 6.50E+05 | 4.96E-04 | 7.63E-10 | nd | | | | | | nd | | |
| NRCoV2-MRed06 | - | - | - | 1.85E+05 | 8.87E-04 | 4.80E-09 | 3.71E+05 | 1.57E-03 | 4.22E-09 | - | - | - |
| NRCoV2-MRed07 | - | - | - | 1.60E+06 | 3.78E-04 | 2.36E-10 | 1.13E+06 | 4.27E-04 | 3.78E-10 | - | - | - |
| NRCoV2-MRed11 | - | - | - | 2.34E+04 | 4.18E-04 | 1.78E-08 | - | - | - | 4.09E+04 | 2.13E-04 | 5.21E-09 |
| NRCoV2-MRed18 | - | - | - | 2.02E+05 | 1.53E-03 | 7.56E-09 | - | - | - | 1.52E+05 | 1.03E-03 | 6.80E-09 |
| NRCoV2-MRed19 | - | - | - | 1.59E+05 | 7.99E-04 | 5.01E-09 | - | - | - | 1.02E+05 | 8.40E-04 | 8.20E-09 |
| NRCoV2-MRed20 | - | - | - | 1.60E+05 | 1.46E-05 | 9.18E-11 | - | - | - | 1.13E+05 | 3.38E-05 | 2.99E-10 |
| NRCoV2-MRed22 | - | - | - | 3.47E+05 | 1.76E-04 | 5.06E-10 | - | - | - | 2.70E+05 | 2.84E-04 | 1.05E-09 |
| NRCoV2-MRed25 | - | - | - | 1.12E+05 | 1.15E-04 | 1.02E-09 | - | - | - | 1.22E+05 | 1.90E-04 | 1.56E-09 |
| $V_HH$-72[2] | 6.82E+05 | 1.26E-01 | 1.85E-07 | 1.06E+06 | 1.50E-01 | 1.42E-07 | 8.30E+05 | 1.61E-01 | 1.94E-07 | - | - | - |
| ACE2-H6[2] | 3.86E+04 | 1.06E-02 | 2.74E-07 | 8.63E+04 | 1.18E-02 | 1.37E-07 | 7.29E+04 | 1.32E-02 | 1.82E-07 | - | - | - |
| NRCsdAb022[2] | - | - | - | - | - | - | - | - | - | - | - | - |

[1]For any given $V_HH$, $K_D$ values across different spike fragments, S1-RBD-Fc, S1, S2 and S were in agreement. Lack of $V_HH$ binding for certain spike fragments was consistent with $V_HHs$' subunit/domain specificities. Binding parameters were determined by flowing monomeric $V_HHs$ over sensorchip surfaces coated with various spike fragments, except for NRCoV2-MRed05, for which binding parameters were obtained by flowing monomeric RBDs over $V_HH$-Fc-captured surfaces. Dashes indicate lack of binding, "nd", not done. [2]$V_HH$-72 (Wrapp et al., 2020) and ACE2-H6 are positive binder controls, EGFR-specific $V_HH$, NRCsdAb022 (Rossotti et al., 2019) is a negative control.

**[00204] Table 10:** ELISA data for the binding of $V_HH$-Fcs to various spike protein fragments

| $V_HH$-Fc[1] | $EC_{50}$app (nM)[2] | | | | Subdomain specificity |
|---|---|---|---|---|---|
| | S | S1 | S1-NTD | S1-RBD | |
| NRCoV2-SR01 | 0.13 | 0.23 | 0.19 | - | S1-NTD |
| NRCoV2-SR02 | 0.11 | 0.13 | 0.34 | - | S1-NTD |
| NRCoV2-SR03 | 0.16 | 0.20 | 0.17 | - | S1-NTD |
| NRCoV2-SR04 | 0.20 | 0.25 | 0.17 | - | S1-NTD |
| NRCoV2-SR13 | 0.43 | 0.43 | 0.23 | - | S1-NTD |
| NRCoV2-SR16 | 0.59 | 2.70 | 0.36 | - | S1-NTD |
| NRCoV2-MRed03 | 0.20 | 0.48 | 0.70 | - | S1-NTD |
| NRCoV2-MRed06 | 0.40 | 0.59 | 0.40 | - | S1-NTD |
| NRCoV2-MRed07 | 1.20 | 1.50 | 0.80 | - | S1-NTD |
| NRCoV2-02 | 0.10 | 0.11 | - | 0.21 | S1-RBD |

[1]S1-specfic $V_HH$s that did not bind to S1-RBD by SPR (**Table 8** and **Table 9**), were tested for specificity against S1-NTD. The S1-RBD-specific NRCoV2-02 internal control gave the expected specificity binding profile. [2]$EC_{50}$app, apparent $EC_{50}$.

**[00205] Table 11:** Kinetic and equilibrium dissociation constants for the binding of $V_HH$s to SARS-CoV-2 Wuhan, SARS-CoV-2 Alpha, SARSCoV-2 Beta and SARS-CoV spike glycoproteins

| $V_HH$/ACE2 | SARS-CoV-2 Wuhan[a] | | | SARS-CoV-2 Alpha[a] | | | SARS-CoV-2 Beta[a] | | | SARS-CoV[a] | | |
|---|---|---|---|---|---|---|---|---|---|---|---|---|
| | $k_a$ (1/Ms) | $k_d$ (1/s) | $K_D$ (M) | $k_a$ (1/Ms) | $k_d$ (1/s) | $K_D$ (M) | $k_a$ (1/Ms) | $k_d$ (1/s) | $K_D$ (M) | $k_a$ (1/Ms) | $k_d$ (1/s) | $K_D$ (M) |
| **RBD-specific $V_HH$** | | | | | | | | | | | | |
| NRCoV2-1d | 1.39E+06 | 1.05E-03 | 7.50E-10 | 1.13E+06 | 1.02E-03 | 9.07E-10 | 8.12E+05 | 9.56E-04 | 1.18E-09 | - | - | - |
| NRCoV2-02 | 2.04E+06 | 1.27E-03 | 6.24E-10 | 1.64E+06 | 2.22E-02 | 1.36E-08 | - | - | - | - | - | - |
| NRCoV2-03 | 1.16E+05 | 1.81E-04 | 1.56E-09 | 1.03E+05 | 1.54E-04 | 1.49E-09 | 5.54E+04 | 2.26E-04 | 4.08E-09 | - | - | - |
| NRCoV2-04 | 1.84E+06 | 1.88E-02 | 1.02E-08 | 1.67E+06 | 1.96E-02 | 1.17E-08 | - | - | - | - | - | - |

| | | | | | | | | | | | | | |
|---|---|---|---|---|---|---|---|---|---|---|---|---|---|
| NRCoV2-05 | 2.76E+06 | 7.09E-03 | 2.57E-09 | 2.28E+06 | 2.61E-02 | 1.14E-08 | - | - | - | - | - | - |
| NRCoV2-06 | 2.05E+04 | 4.56E-03 | 2.23E-07 | 2.05E+04 | 4.68E-03 | 2.29E-07 | 2.48E+04 | 6.14E-03 | 2.48E-07 | - | - | - |
| NRCoV2-07 | 3.78E+05 | 3.55E-04 | 9.39E-10 | 3.39E+05 | 3.78E-04 | 1.12E-09 | 3.05E+05 | 3.21E-04 | 1.05E-09 | 1.20E+05 | 1.46E-03 | 1.22E-08 |
| NRCoV2-10 | 5.81E+05 | 1.16E-04 | 1.99E-10 | 4.84E+05 | 1.02E-04 | 2.10E-10 | 2.70E+05 | 2.62E-03 | 9.73E-09 | - | - | - |
| NRCoV2-11 | 9.64E+05 | 1.71E-05 | 1.77E-11 | 9.28E+05 | 1.59E-05 | 1.71E-11 | 7.57E+05 | 1.72E-05 | 2.27E-11 | 1.93E+06 | 2.70E-05 | 1.40E-11 |
| NRCoV2-12[a] | 7.47E+05 | 3.50E-05 | 4.69E-11 | 9.47E+05 | 4.38E-05 | 4.63E-11 | 9.70E+05 | 3.89E-05 | 4.01E-11 | 3.76E+05 | 1.01E-03 | 2.69E-09 |
| NRCoV2-14 | 3.89E+05 | 1.01E-03 | 2.60E-09 | 3.75E+05 | 9.17E-04 | 2.44E-09 | - | - | - | - | - | - |
| NRCoV2-15 | 6.91E+05 | 2.22E-04 | 3.21E-10 | 6.37E+05 | 1.94E-04 | 3.05E-10 | 1.48E+05 | 3.28E-03 | 2.22E-08 | - | - | - |
| NRCoV2-17 | 6.14E+05 | 9.45E-05 | 1.54E-10 | 6.14E+05 | 7.64E-05 | 1.25E-10 | 1.14E+06 | 5.88E-03 | 5.14E-09 | - | - | - |
| NRCoV2-18 | 2.95E+05 | 9.39E-05 | 3.18E-10 | 2.78E+05 | 9.79E-05 | 3.53E-10 | 2.76E+05 | 1.01E-04 | 3.65E-10 | - | - | - |
| NRCoV2-20 | 2.64E+06 | 1.16E-02 | 4.39E-09 | 2.48E+06 | 1.23E-02 | 4.97E-09 | 2.08E+06 | 1.14E-02 | 5.47E-09 | - | - | - |
| NRCoV2-MRed04 | 1.51E+06 | 1.31E-03 | 8.63E-10 | 1.34E+06 | 1.22E-03 | 9.09E-10 | 1.14E+06 | 1.23E-03 | 1.07E-09 | 3.23E+05 | 9.70E-02 | 3.00E-07 |
| NRCoV2-MRed05[a] | 5.62E+05 | 5.09E-04 | 9.05E-10 | 5.73E+05 | 1.76E-04 | 3.07E-10 | 6.12E+05 | 5.44E-04 | 8.88E-10 | - | | |
| **NTD-specific $V_HH$** | | | | | | | | | | | | |
| NRCoV2-SR01 | 1.43E+06 | 8.05E-04 | 5.64E-10 | 1.01E+06 | 5.94E-04 | 5.91E-10 | 1.09E+06 | 2.21E-04 | 2.02E-10 | 6.81E+05 | 1.05E-04 | 1.54E-10 |
| NRCoV2-SR02 | 4.98E+06 | 6.69E-04 | 1.35E-10 | 4.54E+06 | 2.54E-04 | 5.59E-11 | 4.19E+06 | 6.28E-04 | 1.50E-10 | - | - | - |
| NRCoV2-SR03 | 6.70E+05 | 1.13E-03 | 1.69E-09 | 5.55E+05 | 9.55E-04 | 1.72E-09 | 5.64E+05 | 1.40E-03 | 2.49E-09 | - | - | - |
| NRCoV2-SR04 | 3.68E+06 | 5.15E-04 | 1.40E-10 | 2.80E+06 | 7.50E-04 | 2.67E-10 | 2.24E+06 | 7.23E-04 | 3.24E-10 | - | - | - |
| NRCoV2-SR13 | 1.06E+06 | 3.76E-03 | 3.56E-09 | 5.92E+05 | 3.44E-03 | 5.82E-09 | 5.71E+05 | 4.01E-03 | 7.02E-09 | - | - | - |
| NRCoV2-SR16 | 4.88E+05 | 9.57E-04 | 1.96E-09 | 4.04E+05 | 6.33E-04 | 1.57E-09 | 3.95E+05 | 1.01E-03 | 2.57E-09 | - | - | - |
| NRCoV2-MRed03 | 2.37E+05 | 1.21E-04 | 5.08E-10 | 2.71E+05 | 9.89E-05 | 3.64E-10 | 2.13E+05 | 1.43E-04 | 6.72E-10 | - | - | - |

| | | | | | | | | | | | | |
|---|---|---|---|---|---|---|---|---|---|---|---|---|
| NRCoV2-MRed06 | 1.92E+05 | 9.96E-04 | 5.19E-09 | 2.27E+05 | 1.30E-03 | 5.72E-09 | 1.39E+05 | 1.01E-03 | 7.24E-09 | - | - | - |
| NRCoV2-MRed07 | 4.58E+06 | 4.81E-04 | 1.05E-10 | 3.90E+06 | 1.03E-03 | 2.64E-10 | 2.38E+06 | 5.52E-04 | 2.31E-10 | - | - | - |
| **S2-specific $V_HH$** | | | | | | | | | | | | |
| NRCoV2-S2A3 | 9.83E+04 | 5.51E-05 | 5.61E-10 | 8.70E+04 | 1.89E-04 | 2.18E-09 | 6.69E+04 | 5.71E-05 | 8.53E-10 | - | - | - |
| NRCoV2-S2A4 | 3.49E+04 | 4.46E-04 | 1.28E-08 | 2.48E+05 | 2.36E-03 | 9.52E-09 | 5.88E+4 | 8.98E-4 | 1.53E-8 | - | - | - |
| NRCoV2-S2F3 | 1.56E+05 | 4.73E-04 | 3.03E-09 | | + | | | + | | 2.82E+05 | 1.39E-03 | 4.91E-09 |
| NRCoV2-S2G3 | 3.24E+05 | 6.06E-04 | 1.87E-09 | 2.98E+05 | 5.30E-04 | 1.78E-09 | 3.04E+05 | 5.63E-04 | 1.85E-09 | 1.87E+05 | 8.00E-04 | 4.27E-09 |
| NRCoV2-S2G4 | 8.93E+05 | 2.07E-04 | 2.32E-10 | 1.56E+06 | 2.92E-04 | 1.87E-10 | | + | | 9.20E+05 | 7.35E-04 | 7.99E-10 |
| NRCoV2-MRed11 | 4.57E+04 | 2.83E-04 | 6.20E-09 | 3.11E+04 | 4.26E-04 | 1.37E-08 | 4.54E+04 | 2.82E-04 | 6.21E-09 | - | - | - |
| NRCoV2-MRed18 | 1.97E+05 | 1.19E-03 | 6.03E-09 | 3.82E+05 | 4.93E-03 | 1.29E-08 | 3.69E+05 | 2.39E-03 | 6.48E-09 | 3.00E+05 | 6.77E-03 | 2.25E-08 |
| NRCoV2-MRed19 | 1.31E+05 | 1.18E-03 | 9.07E-09 | 1.83E+05 | 3.70E-03 | 2.02E-08 | 1.29E+05 | 1.04E-03 | 8.07E-09 | 2.49E+05 | 6.14E-03 | 2.46E-08 |
| NRCoV2-MRed20 | 1.60E+05 | 1.46E-05 | 9.18E-11 | 2.78E+05 | 1.53E-04 | 5.50E-10 | 1.39E+05 | 6.33E-05 | 4.55E-10 | 3.80E+05 | 4.06E-03 | 1.07E-08 |
| NRCoV2-MRed22 | 3.47E+05 | 1.76E-04 | 5.06E-10 | 8.96E+05 | 2.20E-04 | 2.46E-10 | | + | | - | - | - |
| NRCoV2-MRed25 | 1.12E+05 | 1.15E-04 | 1.02E-09 | 1.02E+06 | 2.89E-04 | 2.83E-10 | 2.05E+06 | 3.29E-03 | 1.60E-09 | 2.18E+04 | 5.01E-05 | 2.29E-09 |
| **Control** | | | | | | | | | | | | |
| ACE2-$H_6$[b] | 6.38E+04 | 9.79E-03 | 1.53E-07 | 8.52E+04 | 1.56E-03 | 1.83E-08 | 3.66E+04 | 4.78E-03 | 1.31E-07 | 1.11E+05 | 3.89E-02 | 3.51E-07 |
| VHH-72[b] | 1.23E+06 | 1.06E-01 | 8.62E-08 | 1.05E+06 | 1.01E-01 | 9.60E-08 | 8.01E+05 | 9.92E-02 | 1.24E-07 | 1.01E+06 | 6.56E-03 | 6.52E-09 |
| NRCsdAb022[b] | - | - | - | - | - | - | - | - | - | - | - | - |

[a]Binding parameters were determined by flowing monomeric $V_HHs$ over sensorchip surfaces coated with S, except for $V_HH$ NRCoV2-12 and MRed05, which were obtained by flowing monomeric RBDs (aa319-541 [SARS-CoV-2]; aa306-527 [SARS-CoV]) over $V_HH$-Fc-captured surfaces. Dashes indicate lack of binding. nd, not determined. [b]ACE2-$H_6$ and $V_HH$-72 (Wrapp et al., 2020), positive controls, EGFR-specific $V_HH$ NRCsdAb022 (Rossotti et al., 2019) negative control.

**[00206] Table 12.** SPR affinity ($K_D$) of $V_HHs$ against trimeric spikes protein S from the Wuhan-Hu-1 (Wuhan), UK B.1.1.7 (Alpha) and South Africa B.1.351 (Beta) SARS-CoV-2 variants

| $V_HH$/ACE2 | Subunit/domain specificity/epitope bin | $K_D$ (nM) | | |
|---|---|---|---|---|
| | | Wuhan | Alpha | Beta |
| ACE2 | S1-RBD | 153 | 18.3 | 131 |
| NRCoV2-1d | S1-RBD/Bin 1 | 0.75 | 0.91 | 1.2 |
| NRCoV2-07 | | 0.94 | 1.1 | 1.1 |
| NRCoV2-12 | | 0.047 | 0.046 | 0.04 |
| NRCoV2-18 | | 0.32 | 0.35 | 0.37 |
| NRCoV2-20 | | 4.39 | 4.97 | 5.47 |
| NRCoV2-MRed04 | | 0.86 | 0.91 | 1.07 |
| $V_HH$-72[1] | | 86.2 | 96 | 124 |
| NRCoV2-02 | S1-RBD/Bin 2,3 | 0.62 | 13.6 | -[3] |
| NRCoV2-05 | | 2.6 | 11.4 | - |
| NRCoV2-10 | S1-RBD/Bin 2,3,4 | 0.2 | 0.21 | 9.73 |
| NRCoV2-15 | | 0.32 | 0.31 | 22.2 |
| NRCoV2-MRed05 | | 0.91 | 0.31 | 0.89 |
| NRCoV2-14 | S1-RBD/Bin 2,4 | 2.6 | 2.44 | weak binding |
| NRCoV2-17 | S1-RBD/Bin 3,4 | 0.15 | 0.13 | 5.1 |
| NRCoV2-04 | S1-RBD/Bin 4 | 10.2 | 11.7 | - |
| NRCoV2-06 | S1-RBD/Bin 5 | 223 | 229 | 248 |
| NRCoV2-11 | | 0.018 | 0.017 | 0.023 |
| NRCoV2-03 | S1-RBD/Bin 6 | 1.56 | 1.49 | 4.08 |
| NRCoV2-SR01 | S1-NTD/Bin 7,9,10 | 0.56 | 0.59 | 0.2 |
| NRCov2-SR03 | | 1.69 | 1.72 | 2.49 |
| NRCoV2-SR13 | | 3.6 | 5.8 | 7 |
| NRCoV2-SR16 | | 2 | 1.6 | 2.6 |
| NRCoV2-MRed03 | S1-NTD/Bin 8 | 0.51 | 0.36 | 0.67 |
| NRCov2-MRed06 | | 5.2 | 5.72 | 7.24 |
| NRCoV2-MRed07 | S1-NTD/Bin 9 | 0.11 | 0.26 | 0.23 |
| NRCoV2-SR04 | S1-NTD/Bin 7,9 | 0.14 | 0.27 | 0.32 |
| NRCoV2-SR02 | S1-NTD/Bin 10 | 0.47 | 0.11 | 0.53 |
| NRCoV2-S2A3 | S2/Bin 11 | 0.56 | 2.18 | 0.85 |
| NRCoV2-S2A4 | S2/Bin 12 | 12.8 | 9.5 | 15.3 |

| | | | | |
|---|---|---|---|---|
| NRCoV2-S2F3 | | 3.03 | +[4] | +[4] |
| NRCoV2-MRed18 | | 6.03 | 12.9 | 6.48 |
| NRCoV2-MRed19 | S2/Bin 13 | 9.07 | 20.2 | 8.07 |
| NRCoV2-MRed20 | | 0.092 | 0.55 | 0.45 |
| NRCoV2-MRed22 | | 0.51 | 0.25 | +[4] |
| NRCoV2-S2G3 | S2/Bin 14 | 1.87 | 1.78 | 1.85 |
| NRCoV2-S2G4 | S2/Bin 15 | 0.23 | 0.19 | +[4] |
| NRCoV2-MRed11 | S2/Bin 16 | 6.2 | 13.7 | 6.2 |
| NRCoV2-MRed25 | S2/Bin 17 | 1.02 | 0.28 | 1.6 |

[1]$V_HH$-72 is the benchmark (Wrapp et al., 2020); [2]nd, not determined; [3]"-", no binding; [4]"+", $V_HH$ bound, but poor fitting precluded $K_D$ determination. Epitope bin numbers correspond to the bins shown in **Fig. 9G**.

**Example 6: Cell Binding Assays by Flow Cytometry**

***Introduction***

**[00207]** In the previous Examples, lead $V_HHs$ were shown to be binding to SARS-CoV-2 S in its purified form. In this Example, it was confirmed whether the $V_HHs$ also bind to SARS-CoV-2 S in its more natural context, i.e., displayed on the cell membrane of CHO cells.

***Materials and Methods***

**[00208]** A stable Chinese hamster ovary (CHO) cell line CHO$^{BRI\ TM}$/55E1 (Stuible et al., 2021) overexpressing SARS-CoV-2 S (CHO-S) was grown in BalanCD™ CHO Growth A medium (Irvine Scientific) supplemented with 50 µM of methionine sulfoximine (MSX) at 120 rpm and 37°C in a humidified 5% $CO_2$ atmosphere. When the cell count reached 2 x $10^6$/mL, the expression of the membrane anchored SARS-CoV-2 trimeric spike protein (SmT1, described in Stuible et al, 2021) was induced by adding cumate at 2 µg/mL. Expression was carried out for 48 h at 32°C. For flow cytometry experiments, cells were harvested by centrifugation and resuspended at 1 x $10^6$ cells/mL in PBSB (1% PBS containing 1% BSA and 0.05 [v/v] sodium azide). Cells were kept on ice until use. Serially, three-fold dilutions of $V_HH$-Fcs were prepared in V-Bottom 96-well microtest plates (Globe Scientific, Cat# 120130) and mixed with 50 µL of CHO-S cells. Plates were incubated for 1 h on ice, washed twice with PBSB by centrifugation 5 min at 1200 rpm and then incubated for an additional hour with 50 µL of R-Phycoerythrin AffiniPure F(ab')$_2$ Fragment Goat Anti-Human IgG (Jackson Immunoresearch, Cat#109-116-170) at 250 ng/mL diluted in

PBSB. After a final wash, cells were resuspended in 100 µL PBSB and data were acquired on a Beckman Culter CytoFlex S and analyzed by FlowJo™ (FlowJo LLC, v10.6.2, Ashland).

***Results and Discussion***

**[00209]** Interestingly, four $V_HH$-Fcs (NRCoV2-08, NRCoV2-19, NRCoV2-21, NRCoV2-S202) which bound to SARS-CoV-2 S in purified form did not bind to SARS-CoV-2 S-displaying target cells. The remaining 41 $V_HH$-Fcs, however, bound to cells in a dose dependent manner (**Fig. 8A-B**; **Table 13**). Aside from NRCoV2-03 which had a modest apparent affinity ($EC_{50}$app) of ~ 80 nM, the remaining 18 S1-RBD-specific $V_HH$-Fcs bound to S-displaying CHO-S cells with high affinities ($EC_{50}$ range: 0.3 – 8.1 nM; $EC_{50}$ median: 1 nM). For S1-NTD-binders, excluding the outlier NRCoV2-MRed07 ($EC_{50}$ = 132 nM), the apparent $EC_{50}$s for the remaining $V_HH$s were also high (range: 1.2 – 15.1 nM; median: 7 nM). Similarly, affinities for S2-specific $V_HH$-Fcs were also high ($EC_{50}$ range: 0.1 – 6.5; $EC_{50}$ median: 1 nM). $V_HH$-72 benchmark with an $EC_{50}$ of 0.2 nM ranked amongst the strongest S1-RBD-specific binders.

**[00210] Table 13.** Summary of $V_HH$-Fc bindings to SARS-CoV-2 S expressing CHO-S cells

| **S1-RBD-specific** | | | **S1-NTD-specific** | | | **S2-specific** | | |
|---|---|---|---|---|---|---|---|---|
| **$V_HH$-Fc** | **$EC_{50}$ (nM)** | **$B_{max}$** | **$V_HH$-Fc** | **$EC_{50}$ (nM)** | **$B_{max}$** | **$V_HH$-Fc** | **$EC_{50}$ (nM)** | **$B_{max}$** |
| NRCoV2-1a | 1.1 | 17186 | NRCoV2-SR01 | 6.6 | 15389 | NRCoV2-S2A3 | 0.44 | 9819 |
| NRCoV2-1d | 1.1 | 13817 | NRCoV2-SR02 | 1.2 | 14416 | NRCoV2-S2A4 | 0.1 | 6858 |
| NRCoV2-02 | 0.3 | 18553 | NRCoV2-SR03 | 7.1 | 19857 | NRCoV2-S2B3 | 6.5 | 6665 |
| NRCoV2-03 | 78.9 | 16242 | NRCoV2-SR04 | 8.2 | 10119 | NRCoV2-S2F3 | 2.7 | 6953 |
| NRCoV2-04 | 1.3 | 15489 | NRCoV2-SR13 | 7.0 | 17808 | NRCoV2-S2G3 | 0.3 | 7529 |
| NRCoV2-05 | 0.5 | 17419 | NRCoV2-SR16 | 1.4 | 11553 | NRCoV2-S2G4 | 0.3 | 6897 |
| NRCoV2-06 | 8.1 | 13615 | NRCoV2-MRed03 | 15.1 | 11990 | NRCoV2-S2H4 | 1.0 | 7906 |
| NRCoV2-07 | 1.1 | 10620 | NRCoV2-MRed06 | 8.5 | 9023 | NRCoV2-S202 | - | - |
| NRCoV2-08 | - | - | NRCoV2-MRed07 | 132.4 | 8673 | NRCoV2-MRed11 | 2.9 | 3249 |

| | | | | | | | | |
|---|---|---|---|---|---|---|---|---|
| NRCoV2-10 | 1.3 | 28044 | | | | NRCoV2-MRed18 | 0.9 | 10205 |
| NRCoV2-11 | 4.3 | 18230 | | | | NRCoV2-MRed19 | 1.3 | 5482 |
| NRCoV2-11a | 2.0 | 11963 | | | | NRCoV2-MRed20 | 6.5 | 6665 |
| NRCoV2-12 | 0.8 | 21821 | | | | NRCoV2-MRed22 | 0.2 | 5324 |
| NRCoV2-14 | 0.9 | 18801 | | | | NRCoV2-MRed25 | 0.8 | 4421 |
| NRCoV2-15 | 0.8 | 21053 | | | | | | |
| NRCoV2-17 | 0.4 | 19019 | | | | | | |
| NRCoV2-18 | 0.9 | 18266 | | | | | | |
| NRCoV2-19 | - | - | | | | | | |
| NRCoV2-20 | 0.7 | 12056 | | | | | | |
| NRCoV2-21 | - | - | | | | | | |
| NRCoV2-MRed04 | 4.2 | 14916 | | | | | | |
| NRCoV2-MRed05 | 0.5 | 17349 | | | | | | |
| $V_HH$-72 | 0.2 | 8026 | | | | | | |

"-", No detectable binding observed.

**Example 7: Epitope Studies**

***Introduction***

**[00211]** Western blotting experiments were performed to determine if $V_HHs$ bind to conformational or linear epitopes. Additionally, competitive sandwich ELISA as well as SPR were performed to differentiate $V_HHs$ with respect to recognizing non-overlapping epitopes.

***Materials and Methods***

**[00212]** *Epitope typing by sodium dodecyl sulphate-polyacrylamide gel electrophoresis/western blotting (SDS-PAGE/WB)*

**[00213]** A standard SDS-PAGE/WB was performed to detect the binding of $V_HHs$ to nitrocellulose-immobilized, denatured SARS-CoV-2 S. Briefly, 10 µg/lane of S was run on 4–20% Mini-PROTEAN® TGX Stain-Free™ Protein Gels (Bio-Rad, Cat# 4568081), transferred to nitrocellulose (Sigma, Cat#GE10600002) and blocked with 1% PBSC overnight at 4°C. Then, 0.5-cm nitrocellulose strips containing the denatured S were placed on Mini Incubation Trays (Bio-Rad, Cat#1703902) and incubated with 1 mL of 1 µg/mL $V_HH$-Fcs or biotinylated $V_HHs$ ($V_HH$-BAP-$His_6$). After 1 h incubation at room temperature, strips were washed 10 times with PBST and the binding of $V_HH$-Fcs or biotinylated $V_HHs$ to denatured S was probed, respectively, by incubating strips with 1 mL of 100 ng/mL anti-human Ig Fc antibody-peroxidase conjugate or streptavidin-peroxidase conjugate (Jackson ImmunoResearch, Cat#016-030-084) at room temperature for 1 h. Finally, strips were washed 10 times with PBST and peroxidase activity was detected using chemiluminescent reagent (SuperSignal™ West Pico PLUS Chemiluminescent Substrate, ThermoFisher, Cat#34580). Images of developed strips were acquired on Molecular Imager® Gel Doc™ XR System (Bio-Rad, Cat#1708195EDU).

**[00214]** *Epitope binning by SPR*

**[00215]** Standard SPR techniques were used for binding studies. All SPR assays were performed on a Biacore™ T200 instrument (Cytiva) at 25°C with HBS-EP running buffer (10 mM HEPES, 150 mM NaCl, 3 mM EDTA, 0.005 % [v/v] Tween® 20, pH 7.4) and CM5 sensor chips (Cytiva). Prior to SPR analyses all analytes in flow ($V_HHs$, ACE2 receptor) were SEC-purified on a Superdex® 75 Increase 10/300 GL column (Cytiva) in HBS-EP buffer at a flow rate of 0.8 mL/min to obtain monomeric proteins. $V_HH$ epitope binning was performed by SPR dual injection experiments on the SARS-CoV-2 S at a flow rate of 40 µL/min in HBS-EP buffer. Dual injections consisted of injection of $V_HH1$ (at 50 – 100 × $K_D$ concentration) for 150 s, followed by immediate injection of a mixture of $V_HH1$ + $V_HH2$ (both at 50 – 100 × $K_D$ concentration) for 150 s. The opposite orientation was also performed ($V_HH2$ followed by $V_HH2$ + $V_HH1$) (**Fig.9C**). Surfaces were regenerated using a 12 s pulse of 10 mM glycine, pH 1.5, at a flow rate of 100 µL/min. All

pairwise combinations of $V_HHs$ were analyzed and distinct or overlapping epitope bins determined.

**[00216]** *Epitope binning by ELISA*

**[00217]** The pairwise ability of $V_HHs$ to bind to their antigen in a sandwich ELISA format was evaluated as described previously (Rosotti et al., 2015a; Delfin-Riela et al., 2020), (**Fig. 9D**). Briefly, a matrix of 14 wells (row) × 23 wells (column) was generated using six NUNC® MaxiSorp™ 4BX plates (Thermo Fisher) and coated overnight at 4°C with 4 µg/mL streptavidin (Jackson ImmunoResearch, Cat#016-000-113) in 100 µL PBS, pH 7.4. Wells were blocked with 200 µL PBSC for 1 h at room temperature and then biotinylated $V_HHs$ (10 µg/mL in 100 µL PBSCT) were captured in each row (same $V_HH$ in each row; 14 rows for a total of 14 $V_HHs$) for 1 h at room temperature. Wells were washed 5 times with PBST and incubated with 100 ng/mL of SARS-CoV-2 S1 diluted in PBSCT for 1 h. Wells were washed and each column was incubated with the pairing, $V_HH$-Fcs/ACE2-Fc at 1 µg/mL used as detector antibodies (same $V_HH$-Fc in each column; 23 column for a total of 22 $V_HH$-Fcs and ACE2-Fc). The binding of $V_HH$-Fcs/ACE2-Fc to S1 was detected using 100 µL 1 µg/mL HRP-conjugated goat anti-human IgG (SIGMA, Cat#A0170). Finally, plates were washed 10 times with PBST and peroxidase activity was determined as described above. The same procedure was carried out performing a matrix of 17 well (row) x 20 wells (column) as shown in **Fig. 9E**.

***Results and Discussion***

**[00218]** To determine whether $V_HHs$ recognize conformational or linear epitopes, they were subjected to binding analysis against SARS-CoV-2 S by denaturing, SDS-PAGE/Western blot. As shown in **Fig. 9A** using the monomeric $V_HHs$ as probe, three out of 26 $V_HHs$ tested bound to denatured S, indicating they were recognizing linear epitopes, while the remaining $V_HHs$ appeared to be conformational epitope-specific based on their lack of significant binding to denatures S. In assays where $V_HH$-Fc was used instead of $V_HH$, 15 out of 37 $V_HH$-Fcs tested were determined to bind to linear epitopes (**Fig. 9B**). These linear epitope-specific $V_HHs$ give the option of virus detection against denatured S by robust diagnostic techniques such as SDS-PAGE/Western blot, where the additional molecular weight information provided by the SDS-PAGE would serve as a

second, confirmatory piece of information to eliminate/reduce false positives obtained by binding data alone.

**[00219]** To identify the number of distinct (non-overlapping) epitopes, $V_HHs$ were subjected to epitope binning experiments by SPR and sandwich ELISA. In SPR epitope binning assays, the first $V_HH$ ("$V_HH1$") was flowed over a spike protein-immobilized sensorchip and allowed to saturate its epitope, followed by the addition of the second, $V_HH2$ applied as a mixture of $V_HH1$ + $V_HH2$ to keep the $V_HH1$ epitope saturated during the binding of $V_HH2$. Assays were performed in a second orientation as well to cross-confirm results: $V_HH2$ + ($V_HH2$+ $V_HH1$). **Fig. 9C** (left panel) exemplifies a $V_HH$ pair (NRCoV2-02/NRCoV2-05) binding to an overlapping epitope, hence belonging to the same epitope bin, as the addition of the second $V_HH$ does not result in any increased binding (i.e., increase in RU) over that obtained for the addition of the first $V_HH$. **Fig. 9C** (right panel), on the other hand, exemplifies a $V_HH$ pair (NRCoV2-02/NRCoV2-07) binding to non-overlapping epitopes, hence belonging to different epitope bins, as the addition of the second $V_HH$ results in significant increase in binding over that already achieved by the addition of the first $V_HH$. SPR assays were performed with combination pairs of nine $V_HHs$, including $V_HH$-72 against S1-RBD, six $V_HHs$ against S1 and 10 $V_HHs$ against S2. A conceptually similar assay to SPR was performed for 14 more S1-RBD-specific $V_HHs$ by a sandwich ELISA to further expand on epitope bins identified by SPR for the S1-RBD-specific $V_HHs$ (**Figs. 9D** (initial results) and **9E** (further results)). The sandwich ELISA allowed for the rapid identification of antibody pairs that simultaneously bound to the antigen, hence to non-overlapping epitopes. ACE2 and the benchmark $V_HH$, $V_HH$-72, were also included in the epitope binning experiments. The ELISA experiments confirmed the results of epitope binning by SPR, expanded the number of binders within each epitope bin, and identified new epitope bins. The epitope binning results obtained by SPR and ELISA are summarized in **Figs. 9F** (initial results), **9G** (further results) and **Table 14.** Initial binning results identified 14 non-overlapping/partially overlapping bins: six for S1-RBD-specific $V_HHs$, three for S1-NTD-specific $V_HHs$ and five for S2-specific $V_HHs$. Benchmark $V_HH$-72 binned with S1-RBD-specific $V_HHs$ NRCoV2-1a/1c/1d, NRCoV2-07, NRCoV2-12, NRCoV2-18, NRCoV2-20, MRed02 and NRCov2-MRed04. Thirteen out of 22 RBD-specific $V_HHs$ tested, binned with ACE2 (**Fig. 9F**). Further characterization led to the identification of 17 non-overlapping/partially overlapping bins: six for S1-RBD-specific $V_HHs$, four for S1-NTD-specific $V_HHs$ and seven for S2-specific $V_HHs$ (as shown in **Fig. 9G**).

**[00220] Table 14:** Summary of epitope binning results

| $V_HH$ | CDR 1 | SEQ ID NO: | CDR 2 | SEQ ID NO: | CDR 3 | SEQ ID NO: | Domain/subunit specificity | Epitope Bin |
|---|---|---|---|---|---|---|---|---|
| NRCoV2-SR01 | GFTFDNYA | 21 | ISGNGGVT | 65 | AATGIRSTWSVYGCSRLAGPYDY | 111 | S1-NTD | 7/9/10 |
| NRCoV2-SR03 | GSIFSNNH | 23 | ISSGGKT | 67 | NRGGWEYRSSYYIMGPH | 113 | S1-NTD | 7/9/10 |
| NRCoV2-SR13 | GSRFGSKH | 25 | ISSGGST | 69 | NMGGWDYRSNTYIPGSRSDY | 115 | S1-NTD | 7/9/10 |
| NRCoV2-SR16 | GTTFSRYH | 26 | ISTSGAV | 70 | NTGGWDYRSSTFIMGLN | 116 | S1-NTD | 7/9/10 |
| NRCoV2-SR04 | GRTFSSHT | 24 | ISMGGNTNYA | 68 | NTAALVGNRLLPMATIT | 114 | S1-NTD | 7/9 |
| NRCoV2-MRed03 | GFTLDYYA | 20 | ISSSDGST | 81 | ATDAFATCDSWYAQIAQYDF | 126 | S1-NTD | 8 |
| NRCoV2-MRed06 | GFTLAYYA | 37 | ISSSDGSA | 82 | ATDSFSSCSDYESGMDF | 128 | S1-NTD | 8 |
| NRCoV2-MRed07 | GSIGPFNT | 38 | ITRGGVT | 83 | YANYGWAIPY | 129 | S1-NTD | 9 |
| NRCoV2-SR02 | EFTLNYYS | 22 | IRYSGGGI | 66 | AADRLYSRACPTAGGRNY | 112 | S1-NTD | 10 |
| NRCoV2-1a | GSTLDYYA | 1 | VSSSDGST | 45 | AADYSMRPLWVSRWHRDYEY | 90 | S1-RBD | 1 |
| NRCoV2-1c | GSILDYYA | 2 | VSSSDGST | 45 | AADYSMRRFAVGRWHRDYEY | 91 | S1-RBD | 1 |
| NRCoV2-1d | GSTLDYYA | 1 | VSSSDGNT | 46 | AADYSMRPFAVGRWHRDYEY | 92 | S1-RBD | 1 |
| NRCoV2-07 | GVTLDYYA | 8 | ISSNGRRN | 52 | AAVQDVHGDNYYCTSPNEYNV | 98 | S1-RBD | 1 |
| NRCoV2-12 | GRTFRNYV | 13 | VAAISWGGTEI | 57 | AADRGLSYYYTRTTEYNY | 103 | S1-RBD | 1 |
| NRCoV2-18 | GITISGYN | 17 | INSGGST | 61 | SLHTSHDY | 107 | S1-RBD | 1 |
| NRCoV2-20 | GRTFSNYV | 19 | VAVISGSDTET | 63 | AADRGMSYYYTRATEYYY | 109 | S1-RBD | 1 |
| NRCoV2-MRed02 | GNIFSINS | 35 | IWSDSRT | 79 | AADRGFVVRGQYDY | 125 | S1-RBD | 1 |
| NRCoV2-MRed04 | GNSFSINT | 36 | IWSDTTT | 80 | AADRGFVVRGQYDY | 125 | S1-RBD | 1 |
| NRCoV2-04 | GSPFSNVV | 5 | ISGGGIA | 49 | WSSYEST | 95 | S1-RBD | 4 |
| NRCoV2-06 | VSTFSSYA | 7 | IGFVGAT | 51 | NARHYGGSEY | 97 | S1-RBD | 5 |
| NRCoV2-03 | GITFSYYA | 4 | MSNMDST | 48 | NIYGPTYSTRRNEY | 94 | S1-RBD | 6 |
| NRCoV2-08 | GFTLDDYA | 9 | ISRSGTTT | 53 | AADYQYSTYCLGYDAHYEY | 99 | S1-RBD | 6 |
| NRCoV2-11 | GSSLDSYS | 11 | ISRYYSST | 55 | AARSRDFSSPFSATDTYTS | 101 | S1-RBD | 6 |
| NRCoV2-11a | GFTLDSYN | 12 | ISRYYEST | 56 | AARSRDFSSPISATDKYGS | 102 | S1-RBD | 6 |

| | | | | | | | | |
|---|---|---|---|---|---|---|---|---|
| NRCoV2-02 | GFTFSNYA | 3 | ISGRGDDT | 47 | TKGPDLYYFGSGYSD | 93 | S1-RBD | 2,3 |
| NRCoV2-05 | GFIFSNYA | 6 | INSGGGDT | 50 | SKGPVSSYYGSGYDY | 96 | S1-RBD | 2,3 |
| NRCoV2-10 | GNTFSRSN | 10 | ISSRGIS | 54 | YAADDLGDY | 100 | S1-RBD | 2,3,4 |
| NRCoV2-15 | GSTSGRNT | 15 | VSTSGAT | 59 | YAAYGGGGDY | 105 | S1-RBD | 2,3,4 |
| NRCoV2-MRed05 | GFTLDYYA | 20 | ISSSDGST | 81 | ATGPQAYYSGSYYFQCPQAGMDY | 127 | S1-RBD | 2,3,4 |
| NRCoV2-14 | GTTFSHYA | 14 | ISVFGST | 58 | HAVNADIGGDY | 104 | S1-RBD | 2,4 |
| NRCoV2-17 | GSPFSQLA | 16 | ISPTGNR | 60 | QAANVNGGDY | 106 | S1-RBD | 3,4 |
| NRCoV2-19 | GLTLNSYA | 18 | LTSGGTG | 62 | AADRARLRFGCSLNFRREVAYDY | 108 | S1-RBD | ud |
| NRCoV2-21 | GFTLDYYA | 20 | ISSGGST | 64 | AADHRGRSLRFGCSSSTTDYLY | 110 | S1-RBD | ud |
| NRCoV2-S2A3 | GRPYSNYA | 27 | KQRELVAAISSGGTT | 71 | NTGSLSYGGSVYYPSYDN | 117 | S2 | 11 |
| NRCoV2-S2A4 | GSPFRSNV | 28 | ISTGGSR | 72 | HAAARDSHGIYLLLDT | 118 | S2 | 12 |
| NRCoV2-S2F3 | VRILSVPA | 31 | ITSGGST | 75 | NLRDILSQPF | 121 | S2 | 13 |
| NRCoV2-MRed18 | TTVFGRNA | 40 | VSDGGTP | 85 | NYYNYYYGRNF | 131 | S2 | 13 |
| NRCoV2-MRed19 | TIIFKGQT | 41 | MTTSGSA | 86 | YMHSVYYGIDY | 132 | S2 | 13 |
| NRCoV2-MRed20 | GLSFSSYD | 42 | IRESGSGT | 87 | AAKPPFYGSGTYSTPRAYLY | 133 | S2 | 13 |
| NRCoV2-MRed22 | GSVFASNA | 43 | ISSRGST | 88 | NAREFTGFDY | 134 | S2 | 13 |
| NRCoV2-S2G4 | GSTFSGYA | 33 | ISSDGDK | 77 | NKHWWTGDW | 123 | S2 | 14 |
| NRCoV2-S2G3 | GSTFGIFL | 32 | ITSGGAT | 76 | YTTKRDDASVY | 122 | S2 | 15 |
| NRCoV2-MRed11 | GFTFSSYA | 39 | INSGGGST | 84 | ATTISDGSSWSTKSY | 130 | S2 | 16 |
| NRCoV2-MRed25 | GHTFSRYG | 44 | ISWRGDST | 89 | AAEMWGTATIVASRYTY | 135 | S2 | 17 |
| NRCoV2-S2B3 | ASTFGDSA | 29 | ISTGSNT | 73 | NYRSIYYGQNF | 119 | S2 | nd |
| NRCoV2-S2H4 | GFTFNLYS | 30 | INSGDRDSTT | 74 | ALVFGYTSRDYCLTPKRGNY | 120 | S2 | nd |
| NRCoV2-S202 | GITVSRIG | 34 | ISAGGST | 78 | NYGPGYRKAA | 124 | S2 | nd |

nd = no data, ud = undetermined. Epitope bin numbers correspond to the bins shown in **Fig. 9G**.

**Example 8: Surrogate Virus Neutralization Assays**

***Introduction***

**[00221]** Surrogate neutralization assays were performed to identify potential neutralizing $V_HHs/V_HH$-Fcs, i.e., $V_HHs/V_HH$-Fcs inhibiting SARS-CoV-2 viruses from entering host cells. Three different surrogate assays were performed: ELISA, SPR and flow cytometry. In ELISA and SPR, ACE2 and SARS-CoV-2 S acted as surrogates for an ACE2-containing host cell and an S-containing invading virus, respectively. In flow cytometry assays, which were performed directly against the host cell (Vero E6), S1-RBD or S served as surrogate virus. Antibodies that interfered with the binding of spike fragment proteins to ACE2 in the surrogate assays were considered to be neutralizing antibodies.

***Materials and Methods***

**[00222]** *ACE2 competition assay by ELISA*

**[00223]** Wells of NUNC® MaxiSorp™ microtiter plates (Thermo Fisher) were coated overnight at 4°C with 50 ng/well of S in 100 µL PBS, pH 7.4. Next day, plates were blocked with 250 µL PBSC for 1 h at room temperature. For ACE2/$V_HH$ competition binding to SARS-CoV-2 S, 50 µL of ACE2-Fc (ACROBiosystems, Cat#AC2-H5257) at 400 ng/mL was mixed with 50 µL of $V_HH$ at 1 µM, and then transferred to SARS-CoV-2 S coated microtiter plate wells. After 1 h incubation at room temperature, plates were washed 10 times with PBST and the ACE2-Fc binding was detected using 1 µg/mL goat anti-human IgG (Fc specific)–peroxidase antibody (SIGMA, Cat# A0170) in 100 µL PBSCT. After 10 washes with PBST, the peroxidase activity was determined as described above.

**[00224]** *ACE2 competition assay by SPR*

**[00225]** Standard SPR techniques were used for binding studies. All SPR assays were performed on a Biacore™ T200 instrument (Cytiva) at 25°C with HBS-EP running buffer (10 mM HEPES, 150 mM NaCl, 3 mM EDTA, 0.005 % [v/v] Tween® 20, pH 7.4) and CM5 sensor chips (Cytiva). Prior to SPR analyses, all analytes in flow ($V_HHs$, ACE2 receptor) were SEC-purified on a Superdex™ 75 Increase 10/300 GL column (Cytiva) in HBS-EP buffer at a flow rate of 0.8

mL/min to obtain monomeric proteins. $V_HHs$ were analyzed for their ability to block the SARS-CoV-2 spike trimer (S) interaction with ACE2 using SPR dual injection experiments. $V_HHs$ and ACE2 were flowed over the SARS-CoV-2 S surface at 40 µL/min in HBS-EP buffer. Dual injections consisted of injection of ACE2 (1 µM) for 150 s, followed by immediate injection of a mixture of ACE2 (1 µM) + $V_HH$ (at 20 – 40 × $K_D$ concentration) for 150 s. The opposite orientation was also performed ($V_HH$ followed by $V_HH$ + ACE2). Surfaces were regenerated using a 12 s pulse of 10 mM glycine, pH 1.5, at a flow rate of 100 µL/min. All pairwise combinations of $V_HHs$ and ACE2 were analyzed. $V_HHs$ that competed with ACE2 for SARS-CoV-2 spike trimer binding showed no increase in binding response during the second injection. Conversely, a binding response was seen during the second injection for $V_HHs$ that did not compete with ACE2.

**[00226]** *ACE2 competition assay by flow cytometry*

**[00227]** Experiments were performed essentially as described in Example 2. Briefly, 400 ng of chemically biotinylated trimeric SARS-CoV-2 S was mixed with $5 \times 10^4$ Vero E6 cells in the presence of decreasing concentrations of $V_HHs$ or $V_HH$-Fcs in a final volume of 150 µL. Following 1 h incubation on ice, cells were washed twice with PBSB by centrifugation at 1200 rpm for 5 min and then incubated for an additional hour with 50 µL Streptavidin, R-Phycoerythrin Conjugate (SAPE, ThermoFisher, Cat#S866) at 250 ng/mL diluted in PBSB. After a final wash, cells were resuspended in 100 µL PBSB and data were acquired on a CytoFlex™ S flow cytometer (Beckman Culter) and analyzed by FlowJo™ (FlowJo LLC, v10.6.2, Ashland, OR). As an internal reference for competition experiments, a competition assay with recombinant human ACE2-$His_6$ in lieu of $V_HH$ was also included. A20.1, a *C. difficile* toxin A-specific $V_HH$ (Hussack et al., 2011) was used as negative control $V_HH$. Percent inhibition (neutralization) was calculated according to the following formula: % inhibition = 100 x [1 - ($F_n$ - $F_{min}$) / ($F_{max}$ - $F_{min}$)], where, $F_n$ is the measured fluorescence at any given competitor $V_HH$ concentration, $F_{min}$ is the background fluorescence measured in the presence of cells and SAPE only, and $F_{max}$ is the maximum fluorescence, measured in the absence of $V_HH$ competitor.

***Results and Discussion***

**[00228]** Initially, a total of 26 $V_HHs$ (14 S1-RBD-specific, 6 S1-NTD-specific and 6 S2-specific) were subjected to competitive ELISA, to identify those that are neutralizing, i.e., reduce the

binding of ACE2-Fc to S. As shown in **Fig. 10**, the majority of S1-RBD binders were significantly neutralizing, with NRCoV2-1d, NRCoV2-02, NRCoV2-05 and NRCoV2-07 displaying essentially 100% inhibition and outperforming the $V_HH$-72 benchmark. Two of the S1-NTD-specific $V_HHs$ (NRCoV2-SR01, NRCoV2-SR02) showed significant neutralization, with NRCoV2-SR02 essentially neutralizing at 100%. None of the S2 binders showed significant neutralizing activity. A conceptually similar assay to ELISA was performed by a competitive SPR. The results are shown in **Fig. 11** and **Table 16.** The four lead neutralizers identified by ELISA, i.e., NRCoV2-01d, NRCoV2-02, NRCoV2-05 and NRCoV2-07, were confirmed by SPR to be complete neutralizers ('blockers"). NRCoV2-14, NRCoV2-15, NRCoV2-18 and NRCoV2-20 showed partial neutralization ("+/-"; **Table 16**). The remaining $V_HHs$ tested were judged to be non-neutralizing. Although the ELISA and SPR results agreed in the case of the majority of $V_HHs$, there was some disagreement. For example, while NRCoV2-SR02, NRCoV2-06, NRCoV2-10, and NRCoV2-11 were neutralizing by ELISA, they were not found to be neutralizing by SPR. Conversely, NRCoV2-20 was judged to be somewhat neutralizing by SPR, but non-neutralizing by ELISA.

**[00229]** Finally, a quantitative surrogate neutralization assay was performed by flow cytometry, where antibodies were assessed based on their ability to block the interaction of trimeric SARS-CoV-2 S with ACE2 on the surface of Vero E6 cells (African green monkey kidney cells). (Vero E6 cells are known to be highly susceptible to infection by SARS-CoV-2 and SARS-CoV.) Both monomeric $V_HHs$ and bivalent $V_HH$-Fcs were assessed. $IC_{50}$s, $IC_{99}$s and $I_{max}$% values, measures of potency and efficacy were used to rank neutralizing antibodies. A preliminary screen performed at a single concentration with S1-RBD-, S1-NTD- and S2-specfic $V_HHs$ showed that many of the S1-RBD-specific $V_HHs$ were potent neutralizers (**Fig. 12A**). Assays were also performed at multiple $V_HH$ concentrations allowing determination of $IC_{50}$s and $I_{max}$% values (**Fig. 12B; Table 17**). The $I_{max}$% for NRCoV2-SR13 was too low to warrant a reliable $IC_{50}$ determination for this $V_HH$. In agreement with the preliminary results, all of the neutralizers were S1-RBD-specific with many exhibiting high neutralization potencies and efficacies. In particular, NRCoV2-1d, NRCoV2-02, NRCoV2-05 and NRCoV2-07 led others with $IC_{50}$/ $I_{max}$% values of 8.6 nM/72%, 5.1 nM/100%, 9.5 nM/97%, and 7.5 nM/86%, respectively. A second group of $V_HHs$, including NRCoV2-10, NRCoV2-14, NRCoV2-15, NRCoV2-18, NRCoV2-20 and NRCoV2-MRed04 were also potent/efficacious neutralizers (**Table 17**). All of these antibodies outperformed the

benchmark $V_HH$-72, which had a far higher $IC_{50}$ (59 nM). NRCoV2-11 and NRCoV2-17 although showing high potencies ($IC_{50}$s of 16.8 nM and 9.4 nM, respectively), had weak efficacies ($I_{max}$% values of 20% and 18%, respectively). None of the S1-NTD or S2 binders was neutralizing. The results obtained by flow cytometry correlated well with those obtained by ELISA and SPR.

**[00230]** To increase the neutralization potency and efficacy of the $V_HH$s, they were reformatted as bivalent $V_HH$-Fcs. The increase in size (from 16 kDa $V_HH$ to 80 kDa $V_HH$-Fc) as well as avidity (from monovalent $V_HH$ to bivalent $V_HH$-Fc) could sterically hinder the binding of S to ACE2 and increase $V_HH$s' apparent affinity leading to their improved neutralization potency and efficacy. Thus, $V_HH$-Fcs were generated and tested in flow cytometry surrogate neutralization assays as described above. The majority of $V_HH$-Fcs demonstrated high potencies and efficacies (**Figs. 13A-B**; **Table 17**). Reformatting had a significant effect on the neutralization potencies/efficacies of $V_HH$s. As for S1-RBD-specific $V_HH$s, reformatting imparted neutralization capability to NRCoV2-04, and significantly improved the neutralization potency/efficacy of NRCoV2-11, NRCoV2-14, NRCoV2-15, NRCoV2-17, and NRCoV2-18, as well as the $V_HH$-72 benchmark. The potency and efficacy of NRCoV2-1d, NRCoV2-02, NRCoV2-05 and NRCoV2-07 were not essentially affected with reformatting, except for NRCoV2-1d whose $I_{max}$% was increased from 72% ($V_HH$) to 89% ($V_HH$-Fc). Reformatting had a more profound effect on S1-NTD-specific $V_HH$s, transforming six $V_HH$s (NRCoV2-SR01, NRCoV2-SR02, NRCoV2-SR03, NRCoV2-SR04, NRCoV2-SR16, and NRCoV2-MRed07) into neutralizing antibodies, with some displaying strong potencies/efficacies (NRCoV2-SR01, NRCoV2-SR02, and NRCoV2-SR13). As for S2-specfic $V_HH$-Fcs, none was found to be neutralizing. Based on $IC_{99}/I_{max}$% values, many $V_HH$-Fcs outperformed the $V_HH$-72 benchmark. These included S1-RBD-specific $V_HH$-Fcs NRCoV2-1a, NRCoV2-1d, NRCoV2-02, NRCoV2-05, NRCoV2-07, NRCoV2-11, NRCoV2-11a, NRCoV2-12, NRCoV2-14, NRCoV2-15, NRCoV2-17, NRCoV2-20, NRCoV2-MRed04, NRCoV2-MRed05 and the S1-NTD-specific $V_HH$-Fcs NRCoV2-SR02 and NRCoV2-SR03.

**[00231]** The surrogate neutralization assays were then extended to variants Alpha, Beta, Gamma, Delta, Kappa and Omicron using all of the RBD-specific and a subset of NTD-specific $V_HH$-Fcs (**Table 15**). In this assay Wuhan was included and performed again as an internal reference. Several observations were made. First, for cross-neutralizing $V_HH$s, the $IC_{50}$s across variants did not change significantly. Second, while all Wuhan neutralizers also remained Alpha neutralizers,

some lost their capability to inhibit Beta, Gamma, Delta and Kappa with variable cross-neutralizing patterns. In particular, with respect to the RBD-specific $V_HHs$, the cross-neutralization profiles for Beta vs Gamma and Delta vs Kappa were identical, which is likely reflective of the key escape mutations in these variants (K417N, E484K and N501Y for Beta vs K417T, E484K and N501Y for Gamma; L452R and T478K for Delta vs L452R and E484Q for Kappa). Third, and importantly, 12 out of 20 $V_HH$-Fcs (10 RBD-specific, two NTD-specific) were Delta neutralizers, nine of which (eight RBD-specific, one NTD-specific) neutralized across all variants. Fourth, the majority of these nine pan-neutralizers (six RBD-specific, one NTD-specific) also neutralized SARS-CoV. Fifth, Omicron mutations had a major impact on antibodies targeting bin 1, from which only NRCoV2-12 and 20 were able to neutralize with comparable potency to Wuhan or the other variants tested. The neutralization ability of the benchmark VHH-72 was abolished by Omicron mutations. Antibodies from bin 2/3/4 were able to neutralize Omicron with comparable $IC_{50}$ to Wuhan, except for NRCoV-2-02/05 and MRed05, which were negative. NRCoV2-11 (anti-RBD) and SR01 (anti-NTD) were also efficient, achieving neutralization as potent as was observed against Wuhan spike protein. From the list of antibodies tested NRCoV2-12, -20, -11 and -SR01 are the leads, showing efficient pan-neutralization against the SARS-CoV-2 variants generated so far, and outperforming the benchmark VHH-72.

**[00232] Table 15:** Flow cytometry SVNAs against SARS-CoV-2 variants and SARS-CoV

| | | SVNA $IC_{50}$ (nM) | | | | | | | |
|---|---|---|---|---|---|---|---|---|---|
| | $V_HH$-Fc | SARS-CoV-2 S | | | | | | | SARS-CoV S |
| | | Wuhan | Alpha | Beta | Gamma | Delta | Kappa | Omicron | |
| bin | RBD-specific $V_HH$ | | | | | | | | |
| 1 | VHH-72 | 5.6 | 10.6 | 5.1 | 3.3 | 10.5 | 8.5 | - | 7.8 |
| | 1d | 4.7 | 6.1 | 13.1 | 4.8 | 6.4 | 5.5 | - | - |
| | 07 | 4.7 | 5.7 | 3.6 | 3.2 | 2.3 | 3.6 | - | 4.2 |
| | 12 | 3.5 | 5.2 | 8 | 3.4 | 6.4 | 6.2 | 17.2 | 3.1 |
| | 18 | 9.1 | 12.2 | 16.6 | 12.1 | 10.2 | 17.4 | - | 12.7 |
| | 20 | 6.5 | 5.2 | 11.9 | 7.5 | 12.6 | 4.1 | 13.1 | 10.3 |
| | MRed04 | 5 | 6.4 | 24.4 | 8.7 | 11.8 | 10.4 | - | 24.6 |
| 2,3 | 02 | 4.7 | 4.2 | - | - | 8.4 | 7.2 | - | - |
| | 05 | 4.9 | 4.8 | - | - | 7.6 | 6.8 | - | - |
| 2,4 | 14 | 7.5 | 18 | 58 | 177 | - | - | 5.2 | - |

| | | | | | | | | | |
|---|---|---|---|---|---|---|---|---|---|
| 3,4 | 17 | 8.6 | 10.6 | 26.4 | 214 | - | - | 3.4 | - |
| 2,3,4 | 10 | 8.8 | 11.3 | 10.8 | 21.8 | - | - | 4.3 | - |
| | 15 | 5.8 | 9.8 | 12.2 | 10.8 | - | - | 3 | - |
| | MRed05 | 4.3 | 4.2 | 4.4 | 4.7 | 4.8 | 4.8 | - | - |
| 4 | 04 | 10.8 | 21.9 | - | - | - | - | 18.4 | - |
| 5 | 06 | - | - | - | - | - | - | - | - |
| 6 | 03 | - | - | - | - | - | - | - | - |
| | 11 | 3.2 | 6.6 | 10.7 | 4.7 | 7.7 | 3.3 | 8.8 | 7.7 |
| **bin** | **NTD-specific $V_HH$** | | | | | | | | |
| 7,9,10 | SR01 | 4.2 | 3.1 | 8.8 | 2.1 | 3.1 | 2.3 | 4.4 | 5.1 |
| | SR13 | 7.7 | 22.4 | - | 16.5 | - | 12.2 | - | 15 |
| 10 | SR02 | 1.7 | 7.3 | - | 4.7 | 6.1 | 3.1 | - | - |

"-" dash indicates lack of surrogate neutralization

**[00233] Table 16:** Eva Green $V_HH$ binding data obtained by tandem SPR surrogate virus neutralization assays against surface-immobilized SARS-CoV-2 S. $V_HHs$ were used at 20 – 40x $K_D$ concentrations, ACE2 at 1 μM. [1]inj, injection.

| **Summary orientation #1: $V_HH$ followed by $V_HH$ + ACE2** | | | | | | | **Summary orientation #2: ACE2 followed by ACE2 + $V_HH$** | | | | | | |
|---|---|---|---|---|---|---|---|---|---|---|---|---|---|
| **Cycle** | **Solution 1** | **Solution 2** | **End 1st inj[1] (RU)** | **End 2nd inj[1] (RU)** | **inj 2-1 (ΔRU)** | **Blocker** | **Cycle** | **Solution 1** | **Solution 2** | **End 1st inj[1] (RU)** | **End 2nd inj[1] (RU)** | **inj 2-1 (ΔRU)** | **Blocker** |
| 1 | Buffer | ACE2 | -3.1 | 56 | 59.1 | No | 1 | - | - | - | - | - | - |
| 2 | NRCoV2-1d | NRCoV2-1d+ACE2 | 26.3 | 40 | 13.7 | Yes | 2 | ACE2 | NRCoV2-1d+ACE2 | 57.1 | 56.4 | -0.7 | Yes |
| 3 | NRCoV2-02 | NRCoV2-02+ACE2 | 33 | 39.3 | 6.3 | Yes | 3 | ACE2 | NRCoV2-02+ACE2 | 55.8 | 59.6 | 3.8 | Yes |
| 4 | NRCoV2-03 | NRCoV2-03+ACE2 | 18.1 | 82.3 | 64.2 | No | 4 | ACE2 | NRCoV2-03+ACE2 | 52.8 | 75.3 | 22.5 | No |
| 5 | NRCoV2-04 | NRCoV2-04+ACE2 | 41.4 | 95.8 | 54.4 | No | 5 | ACE2 | NRCoV2-04+ACE2 | 52.4 | 98.8 | 46.4 | No |
| 6 | NRCoV2-05 | NRCoV2-05+ACE2 | 36.9 | 46.8 | 9.9 | Yes | 6 | ACE2 | NRCoV2-05+ACE2 | 52.2 | 60.5 | 8.3 | Yes |
| 7 | NRCoV2-06 | NRCoV2-06+ACE2 | 38.5 | 92.2 | 53.7 | No | 7 | ACE2 | NRCoV2-06+ACE2 | 52.3 | 94.4 | 42.1 | No |
| 8 | NRCoV2-07 | NRCoV2-07+ACE2 | 19.1 | 37.5 | 18.4 | Yes | 8 | ACE2 | NRCoV2-07+ACE2 | 52 | 59.1 | 7.1 | Yes |
| 10 | NRCoV2-10 | NRCoV2-10+ACE2 | 9.6 | 58.8 | 49.2 | No | 10 | ACE2 | NRCoV2-10+ACE2 | 52.1 | 64.1 | 12 | No |
| 11 | NRCoV2-11 | NRCoV2-11+ACE2 | 21.8 | 80.7 | 58.9 | No | 11 | ACE2 | NRCoV2-11+ACE2 | 52.3 | 83.6 | 31.3 | No |
| 12 | NRCoV2-SR13 | NRCoV2-SR13+ACE2 | 36.9 | 86.8 | 49.9 | No | 12 | ACE2 | NRCoV2-SR13+ACE2 | 52.3 | 92.8 | 40.5 | No |
| 13 | NRCoV2-14 | NRCoV2-14+ACE2 | 26.9 | 70.4 | 43.5 | +/- | 13 | ACE2 | NRCoV2-14+ACE2 | 52.3 | 75.9 | 23.6 | No |

| | | | | | | | | | | | |
|---|---|---|---|---|---|---|---|---|---|---|---|
| 14 | NRCoV2-15 | NRCoV2-15+ACE2 | 10.1 | 50.7 | 40.6 | +/- | 14 | ACE2 | NRCoV2-15+ACE2 | 50 | 59.7 | 9.7 | No |
| 15 | NRCoV2-SR16 | NRCoV2-SR16+ACE2 | 37.4 | 88.8 | 51.4 | No | 15 | ACE2 | NRCoV2-SR16+ACE2 | 52.1 | 95.7 | 43.6 | No |
| 16 | NRCoV2-17 | NRCoV2-17+ACE2 | 16.7 | 69.5 | 52.8 | No | 16 | ACE2 | NRCoV2-17+ACE2 | 52 | 71.7 | 19.7 | No |
| 17 | NRCoV2-18 | NRCoV2-18+ACE2 | 12.6 | 52.5 | 39.9 | +/- | 17 | ACE2 | NRCoV2-18+ACE2 | 50.9 | 61.7 | 10.8 | +/- |
| 18 | NRCoV2-20 | NRCoV2-20+ACE2 | 27.1 | 60.5 | 33.4 | +/- | 18 | ACE2 | NRCoV2-20+ACE2 | 51.3 | 66.2 | 14.9 | +/- |
| 19 | NRCoV2-SR01 | NRCoV2-SR01+ACE2 | 39.4 | 92 | 52.6 | No | 19 | ACE2 | NRCoV2-SR01+ACE2 | 51.4 | 97.2 | 45.8 | No |
| 20 | NRCoV2-SR02 | NRCoV2-SR02+ACE2 | 10.3 | 60.2 | 49.9 | No | 20 | ACE2 | NRCoV2-SR02+ACE2 | 49.1 | 67.8 | 18.7 | No |
| 21 | NRCoV2-SR03 | NRCoV2-SR03+ACE2 | 18.5 | 70.7 | 52.2 | No | 21 | ACE2 | NRCoV2-SR03+ACE2 | 50 | 76.4 | 26.4 | No |
| 22 | NRCoV2-SR04 | NRCoV2-SR04+ACE2 | 10.9 | 63.6 | 52.7 | No | 22 | ACE2 | NRCoV2-SR04+ACE2 | 50.5 | 68.5 | 18 | No |
| 23 | NRCoV2-S2A3 | NRCoV2-S2A3+ACE2 | 15 | 82 | 67 | No | 23 | ACE2 | NRCoV2-S2A3+ACE2 | 50.8 | 72.2 | 21.4 | No |
| 24 | NRCoV2-S2A4 | NRCoV2-S2A4+ACE2 | 11.6 | 73.3 | 61.7 | No | 24 | ACE2 | NRCoV2-S2A4+ACE2 | 50.9 | 71.1 | 20.2 | No |
| 25 | NRCoV2-S2G3 | NRCoV2-S2G3+ACE2 | 59 | 113.2 | 54.2 | No | 25 | ACE2 | NRCoV2-S2G3+ACE2 | 51 | 114.1 | 63.1 | No |
| 26 | NRCoV2-S2G4 | NRCoV2-S2G4+ACE2 | 21.3 | 81.7 | 60.4 | No | 26 | ACE2 | NRCoV2-S2G4+ACE2 | 50.9 | 79.3 | 28.4 | No |
| 27 | NRCoV2-S2F3 | NRCoV2-S2F3+ACE2 | 50 | 111.1 | 61.1 | No | 27 | ACE2 | NRCoV2-S2F3+ACE2 | 50.7 | 106.9 | 56.2 | No |
| 28 | $V_HH$-72 | $V_HH$-72+ACE2 | 25.8 | 37.8 | 12 | Yes | 28 | ACE2 | $V_HH$-72+ACE2 | 51 | 51.2 | 0.2 | Yes |

**[00234] Table 17:** Neutralization capabilities of SARS-CoV-2-specific $V_HHs$/$V_HH$-Fcs obtained by surrogate virus neutralization flow cytometry assays against SARS-CoV-2 S (Wuhan)

| **$V_HH$/ACE2** | **Domain/ subdomain specificity** | **$V_HH$/ACE2-$H_6$[2]** | | | **$V_HH$-Fc/ACE2-Fc[2]** | | |
|---|---|---|---|---|---|---|---|
| | | $IC_{50}$[3] (nM) | $IC_{99}$[3] (nM) | $I_{max}$%[3] | $IC_{50}$[3] (nM) | $IC_{99}$[3] (nM) | $I_{max}$%[3] |
| ACE2 | S1-RBD | 24.5 | 1506 | 94% | 5.1 | 328.1 | 97% |
| $V_HH$-72[1] | S1-RBD | 59 | 9409 | 43% | 7.2 | 238.5 | 57% |
| NRCoV2-1a | S1-RBD | nd | nd | nd | 9.2 | 89.4 | 94% |
| NRCoV2-1d | S1-RBD | 8.6 | 40.8 | 72% | 5.4 | 42 | 89% |
| NRCoV2-02 | S1-RBD | 5.1 | 15.5 | 100% | 5 | 30 | 94% |
| NRCoV2-03 | S1-RBD | - | - | - | - | - | - |
| NRCoV2-04 | S1-RBD | - | - | - | 11.7 | 420.4 | 51% |
| NRCoV2-05 | S1-RBD | 9.5 | 14.2 | 97% | 6.7 | 37 | 95% |
| NRCoV2-06 | S1-RBD | - | - | - | - | - | - |
| NRCoV2-07 | S1-RBD | 7.5 | 65.3 | 86% | 6.8 | 98.9 | 89% |
| NRCoV2-08 | S1-RBD | nd | nd | nd | - | - | - |
| NRCoV2-10 | S1-RBD | 16.1 | 121 | 50% | 7.7 | 77.3 | 91% |
| NRCoV2-11 | S1-RBD | - | - | - | 9.7 | 99.8 | 63% |
| NRCoV2-11a | S1-RBD | nd | nd | nd | 9.7 | 67.6 | 46% |
| NRCoV2-12 | S1-RBD | nd | nd | nd | 7.3 | 839.9 | 90% |
| NRCoV2-14 | S1-RBD | 21.3 | 17352 | 54% | 9.9 | 160.5 | 83% |
| NRCoV2-15 | S1-RBD | 12.1 | 233 | 44% | 8.1 | 71.5 | 95% |
| NRCoV2-17 | S1-RBD | - | - | - | 8.6 | 100.6 | 88% |
| NRCoV2-18 | S1-RBD | 8.9 | 133 | 51% | 12 | 680.5 | 90% |
| NRCoV2-19 | S1-RBD | nd | nd | nd | - | - | - |
| NRCoV2-20 | S1-RBD | 5.1 | 1371 | 43% | 8.7 | 70.3 | 66% |
| NRCoV2-21 | S1-RBD | nd | nd | nd | - | - | - |
| NRCoV2-MRed04 | S1-RBD | 6.1 | 124 | 53% | 4.6 | 262 | 73% |
| NRCoV2-MRed05 | S1-RBD | 15 | 184 | 88% | 6.1 | 36.3 | 95% |
| NRCoV2-SR01 | S1-NTD | - | - | - | 6.6 | 56.9 | 59% |
| NRCoV2-SR02 | S1-NTD | - | - | - | 5.8 | 49.8 | 53% |
| NRCoV2-SR03 | S1-NTD | - | - | - | - | - | - |
| NRCoV2-SR04 | S1-NTD | - | - | - | - | - | - |
| NRCoV2-SR13 | S1-NTD | - | - | - | 23.8 | 1974.5 | 82% |
| NRCoV2-SR16 | S1-NTD | - | - | - | - | - | - |
| NRCoV2-MRed03 | S1-NTD | - | - | - | - | - | - |
| NRCoV2-MRed06 | S1-NTD | - | - | - | - | - | - |
| NRCoV2-MRed07 | S1-NTD | - | - | - | - | - | - |
| NRCoV2-S2A3 | S2 | - | - | - | - | - | - |

| | | | | | | | |
|---|---|---|---|---|---|---|---|
| NRCoV2-S2A4 | S2 | - | - | - | - | - | - |
| NRCoV2-S2F3 | S2 | - | - | - | - | - | - |
| NRCoV2-S2G3 | S2 | - | - | - | - | | - |
| NRCoV2-S2G4 | S2 | - | - | - | - | - | - |
| NRCoV2-S2H4 | S2 | nd | nd | nd | - | - | - |
| NRCoV2-S202 | S2 | nd | nd | nd | - | - | - |
| NRCoV2-MRed11 | S2 | - | - | - | - | - | - |
| NRCoV2-MRed18 | S2 | - | - | - | - | - | - |
| NRCoV2-MRed19 | S2 | - | - | - | - | - | - |
| NRCoV2-MRed20 | S2 | - | - | - | - | - | - |
| NRCoV2-MRed22 | S2 | - | - | - | - | - | - |
| NRCoV2-MRed25 | S2 | - | - | - | - | - | - |

[1]$V_HH$-72 benchmark is SARS-CoV S-specific $V_HH$ that cross-reacts with SARS-CoV-2 S (Wrapp et al., 2020). [2]ACE2-$H_6$ is $His_6$-tagged monomeric ACE2, ACE2-Fc, human Ig Fc-fused dimeric ACE2. [3]$IC_{50}$, concentration of $V_HH/V_HH/Fc$ giving 50% neutralization; $IC_{99}$, concentration of $V_HH/V_HH/Fc$ giving 99% neutralization; $I_{max}$%, maximal inhibitory effect; $IC_{50}$, $IC_{99}$ and $I_{max}$% values were extracted from graphs exemplified in **Figs. 12B** and **Figs. 13B**. Dash indicate $V_HH/V_HH$-Fc does not neutralize the interaction between Vero E6 cell-displayed ACE2 and soluble S. [4]*IC*s cannot be determined with certainty due to low $I_{max}$% values. nd, not determined, due to lack of sufficient quantities and/or neutralization as $V_HH$-Fc.

**Example 9: Live-Virus Neutralization Assays**

***Introduction***

**[00235]** $V_HH$-Fcs were subjected to authentic-virus neutralizations assays, i.e., micro-neutralization assays, to identify those that neutralized infection of host cells by the invading SARS-CoV-2 virus.

***Materials and Methods***

*Authentic-virus neutralizations assays*

**[00236]** Neutralization activity of antibodies to SARS-CoV-2 was determined with the microneutralization assay. In brief, antibody ($V_HH$-Fc and $V_HH$) stocks were prepared at 1 mg/mL in PBS and sterilized by passing through 0.22 µM filters. 1:5 serial dilutions of 50 µg/mL of each antibody was carried out in DMEM, high glucose media supplemented with 1 mM sodium pyruvate, 1mM non-essential amino acids, 100 U/ml penicillin-streptomycin, and 1% heat-

inactivated fetal bovine serum. SARS-CoV-2 (strain SARS-CoV-2/*Canada/VIDO-01/2020*) was incubated at 250 pfu with antibody dilution in 1:1 ratio at 37°C for 1 h. Vero E6 cells seeded in 96-well plates were infected with virus/antibody mix and incubated at 37°C in humidified/5% $CO_2$ incubator for 72 hours post-infection (hpi). Cells were then fixed in 10% formaldehyde overnight and virus infection was detected with mouse anti-SARS-CoV-2 nucleocapsid antibody (R&D Systems, clone #1035111) and counterstained with rabbit anti-mouse IgG-HRP (Rockland Inc.). Colorimetric development was obtained with o-phenylenediamine dihydrochloride peroxidate substrate (Sigma-Aldrich) and detected on Biotek Synergy H1 plate reader at 490 nm. $IC_{50}$ was determined from non-linear regression on GraphPad Prism 9. For determining neutralization potencies by measuring cytopathic effect (CPE), infected Vero E6 cells were incubated at 37°C for 96 h until the virus-only control wells had nearly 100% CPE (cell-only controls were also included). Neutralization was scored by $MN_{100}$, lowest antibody concentration that gave no CPE, i.e., 100% neutralization. Assays were performed in technical duplicates.

**[00237]** ***Results and Discussion***

**[00238]** A select set of lead $V_HH$-Fcs were subjected to preliminary authentic-virus micro-neutralization assays to assess their SARS-CoV-2 virus-neutralizing activity. These included five S1-RBD-specific $V_HH$s and two S1-NTD-specfic $V_HH$s. Neutralization was scored by $MN_{100}$, the lowest antibody concentration that gave no cytopathic effect (100% neutralization). Results are shown in **Figs. 14A-B** and **Table 18**. All $V_HH$-Fcs demonstrated significant neutralization capabilities, with $MN_{100}$s ranging from 6.25 nM (lowest neutralization capability) to ≤0.01 nM (highest neutralization capability). The most potent neutralizers were amongst the S1-RBD binders: NRCoV2-02 ($MN_{100}$ ≤0.01 nM); NRCoV2-1d ($MN_{100}$ 0.25 nM); NRCoV2-04 and NRCoV2-07 ($MN_{100}$ 1.25 nM); NRCoV2-03 ($MN_{100}$ 6.25 nM). NRCoV2-02 and NRCoV2-1d were far more potent neutralizers than the benchmark ($V_HH$-72), by five- and 125-fold, respectively. S1-NTD binders had $MN_{100}$s of 6.25 nM (NRCoV2-SR01, NRCoV2-SR02). The lead antibody, NRCoV2-02 also outperformed the benchmark in $V_HH$ format by 125-fold (**Fig. 14A** inset).

To explore the contribution of bivalency to the neutralization potency of $V_HH$-Fcs, monovalent $V_HH$-Fc versions of select $V_HH$-Fcs were generated. Based on $MN_{100}$ values, neutralization potencies were decreased by five-fold for NRCoV2-SR01, 25-fold for NRCoV2-1d and NRCoV2-

07 and more than 125-fold for NRCoV2-02, with their conversion from bivalent to monovalent $V_HH$-Fcs, demonstrating the sizable contribution of bivalency to their neutralization potency. In the case of NRCoV2-02, the identical $MN_{100}$ for its monovalent $V_HH$ and monovalent $V_HH$-Fc versions indicates that the observed dramatic increase in neutralization potency in going from $V_HH$ to bivalent $V_HH$-Fc was likely due solely to an increase in valency, not size (steric hindrance). The loss of bivalency also had drastic effect on $V_HH$-72, rendering it non-neutralizing at the highest concentration tested.

**[00239]** A more comprehensive authentic neutralization assay was performed to determine the $IC_{50}$ of $V_HH$-Fcs (**Fig. 15 A-D; Table 19**). Most potent neutralizers were amongst the S1-RBD binders with 17 out of 20 $V_HH$-Fcs tested being neutralizing. The most potent $V_HH$-Fcs recognized epitopes 2/3/4 and had $IC_{50}$s of 0.0008- 3.1 nM (**Fig. 15E** and **Fig. 30; Table 19**). The leads were NRCoV-05 ($IC_{50}$ 0.0008 nM) followed closely by NRCoV-02 ($IC_{50}$ 0.12 nM) and NRCoV2-MRed 05 ($IC_{50}$ 0.17 nM). $V_HH$-Fcs recognizing epitope 1 showed intermediate potencies with $IC_{50}$s of 1.94 – 9.6 nM, with $V_HH$-72 (belonging to the same bin 1) having similar $IC_{50}$ (8.46 nM). $V_HH$-Fcs recognizing epitope 5 and 6 showed $IC_{50}$s of 9.96 – 76 nM. As for S1-NTD-specific $V_HH$, six out of nine $V_HH$-Fcs tested were neutralizing, with the lead $V_HH$-Fcs having $IC_{50}$s of 9.42, 14.31 and 54.2 nM. The remaining two had $IC_{50}$s in the high nM - micromolar range. Out of 13 S2-specific $V_HH$-Fcs tested, three, NRCoV2-S2A3, NRCoV2-S2G3 and NRCoV2-S2G4, were neutralizing with $IC_{50}$s from 12.2 nM for S2A3 to high nM - micromolar range for S2G3 and S2G4. These belonged to three different epitope bins. Nine $V_HH$-Fcs outperformed the $V_HH$-72 benchmark by 2.5 – 10,000-fold. In particular, the NRCoV2-05, NRCoV2-02 and NRCoV2-MRed05 leads showed 10,000-fold, 70-fold and 50-fold higher potency than $V_HH$-72, respectively. We provide the first examples of single domain antibodies that neutralize the SARS-CoV-2 virus by targeting the non-S1-RBD region of S, i.e., S1-NTD and S2.

**[00240]** The live virus neutralization assays were then extended to include Alpha and Beta variants. With the exception of $V_HH$-Fc NRCoV2-06, all remaining 16 RBD-specific Wuhan neutralizers maintained their ability to neutralize Alpha (**Table 19**, **Fig. 30, Fig. 31A**, and **Fig. 31C**). Interestingly, many $V_HH$s from across different epitope bins showed improved $IC_{50}$s by as high as 15-fold. Except for NRCoV2-05, which despite showing a reduced potency towards the Alpha variant (~40-fold) still exhibited the highest potency of all against the variant, the remaining

$V_HHs$ demonstrated comparable potencies. Of the 16 Wuhan/Alpha neutralizers, 13 also neutralized the Beta variant (**Fig. 31B** and **Fig. 31D**), with the majority (10 of 13) demonstrating comparable potencies and two (NRCoV2-14 and NRCoV2-17) showing reductions (~10-fold). Although from the most potent bin (2/3/4), NRCoV2-02, NRCoV2-04 and NRCoV2-05, consistent with the cross-reactivity data (**Fig. 6B**), were completely abrogated presumably by the Beta mutations in the RBD (K417N, E484K, N501Y), several others including NRCoV2-MRed05, NRCoV2-10 and NRCov2-15 did retain their high neutralizing potencies against both Alpha and Beta variants. A similar trend was observed for the NTD-specific neutralizing $V_HHs$: against the Alpha variant, potencies either remained essentially the same as those for the Wuhan variant or improved, while against the Beta variant, potencies diminished (**Fig. 30** and **Figs. 31 A-D**). Nonetheless, NRCoV2-SR01 and NRCoV2-SR16 maintained respectable neutralization potencies against Beta. The potencies of S2-specific neutralizers (S2A3, S2G3, S2G4) were also decreased with variants. However, the lead NRCoV2-S2A3 still maintained comparable potencies across all three variants ($IC_{50}$ of 12.2 nM, 31 nM and 54 nM for Wuhan, Alpha and Beta [**Table 19**]). Collectively, the neutralization profiles across Wuhan, Alpha and Beta variants were consistent with cross-reactivity profiles (**Fig. 6B**). Based on the cross-reactivity (**Fig. 6B**) and surrogate cross-neutralization data (**Table 15**), it is likely that many $V_HHs$ would also neutralize the Gamma, Kappa, Delta, and Omicron variants in live virus neutralization assays.

**[00241] Table 18:** Neutralization capabilities ($MN_{100}$) of SARS-CoV-2-specific $V_HH$-Fcs obtained by authentic-virus (aka live virus) neutralization assays

| **$V_HH$** | **Domain/subunit specificity** | **$MN_{100}$ (nM)[2]** |
|---|---|---|
| NRCoV2-1d | S1-RBD | 0.25 |
| NRCoV2-02 | S1-RBD | ≤0.01[3] |
| NRCoV2-03 | S1-RBD | 6.25 |
| NRCoV2-04 | S1-RBD | 1.25 |
| NRCoV2-07 | S1-RBD | 1.25 |
| NRCoV2-SR01 | S1-NTD | 6.25 |
| NRCoV2-SR02 | S1-NTD | 6.25 |
| NRCoV2-15 x A26.8 | S1-RBD x null | 1.25 |
| $V_HH$72 x A26.8 | S1-RBD x null | - |
| NRCoV2-S2A4 x A26.8 | S2 x null | - |

| | | |
|---|---|---|
| NRCoV2-07 x A26.8 | S1-RBD x null | 31.25 |
| NRCoV2-1d x A26.8 | S1-RBD x null | 6.25 |
| NRCoV2-SR01 x A26.8 | S1-NTD x null | 31.25 |
| NRCoV2-02 x A26.8 | S1-RBD x null | 1.25 |
| $V_HH$-72[1] | S1-RBD | 1.25[3] |
| A20.1[1] | null | - |

[1]$V_HH$-72 benchmark is a SARS-CoV S-specific $V_HH$ that cross-reacts with SARS-CoV-2 S (Wrapp et al., 2020); A20.1 and A26.8 are *C. difficile* toxin A-specific negative control $V_HH$ (Hussack et al., 2011). [2]$MN_{100}$ is the lowest antibody concentration that gave no cytopathic effect (100% neutralization). Dash indicate $V_HH$-Fc does not neutralize SARS-CoV-2 virus at the highest $V_HH$-Fc concentration used. $MN_{100}$ values were used to construct **Fig. 14A-B** graphs. [3]The $MN_{100}$ of monovalent $V_HH$-72 and NRCoV2-02 $V_HH$s were 156.25 and 1.25 nM, respectively.

**[00242] Table 19:** Neutralization capabilities ($IC_{50}$) of SARS-CoV-2-specific $V_HH$-Fcs obtained by authentic-virus (aka live virus) neutralization assays

| **$V_HH$-Fc** | **Epitope bin** | **LVNA $IC_{50}$ (nM)** | | |
|---|---|---|---|---|
| | | **Wuhan** | **Alpha** | **Beta** |
| **RBD-specific $V_HH$** | | | | |
| 1d | 1 | 1.94 | 0.37 | 2.14 |
| 07 | | 6.15 | 0.42 | 3.18 |
| 12 | | 2.82 | 1.35 | 2.62 |
| 18 | | 6.4 | 2.82 | 9.48 |
| 20 | | 11.2 | 1.94 | 2.88 |
| MRed04 | | 9.61 | 4.5 | 5.73 |
| 02 | 2,3 | 0.12 | 0.09 | - |
| 05 | | 0.0008 | 0.03 | - |
| 14 | 2,4 | 3.1 | 0.88 | 32.8 |
| 17 | 3,4 | 2.82 | 0.61 | 34.7 |
| 10 | 2,3,4 | 1.28 | 0.47 | 2.25 |
| 15 | | 0.73 | 0.16 | 0.43 |
| MRed05 | | 0.17 | 0.13 | 0.11 |
| 04 | 4 | 1.65 | 2.3 | - |
| 06 | 5 | 76 | - | - |
| 03 | 6 | 58 | 16 | 62 |
| 11 | | 9.9 | 2.3 | 18.5 |

| | | | | |
|---|---|---|---|---|
| **NTD-specific $V_HH$** | | | | |
| SR01 | 7,9,10 | 9.42 | 3.77 | 70.3 |
| SR03 | | ~500 | 22.2 | - |
| SR13 | | ~100 | ~100 | - |
| SR16 | | 54.2 | 17.8 | 100 |
| SR04 | 7/9 | ~500 | - | - |
| MRed03 | 8 | - | - | - |
| MRed06 | 8 | - | - | - |
| MRed07 | 9 | - | - | - |
| SR02 | 10 | 14.13 | 9.05 | ~300 |
| **S2-specific $V_HH$** | | | | |
| S2A3 | 11 | 12.2 | 31 | 54 |
| S2A4 | 12 | - | - | - |
| S2F3 | 13 | - | - | - |
| MRed18 | | - | ~400 | - |
| MRed19 | | - | - | - |
| MRed20 | | - | - | - |
| MRed22 | | - | - | - |
| S2G3 | 14 | ~200 | - | - |
| S2G4 | 15 | ~200 | - | - |
| MRed11 | 16 | - | - | - |
| MRed25 | 17 | - | - | - |
| **Reference** | | | | |
| VHH-72[1] | 1 | 8.46 | 1.86 | 9.34 |
| A20.1[1] | null | - | - | - |

[1]$V_HH$-72 benchmark is a SARS-CoV S-specific $V_HH$ that cross-reacts with SARS-CoV-2 S (Wrapp et al., 2020); A20.1 is *C. difficile* toxin A-specific negative control $V_HH$ (Hussack et al., 2011. Epitope bin numbers correspond to the bins shown in **Fig. 9G**.

**Example 10: Stability of $V_HH$s against Aerosolization**

***Introduction***

**[00243]** One effective therapeutic approach against COVID-19 might be the direct delivery of aerosolized antibodies to the nasal and lung epithelia by inhalation. $V_HH$s in particular, are advantageously fit for such administration approach due to their high stability and robustness. Since aerosolization could compromise the structural integrity and function of antibodies that lack

sufficient stability, such as mAbs (Detalle et al., 2016; Respaud et al., 2015), the effect of aerosolization on the stability of $V_HHs$ was tested.

***Materials and Methods***

**[00244]** *Aerosolization studies*

**[00245]** Prior to aerosolization, 4 mg of each $V_HH$ was purified by size-exclusion chromatography using a Superdex™ 75 GL column (Cytiva) and PBS as running buffer, as described above. Protein fractions corresponding to the chromatogram's monomeric peak were pooled, quantified and the concentration adjusted to 0.5 mg/mL. One mL of each $V_HH$ was subsequently aerosolized at room temperature with a portable mesh nebulizer (AeroNeb® Solo, Aerogen, Galway, Ireland), which produces 3.4-µm particles. Aerosolized $V_HHs$ were collected into 15 mL Round-Bottom Polypropylene test tubes (Falcon, Cat#C352059) for 5 min to allow condensation and were subsequently quantified and kept at 4°C until use. Then 200 µL aliquots of pre- and post- aerosolized $V_HHs$ were subjected to SEC to obtain chromatogram profiles. Additionally, condensed $V_HHs$ were closely monitored for the formation of any visible aggregates, and in cases where aggregate formation was observed, aggregates were removed by centrifugation prior to concentration determination, SEC analysis and ELISA. % soluble aggregate was determined as the proportion of a $V_HH$ that gave elution volumes ($V_e$s) smaller than that of the monomeric $V_HH$ fraction. % recovery was determined as the proportion of a $V_HH$ that remained monomerically soluble following aerosolization.

**[00246]** To assess the effect of aerosolization on the functionality of $V_HHs$, the activities of post-aerosolized $V_HHs$ were determined by ELISA and compared to those for pre-aerosolized $V_HHs$. To perform ELISA, S1-Fc (ACRO Biosystems, Cat#S1N-C5255) was diluted in PBS to 500 ng/mL, and 100 µL/well were coated overnight at 4°C. The next day, plates were washed with PBST and blocked with 200 µL PBSC for 1 h at room temperature. After five washes with PBST, serial dilutions of the pre- and post- aerosolized $V_HHs$ were added to wells and incubated for 1 h at room temperature. Then plates were washed 10 times with PBST and binding of $V_HHs$ to S1-Fc was detected with rabbit anti-6xHis Tag antibody HRP Conjugate (Bethyl, Cat#A190-114P), diluted at 10 ng/mL in PBST and added at 100 µL/well. Finally, after 1 h incubation at room temperature, peroxidase activity was detected as described previously.

***Results and Discussion***

**[00247]** $V_HHs$ including the benchmark $V_HH$-72 were examined for their aggregation resistance/stability against aerosolization. For a few $V_HHs$, e.g., NRCoV2-MRed20, NRCoV2-S2A4, as well as the $V_HH$-72 benchmark, aerosolization induced some soluble aggregation formation as determined by SEC (**Fig. 16A**; **Table 20**). Several $V_HHs$, e.g., NRCoV2-11, NRCoV2-SR03, formed visible aggregates, which led to their reduced % recovery (**Fig. 16A-C; Table 20**). However, the majority of $V_HHs$ (20 out of 30 $V_HHs$ tested) were highly stable against aerosolization, that is, they did not form any soluble or visible aggregates and demonstrated high % recovery upon aerosolization treatment. Examples include NRCoV2-1c/1d, NRCoV2-02, NRCoV2-07, NRCoV2-17, NRCoV2-18 and NRCoV2-20. High % recovery indicates these $V_HHs$ advantageously lack non-specific binding to nebulizer surfaces. For therapeutic $V_HHs$, this is expected to translate to a more effective drug delivery to the site of viral infection. Several $V_HHs$, i.e., NRCoV2-04, NRCoV2-14, NRCoV2-15, NRCoV2-SR04 and NRCoV2-MRed04, while forming some visible aggregates, still showed a good % recovery upon aerosolization (52 – 69 %). To assess the effect of aerosolization on the functionality of $V_HHs$, the activities ($EC_{50}$s) of post-aerosolized $V_HHs$ were determined by ELISA and compared to those for pre-aerosolized $V_HHs$. ELISAs were performed on a sample of four $V_HHs$: NRCoV2-1d, NRCoV2-02, NRCoV2-07 and NRCoV2-11 (**Fig. 16D**). Comparison of $EC_{50}$s for post-aerosolized $V_HHs$ *vs* pre-aerosolized $V_HHs$ demonstrated that aerosolization did not compromise the functionality of $V_HHs$ (**Fig. 16D; Table 21**).

**[00248] Table 20:** Stability of $V_HHs$ against aerosolization

| $V_HH$ | Recovery (%)[1] | Soluble aggregates (%)[2] | | ΔSoluble agg.[3] | Visible aggregates |
|---|---|---|---|---|---|
| | | Pre-aerosolization | Post-aerosolization | | |
| NRCoV2-1c | 91 | 3 | 5 | 2 | No |
| NRCoV2-1d | 83 | 2 | 4 | 2 | No |
| NRCoV2-02 | 89 | 2 | 2 | 0 | No |
| NRCoV2-03 | 81 | 2 | 1 | -1 | No |
| NRCoV2-04 | 62 | 6 | 5 | -1 | Yes |
| NRCoV2-05 | 89 | 2 | 5 | 3 | No |
| NRCoV2-06 | 51 | 7 | 5 | -2 | Yes |
| NRCoV2-07 | 75 | 2 | 3 | 1 | No |
| NRCoV2-10 | 83 | 5 | 5 | 0 | No |

| | | | | | |
|---|---|---|---|---|---|
| NRCoV2-11 | 24 | 6 | 5 | -1 | Yes |
| NRCoV2-14 | 55 | 6 | 6 | 0 | Yes |
| NRCoV2-15 | 69 | 4 | 5 | 1 | Yes |
| NRCoV2-17 | 85 | 5 | 6 | 1 | No |
| NRCoV2-18 | 99 | 9 | 5 | -4 | No |
| NRCoV2-20 | 97 | 2 | 1 | -1 | No |
| NRCoV2-SR03 | 43 | 3 | 11 | 8 | Yes |
| NRCoV2-SR04 | 52 | 5 | 3 | -2 | Yes |
| NRCoV2-SR13 | 83 | 4 | 6 | 2 | No |
| NRCoV2-S2A4 | 84 | 7 | 11 | 4 | No |
| NRCoV2-S2G4 | 91 | 3 | 6 | 3 | No |
| NRCoV2-MRed02 | 73 | 1 | 1 | 0 | No |
| NRCoV2-MRed03 | 96 | 3 | 2 | -1 | No |
| NRCoV2-MRed04 | 59 | 4 | 4 | 0 | Yes |
| NRCoV2-MRed07 | 90 | 10 | 3 | -7 | No |
| NRCoV2-MRed11 | 89 | 4 | 5 | 1 | No |
| NRCoV2-MRed18 | 96 | 3 | 10 | 7 | No |
| NRCoV2-MRed19 | 87 | 5 | 9 | 4 | No |
| NRCoV2-MRed20 | 76 | 2 | 18 | 16 | No |
| NRCoV2-MRed22 | 86 | 3 | 9 | 6 | No |
| NRCoV2-MRed25 | 44 | 3 | 3 | 0 | Yes |
| $V_HH$-72 | 78 | 1 | 14 | 13 | No |

[1]% recovery were determined as described in Examples 10. [2]% soluble aggregate was determined as the proportion of a $V_HH$ that gave elution volumes ($V_e$s) smaller than that of the monomeric $V_HH$ fraction. [3]ΔSoluble agg. = "Post-aerosolization" – "Pre-aerosolization".

**[00249] Table 21**. Affinities ($EC_{50}$s) of pre-aerosolized ("Pre") *vs* post-aerosolized ("Post") $V_HH$s

| **$V_HH$** | ***$EC_{50}$* (nM)** | |
|---|---|---|
| | **Pre** | **Post** |
| NRCoV2-1d | 1.1 | 1.3 |
| NRCoV2-02 | 0.2 | 0.2 |
| NRCoV2-07 | 1.1 | 1 |
| NRCoV2-11 | 0.2 | 0.2 |

**Example 11: $V_HH$s for Diagnosis and Capture of SARS-CoV-2**

*Introduction*

**[00250]** $V_HHs$ described herein are promising diagnostic/capture agents against SARS-CoV-2, SARS-CoV and related viruses as well as their spike proteins. To explore the use of these $V_HHs$ as capture agents, four of the $V_HHs$ were tested in sandwich ELISA for their diagnostic/capturing capability against SARS-CoV-2.

*Materials and Methods*

*Sandwich ELISA*

**[00251]** NUNC® MaxiSorp™ 4 HBX plates (Thermo Fisher) were coated overnight at 4°C with 4 µg/mL streptavidin (Jackson ImmunoResearch, Cat#016-000-113) in 100 µL PBS, pH 7.4. Wells were blocked with 200 µL PBSC for 1 h at room temperature followed by capturing biotinylated NRCoV2-02 $V_HH$ (10 µg/mL in 100 µL PBSCT) for 1 h at room temperature. Wells were washed five times with PBST and incubated with variable concentrations of SARS-CoV-2 S, S1 or S1-RBD diluted in PBSCT for 1 h. Well were washed and incubated with detecting $V_HH$-Fcs at 1 µg/mL. The binding of $V_HH$-Fcs to spike protein fragments was probed using 100 µL 1 µg/mL HRP-conjugated goat anti-human IgG (SIGMA, Cat#A0170). Finally, plates were washed 10 times with PBST and peroxidase activity was determined as described above.

*Results and Discussion*

**[00252]** To provide proof of concept for the utility of the $V_HHs$ as detecting / capturing agents against SARS-CoV-2, SARS-CoV and related viruses, sandwich ELISAs were performed with four $V_HHs$ using SARS-CoV-2 spike protein fragments as surrogates for the virus. Wells were coated with NRCoV2-02 $V_HH$ as the capturing antibody, followed by the capture of antigens S, S1, or S1-RBD added at variable concentrations. Then a second, $V_HH$-Fc that binds to a non-overlapping epitope in relation to NRCoV2-02 was added as the detecting antibody followed by the addition of a HRP-conjugated probing antibody binding to the detecting antibody. The different $V_HH$-Fcs tested as detecting antibodies were: NRCoV2-1d, NRCoV2-04, NRCoV2-07, and NRCoV2-11. Very low $SC_{50}$ values were obtained in ELISA assays (**Fig. 17, Table 22**). In addition, limit of detection values as low as 0.08 ng/mL (8 picogram) spike protein could be

detected with confidence (**Table 23**). These results indicate that the $V_HHs$ are promising virus detecting / capturing agents.

**[00253] Table 22:** $SC_{50}$ values obtained in ELISA assays

| | $SC_{50}$ (ng/mL) | | |
|---|---|---|---|
| | **S** | **S1** | **S1-RBD** |
| NRCoV2-1d | 25 | 16 | 1.7 |
| NRCoV2-04 | 39 | 25 | 3.3 |
| NRCoV2-07 | 18 | 5 | 0.7 |
| NRCoV2-11 | 20 | 6 | 0.8 |

**[00254] Table 23:** Limit of detection (ng/mL)

| | **NRCoV2-1d** | **NRCoV2-04** | **NRCoV2-07** | **NRCoV2-11** |
|---|---|---|---|---|
| **S** | 1.4 | 4.1 | 1.4 | 1.4 |
| **S1** | 1.37 | 4.12 | 0.46 | 0.46 |
| **S1-RBD** | 0.15 | 0.46 | 0.08 | 0.08 |

**Example 12: In vivo therapeutic efficacy of $V_HH$-Fcs**

**[00255]** Before testing $V_HH$-Fcs in hamsters for in vivo efficacy, they were assessed for in vivo stability and persistence. NRCov2-1d $V_HH$-Fc was chosen as a representative $V_HH$ and VHH-72 $V_HH$-Fc, whose modified/enhanced version is currently in a phase 1 clinical trial, was included as a reference. Hamsters were injected intraperitoneally (IP) with 1 mg of each antibody and serum antibody concentration was monitored for up to four days by ELISA. Significant and comparable VHH-Fc concentrations were present in the hamster sera for both 1d and VHH-72 $V_HH$-Fcs on days 1 and 4 post injection (**Fig. 32**), indicating that $V_HH$-Fcs would have the required serum stability and persistence in vivo for the duration of the animal studies.

**[00256]** The in vivo therapeutic efficacy of $V_HH$-Fcs which were neutralizing by live virus neutralization assay was then assessed in a hamster model of SARS-CoV-2 infection. Five $V_HH$-Fcs were selected to cover a wide range of important attributes including in vitro neutralization

potencies and breadth, epitope bin, subunit/domain specificity and cross-reactivity pattern. These included three RBD-specific (1d, 05, MRed05), one NTD-specific (SR01) and one S2-specific (S2A3) $V_HH$-Fcs. Cocktails of two $V_HH$-Fcs were also included to explore synergy between the antibody pairs recognizing distinct epitopes within the RBD (1d/MRed05) or RBD and NTD (1d/SR01).

**[00257]** Hamsters were administered IP with 1 mg of $V_HH$-Fcs 24 h prior to intranasal challenge with SARS-CoV-2 Wuhan isolate. Daily weight change and clinical symptoms were monitored. At 5 dpi, lungs were collected to determine viral titers. Viral titer decrease and reversal of weight loss in antibody treated versus control animals were taken as measures of antibody efficacy. Animals treated with RBD binders 1d, 05, and MRed05 showed reduced lung viral burden by three, five and six orders of magnitude, respectively, relative to PBS or VHH-Fc isotype controls, with 05 and MRed05 reducing viral burden to below detectable levels (**Fig. 22A**). The RBD-specific VHH-72 benchmark caused a mean viral decrease of four orders of magnitude. The NTD binder SR01, and interestingly, the S2 binder S2A3, were also effective neutralizers, decreasing mean viral titers by four and three orders of magnitude, respectively. Both 1d/SR01 and 1d/MRed05 cocktails decreased viral titers by 6 orders of magnitude to undetectable levels of virus infection. While it was not possible to unravel potential synergies for 1d/MRed05, as MRed05 alone displayed essentially the same efficacy as the 1d/MRed05 combination, it was apparent that the 1d/SR01 combination benefited from synergy, decreasing viral titers by a further 2 - 3 orders of magnitude to undetectable levels, relative to 1d or SR01 alone. Moreover, in accordance with the viral titer decreases, a gradual reversal of weight loss in infected animals was observed with antibody treatment starting on 2 dpi (**Figs. 22B** and **22C**). A strong negative correlation ($r = -0.9436$; $p < 0.0001$) was observed between weight change and viral titer at 5 dpi (**Fig. 22D**).

**[00258]** Subsequent immunohistochemistry studies corroborated the viral titer and weight change results. First, in agreement with the viral titer observations, substantial viral antigen (nucleocapsid) reductions in hamster lungs were observed with antibody treatments (**Fig. 23**; compare non-treated PBS and isotype controls to treated profiles). Although, small foci of viral antigen expression were detected in VHH-72-, 1d-, SR01- and S2A3-treated animals, none were detected in 05-, MRed05-, 1d/SR01- and 1d/MRed05-treated animals. Second, SARS-CoV-2 infection is characterized by

an overt inflammatory response in the respiratory tract accompanied by an increased infiltration of inflammatory immune cells, e.g., macrophages and T lymphocytes, in the lung parenchyma 70. As expected, this was the case for the non-treated PBS and isotype control groups. In contrast, we observed a substantial reduction of macrophages and T lymphocytes infiltrate in lung parenchyma with antibody treatment (**Figs. 24, 25**). The most dramatic decreases in the number of macrophages and T lymphocytes were seen with 05, MRed05, 1d/MRed05 and 1d/SR01 treatments. Interestingly, a reduction in inflammatory responses was also associated with a decrease in the number of apoptotic cells in antibody-treated animals (**Fig. 26**). Altogether, the viral titer, weight change and immunohistochemistry results consistently demonstrate that a single dose of several of the $V_HH$-Fcs reduced viral burden, immune cell infiltration and apoptosis in the lungs of infected hamsters.

**[00259]** The preceding examples have been provided to illustrate various aspects of the disclosure and are non-limiting. The scope of the claims is not limited to specific details provided in the examples; rather the claims are to be given the broadest interpretation consistent with the teachings of the disclosure as a whole.

**[00260] Table 24:** List of sequences described in the specification

| SEQ ID NO: | Sequence | Seq. Type | Antibody(ies) including sequence |
|---|---|---|---|
| 1 | GSTLDYYA | CDR1 | NRCoV2-1a<br>NRCoV2-1d |
| 2 | GSILDYYA | CDR1 | NRCoV2-1c |
| 3 | GFTFSNYA | CDR1 | NRCoV2-02 |
| 4 | GITFSYYA | CDR1 | NRCoV2-03 |
| 5 | GSPFSNVV | CDR1 | NRCoV2-04 |
| 6 | GFIFSNYA | CDR1 | NRCoV2-05 |
| 7 | VSTFSSYA | CDR1 | NRCoV2-06 |
| 8 | GVTLDYYA | CDR1 | NRCoV2-07 |
| 9 | GFTLDDYA | CDR1 | NRCoV2-08 |
| 10 | GNTFSRSN | CDR1 | NRCoV2-10 |
| 11 | GSSLDSYS | CDR1 | NRCoV2-11 |
| 12 | GFTLDSYN | CDR1 | NRCoV2-11a |
| 13 | GRTFRNYV | CDR1 | NRCoV2-12 |
| 14 | GTTFSHYA | CDR1 | NRCoV2-14 |

| | | | |
|---|---|---|---|
| 15 | GSTSGRNT | CDR1 | NRCoV2-15 |
| 16 | GSPFSQLA | CDR1 | NRCoV2-17 |
| 17 | GITISGYN | CDR1 | NRCoV2-18 |
| 18 | GLTLNSYA | CDR1 | NRCoV2-19 |
| 19 | GRTFSNYV | CDR1 | NRCoV2-20 |
| 20 | GFTLDYYA | CDR1 | NRCoV2-21<br>NRCoV2-MRed03<br>NRCoV2-MRed05 |
| 21 | GFTFDNYA | CDR1 | NRCoV2-SR01 |
| 22 | EFTLNYYS | CDR1 | NRCoV2-SR02 |
| 23 | GSIFSNNH | CDR1 | NRCoV2-SR03 |
| 24 | GRTFSSHT | CDR1 | NRCoV2-SR04 |
| 25 | GSRFGSKH | CDR1 | NRCoV2-SR13 |
| 26 | GTTFSRYH | CDR1 | NRCoV2-SR16 |
| 27 | GRPYSNYA | CDR1 | NRCoV2-S2A3 |
| 28 | GSPFRSNV | CDR1 | NRCoV2-S2A4 |
| 29 | ASTFGDSA | CDR1 | NRCoV2-S2B3 |
| 30 | GFTFNLYS | CDR1 | NRCoV2-S2H4 |
| 31 | VRILSVPA | CDR1 | NRCoV2-S2F3 |
| 32 | GSTFGIFL | CDR1 | NRCoV2-S2G3 |
| 33 | GSTFSGYA | CDR1 | NRCoV2-S2G4 |
| 34 | GITVSRIG | CDR1 | NRCoV2-S202 |
| 35 | GNIFSINS | CDR1 | NRCoV2-MRed02 |
| 36 | GNSFSINT | CDR1 | NRCoV2-MRed04 |
| 37 | GFTLAYYA | CDR1 | NRCoV2-MRed06 |
| 38 | GSIGPFNT | CDR1 | NRCoV2-MRed07 |
| 39 | GFTFSSYA | CDR1 | NRCoV2-MRed11 |
| 40 | TTVFGRNA | CDR1 | NRCoV2-MRed18 |
| 41 | TIIFKGQT | CDR1 | NRCoV2-MRed19 |
| 42 | GLSFSSYD | CDR1 | NRCoV2-MRed20 |
| 43 | GSVFASNA | CDR1 | NRCoV2-MRed22 |
| 44 | GHTFSRYG | CDR1 | NRCoV2-MRed25 |
| 45 | VSSSDGST | CDR2 | NRCoV2-1a<br>NRCoV2-1c |
| 46 | VSSSDGNT | CDR2 | NRCoV2-1d |
| 47 | ISGRGDDT | CDR2 | NRCoV2-02 |
| 48 | MSNMDST | CDR2 | NRCoV2-03 |
| 49 | ISGGGIA | CDR2 | NRCoV2-04 |
| 50 | INSGGGDT | CDR2 | NRCoV2-05 |
| 51 | IGFVGAT | CDR2 | NRCoV2-06 |
| 52 | ISSNGRRN | CDR2 | NRCoV2-07 |

| | | | |
|---|---|---|---|
| 53 | ISRSGTTT | CDR2 | NRCoV2-08 |
| 54 | ISSRGIS | CDR2 | NRCoV2-10 |
| 55 | ISRYYSST | CDR2 | NRCoV2-11 |
| 56 | ISRYYEST | CDR2 | NRCoV2-11a |
| 57 | VAAISWGGTEI | CDR2 | NRCoV2-12 |
| 58 | ISVFGST | CDR2 | NRCoV2-14 |
| 59 | VSTSGAT | CDR2 | NRCoV2-15 |
| 60 | ISPTGNR | CDR2 | NRCoV2-17 |
| 61 | INSGGST | CDR2 | NRCoV2-18 |
| 62 | LTSGGTG | CDR2 | NRCoV2-19 |
| 63 | VAVISGSDTET | CDR2 | NRCoV2-20 |
| 64 | ISSGGST | CDR2 | NRCoV2-21 |
| 65 | ISGNGGVT | CDR2 | NRCoV2-SR01 |
| 66 | IRYSGGGI | CDR2 | NRCoV2-SR02 |
| 67 | ISSGGKT | CDR2 | NRCoV2-SR03 |
| 68 | ISMGGNTNYA | CDR2 | NRCoV2-SR04 |
| 69 | ISSGGST | CDR2 | NRCoV2-SR13 |
| 70 | ISTSGAV | CDR2 | NRCoV2-SR16 |
| 71 | KQRELVAAISSGGTT | CDR2 | NRCoV2-S2A3 |
| 72 | ISTGGSR | CDR2 | NRCoV2-S2A4 |
| 73 | ISTGSNT | CDR2 | NRCoV2-S2B3 |
| 74 | INSGDRDSTT | CDR2 | NRCoV2-S2H4 |
| 75 | ITSGGST | CDR2 | NRCoV2-S2F3 |
| 76 | ITSGGAT | CDR2 | NRCoV2-S2G3 |
| 77 | ISSDGDK | CDR2 | NRCoV2-S2G4 |
| 78 | ISAGGST | CDR2 | NRCoV2-S202 |
| 79 | IWSDSRT | CDR2 | NRCoV2-MRed02 |
| 80 | IWSDTTT | CDR2 | NRCoV2-MRed04 |
| 81 | ISSSDGST | CDR2 | NRCoV2-MRed03<br>NRCoV2-MRed05 |
| 82 | ISSSDGSA | CDR2 | NRCoV2-MRed06 |
| 83 | ITRGGVT | CDR2 | NRCoV2-MRed07 |
| 84 | INSGGGST | CDR2 | NRCoV2-MRed11 |
| 85 | VSDGGTP | CDR2 | NRCoV2-MRed18 |
| 86 | MTTSGSA | CDR2 | NRCoV2-MRed19 |
| 87 | IRESGSGT | CDR2 | NRCoV2-MRed20 |
| 88 | ISSRGST | CDR2 | NRCoV2-MRed22 |
| 89 | ISWRGDST | CDR2 | NRCoV2-MRed25 |
| 90 | AADYSMRPLWVSRWHRDYEY | CDR3 | NRCoV2-1a |
| 91 | AADYSMRRFAVGRWHRDYEY | CDR3 | NRCoV2-1c |
| 92 | AADYSMRPFAVGRWHRDYEY | CDR3 | NRCoV2-1d |

| | | | |
|---|---|---|---|
| 93 | TKGPDLYYFGSGYSD | CDR3 | NRCoV2-02 |
| 94 | NIYGPTYSTRRNEY | CDR3 | NRCoV2-03 |
| 95 | WSSYEST | CDR3 | NRCoV2-04 |
| 96 | SKGPVSSYYGSGYDY | CDR3 | NRCoV2-05 |
| 97 | NARHYGGSEY | CDR3 | NRCoV2-06 |
| 98 | AAVQDVHGDNYYCTSPNEYNV | CDR3 | NRCoV2-07 |
| 99 | AADYQYSTYCLGYDAHYEY | CDR3 | NRCoV2-08 |
| 100 | YAADDLGDY | CDR3 | NRCoV2-10 |
| 101 | AARSRDFSSPFSATDTYTS | CDR3 | NRCoV2-11 |
| 102 | AARSRDFSSPISATDKYGS | CDR3 | NRCoV2-11a |
| 103 | AADRGLSYYYTRTTEYNY | CDR3 | NRCoV2-12 |
| 104 | HAVNADIGGDY | CDR3 | NRCoV2-14 |
| 105 | YAAYGGGGDY | CDR3 | NRCoV2-15 |
| 106 | QAANVNGGDY | CDR3 | NRCoV2-17 |
| 107 | SLHTSHDY | CDR3 | NRCoV2-18 |
| 108 | AADRARLRFGCSLNFRREVAYDY | CDR3 | NRCoV2-19 |
| 109 | AADRGMSYYYTRATEYYY | CDR3 | NRCoV2-20 |
| 110 | AADHRGRSLRFGCSSSTTDYLY | CDR3 | NRCoV2-21 |
| 111 | AATGIRSTWSVYGCSRLAGPYDY | CDR3 | NRCoV2-SR01 |
| 112 | AADRLYSRACPTAGGRNY | CDR3 | NRCoV2-SR02 |
| 113 | NRGGWEYRSSYYIMGPH | CDR3 | NRCoV2-SR03 |
| 114 | NTAALVGNRLLPMATIT | CDR3 | NRCoV2-SR04 |
| 115 | NMGGWDYRSNTYIPGSRSDY | CDR3 | NRCoV2-SR13 |
| 116 | NTGGWDYRSSTFIMGLN | CDR3 | NRCoV2-SR16 |
| 117 | NTGSLSYGGSVYYPSYDN | CDR3 | NRCoV2-S2A3 |
| 118 | HAAARDSHGIYLLDT | CDR3 | NRCoV2-S2A4 |
| 119 | NYRSIYYGQNF | CDR3 | NRCoV2-S2B3 |
| 120 | ALVFGYTSRDYCLTPKRGNY | CDR3 | NRCoV2-S2H4 |
| 121 | NLRDILSQPF | CDR3 | NRCoV2-S2F3 |
| 122 | YTTKRDDASVY | CDR3 | NRCoV2-S2G3 |
| 123 | NKHWWTGDW | CDR3 | NRCoV2-S2G4 |
| 124 | NYGPGYRKAA | CDR3 | NRCoV2-S202 |
| 125 | AADRGFVVRGQYDY | CDR3 | NRCoV2-MRed02<br>NRCoV2-MRed04 |
| 126 | ATDAFATCDSWYAQIAQYDF | CDR3 | NRCoV2-MRed03 |
| 127 | ATGPQAYYSGSYYFQCPQAGMDY | CDR3 | NRCoV2-MRed05 |
| 128 | ATDSFSSCSDYESGMDF | CDR3 | NRCoV2-MRed06 |
| 129 | YANYGWAIPY | CDR3 | NRCoV2-MRed07 |
| 130 | ATTISDGSSWSTKSY | CDR3 | NRCoV2-MRed11 |
| 131 | NYYNYYYGRNF | CDR3 | NRCoV2-MRed18 |
| 132 | YMHSVYYGIDY | CDR3 | NRCoV2-MRed19 |

| | | | |
|---|---|---|---|
| 133 | AAKPPFYGSGTYSTPRAYLY | CDR3 | NRCoV2-MRed20 |
| 134 | NAREFTGFDY | CDR3 | NRCoV2-MRed22 |
| 135 | AAEMWGTATIVASRYTY | CDR3 | NRCoV2-MRed25 |
| 136 | EVKLVQSGGGSVQPGGSLRLSCAAS**GSTLDYYA**IGWF RQAPGKEREWVSC**VSSSDGST**LYADSVKGRFTISRDNA KNTVYLQMNSLKPEDTAVYVC**AADYSMRPLWVSRWH RDYEY**WGQGTQVTVSS | $V_HH$ | NRCoV2-1a |
| 137 | EVQLVESGGGSVQPGGSLRLSCAAS**GSILDYYA**VGWF RQAPGKEREWVSS**VSSSDGST**LYADSVKGRFTISRDDA KNTIYLQMDNLEPEDTAVYVC**AADYSMRRFAVGRWHR DYEY**WGQGTQVTVSS | $V_HH$ | NRCoV2-1c |
| 138 | EVQLVESGGGSVQPGGSLRLSCAAS**GSTLDYYA**IGWF RQAPGKEREWVSS**VSSSDGNT**LYADSVKGRFTISRDNA KNTVYLQMNSLKAEDTAVYVC**AADYSMRPFAVGRWH RDYEY**WGQGTQVTVSS | $V_HH$ | NRCoV2-1d |
| 139 | EVQLVESGGGLVQAGGSLRLSCAAS**GFTFSNYA**MNWV RQAPGKGLEWVSG**ISGRGDDT**RYADSVKGRFTISRDN AKNTLFLQMRSLRPEDTGVYRC**TKGPDLYYFGSGYSD** RGQGTQVTVSS | $V_HH$ | NRCoV2-02 |
| 140 | EVQLVSSGGGLVQAGGSLRLSCTAS**GITFSYYA**MGWY RQAPGQPRELVAS**MSNMDST**IYADSVKGRFTISRDNAK TTIYLQMNNLKPEDTAVYFC**NIYGPTYSTRRNEY**WGQG TQVTVSS | $V_HH$ | NRCoV2-03 |
| 141 | AVQLVDSGGGLVQPGGSLRLSCAAS**GSPFSNVV**MAWY RQAPGKQRERVAF**ISGGGIA**DYIMSVKGRFTISRDNAKN TVYLQMNSLKPEDTAVYYC**WSSYEST**WGQGTQVTVSS | $V_HH$ | NRCoV2-04 |
| 142 | EVKLVQSGGGLVQPGGSLRLSCAAS**GFIFSNYA**MNWV RQAPGKGLEWVSG**INSGGGDT**RYADSVKGRFTVSRDN AKNTLYLQMNSLKPEDTGVYYC**SKGPVSSYYGSGYDY**R GQGTQVTVSS | $V_HH$ | NRCoV2-05 |
| 143 | EVQLVQSGGGLVQAGESLRLSCAAS**VSTFSSYA**MGWY RQAPGKQRELVAS**IGFVGAT**YYIDSVKGRFTISRDNAKK TAYLQMNDLKPDDTAVYYC**NARHYGGSEY**WGQGTQV TVSS | $V_HH$ | NRCoV2-06 |
| 144 | QVQLVQSGGGLVQPGGSLRLSCAAS**GVTLDYYA**IGWF RQAPGKEREAVSC**ISSNGRRN**HYVASVRGRFTISRDNA KSTVYLQMNSLKPEDTAVYYC**AAVQDVHGDNYYCTSP NEYNV**WGQGTQVTVSS | $V_HH$ | NRCoV2-07 |
| 145 | EVQLQQSGGGLVQPGGSLRLSCAAS**GFTLDDYA**IGWF RQSPGKEREWVTC**ISRSGTTT**YYTASVKGRFTFSRDNA KNTAYLQMNSLRPEDTAVYYC**AADYQYSTYCLGYDAH YEY**WGQGTQVTVSS | $V_HH$ | NRCoV2-08 |

| | | | |
|---|---|---|---|
| 146 | QLQLQESGGGLVQPGGSLTLSCAAS**GNTFSRSN**MHWY RQAPGAQREWVAA**ISSRGIS**TYAYSAKGRFTISRDNAKN TVSLQMNSLKPEDTAVYYC**YAADDLGDY**WGQGTQVTV SS | $V_HH$ | NRCoV2-10 |
| 147 | EVQLVSSGGGLVQPGGSLRLSCAAS**GSSLDSYS**VSWFR QAPGKEREWISF**ISRYYSST**YYTDSVKGRFTTSRDGDQ KTVHLQMNSLKPEDTAVYYC**AARSRDFSSPFSATDTYT S**WGQGTQVTVSS | $V_HH$ | NRCoV2-11 |
| 148 | EVQLQQSGGGLVQPGGSLRLSCAAS**GFTLDSYN**IAWF RQAPGKEREWISY**ISRYYEST**YYSDSVKGRFTTSRDGD KKTVSLQMNSLKSEDTAVYYC**AARSRDFSSPISATDKY GS**WGQGTQVTVSS | $V_HH$ | NRCoV2-11a |
| 149 | EVQLQQSGGGLVQAGGSLRLSCAAS**GRTFRNYV**MGW FRQAPQAPGKDHEF**VAAISWGGTEI**YYADSVKGRFTIS RDNAKNTVYLQMNSLKPEDTAVYYC**AADRGLSYYYTR TTEYNY**WGQGTQVTVSS | $V_HH$ | NRCoV2-12 |
| 150 | EVQLVSSGGGLVQAGGSLRLSCEAS**GTTFSHYA**VGWY RQAPGKQREWVAS**ISVFGST**TYGGSVAGRFTISRDNDK NTVDLQMNSLKPEDTAVYYC**HAVNADIGGDY**WGQGTQ VTVSS | $V_HH$ | NRCoV2-14 |
| 151 | EVQLVSSGGGLVEAGGSLRLSCIAS**GSTSGRNT**MGWF RQAPGKQREWVAI**VSTSGAT**NYAGSVKGRFTLSRDNA KNAVYLQMNNLKPEDTAVYYC**YAAYGGGGDY**WGQGT QVTVSS | $V_HH$ | NRCoV2-15 |
| 152 | EVQLQQSGGGLVQTGGSLRLSCAAA**GSPFSQLA**MSWY RQISGKERAWVAS**ISPTGNR**SYSKIAKGRFTISRDNAKN TVTLQMTSLKPEDTAAYIC**QAANVNGGDY**WGQGTQVT VSS | $V_HH$ | NRCoV2-17 |
| 153 | EVQLVESGGGLVQAGGSLRLSCVAS**GITISGYN**MAWW RQTRGKQTERVAF**INSGGST**TYSDSVKGRFTISRDNGK NTAYLQMNSLNAEDTADYFC**SLHTSHDY**WGQGTQVTV SS | $V_HH$ | NRCoV2-18 |
| 154 | EVQLLESGGGLVLPGGSLRLSCAVS**GLTLNSYA**IGWFR QAPGKEREGLSC**LTSGGTG**VYAESVKGRFTISRDNAEN TVYLQMNSLKPEDTAVYYC**AADRARLRFGCSLNFRRE VAYDY**WGQGTQVTVSS | $V_HH$ | NRCoV2-19 |
| 155 | EVQLQQSGGGLVQPGGSLRLSCAAS**GRTFSNYV**VGWF RQAPQAPGKDHEF**VAVISGSDTET**YYADSVKGRFTISR DNAKNTVYLQMNSLKPEDTAVYYC**AADRGMSYYYTRA TEYYY**WGQGTQVTVSS | $V_HH$ | NRCoV2-20 |
| 156 | EVQLVESGGGLVQPGGSLRLSCATS**GFTLDYYA**IGWFR QAPGKEREWVSC**ISSGGST**FYVDSVKGRFTISRDNAKD TVYLQMSSLKPDDTAVYYC**AADHRGRSLRFGCSSSTT DYLY**WGQGTQVTVSS | $V_HH$ | NRCoV2-21 |

| | | | |
|---|---|---|---|
| 157 | EVQLVQSGGGSVQAGGSLRLSCVAS**GFTFDNYA**IGWF RQAPGKEREGVSC**ISGNGGVT**IYADSVKGRFTISRDNA KNLVYLQMNSLKPEDTAVYYC**AATGIRSTWSVYGCSRL AGPYDY**WGQGTQVTVSS | $V_HH$ | NRCoV2-SR01 |
| 158 | EVQLVDSGGGLVQAGGSLRLSCTAS**EFTLNYYS**IGWFR QSPGKEREGVSC**IRYSGGGI**DYADSVKGRFTISRDNAK NTVYLTMNSLKPEDTAVYYC**AADRLYSRACPTAGGRN Y**WGQGTQVTVSS | $V_HH$ | NRCoV2-SR02 |
| 159 | AVQLVDSGGGLVQAGGSLRLSCAAS**GSIFSNNH**MGWY RQAPGKQRELVAA**ISSGGKT**NYADFAKGRFTISRDNAK NMVYLQMNSLKPEDTAVYYC**NRGGWEYRSSYYIMGPH** WGQGTQVTVSS | $V_HH$ | NRCoV2-SR03 |
| 160 | QVQLVESGGGLVQAGGSLRLSCAAS**GRTFSSHT**VGWY RQAPGKQRDLVAA**ISMGGNTNYA**DYADSVKGRFTISRD NAKNTLYLQMNSLKPEDTAVYYC**NTAALVGNRLLPMAT IT**WGQGTQVTVSS | $V_HH$ | NRCoV2-SR04 |
| 161 | EVQLVESGGGLVTTGGSLRLSCATS**GSRFGSKH**MAWY RQAPGKQRDLVAA**ISSGGST**HYGSSVKGRFTISRDNAK STVYLQMNSLNPEDTAVFYC**NMGGWDYRSNTYIPGSR SDY**WGQGTQVTVSS | $V_HH$ | NRCoV2-SR13 |
| 162 | QVQLVQSAGGLVQAGGSLRLSCVVS**GTTFSRYH**MGW HRQAPGKQRDFVAG**ISTSGAV**TYADSAKGRFTISRDNA KNTVYLEMNSLKLEDTALYYC**NTGGWDYRSSTFIMGL N**WGQGTQVTVSS | $V_HH$ | NRCoV2-SR16 |
| 163 | EVQLQQSGGGLVQAGGSLRLSCAAS**GRPYSNYA**MAWY RQAPGKQHELVAG**KQRELVAAISSGGTT**KYADSVKAR FTISRDNAKNTVYLQMNILRPEDTAVYYC**NTGSLSYGGS VYYPSYDN**WGQGTQVTVSS | $V_HH$ | NRCoV2-S2A3 |
| 164 | QVQLVQSGGGLVQAGGSLRLSCAVS**GSPFRSNV**MEWY RQAPGKQRELVAS**ISTGGSR**TYTDSVKGRFTISRDNAK NEAFLQMNSLKPEDTAVYYC**HAAARDSHGIYLLDT**WG QGTQVTVSS | $V_HH$ | NRCoV2-S2A4 |
| 165 | QVQLVDSGGGLVQAGGSLRLSCAAS**ASTFGDSA**MGYY RQAPGKQRELVAT**ISTGSNT**NYADSVKGRFTISRDDAK NTVYLQMNSLKPEDTAVYYC**NYRSIYYGQNF**WGQGTQ VTVSS | $V_HH$ | NRCoV2-S2B3 |
| 166 | QVQLVQSGGGLVQAGGSLRLSCAAS**GFTFNLYS**IAWFR QAPGKEREGVSC**INSGDRDSTT**YYADSVKGRFTISRDN AKHTAYLQMDSLKPEDTAVYYC**ALVFGYTSRDYCLTPK RGNY**WGQGTQVTVSS | $V_HH$ | NRCoV2-S2H4 |
| 167 | EVQLVQSGGGLVQAGGSLRLSCATS**VRILSVPA**MGWY RQAPGKEREMVAV**ITSGGST**NYADSVKGRFTISRDNAK NTVYLQMNSLKLEDTAVYQC**NLRDILSQPF**WGQGTQV TVSS | $V_HH$ | NRCoV2-S2F3 |

| | | | |
|---|---|---|---|
| 168 | QVQLVQSGGGSVQAGGSLRLSCAAS**GSTFGIFL**MGWR RQAPGKQRELVAH**ITSGGAT**NYADSVKGRFTISRDNAK NTVYLQMNSLEPEDTAVYYC**YTTKRDDASVY**WGQGTQ VTVSS | $V_HH$ | NRCoV2-S2G3 |
| 169 | QVQLVQSGGGLVQAGGSLTLSCAPS**GSTFSGYA**TNWY RQAPGKQRELVAT**ISSDGDK**NYADSVKGRFTISRDNAK NTVYLQMNSLKPEDTAVYYC**NKHWWTGDW**WGQGTQ VTVSS | $V_HH$ | NRCoV2-S2G4 |
| 170 | QVQLVQSGGGLVQAGGSLRLSCAAS**GITVSRIG**MGWY RQAPGKQRDMVAV**ISAGGST**NYADSVKGRFTISRDNAK NTVYLQMDSLKPEDTAVYYC**NYGPGYRKAA**WGQGTQ VTVSS | $V_HH$ | NRCoV2-S202 |
| 171 | EVQLVESGGGLVQPGGSLRLSCAAS**GNIFSINS**MGWFR QAPGKERDVVAT**IWSDSRT**SYADSVKGRFTISTDNTRT KVYLQMSSLNPEDTAVYYC**AADRGFVVRGQYDY**WGQ GTQVTVSS | $V_HH$ | NRCoV2-MRed02 |
| 172 | EVQLVESGGGLVQPGGSLRLSCAAI**GFTLDYYA**IGWFR QAPGKEREGVSC**ISSSDGST**YYADSVKGRFTISRDNAK NTVYLQMNSLKPEDTAVYYC**ATDAFATCDSWYAQIAQ YDF**RGQGTQVTVSS | $V_HH$ | NRCoV2-MRed03 |
| 173 | EVQLVESGGGLVQPGRSLRLSCAAS**GNSFSIST**MGWF RQAPGKERELVAS**IWSDTTT**SYADSVKGRFTISTDNTRT KVYLQMSSLNPEDTAVYYC**AADRGFVVRGQYDY**WGQ GTQVTVSS | $V_HH$ | NRCoV2-MRed04 |
| 174 | EVQLVESGGGLVQPGGSLRLSCAAS**GFTLDYYA**IGWFR QAPGKEREGVSC**ISSSDGST**LYADSVKGRFTISRDNAK NTVYLQMNSLKPEDTAVYYC**ATGPQAYYSGSYYFQCP QAGMDY**WGKGTQVTVSS | $V_HH$ | NRCoV2-MRed05 |
| 175 | EVQLVESGGGLVQAGGSLRLSCAAS**GFTLAYYA**IGWFR QAPGKEREGVSC**ISSSDGSA**HYADSVKGRFTISRDNAK NTVSLQMNSLKPEDTAVYYC**ATDSFSSCSDYESGMDF** WGKGTQVTVSS | $V_HH$ | NRCoV2-MRed06 |
| 176 | EVQLVESGGGLVQPGGSLTLSCAAS**GSIGPFNT**MGWY RQAPGNQREPAAI**ITRGGVT**NYADSVKGRFTISRDNAK NAVYLQMDSLKPDDTAVYYC**YANYGWAIPY**WGNGTQV TVSS | $V_HH$ | NRCoV2-MRed07 |
| 177 | EVQLVESGGGLVQAGGSLRLSCAAS**GFTFSSYA**MSWH RQAPGKGLEWVSA**INSGGGST**SYADSVKGRFAISRDNA KNTLYLQMNSLKPEDTAVYYC**ATTISDGSSWSTKSY**RG QGTQVTVSS | $V_HH$ | NRCoV2-MRed11 |
| 178 | EVQLVESGGGLVQPGGSLRLSCAAS**TTVFGRNA**MGWY RQAPGKERELVAT**VSDGGTP**NYADSVKGRFTISRDNAK NTIYLQMNSLEPEDTAVYYC**NYYNYYYGRNF**WGQGTQ VTVSS | $V_HH$ | NRCoV2-MRed18 |

| | | | |
|---|---|---|---|
| 179 | EVQLVESGGGLVQPGGSLRLSCAAS**TIIFKGQT**MGWF RQAPGNERELVAT**MTTSGSA**NYADSVKGRFTISRDNEK TVTLQMNSLKPEDTALYYC**YMHSVYYGIDY**WGKGTQV TVSS | $V_HH$ | NRCoV2-MRed19 |
| 180 | EVQLVESGGGSVQAGGSLRLSCAAS**GLSFSSYD**MGWF RQAPGKEREFVAA**IRESGSGT**YYADSVKGRFTISRDNA KNTVYLQVSSLKPEDTAVYTC**AAKPPFYGSGTYSTPRA YLY**WGQGTQVTVSS | $V_HH$ | NRCoV2-MRed20 |
| 181 | EVQLVESGGGLVQPGGSLRLSCAAS**GSVFASNA**MGWY RQAPGKQRELVAT**ISSRGST**NYADSVKGRFTISRDNAK NTVYLQMNSLGPEDTAVYYC**NAREFTGFDY**WGQGTQV TVSS | $V_HH$ | NRCoV2-MRed22 |
| 182 | EVQLVESGGGLVQAGGSLRLSCAAS**GHTFSRYG**MGW FRQAPGKEREFVAA**ISWRGDST**YYRDSVNGRFTISRDN AKNTVYLGMNSLKPEDTAVYYC**AAEMWGTATIVASRY TY**WGQGTQVTVSS | $V_HH$ | NRCoV2-MRed25 |
| 183 | XXXLXXSXGGXVXXGXSLXLSCXXXXXXXXXXXXXXXX RQXXXXXGXXXXXXXXXXXXXXXXXXXXXXXXXXXXX XXXXXRFXXSXDXXXXXXXLXXXXLXXXDTXXXXCXX XXXXXXXXXXXXXXXXXXXXXXXGXGTQVTVSS<br><br>X at position 1 is Ala, Glu, or Gln<br>X at position 2 is Leu or Val<br>X at position 3 is Lys or Gln<br>X at position 5 is Leu, Gln, or Val<br>X at position 6 is Asp, Glu, Gln, or Ser<br>X at position 8 is Ala or Gly<br>X at position 11 is Leu or Ser<br>X at position 13 is Glu, Leu, Gln, or Thr<br>X at position 14 is Ala, Pro, or Thr<br>X at position 16 is Glu, Gly, or Arg<br>X at position 19 is Arg or Thr<br>X at position 23 is Ala, Glu, Ile, Thr, or Val<br>X at position 24 is Ala, Pro, Thr, or Val<br>X at position 25 is Ala, Ile, or Ser<br>X at position 26 is Ala, Glu, Gly, Thr, or Val<br>X at position 27 is Phe, His, Ile, Leu, Asn, Arg, Ser, Thr, or Val<br>X at position 28 is Ile, Pro, Arg, Ser, Thr, or Val<br>X at position 29 is Phe, Gly, Ile, Leu, Ser, Val, or Tyr<br>X at position 30 is Ala, Asp. Gly, Lys, Asn, Pro, Arg, or Ser<br>X at position 31 is Asp, Phe, Gly, His, Ile, Leu, Asn, Gln, Arg, Ser, Val, Tyr<br>X at position 32 is Phe, His, Ile, Lys, Leu, Asn, Pro, Gln, Ser, Val, or Tyr<br>X at position 33 is Ala, Asp, Gly, His, Leu, Asn, Ser, Thr, or Val<br>X at position 34 is Ile, Met, Thr, or Val | $V_HH$ cons. seq. | Consensus sequence for $V_HH$ sequences, generated based on the sequence alignment shown in **Fig. 18** |

| | | | |
|---|---|---|---|
| | X at position 35 is Ala, Glu, Gly, His, Asn, or Ser<br>X at position 36 is Trp or Tyr<br>X at position 37 is Phe, His, Arg, Val, Trp, or Tyr<br>X at position 40 is Ala, Ile, Ser, or Thr<br>X at position 41 is Pro or absent<br>X at position 42 is Gln or absent<br>X at position 43 is Ala or absent<br>X at position 44 is Pro, Arg, or Ser<br>X at position 46 is Ala, Lys, Asn, or Gln<br>X at position 47 is Asp, Glu, Gly, Pro, or Gln<br>X at position 48 is His or absent<br>X at position 49 is Glu or absent<br>X at position 50 is Leu or absent<br>X at position 51 is Val or absent<br>X at position 52 is Ala or absent<br>X at position 53 is Gly or absent<br>X at position 54 is Lys or absent<br>X at position 55 is Gln or absent<br>X at position 56 is His, Leu, Arg, or Thr<br>X at position 57 is Ala, Asp, or Glu<br>X at position 58 is Ala, Phe, Gly, Leu, Met, Pro, Arg, Val, or Trp<br>X at position 59 is Ala, Ile, Leu, or Val<br>X at position 60 is Ala, Ser, or Thr<br>X at position 61 is Ala, Cys, Phe, Gly, His, Ile, Ser, Thr, Val, or Tyr<br>X at position 62 is Ile, Leu, Met, or Val<br>X at position 63 is Gly, Asn, Arg, Ser, Thr, or Trp<br>X at position 64 is Ala, Asp, Glu, Phe, Gly, Met, Asn, Pro, Arg, Ser, Thr, Val, Trp, or Tyr<br>X at position 65 is Asp, Phe, Gly, Met, Asn, Arg, Ser, Thr, Val, Tyr, or absent<br>X at position 66 is Asp, Gly, Ser, Thr, or Tyr<br>X at position 67 is Ala, Asp, Glu, Gly, Ile, Lys, Asn, Arg, Ser, Thr, or Val<br>X at position 68 is Ala, Asp, Glu, Gly, Lys, Asn, Pro, Arg, Ser, Thr, or Val<br>X at position 69 is Asn, Ser, or absent<br>X at position 70 is Thr, Tyr, or absent<br>X at position 71 is Ala, Gly, Ile, Asn, Thr, or absent<br>X at position 72 is Asp, Phe, His, Ile, Lys, Leu, Asn, Arg, Ser, Thr, Val, Tyr, or absent<br>X at position 73 is Tyr or absent<br>X at position 74 is Ala, Gly, Ile, Arg, Ser, Thr, or Val<br>X at position 75 is Ala, Asp, Glu, Gly, Lys, Met, Ser, or Tyr<br>X at position 76 is Phe, Ile, or Ser<br>X at position 77 is Ala or Val<br>X at position 78 is Ala, Lys, Asn, or Val<br>X at position 79 is Ala or Gly | | |

| | | | |
|---|---|---|---|
| | X at position 82 is Ala or Thr<br>X at position 83 is Phe, Ile, Leu, Thr, or Val<br>X at position 85 is Arg or Thr<br>X at position 87 is Asp, Gly, or Asn<br>X at position 88 is Ala, Asp, Glu, Gly, or Thr<br>X at position 89 is Glu, Lys, Gln, or Arg<br>X at position 90 is Asp, His, Lys, Asn, Ser, Thr, or absent<br>X at position 91 is Ala, Glu, Lys, Leu, Met, or Thr<br>X at position 92 is Ala, Ile, Leu, or Val<br>X at position 93 is Asp, Phe, His, Ser, Thr, or Tyr<br>X at position 95 is Glu, Gly, Gln, or Thr<br>X at position 96 is Met or Val<br>X at position 97 is Asp, Asn, Arg, Ser, or Thr<br>X at position 98 is Asp, Ile, Asn, or Ser<br>X at position 100 is Glu, Gly, Lys, Asn, or Arg<br>X at position 101 is Ala, Leu, Pro, or Ser<br>X at position 102 is Asp or Glu<br>X at position 105 is Ala or Gly<br>X at position 106 is Ala, Asp, Leu, or Val<br>X at position 107 is Phe or Tyr<br>X at position 108 is Phe, Ile, Gln, Arg, Thr, Val, or Tyr<br>X at position 110 is Ala, His, Asn, Gln, Ser, Thr, Trp, or Tyr<br>X at position 111 is Ala, Ile, Lys, Leu, Met, Arg, Ser, Thr, or Tyr<br>X at position 112 is Ala, Asp, Glu, Gly, His, Lys, Asn, Arg, Ser, Thr, Val, or Tyr<br>X at position 113 is Ala, Asp, Glu, Phe, Gly, His, Ile, Lys, Asn, Pro, Gln, Arg, Ser, Thr, Tyr, or absent<br>X at position 114 is Ala, Asp, Phe, Gly, Ile, Leu, Pro, Gln, Arg, Ser, Val, Trp, or absent<br>X at position 115 is Ala, Asp, Glu, Phe, Gly, Leu, Met, Arg, Ser, Thr, Val, Tyr, or absent<br>X at position 116 is Phe, Gly, His, Leu, Ser, Thr, Trp, Tyr, or absent<br>X at position 117 is Cys, Gly, His, Asn, Arg, Ser, Thr, Tyr, or absent<br>X at position 118 is Ala, Asp, Phe, Gly, Arg, Ser, Thr, Trp, or absent<br>X at position 119 is Ala, Cys, Asp, Gly, Ile, Leu, Asn, Pro, Arg, Ser, Tyr, or absent<br>X at position 120 is Cys, Gly, Ile, Asn, Pro, Arg, Ser, Thr, Val, Trp, Tyr, or absent<br>X at position 121 is Asp, Phe, Gly, Leu, Ser, Trp, Tyr, or absent<br>X at position 122 is Ala, Asp, Gly, Ile, Leu, Thr, Val, Trp, Tyr, or absent<br>X at position 123 is Cys, Phe, Asn, Val, or absent | | |

| | | | |
|---|---|---|---|
| | X at position 124 is Phe, Gly, Ile, Leu, Gln, Ser, Tyr, or absent<br>X at position 125 is Ala, Cys, Asp, Gly, Pro, Arg, Ser, Thr, or absent<br>X at position 126 is Ala, Phe, Gly, Leu, Met, Pro, Gln, Arg, Ser, Thr, Val, Trp, Tyr, or absent<br>X at position 127 is Ala, Asp, Glu, Gly, His, Ile, Pro, Gln, Arg, Ser, Thr, Trp, or absent<br>X at position 128 is Ala, Asp, Gly, Ile, Lys, Met, Asn, Arg, Ser, Thr, Val, Trp, Tyr, or absent<br>X at position 129 is Ala, Asp, Glu, Gly, His, Lys, Leu, Pro, Gln, Arg, Ser, Thr, or absent<br>X at position 130 is Glu, Phe, Gly, His, Ile, Lys, Leu, Met, Asn, Gln, Arg, Ser, Thr, or Tyr<br>X at position 131 is Ala, Asp, Glu, Gly, Ile, Leu, Asn, Pro, Ser, Thr, Val, or Tyr<br>X at position 132 is Ala, Asp, Phe, His, Asn, Ser, Thr, Val, Trp, or Tyr<br>X at position 133 is Arg or Trp<br>X at position 135 is Lys, Asn, or Gln | | |
| 184 | XVQLVXSXGGXVXXGGSLXLSCXXXXXXXXXXXXXXWX<br>RQXPGXXRXXXXXIXXXXGXXXYXXXXXXXXKGRFTISR<br>DNAKXXXXLXMXSLXXXDTAXXYCXXXXXXXXXXXXX<br>XXXXXXXXXXXXGXGTQVTVSS<br><br>X at position 1 is Ala, Glu, or Gln<br>X at position 6 is Asp. Glu, or Gln<br>X at position 8 is Ala or Gly<br>X at position 11 is Leu or Ser<br>X at position 13 is Gln or Thr<br>X at position 14 is Ala, Pro, or Thr<br>X at position 19 is Arg or Thr<br>X at position 23 is Ala, Thr, or Val<br>X at position 24 is Ala, Thr, or Val<br>X at position 25 is Ile or Ser<br>X at position 26 is Glu or Gly<br>X at position 27 is Phe, Arg, Ser, or Thr<br>X at position 28 is Ile, Arg, or Thr<br>X at position 29 is Phe, Gly, or Leu<br>X at position 30 is Asp, Ala, Gly, Asn, Pro, or Ser<br>X at position 31 is Phe, Asn, Arg, Ser, or Tyr<br>X at position 32 is His, Lys, Asn, or Tyr<br>X at position 33 is Ala, His, Ser, or Thr<br>X at position 34 is Ile, Met, or Val<br>X at position 35 is Ala or Gly<br>X at position 37 is Phe, His, or Tyr<br>X at position 40 is Ala or Ser<br>X at position 43 is Lys or Asn<br>X at position 44 is Glu or Gln<br>X at position 46 is Asp or Glu | $V_HH$ cons. seq. | Consensus sequence for S1-NTD specific $V_HHs$, generated based on the sequence alignment shown in **Fig. 19** |

| | | | |
|---|---|---|---|
| | X at position 47 is Phe, Gly, Leu, or Pro<br>X at position 48 is Ala or Val<br>X at position 49 is Ala or Ser<br>X at position 50 is Ala, Cys, Gly, or Ile<br>X at position 52 is Arg, Ser, or Thr<br>X at position 53 is Gly, Met, Arg, Ser, Thr, or Tyr<br>X at position 54 is Gly, Asn, or Ser<br>X at position 55 is Asp, Gly, or absent<br>X at position 57 is Ala, Gly, Lys, Asn, Ser, or Val<br>X at position 58 is Ala, Ile, Thr, or Val<br>X at position 59 is Asp, His, Ile, Asn, Thr, or Tyr<br>X at position 61 is Ala, Gly, or absent<br>X at position 62 is Asp or absent<br>X at position 63 is Tyr or absent<br>X at position 64 is Ala or absent<br>X at position 65 is Asp or Ser<br>X at position 66 is Phe or Ser<br>X at position 67 is Ala or Val<br>X at position 80 is Asn or Ser<br>X at position 81 is Ala, Leu, Met, or Thr<br>X at position 82 is Leu or Val<br>X at position 83 is Ser or Tyr<br>X at position 85 is Glu, Gln, or Thr<br>X at position 87 is Asp or Asn<br>X at position 90 is Lys or Asn<br>X at position 91 is Leu or Pro<br>X at position 92 is Asp or Glu<br>X at position 96 is Leu or Val<br>X at position 97 is Phe or Tyr<br>X at position 100 is Ala, Asn, or Tyr<br>X at position 101 is Ala, Met, Arg, or Thr<br>X at position 102 is Asp, Ala, Gly, Asn, or Thr<br>X at position 103 is Ala, Gly, Arg, Ser, or absent<br>X at position 104 is Phe, Ile, Leu, Trp, or absent<br>X at position 105 is Asp, Glu, Ala, Arg, Ser, Val, Tyr, or absent<br>X at position 106 is Gly, Ser, Thr, Tyr, or absent<br>X at position 107 is Cys, Asn, Arg, Thr, or absent<br>X at position 108 is Asp, Ser, Trp, or absent<br>X at position 109 is Asp, Asn, Ser, or absent<br>X at position 110 is Thr, Val, Trp, Tyr, or absent<br>X at position 111 is Glu, Phe, Arg, Tyr, or absent<br>X at position 112 is Gly or absent<br>X at position 113 is Ala, Cys, or absent<br>X at position 114 is Cys, Ser, or absent<br>X at position 115 is Ala, Ile, Leu, Pro, Arg, Ser, or absent<br>X at position 116 is Gln, Leu, Met, Pro, Thr, Tyr, or absent<br>X at position 117 is Ala, Gly, Ile, Pro, or absent | | |

| | | | |
|---|---|---|---|
| | X at position 118 is Ala, Gly, Leu, Met, Pro, Ser, Trp, or absent<br>X at position 119 is Gln, Ala, Gly, Pro, Arg, or absent<br>X at position 120 is Ile, Met, Arg, Ser, Thr, Tyr, or absent<br>X at position 121 is Asp, Ile, Asn, Pro, or absent<br>X at position 122 is Phe, His, Asn, Thr, or Tyr<br>X at position 123 is Arg or Trp<br>X at position 125 is Gln, Lys, or Asn | | |
| 185 | XVQLXXSGGGXVQXGGSLXLSCAXSXXXXXXXXXXXX<br>RQAPGXXXXXXXXXXXXXVXXXXXXXXXXXXXXYXDSV<br>XXRFXISRDXXKXXXXLXXXXLXXEDTAXYXCXXXXXX<br>XXXXXXXXXXXXXXXGXGTQVTVSS<br><br>X at position 1 is Ala or Pro<br>X at position 5 is Pro or Val<br>X at position 6 is Gln, Ala, or Pro<br>X at position 11 is Lys or Ser<br>X at position 14 is Asp or Asn<br>X at position 19 is Arg or Thr<br>X at position 24 is Asp, Asn, Thr, or Val<br>X at position 26 is Asp, Phe, Thr, or Val<br>X at position 27 is Cys, Gly, His, Lys, Arg, Ser, or Thr<br>X at position 28 is His, Asn, Ser, Thr, or Val<br>X at position 29 is Cys, Lys, Val, or Tyr<br>X at position 30 is Asp, Phe, Ile, Met, Arg, or Ser<br>X at position 31 is Gln, Phe, His, Lys, Met, Arg, Ser, or Val<br>X at position 32 is Cys, His, Met, Asn, Pro, Ser, or Tyr<br>X at position 33 is Asp, Gln, Phe, Lys, Ser, Thr, or Val<br>X at position 34 is His, Leu, or Thr<br>X at position 35 is Asp, Ala, Phe, Met, or Ser<br>X at position 36 is Trp or Tyr<br>X at position 37 is Cys, Gly, Arg, or Tyr<br>X at position 43 is Ile or Met<br>X at position 44 is Ala, Phe, or Pro<br>X at position 45 is Gly, Lys, or absent<br>X at position 46 is Ala or absent<br>X at position 47 is Lys or absent<br>X at position 48 is Val or absent<br>X at position 49 is Asp or absent<br>X at position 50 is Phe or absent<br>X at position 51 is Ile or absent<br>X at position 52 is Pro or absent<br>X at position 53 is Arg or absent<br>X at position 54 is Gln or Ala<br>X at position 55 is Cys, Phe, Lys, Leu, or Trp<br>X at position 57 is Asp or Ser<br>X at position 58 is Asp, Glu, Gly, Ser, Thr, or Val<br>X at position 59 is His, Leu, or Val | $V_HH$ cons. seq. | Consensus sequence for S2 specific $V_HHs$, generated based on the sequence alignment shown in **Fig. 20** |

| | | | |
|---|---|---|---|
| | X at position 60 is Met, Arg, Ser, or absent<br>X at position 61 is Ala, Ser, Thr, or Trp<br>X at position 62 is Asp, Gln, Phe, Arg, Ser, or Thr<br>X at position 63 is Gln or absent<br>X at position 64 is Arg or absent<br>X at position 65 is Gln, Phe, Arg, or Ser<br>X at position 66 is Gln, Phe, or Ser<br>X at position 67 is Asp, Gln, Phe, Met, Ser, or Thr<br>X at position 68 is Asp, Ile, Asn, Arg, or Thr<br>X at position 69 is Ile, Met, Ser, Thr, or Tyr<br>X at position 71 is Asp, Arg, or Thr<br>X at position 75 is Ile or Met<br>X at position 76 is Asp or Phe<br>X at position 79 is Asp or Thr<br>X at position 84 is Gln or Met<br>X at position 85 is Asp or Ala<br>X at position 87 is Gly, Met, or absent<br>X at position 88 is Ala or Thr<br>X at position 89 is Asp, His, Lys, or Val<br>X at position 90 is Cys, Thr, or Tyr<br>X at position 92 is Phe or Pro<br>X at position 93 is Leu or Val<br>X at position 94 is Gln, Met, or Ser<br>X at position 95 is His or Ser<br>X at position 97 is Ala, Phe, Ile, or Arg<br>X at position 98 is Lys or Asn<br>X at position 103 is Lys or Val<br>X at position 105 is Pro, Thr, or Tyr<br>X at position 107 is Asp, Gly, Met, or Tyr<br>X at position 108 is Asp, ile, Lys, Leu, Thr, or Tyr<br>X at position 109 is Asp, Ala, Phe, Gly, Ile, Arg, Thr, Val, or Tyr<br>X at position 110 is Asp, Gln, Ala, Cys, His, Ile, Met, Asn, Ser, or absent<br>X at position 111 is Phe, His, Lys, Asn, Arg, Ser, Val, Tyr, or absent<br>X at position 112 is Gln, Cys, Leu, Ser, Tyr, or absent<br>X at position 113 is Phe, Ser, Thr, Trp, Tyr, or absent<br>X at position 114 is Phe, Gly, Ser, or absent<br>X at position 115 is Phe, Arg, Ser, Thr, or absent<br>X at position 116 is Asp, Gln, Phe, or absent<br>X at position 117 is Thr, Tyr, or absent<br>X at position 118 is Glu, His, Ser, Tyr, or absent<br>X at position 119 is Lys, Ser, Val, or absent<br>X at position 120 is Ser, Thr, Val, Tyr, or absent<br>X at position 121 is Asp, Gln, Cys, His, Asn, Trp, Tyr, or absent<br>X at position 122 is Gln, Ile, Lys, Asn, Arg, Ser, Thr, Trp, or Tyr<br>X at position 123 is Asp, Phe, Lys, Arg, Ser, or Thr | | |

| | | | |
|---|---|---|---|
| | X at position 124 is Cys, Phe, His, Ile, Lys, Pro, Arg, Ser, or Tyr<br>X at position 125 is Asp, Gln, Lys, Met, Asn, Ser, Thr, or Val<br>X at position 126 is Asp, Cys, Met, Thr, Trp, or Tyr<br>X at position 127 is Arg or Trp<br>X at position 129 is Ile or Pro | | |
| 186 | XXXLXXSGGGXVXXGXSLXLSCXXXXXXXXXXXXXXWX RQXXXXXGXXXXXXXXXXXXXXXXXXYXXXXXGRFTXS XDXXXXXXXLQMXXLXXXDTXXYXCXXXXXXXXXXXX XXXXXXXXXXXXXGXGTQVTVSS<br><br>X at position 1 is Asp, Ala, or Pro<br>X at position 2 is Lys or Val<br>X at position 3 is Ile or Pro<br>X at position 5 is Lys, Pro, or Val<br>X at position 6 is Gln, Ala, Pro, or Ser<br>X at position 11 is Lys or Ser<br>X at position 13 is Ala, Lys, or Pro<br>X at position 14 is Asp, Asn, or Thr<br>X at position 16 is Ala, Phe, or Arg<br>X at position 19 is Arg or Thr<br>X at position 23 is Asp, Ala, His, Thr, or Val<br>X at position 24 is Asp, Thr, or Val<br>X at position 25 is Asp or Ser<br>X at position 26 is Phe or Val<br>X at position 27 is Cys, His, Lys, Met, Arg, Ser, Thr, or Val<br>X at position 28 is His, Asn, Ser, or Thr<br>X at position 29 is Cys, His, Lys, or Ser<br>X at position 30 is Gln, Phe, Met, Arg, or Ser<br>X at position 31 is Gln, Phe, Gly, His, Met, Pro, Arg, Ser, or Tyr<br>X at position 32 is Lys, Met, Ser, Val, or Tyr<br>X at position 33 is Asp, Met, Ser, Thr, or Val<br>X at position 34 is His, Leu, or Val<br>X at position 35 is Asp, Phe, Gly, Met, or Ser<br>X at position 37 is Cys, Val, Trp, or Tyr<br>X at position 40 is Asp, His, Ser, or Thr<br>X at position 41 is Asn or absent<br>X at position 42 is Pro or absent<br>X at position 43 is Asp or absent<br>X at position 44 is Asn, Arg, or Ser<br>X at position 46 is Asp, Ile, or Pro<br>X at position 47 is Gln, Ala, Phe, Asn, or Pro<br>X at position 48 is Gly, Lys, Arg, or Thr<br>X at position 49 is Asp, Gln, or Ala<br>X at position 50 is Asp, Cys, Phe, Lys, Arg, Val, or Trp<br>X at position 51 is His, Lys, or Val<br>X at position 52 is Asp, Ser, or Thr | $V_HH$ cons. seq. | Consensus sequence for S1-RBD specific $V_HHs$, generated based on the sequence alignment shown in **Fig. 21** |

| | | | |
|---|---|---|---|
| | X at position 53 is Asp, Glu, Cys, Phe, His, Ser, Thr, Val, or Tyr<br>X at position 54 is His, Lys, Leu, or Val<br>X at position 55 is Phe, Met, Ser, Thr, or Trp<br>X at position 56 is Cys, Phe, Met, Asn, Arg, Ser, Thr, Val, Trp, or absent<br>X at position 57 is Phe, Met, Arg, Ser, Tyr, or absent<br>X at position 58 is Gln, Cys, Phe, Leu, Arg, Ser, Thr, Val, or Tyr<br>X at position 59 is Gln, Ala, Phe, Arg, Ser, or Thr<br>X at position 60 is Asp, Gln, Ala, His, Met, Arg, Ser, or Thr<br>X at position 61 is Asp, Phe, His, Met, Arg, Ser, or Thr<br>X at position 62 is Gln, Cys, Gly, His, Lys, Met, Arg, Ser, Thr, Val, or Tyr<br>X at position 64 is Asp, Phe, His, Ser, Thr, or Val<br>X at position 65 is Asp, Gln, Ala, Phe, Ile, Leu, or Tyr<br>X at position 66 is His or Ser<br>X at position 67 is Asp or Val<br>X at position 68 is Asp, Ile, or Arg<br>X at position 73 is Cys, His, Lys, Thr, or Val<br>X at position 75 is Arg or Thr<br>X at position 77 is Gln, Phe, or Met<br>X at position 78 is Asp, Gln, Phe, or Thr<br>X at position 79 is Ala, Ile, Pro, or Arg<br>X at position 80 is Gln, Ile, Met, Ser, or Thr<br>X at position 81 is Asp, Ile, or Thr<br>X at position 82 is Asp, His, Lys, or Val<br>X at position 83 is Gln, Cys, Gly, Ser, Thr, or Tyr<br>X at position 87 is Gln, Met, Arg, Ser, or Thr<br>X at position 88 is Gln, Met, or Ser<br>X at position 90 is Ala, Ile, Met, or Arg<br>X at position 91 is Asp, Asn, or Ser<br>X at position 92 is Gln or Ala<br>X at position 95 is Asp or Phe<br>X at position 96 is Asp, Gln, or Val<br>X at position 98 is Cys, His, Arg, Val, or Tyr<br>X at position 100 is Asp, Gly, Met, Pro, Ser, Thr, Trp, or Tyr<br>X at position 101 is Asp, His, Ile, Lys, Ser, or Thr<br>X at position 102 is Asp, Gln, Phe, Gly, Arg, Ser, Val, or Tyr<br>X at position 103 is Phe, Gly, Met, Asn, Pro, Arg, Ser, Tyr, or absent<br>X at position 104 is Asp, Gln, Phe, Asn, Pro, Arg, Val, or absent<br>X at position 105 is Asp, Gln, Cys, Phe, Lys, Leu, Arg, Ser, Thr, Val, Tyr, or absent<br>X at position 106 is Cys, Gly, Lys, Met, Arg, Ser, Val, Tyr, or absent | | |

| | | | |
|---|---|---|---|
| | X at position 107 is Asp, Ala, Arg, Ser, Val, Tyr, or absent<br>X at position 108 is Cys, Phe, Lys, Leu, Ser, Tyr, or absent<br>X at position 109 is Gln, Phe, Arg, or absent<br>X at position 110 is Glu, Met, Asn, Arg, Ser, or absent<br>X at position 111 is Cys, Lys, Ser, Thr, Tyr, or absent<br>X at position 112 is Asp, Phe, Lys, Trp, Tyr, or absent<br>X at position 113 is Glu, Cys, Met, Asn, Val, Tyr, or absent<br>X at position 114 is Cys, Phe, His, Lys, Pro, Ser, Tyr, or absent<br>X at position 115 is Glu, Phe, Arg, Ser, Thr, or absent<br>X at position 116 is Asp, Asn, Arg, Ser, Trp, Tyr, or absent<br>X at position 117 is Asp, Gln, Ala, Phe, Gly, Asn, Pro, Arg, Thr, Val, Tyr, or absent<br>X at position 118 is Asp, Gln, Phe, His, Met, Arg, Ser, Thr, Val, or absent<br>X at position 119 is Asp, Gln, Ala, Phe, Gly, Ile, Lys, Pro, Arg, Ser, Thr, or absent<br>X at position 120 is Phe, Gly, Leu, Met, Ser, Tyr, or absent<br>X at position 121 is Gln, Ala, Phe, Lys, Met, Ser, Thr, or Tyr<br>X at position 122 is Gln, Ser, Thr, Val, or Tyr<br>X at position 123 is Arg or Trp<br>X at position 125 is Ile or Pro | | |

Bold highlighting in $V_HH$ sequences indicates the locations of CDR sequences, as defined using the IMGT numbering system described in Lefranc et al (2003).

## References

All publications identified herein, including each of the references listed below and any published sequences that are identified by name and/or accession number, are hereby incorporated by reference in their entirety.

Adejare, A. (ed.) (2021) "Remington (23rd Edition), The Science and Practice of Pharmacy" Academic Press, ISBN 978-0-12-820007-0.

Akache B, et al. Immunogenic and efficacious SARS-CoV-2 vaccine based on resistin-trimerized spike antigen SmT1 and SLA archaeosome adjuvant. Sci Rep 11, 21849 (2021).

Algaissi, A., and Hashem, A. M. (2020) Evaluation of MERS-CoV Neutralizing Antibodies in Sera Using Live Virus Microneutralization Assay. Methods Mol Biol 2099, 107-116.

Altschul, S.F., Gish, W., Miller, W., Myers, E.W., Lipman, D.J., Basic local alignment search tool, Journal of Molecular Biology, 1990, 215(3): 403-410.

Altschul, S.F., Madden, T.L., Schäffer, A.A., Zhang, J., Zhang, Z., Miller, W., Lipman, D.J., Gapped BLAST and PSI-BLAST: a new generation of protein database search programs, Nucleic Acids Research, 1997, 25(17):3389-402.

Arbabi-Ghahroudi, M. Desmyter A, Wyns L, Hamers R., and Muyldermans S (1997) Selection and identification of single domain antibody fragments from camel heavy-chain antibodies, FEBS Lett 414, 521-526.

Arora, P, Jafferany, M, Lotti, T, Sadoughifar, R, Goldust, M. Learning from history: Coronavirus outbreaks in the past. Dermatologic Therapy. 2020; 33:e13343.

Chi, X., Yan, R., Zhang, J., Zhang, G., Zhang, Y., Hao, M., Zhang, Z., Fan, P., Dong, Y., Yang, Y., Chen, Z., Guo, Y., Zhang, J., Li, Y., Song, X., Chen, Y., Xia, L., Fu, L., Hou, L., Xu, J., Yu, C., Li, J., Zhou, Q., and Chen, W. (2020) A neutralizing human antibody binds to the N-terminal domain of the Spike protein of SARS-CoV-2. Science 369, 650-655.

Colwill K, et al. A "Made-in-Canada" serology solution for profiling humoral immune responses to SARS-CoV-2 infection and vaccination. medRxiv, 2021.2010.2025.21265476 (2021).

Coughlin, M. M., Babcook, J., and Prabhakar, B. S. (2009) Human monoclonal antibodies to SARS-coronavirus inhibit infection by different mechanisms. Virology 394, 39-46.

Davies J., and L. Riechmann, Affinity improvement of single antibody VH domains: residues in all three hypervariable regions affect antigen binding. Immunotechnology 2 (1996) 169-179.

Delfin-Riela, T., Rossotti, M. A., Alvez-Rosado R, Leizagoyen C, and Gonzalez-Sapienza, G. (2020) Highly Sensitive Detection of Zika Virus Nonstructural Protein 1 in Serum Samples by a Two-Site Nanobody ELISAA nanobody-based test for highly sensitive detection of hemoglobin in fecal samples. Biomolecules, 10 (12):1652.

Detalle, L., Stohr, T., Palomo, C., Piedra, P. A., Gilbert, B. E., Mas, V., Millar, A., Power, U. F., Stortelers, C., Allosery, K., Melero, J. A., and Depla, E. (2016) Generation and Characterization of ALX-0171, a Potent Novel Therapeutic Nanobody for the Treatment of Respiratory Syncytial Virus Infection. Antimicrob Agents Chemother 60, 6-13.

Dondelinger, M., Filée, P., Sauvage, E., Quinting, B., Muyldermans, S., Galleni, M., & Vandevenne, M. S. (2018). Understanding the Significance and Implications of Antibody Numbering and Antigen-Binding Surface/Residue Definition. Frontiers in immunology, 9, 2278.

Dumoulin, M., Conrath, K., Van Meirhaighe, A., Meersman, F., Heremans, K., Frenken, L.G., Muyldermans, S., Wyns, L, and Matagne, A. (2002) Protein Sci 11, 500-515.

Galipeau Y, et al. Relative Ratios of Human Seasonal Coronavirus Antibodies Predict the Efficiency of Cross-Neutralization of SARS-CoV-2 Spike Binding to ACE2. EBioMedicine 74, 103700 (2021).

Hamers-Casterman, C, Atarhouch, T., Muyldermans, S., Robinson, G., Hamers, C, Songa, E.B., Bendahman, N., and Hamers, R. (1993) Nature 363, 446-448 Henry, K. A., Hussack, G., Collins, C., Zwaagstra, J. C., Tanha, J., and MacKenzie, C. R. (2016) Isolation of TGF-beta-neutralizing single-domain antibodies of predetermined epitope specificity using next-generation DNA sequencing. Protein Eng Des Sel 29, 439-443.

Henry, K. A., Kim, D. Y., Kandalaft, H., Lowden, M. J., Yang, Q., Schrag, J. D., Hussack, G., MacKenzie, C. R., and Tanha, J. (2017) Stability-Diversity Tradeoffs Impose Fundamental Constraints on Selection of Synthetic Human VH/VL Single-Domain Antibodies from In Vitro Display Libraries. Front Immunol 8, 1759.

Henry, K. A., Tanha, J., and Hussack, G. (2015) Identification of cross-reactive single-domain antibodies against serum albumin using next-generation DNA sequencing. Protein Eng Des Sel 28, 379-383.

Hussack, G., Arbabi-Ghahroudi, M., van Faassen, H., Songer, J. G., Ng, K. K., MacKenzie, R., and Tanha, J. (2011) Neutralization of Clostridium difficile toxin A with single-domain antibodies targeting the cell receptor binding domain. J Biol Chem 286, 8961-8976.

Jespers, L, Schon, O., Famm, K., and Winter, G. (2004) Nat. Biotechnol. 22, 1161-1165.

Karlin, S., Altschul, S.F., Applications and statistics for multiple high-scoring segments in molecular sequences. PNAS, 1993, 90(12): 5873-5877.

Karlin, S., Altschul, S.F., Methods for assessing the statistical significance of molecular sequence features by using general scoring schemes. PNAS, 1990, 87(6): 2264-2268.

Kim, D.Y., Kandalaft, H., Ding, W., Ryan, S., van Fassen, H., Hirama, T., Foote, S.J., MacKenzie, R., and Tanha, J. (2012) PEDS advance access August 30, 2012, 1-9.

Lan, J., Ge, J., Yu, J., Shan, S., Zhou, H., Fan, S., Zhang, Q., Shi, X., Wang, Q., Zhang, L., Wang, X. (2020), Structure of the SARS-CoV-2 spike receptor-binding domain bound to the ACE2 receptor. Nature 581, 215-220.

Lefranc, M.-P. et al., (2003) Dev. Comp. Immunol., 27, 55-77.

Li, R. (2016) Structure, Function, and Evolution of Coronavirus Spike Proteins, Annual Review of Virology 3, 237-261.

Li S, Zheng W, Kuolee R, Hirama T, Henry M, Makvandi-Nejad S, Fjallman T, Chen W, Zhang J. Pentabody-mediated antigen delivery induces antigen-specific mucosal immune response. Mol Immunol 2009; 46:1718-26.

Myers, E.W., Miller, W., Optimal alignments in linear space, Bioinformatics, 4(1): 11-17.Sliepen K, van Montfort T, Melchers M, Isik G, Sanders RW, 2015. Immunosilencing a highly immunogenic protein trimerization domain. J Biol Chem 290, 7436-7442.

Nuttall, S.D., Krishnan, U.V., Doughty, L., Pearson, K., Ryan, M.T., Hoogenraad, N.J., Hattarki, M., Carmichael, J.A., Irving, R.A., and Hudson, P.J. (2003) Eur. J. Biochem. 270, 3543-3554.

Ravichandran, S., Coyle, E. M., Klenow, L., Tang, J., Grubbs, G., Liu, S., Wang, T., Golding, H., and Khurana, S. (2020) Antibody signature induced by SARS-CoV-2 spike protein immunogens in rabbits. Sci Transl Med 12.

Respaud, R., Vecellio, L., Diot, P., and Heuze-Vourc'h, N. (2015) Nebulization as a delivery method for mAbs in respiratory diseases. Expert Opin Drug Deliv 12, 1027-1039.

Rogers, T. F., Zhao, F., Huang, D., Beutler, N., Burns, A., He, W. T., Limbo, O., Smith, C., Song, G., Woehl, J., Yang, L., Abbott, R. K., Callaghan, S., Garcia, E., Hurtado, J., Parren, M., Peng, L., Ramirez, S., Ricketts, J., Ricciardi, M. J., Rawlings, S. A., Wu, N. C., Yuan, M., Smith, D. M., Nemazee, D., Teijaro, J. R., Voss, J. E., Wilson, I. A., Andrabi, R., Briney, B., Landais, E., Sok,

D., Jardine, J. G., and Burton, D. R. (2020) Isolation of potent SARS-CoV-2 neutralizing antibodies and protection from disease in a small animal model. Science 369, 956-963.

Rossotti, M. A., Henry, K. A., van Faassen, H., Tanha, J., Callaghan, D., Hussack, G., Arbabi-Ghahroudi, M., and MacKenzie, C. R. (2019) Camelid single-domain antibodies raised by DNA immunization are potent inhibitors of EGFR signaling. Biochem J 476, 39-50.

Rossotti, M. A., Pirez, M., Gonzalez-Techera, A., Cui, Y., Bever, C. S., Lee, K. S., Morisseau, C., Leizagoyen, C., Gee, S., Hammock, B. D., and Gonzalez-Sapienza, G. (2015a) Method for Sorting and Pairwise Selection of Nanobodies for the Development of Highly Sensitive Sandwich Immunoassays. Anal Chem 87, 11907-11914.

Rossotti, M., Tabares, S., Alfaya, L., Leizagoyen, C., Moron, G., and Gonzalez-Sapienza, G. (2015b) Streamlined method for parallel identification of single domain antibodies to membrane receptors on whole cells. Biochim Biophys Acta 1850, 1397-1404.

Stuible, M. Gervais, C., Lord-Dufour, S., Perret, S., L'Abbe, D., Schrag, J., St-Laurent, G., Durocher, Y. (2021), Rapid, high-yield production of full-length SARS-CoV-2 spike ectodomain by transient gene expression in CHO cells. Journal of Biotechnology 326, 21-27.

Sulea T, Baardsnes J, Stuible M, Rohani N, Tran A, Parat M, Cepero Donates Y, Duchesne M, Plante P, Kour G, Durocher Y. (2022) Structure-based dual affinity optimization of a SARS-CoV-1/2 cross-reactive single-domain antibody. PLoS One. 17(3):e0266250.

Wrapp, D., De Vlieger, D., Corbett, K. S., Torres, G. M., Wang, N., Van Breedam, W., Roose, K., van Schie, L., Team, V.-C. C.-R., Hoffmann, M., Pohlmann, S., Graham, B. S., Callewaert, N., Schepens, B., Saelens, X., and McLellan, J. S. (2020) Structural Basis for Potent Neutralization of Betacoronaviruses by Single-Domain Camelid Antibodies. Cell 181, 1004-1015 e1015.

Wrapp D, et al. Cryo-EM structure of the 2019-nCoV spike in the prefusion conformation. Science 367, 1260-1263 (2020).

Zheng M, Zhao X, Zheng S, et al. Bat SARS-Like WIV1 coronavirus uses the ACE2 of multiple animal species as receptor and evades IFITM3 restriction via TMPRSS2 activation of membrane fusion. Emerg Microbes Infect. 2020;9(1):1567-1579.

Zhou, P., Yang, XL., Wang, XG. et al. (2020) A pneumonia outbreak associated with a new coronavirus of probable bat origin. Nature 579, 270–273.

WHAT IS CLAIMED IS:

1. An isolated or purified antibody that specifically recognizes at least one coronavirus spike polypeptide, wherein the antibody comprises an antigen binding portion of an antibody heavy chain, wherein the antigen binding portion comprises a first complementarity determining region (CDR1), a second complementarity determining region (CDR2), and a third complementarity determining region (CDR3), and wherein CDR1, CDR2, and CDR3, respectively, comprise the amino acid sequence set forth in:

SEQ ID NO: 1, SEQ ID NO: 45, and SEQ ID NO: 90;
SEQ ID NO: 2, SEQ ID NO: 45, and SEQ ID NO: 91;
SEQ ID NO: 1, SEQ ID NO: 46, and SEQ ID NO: 92;
SEQ ID NO: 3, SEQ ID NO: 47, and SEQ ID NO: 93;
SEQ ID NO: 4, SEQ ID NO: 48, and SEQ ID NO: 94;
SEQ ID NO: 5, SEQ ID NO: 49, and SEQ ID NO: 95;
SEQ ID NO: 6, SEQ ID NO: 50, and SEQ ID NO: 96;
SEQ ID NO: 7, SEQ ID NO: 51, and SEQ ID NO: 97;
SEQ ID NO: 8, SEQ ID NO: 52, and SEQ ID NO: 98;
SEQ ID NO: 9, SEQ ID NO: 53, and SEQ ID NO: 99;
SEQ ID NO: 10, SEQ ID NO: 54, and SEQ ID NO: 100;
SEQ ID NO: 11, SEQ ID NO: 55, and SEQ ID NO: 101;
SEQ ID NO: 12, SEQ ID NO: 56, and SEQ ID NO: 102;
SEQ ID NO: 13, SEQ ID NO: 57, and SEQ ID NO: 103;
SEQ ID NO: 14, SEQ ID NO: 58, and SEQ ID NO: 104;
SEQ ID NO: 15, SEQ ID NO: 59, and SEQ ID NO: 105;
SEQ ID NO: 16, SEQ ID NO: 60, and SEQ ID NO: 106;
SEQ ID NO: 17, SEQ ID NO: 61, and SEQ ID NO: 107;
SEQ ID NO: 18, SEQ ID NO: 62, and SEQ ID NO: 108;
SEQ ID NO: 19, SEQ ID NO: 63, and SEQ ID NO: 109;
SEQ ID NO: 20, SEQ ID NO: 64, and SEQ ID NO: 110;
SEQ ID NO: 21, SEQ ID NO: 65, and SEQ ID NO: 111;
SEQ ID NO: 22, SEQ ID NO: 66, and SEQ ID NO: 112;
SEQ ID NO: 23, SEQ ID NO: 67, and SEQ ID NO: 113;

SEQ ID NO: 24, SEQ ID NO: 68, and SEQ ID NO: 114;
SEQ ID NO: 25, SEQ ID NO: 69, and SEQ ID NO: 115;
SEQ ID NO: 26, SEQ ID NO: 70, and SEQ ID NO: 116;
SEQ ID NO: 27, SEQ ID NO: 71, and SEQ ID NO: 117;
SEQ ID NO: 28, SEQ ID NO: 72, and SEQ ID NO: 118;
SEQ ID NO: 29, SEQ ID NO: 73, and SEQ ID NO: 119;
SEQ ID NO: 30, SEQ ID NO: 74, and SEQ ID NO: 120;
SEQ ID NO: 31, SEQ ID NO: 75, and SEQ ID NO: 121;
SEQ ID NO: 32, SEQ ID NO: 76, and SEQ ID NO: 122;
SEQ ID NO: 33, SEQ ID NO: 77, and SEQ ID NO: 123;
SEQ ID NO: 34, SEQ ID NO: 78, and SEQ ID NO: 124;
SEQ ID NO: 35, SEQ ID NO: 79, and SEQ ID NO: 125;
SEQ ID NO: 36, SEQ ID NO: 80, and SEQ ID NO: 125;
SEQ ID NO: 20, SEQ ID NO: 81, and SEQ ID NO: 126;
SEQ ID NO: 20, SEQ ID NO: 81, and SEQ ID NO: 127;
SEQ ID NO: 37, SEQ ID NO: 82, and SEQ ID NO: 128;
SEQ ID NO: 38, SEQ ID NO: 83, and SEQ ID NO: 129;
SEQ ID NO: 39, SEQ ID NO: 84, and SEQ ID NO: 130;
SEQ ID NO: 40, SEQ ID NO: 85, and SEQ ID NO: 131;
SEQ ID NO: 41, SEQ ID NO: 86, and SEQ ID NO: 132;
SEQ ID NO: 42, SEQ ID NO: 87, and SEQ ID NO: 133;
SEQ ID NO: 43, SEQ ID NO: 88, and SEQ ID NO: 134; or
SEQ ID NO: 44, SEQ ID NO: 89, and SEQ ID NO: 135.

2. The antibody of claim 1, wherein the antibody is a neutralizing antibody and wherein CDR1, CDR2, and CDR3, respectively, comprise the amino acid sequence set forth in:

SEQ ID NO: 11, SEQ ID NO: 55, and SEQ ID NO: 101;
SEQ ID NO: 13, SEQ ID NO: 57, and SEQ ID NO: 103;
SEQ ID NO: 19, SEQ ID NO: 63, and SEQ ID NO: 109; or
SEQ ID NO: 21, SEQ ID NO: 65, and SEQ ID NO: 111.

3. The antibody of claim 1, wherein the antibody comprises the amino acid sequence set forth in SEQ ID NO: 183, SEQ ID NO: 184, SEQ ID NO: 185, or SEQ ID NO: 186.

4. The antibody of claim 1, wherein the antibody comprises the amino acid sequence set forth in SEQ ID NO: 136, SEQ ID NO: 137, SEQ ID NO: 138, SEQ ID NO: 139, SEQ ID NO: 140, SEQ ID NO: 141, SEQ ID NO: 142, SEQ ID NO: 143, SEQ ID NO: 144, SEQ ID NO: 145, SEQ ID NO: 146, SEQ ID NO: 147, SEQ ID NO: 148, SEQ ID NO: 149, SEQ ID NO: 150, SEQ ID NO: 151, SEQ ID NO: 152, SEQ ID NO: 153, SEQ ID NO: 154, SEQ ID NO: 155, SEQ ID NO: 156, SEQ ID NO: 157, SEQ ID NO: 158, SEQ ID NO: 159, SEQ ID NO: 160, SEQ ID NO: 161, SEQ ID NO: 162, SEQ ID NO: 163, SEQ ID NO: 164, SEQ ID NO: 165, SEQ ID NO: 166, SEQ ID NO: 167, SEQ ID NO: 168, SEQ ID NO: 169, SEQ ID NO: 170, SEQ ID NO: 171, SEQ ID NO: 172, SEQ ID NO: 173, SEQ ID NO: 174, SEQ ID NO: 175, SEQ ID NO: 176, SEQ ID NO: 177, SEQ ID NO: 178, SEQ ID NO: 179, SEQ ID NO: 180, SEQ ID NO: 181, or SEQ ID NO: 182, or an amino acid sequence having at least 75% sequence identity to the full length of the amino acid sequence set forth in SEQ ID NO: 136, SEQ ID NO: 137, SEQ ID NO: 138, SEQ ID NO: 139, SEQ ID NO: 140, SEQ ID NO: 141, SEQ ID NO: 142, SEQ ID NO: 143, SEQ ID NO: 144, SEQ ID NO: 145, SEQ ID NO: 146, SEQ ID NO: 147, SEQ ID NO: 148, SEQ ID NO: 149, SEQ ID NO: 150, SEQ ID NO: 151, SEQ ID NO: 152, SEQ ID NO: 153, SEQ ID NO: 154, SEQ ID NO: 155, SEQ ID NO: 156, SEQ ID NO: 157, SEQ ID NO: 158, SEQ ID NO: 159, SEQ ID NO: 160, SEQ ID NO: 161, SEQ ID NO: 162, SEQ ID NO: 163, SEQ ID NO: 164, SEQ ID NO: 165, SEQ ID NO: 166, SEQ ID NO: 167, SEQ ID NO: 168, SEQ ID NO: 169, SEQ ID NO: 170, SEQ ID NO: 171, SEQ ID NO: 172, SEQ ID NO: 173, SEQ ID NO: 174, SEQ ID NO: 175, SEQ ID NO: 176, SEQ ID NO: 177, SEQ ID NO: 178, SEQ ID NO: 179, SEQ ID NO: 180, SEQ ID NO: 181, or SEQ ID NO: 182.

5. The antibody of any one of claims 1 to 4, wherein the antibody is a single domain antibody.

6. The antibody of claim 5, wherein the antibody is a $V_HH$.

7. The antibody of any one of claims 1 to 6, wherein the antibody is of camelid origin.

8. The antibody of any one of claims 1 to 7, wherein the antibody is in a multivalent display format.

9. The antibody of claim 8, wherein the antibody is linked to an Fc fragment.

10. The antibody of claim 9, wherein the antibody is in a bivalent display format.

11. A nucleic acid molecule encoding an antibody as described in any one of claims 1 to 10.

12. A vector comprising the nucleic acid molecule of claim 11.

13. The vector of claim 12, wherein the nucleic acid molecule is operably linked to at least one promoter and/or regulatory element to enable expression in a host cell.

14. A host cell comprising the vector of claim 12 or 13.

15. A pharmaceutical composition comprising at least one antibody as defined in any one of claims 1 to 10 and a pharmaceutically acceptable carrier and/or diluent.

16. The pharmaceutical composition of claim 15, wherein the composition is for delivery by inhalation or nebulization.

17. A composition comprising at least one antibody as defined in any one of claims 1 to 10 linked to another molecule.

18. The composition of claim 17, wherein the other molecule is a label or polypeptide.

19. The composition of claim 17, wherein the other molecule is an ACE2 polypeptide or a fragment thereof.

20. A composition comprising at least one antibody as defined in any one of claims 1 to 10 immobilized on a substrate.

21. Use of the antibody of any one of claims 1 to 10 or the composition of any one of claims 15 to 19 to treat or detect a coronavirus infection.

22. The use of claim 21, wherein the coronavirus infection is caused by at least one coronavirus that specifically binds an ACE2 receptor.

23. The use of claim 21 or 22, wherein the coronavirus infection is caused by SARS-CoV-2 and/or SARS-CoV.

24. Use of the antibody of any one of claims 1 to 10 or the composition of any one of claims 15 to 20 to detect, quantify and/or capture a coronavirus; or to detect, quantify and/or capture a coronavirus spike polypeptide or fragment thereof.

25. The use of claim 24, wherein the coronavirus is a coronavirus that specifically binds an ACE2 receptor or the coronavirus spike polypeptide is a coronavirus spike polypeptide that specifically binds an ACE2 receptor.

26. The use of claim 25, wherein the coronavirus is SARS-CoV-2 or SARS-CoV.

27. A method for treating or preventing a coronavirus infection, the method comprising administering at least one antibody as defined in any one of claims 1 to 10 or a composition as defined in any one of claims 15 to 19 to a subject in need thereof.

28. The method of claim 27, wherein the coronavirus infection is caused by at least one coronavirus that specifically binds an ACE2 receptor.

29. The method of claim 27 or 276, wherein the coronavirus infection is caused by SARS-CoV-2 and/or SARS-CoV.

30. The method of any one of claims 27 to 29, wherein the administration is by inhalation or nebulization.

31. A method for detecting the presence of a coronavirus or a coronavirus spike polypeptide or fragment thereof in a sample, the method comprising exposing the sample to at least one antibody as defined in any one of claims 1 to 10 or a composition as defined in any one of claims 15 to 20 and assaying for specific binding between the at least one antibody and the sample, wherein specific binding indicates a presence of the at least one coronavirus or coronavirus spike polypeptide or fragment thereof in the sample.

32. A method for capturing a coronavirus or a coronavirus spike polypeptide or fragment thereof from a sample, the method comprising exposing the sample to the composition as defined in claim 20.

33. The method of claim 31 or 32, wherein the coronavirus is a coronavirus that specifically binds an ACE2 receptor or the coronavirus spike polypeptide is a coronavirus spike polypeptide that specifically binds an ACE2 receptor.

34. The method of any one of claims 31 to 33, wherein the coronavirus is SARS-CoV-2 or SARS-CoV, or the coronavirus spike polypeptide or fragment thereof is a SARS-CoV-2 or SARS-CoV coronavirus spike polypeptide or fragment thereof.

35. The antibody of any one of claims 1 to 10 or the composition of any one of claims 15 to 19 for use to detect or treat a coronavirus infection.

36. The antibody of claim 35, wherein the coronavirus infection is caused by at least one coronavirus that specifically binds an ACE2 receptor.

37. The antibody of claim 35 or 36, wherein the at least one coronavirus is SARS-CoV-2 and/or SARS-CoV.

38. The antibody of any one of claims 1 to 10 or the composition of any one of claims 15 to 19 for use to detect, quantify and/or capture a coronavirus; or to detect, quantify and/or capture a coronavirus spike polypeptide or fragment thereof.

39. The antibody of claim 38, wherein the coronavirus is a coronavirus that specifically binds an ACE2 receptor, or the coronavirus spike polypeptide is a coronavirus spike polypeptide that specifically binds an ACE2 receptor.

40. The antibody of claim 38 or 39, wherein the coronavirus is SARS-CoV-2 or SARS-CoV or the coronavirus spike polypeptide or fragment thereof is a SARS-CoV-2 or SARS-CoV spike polypeptide or fragment thereof.

41. Use of the antibody of any one of claims 1 to 10 in the manufacture of a medicament for prevention or treatment of a coronavirus infection.

42. The use of claim 41, wherein the coronavirus infection is caused by at least one coronavirus that specifically binds an ACE2 receptor.

43. The use of claim 42, wherein the at least one coronavirus is SARS-CoV-2 and/or SARS-CoV.

44. The use of any one of claims 41 to 43, wherein the medicament is for delivery by inhalation or nebulization.

45. An antibody cocktail composition comprising two or more of the antibodies as defined in any one of claims 1 to 10.

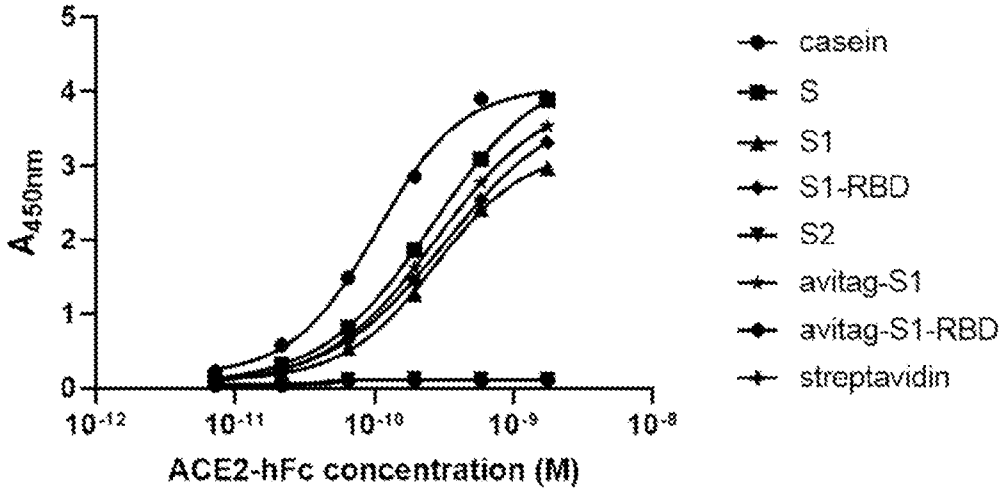
A450nm
ACE2-hFc concentration (M)
casein
S
S1
S1-RBD
S2
avitag-S1
avitag-S1-RBD
streptavidin

FIG. 1A

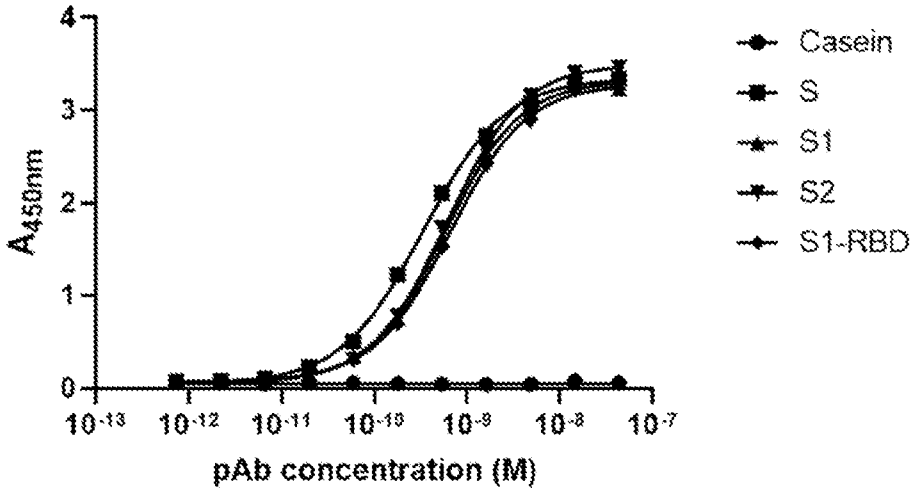
A450nm
pAb concentration (M)
Casein
S
S1
S2
S1-RBD

FIG. 1B

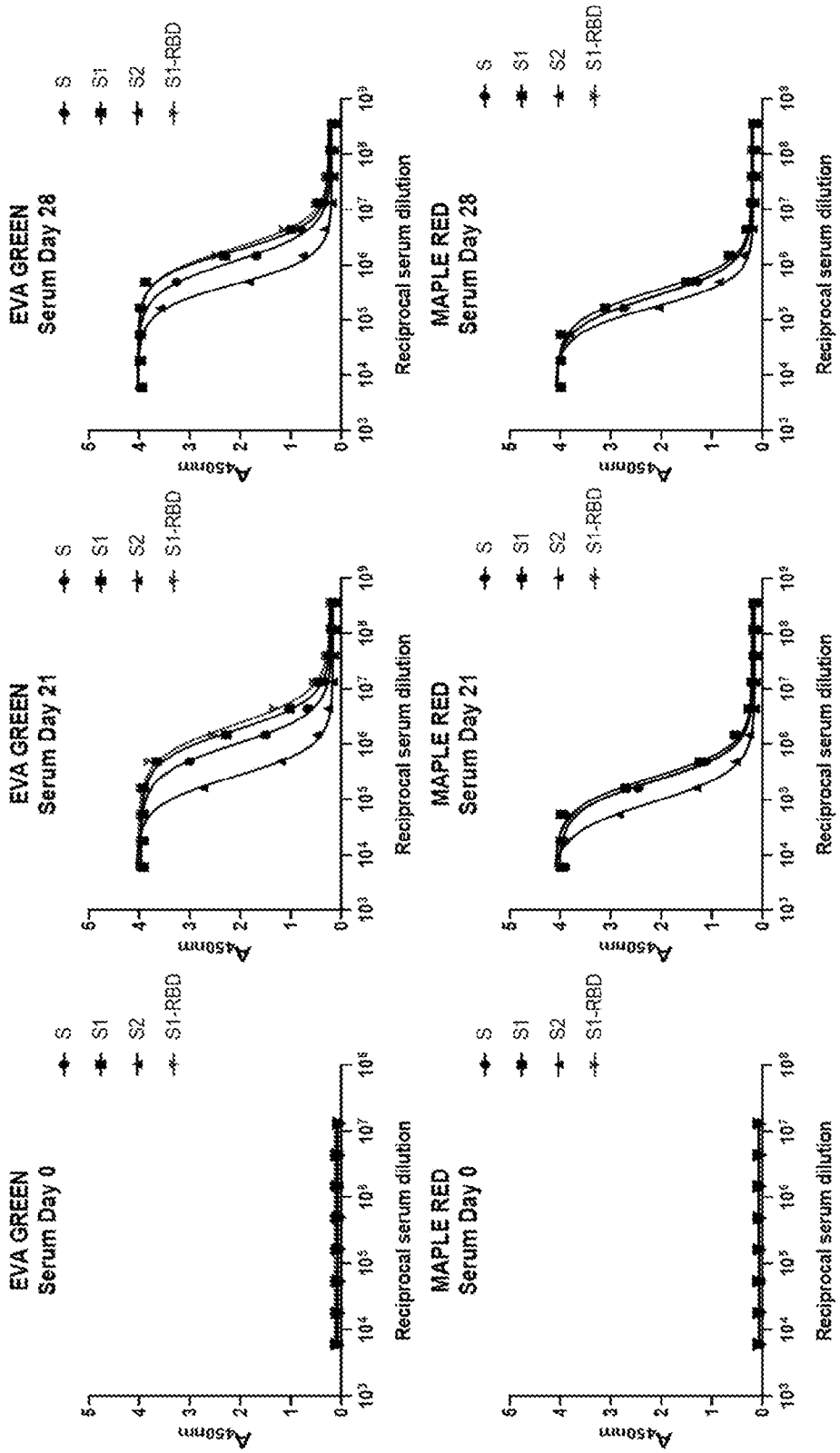
EVA GREEN
Serum Day 0
MAPLE RED
Serum Day 0
EVA GREEN
Serum Day 21
MAPLE RED
Serum Day 21
EVA GREEN
Serum Day 28
MAPLE RED
Serum Day 28
S
S1
S2
S1-RBD
A450nm
Reciprocal serum dilution

FIG. 2A

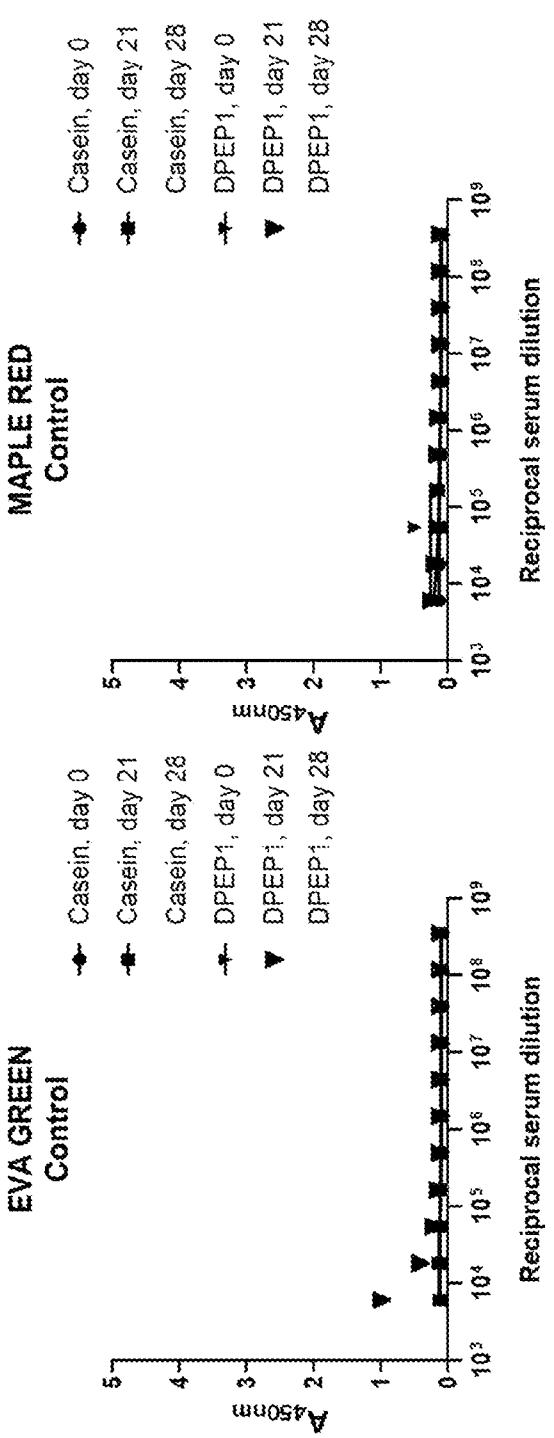


FIG. 2A (cont.)

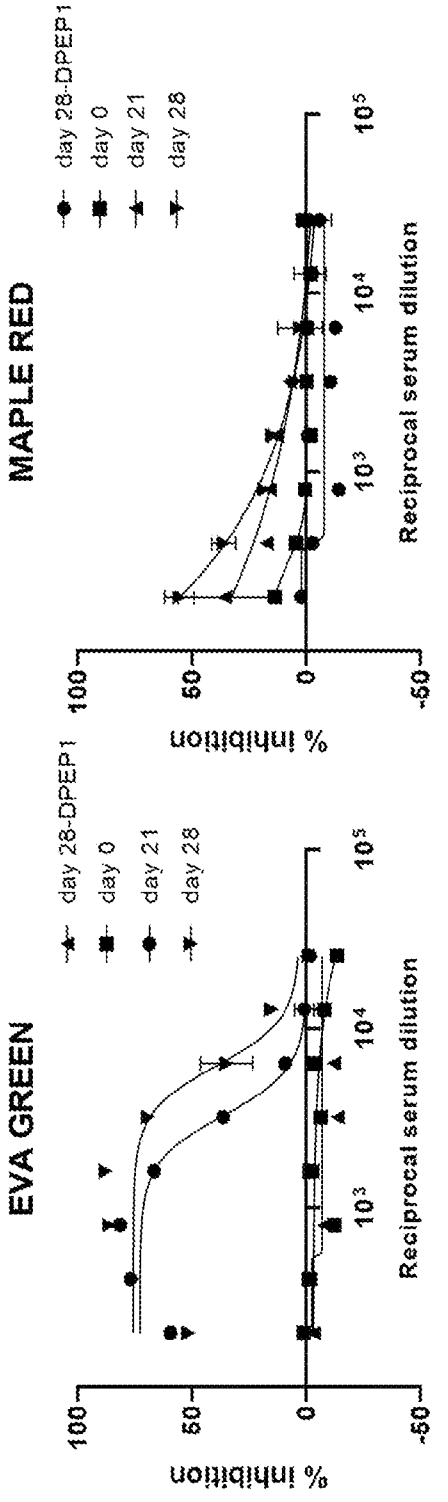


FIG. 2B

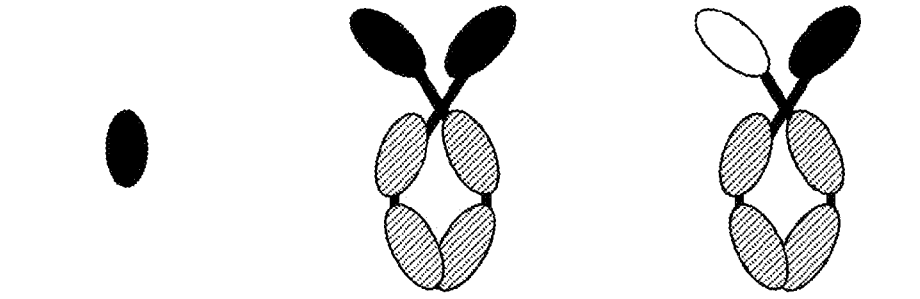

SARS-CoV-2 S-specific monomeric $V_HH$

SARS-CoV-2 S-specific bivalent $V_HH$-Fc

SARS-CoV-2 S-specific monovalent $V_HH$-Fc

FIG. 3

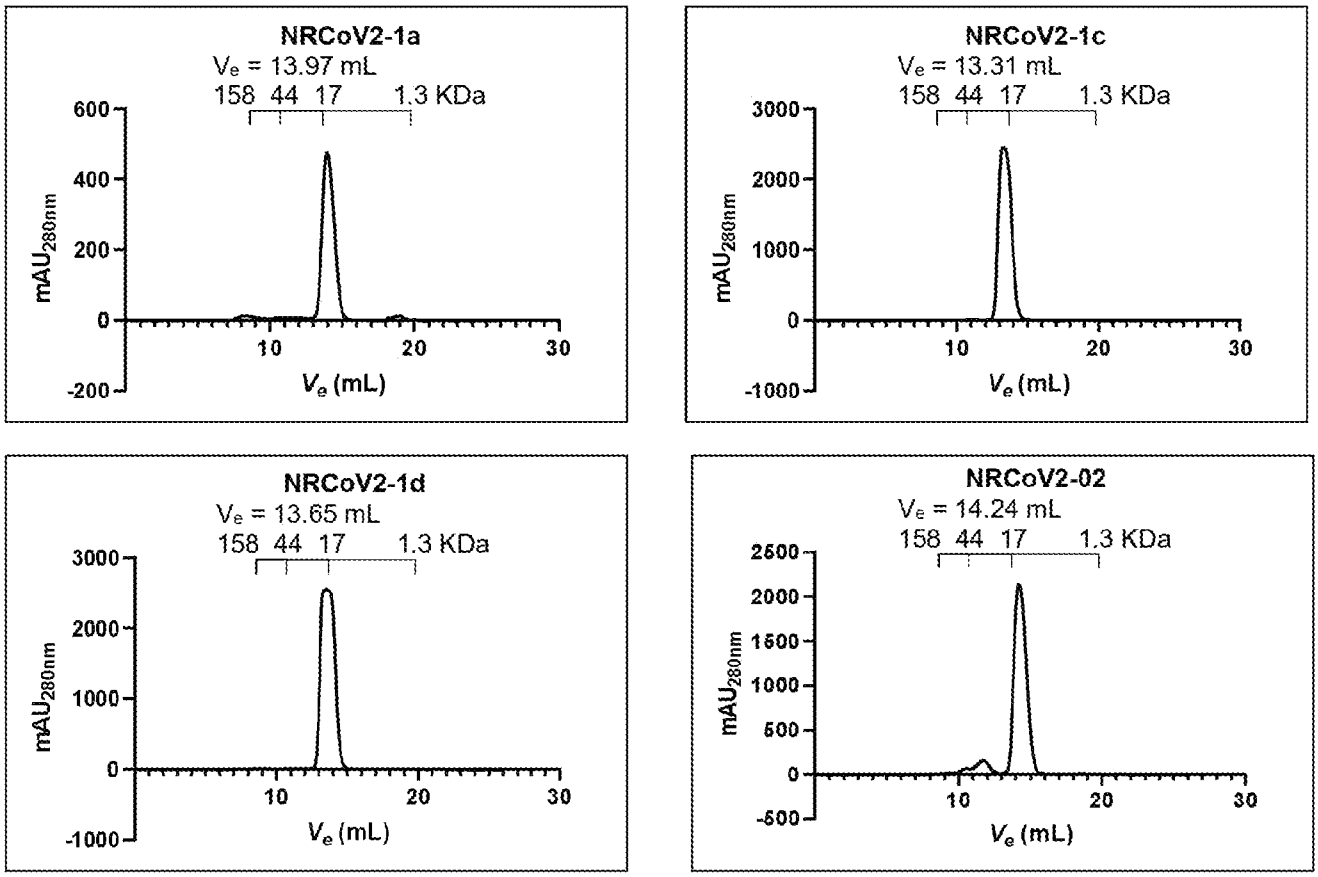


FIG. 4A

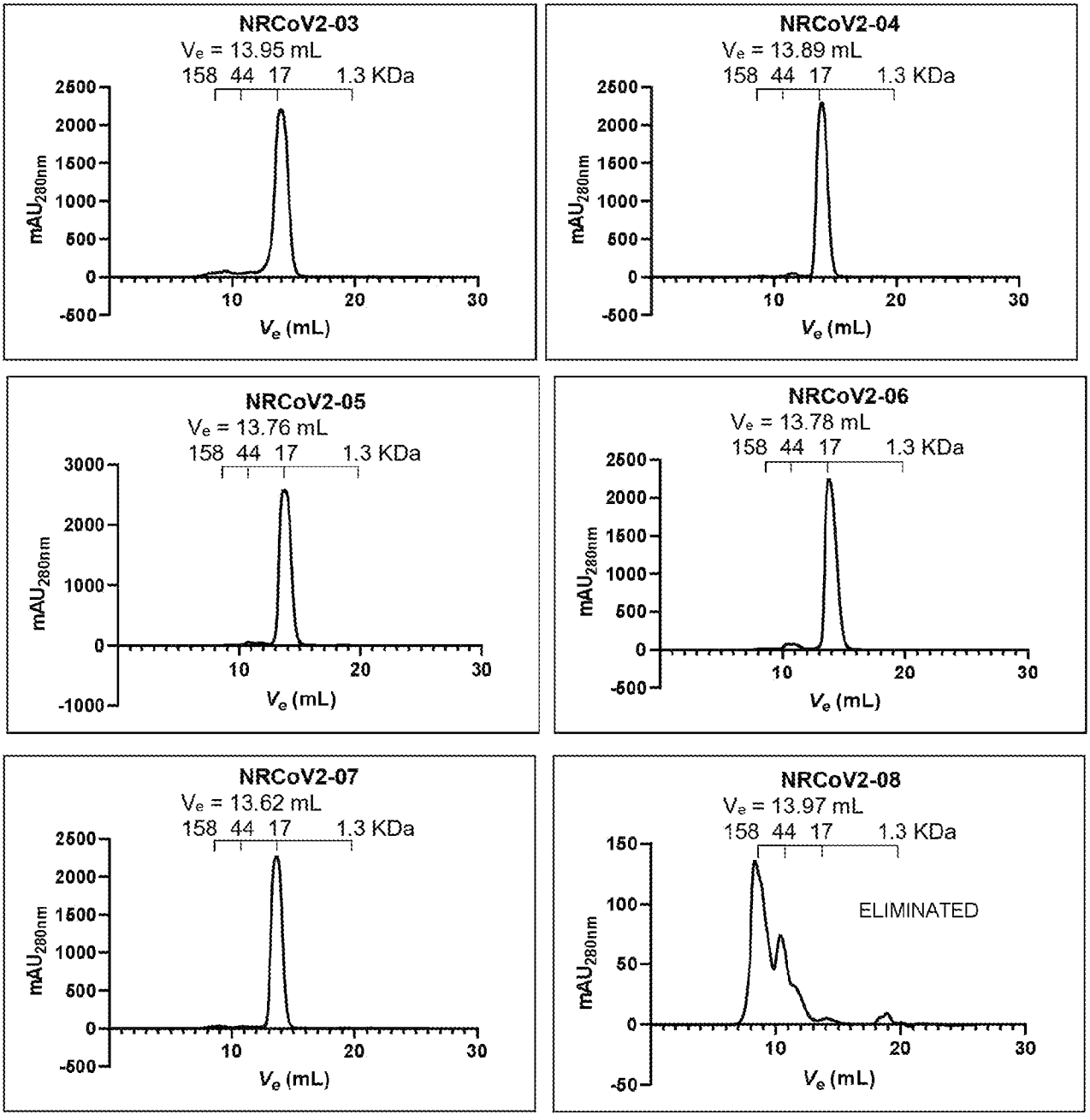
NRCoV2-03
Ve = 13.95 mL
158 44 17 1.3 KDa
mAU280nm
Ve (mL)
NRCoV2-04
Ve = 13.89 mL
158 44 17 1.3 KDa
mAU280nm
Ve (mL)
NRCoV2-05
Ve = 13.76 mL
158 44 17 1.3 KDa
mAU280nm
Ve (mL)
NRCoV2-06
Ve = 13.78 mL
158 44 17 1.3 KDa
mAU280nm
Ve (mL)
NRCoV2-07
Ve = 13.62 mL
158 44 17 1.3 KDa
mAU280nm
Ve (mL)
NRCoV2-08
Ve = 13.97 mL
158 44 17 1.3 KDa
ELIMINATED
mAU280nm
Ve (mL)

FIG. 4A (cont.)

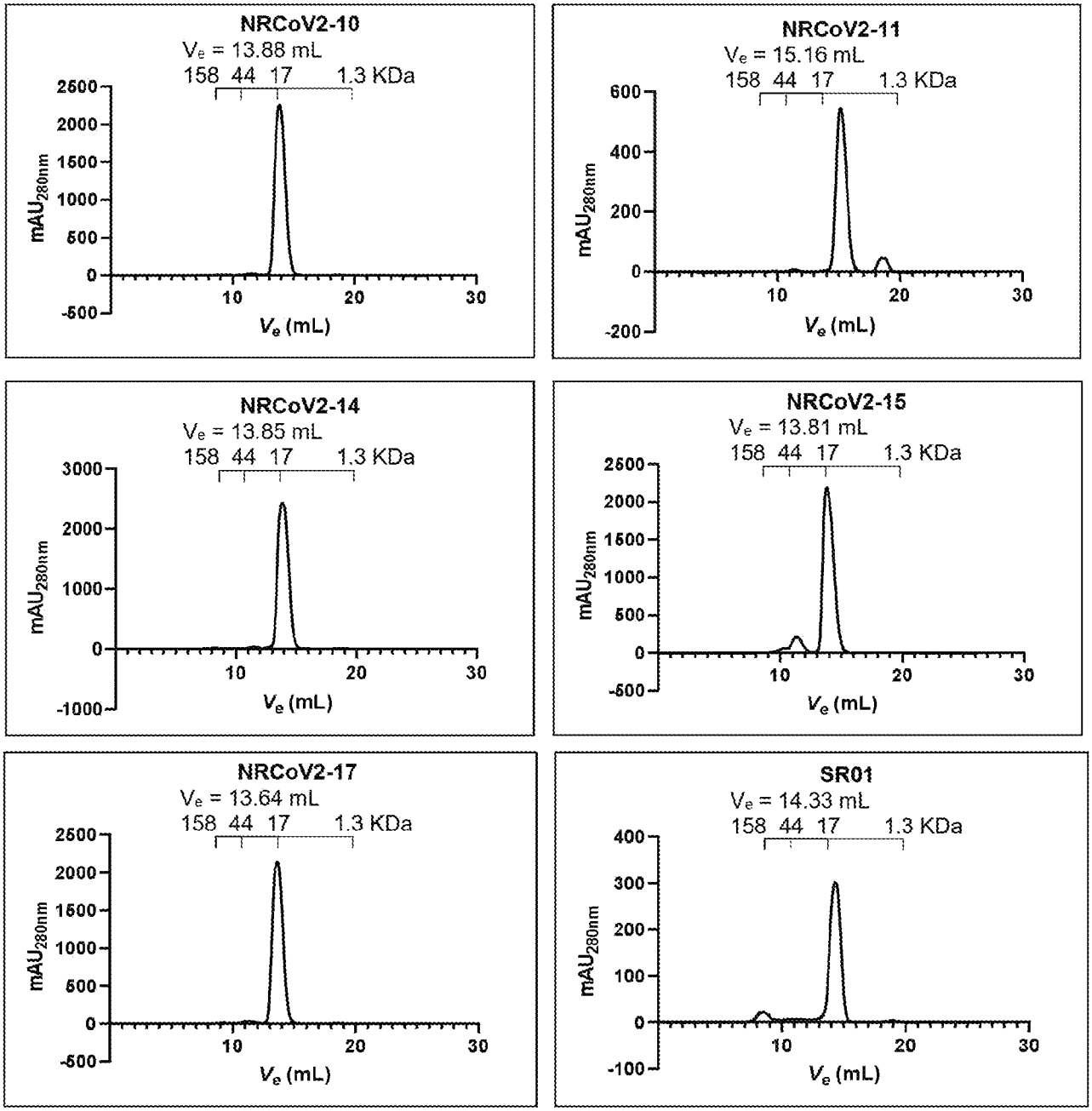
NRCoV2-10
Ve = 13.88 mL
158 44 17 1.3 KDa
mAU280nm
Ve (mL)
NRCoV2-11
Ve = 15.16 mL
158 44 17 1.3 KDa
mAU280nm
Ve (mL)
NRCoV2-14
Ve = 13.85 mL
158 44 17 1.3 KDa
mAU280nm
Ve (mL)
NRCoV2-15
Ve = 13.81 mL
158 44 17 1.3 KDa
mAU280nm
Ve (mL)
NRCoV2-17
Ve = 13.64 mL
158 44 17 1.3 KDa
mAU280nm
Ve (mL)
SR01
Ve = 14.33 mL
158 44 17 1.3 KDa
mAU280nm
Ve (mL)

FIG. 4A (cont.)

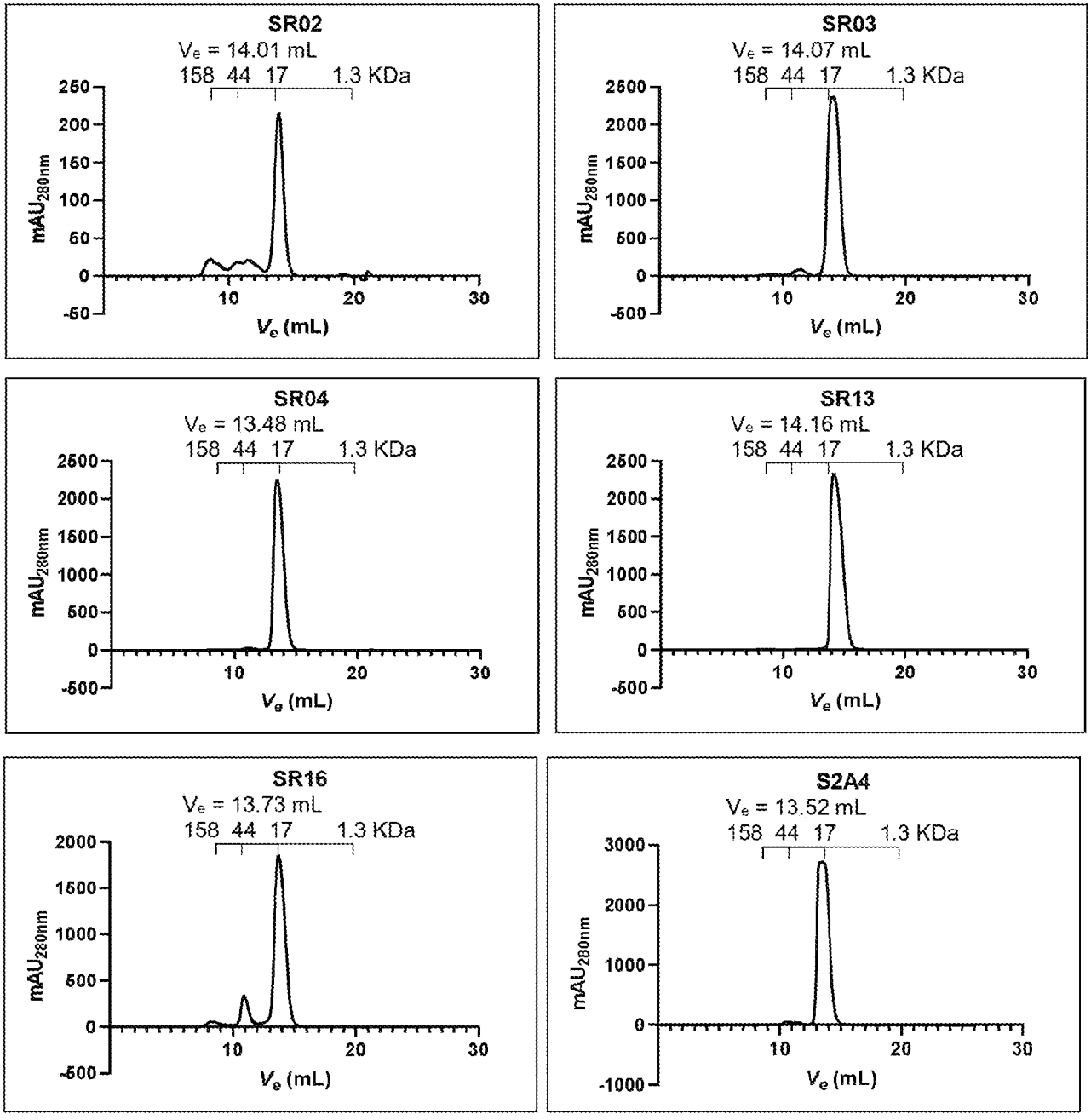
SR02
Ve = 14.01 mL
158 44 17 1.3 KDa
mAU280nm
Ve (mL)
SR03
Ve = 14.07 mL
158 44 17 1.3 KDa
mAU280nm
Ve (mL)
SR04
Ve = 13.48 mL
158 44 17 1.3 KDa
mAU280nm
Ve (mL)
SR13
Ve = 14.16 mL
158 44 17 1.3 KDa
mAU280nm
Ve (mL)
SR16
Ve = 13.73 mL
158 44 17 1.3 KDa
mAU280nm
Ve (mL)
S2A4
Ve = 13.52 mL
158 44 17 1.3 KDa
mAU280nm
Ve (mL)

FIG. 4A (cont.)

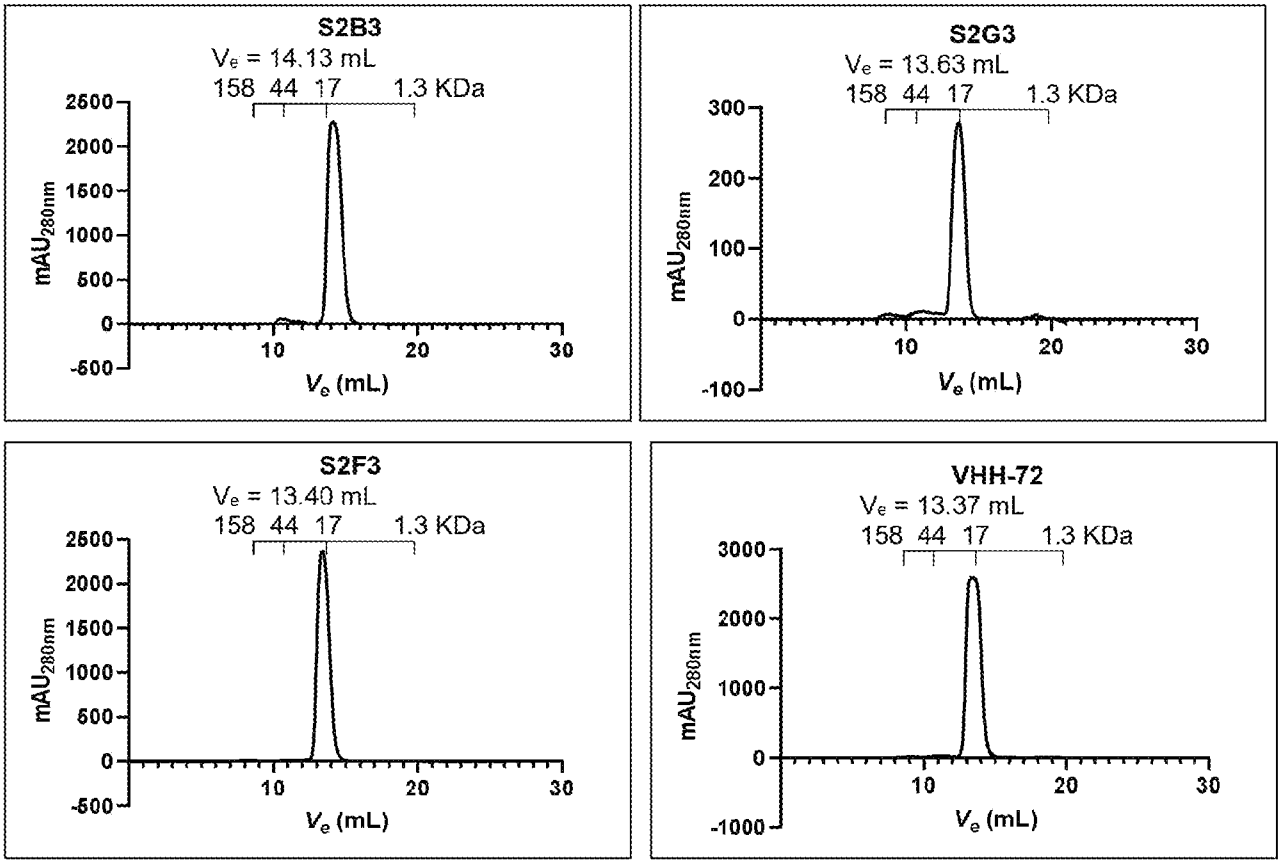
S2B3
Ve = 14.13 mL
158 44 17 1.3 KDa
mAU280nm
Ve (mL)
S2G3
Ve = 13.63 mL
158 44 17 1.3 KDa
mAU280nm
Ve (mL)
S2F3
Ve = 13.40 mL
158 44 17 1.3 KDa
mAU280nm
Ve (mL)
VHH-72
Ve = 13.37 mL
158 44 17 1.3 KDa
mAU280nm
Ve (mL)

FIG. 4A (cont.)

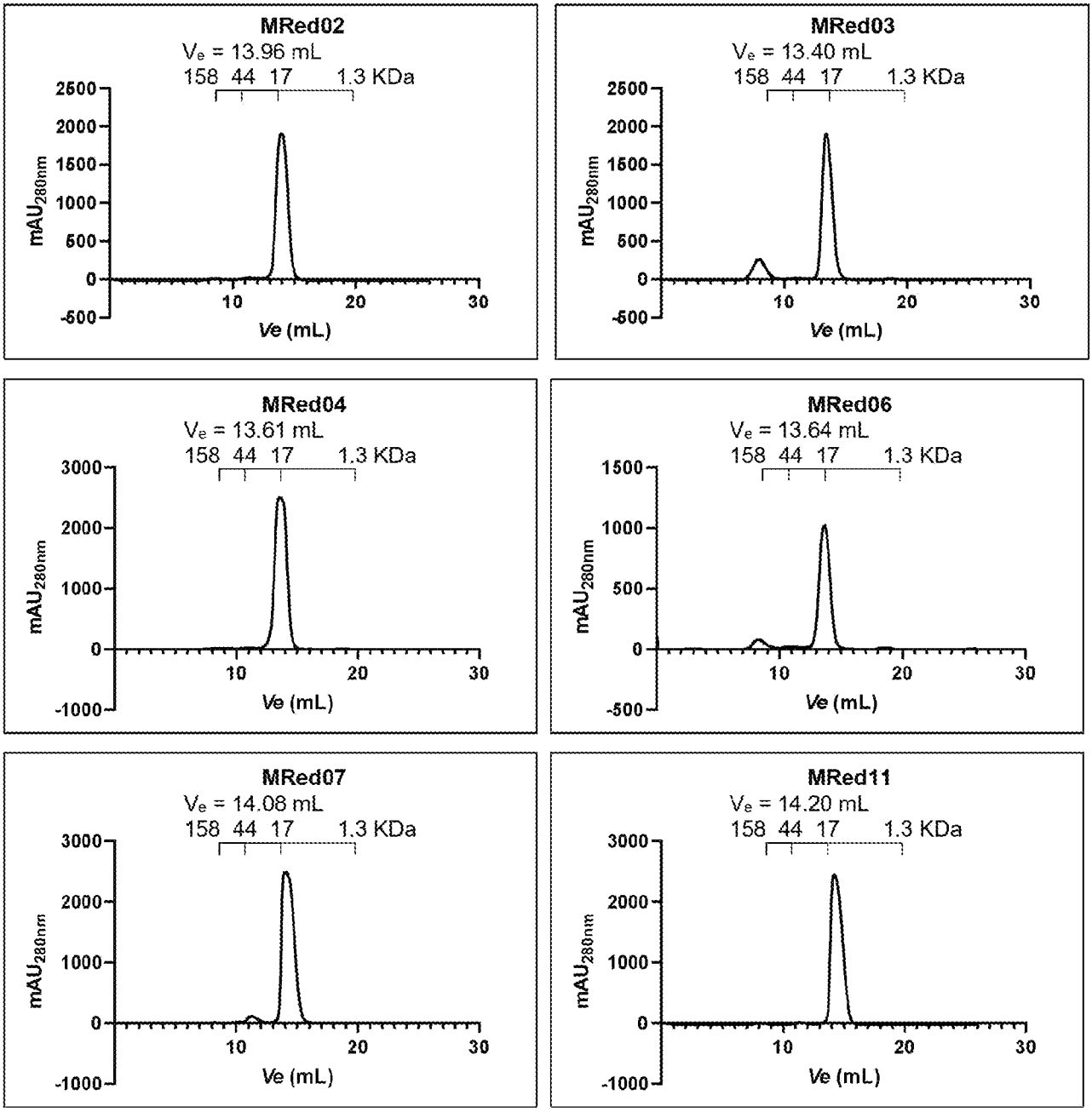
MRed02
Ve = 13.96 mL
158 44 17 1.3 KDa
mAU280nm
Ve (mL)
MRed03
Ve = 13.40 mL
158 44 17 1.3 KDa
mAU280nm
Ve (mL)
MRed04
Ve = 13.61 mL
158 44 17 1.3 KDa
mAU280nm
Ve (mL)
MRed06
Ve = 13.64 mL
158 44 17 1.3 KDa
mAU280nm
Ve (mL)
MRed07
Ve = 14.08 mL
158 44 17 1.3 KDa
mAU280nm
Ve (mL)
MRed11
Ve = 14.20 mL
158 44 17 1.3 KDa
mAU280nm
Ve (mL)

FIG. 4B

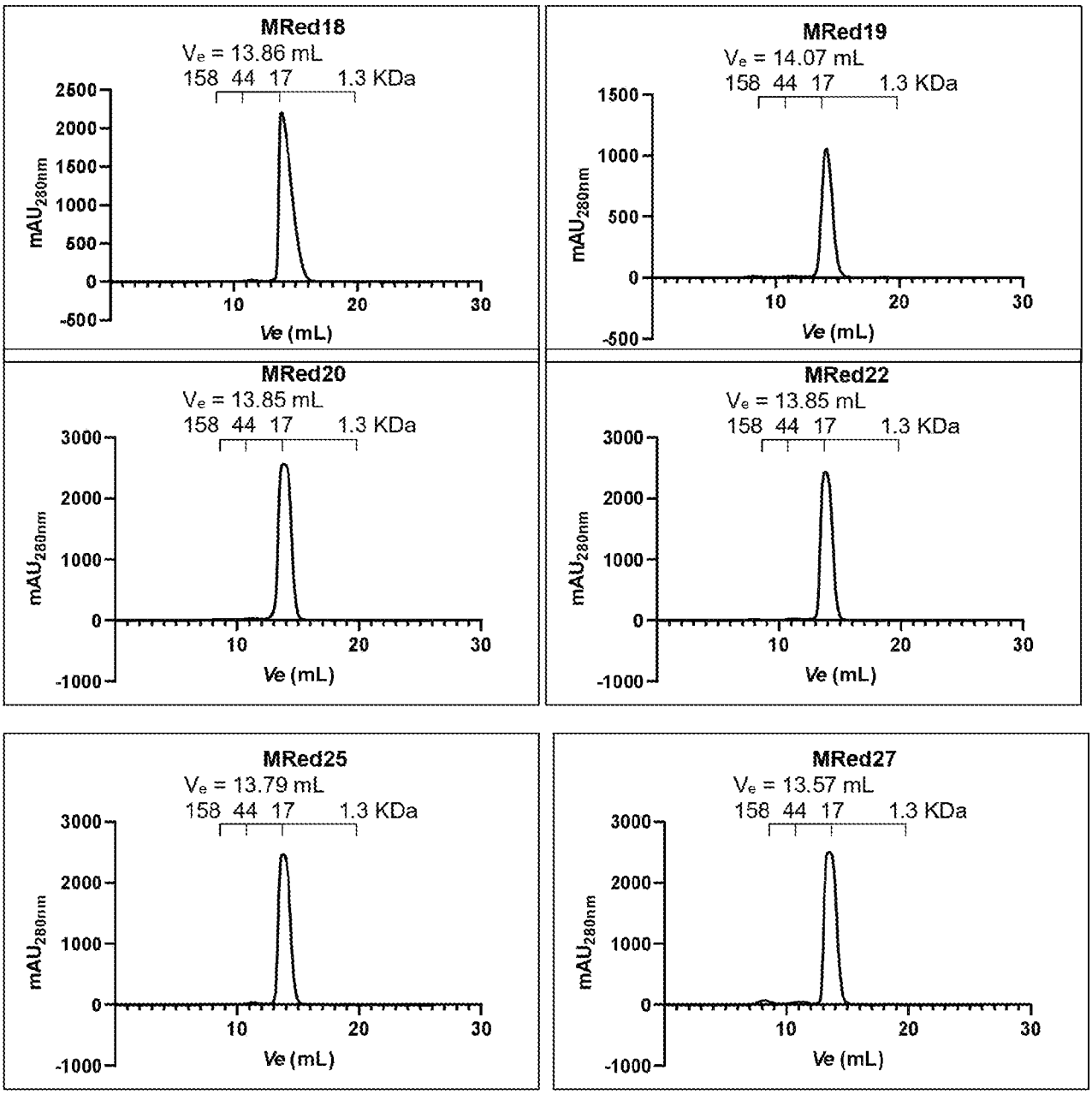
MRed18
Ve = 13.86 mL
158 44 17 1.3 KDa
mAU280nm
Ve (mL)
MRed19
Ve = 14.07 mL
158 44 17 1.3 KDa
mAU280nm
Ve (mL)
MRed20
Ve = 13.85 mL
158 44 17 1.3 KDa
mAU280nm
Ve (mL)
MRed22
Ve = 13.85 mL
158 44 17 1.3 KDa
mAU280nm
Ve (mL)
MRed25
Ve = 13.79 mL
158 44 17 1.3 KDa
mAU280nm
Ve (mL)
MRed27
Ve = 13.57 mL
158 44 17 1.3 KDa
mAU280nm
Ve (mL)

FIG. 4B (cont.)

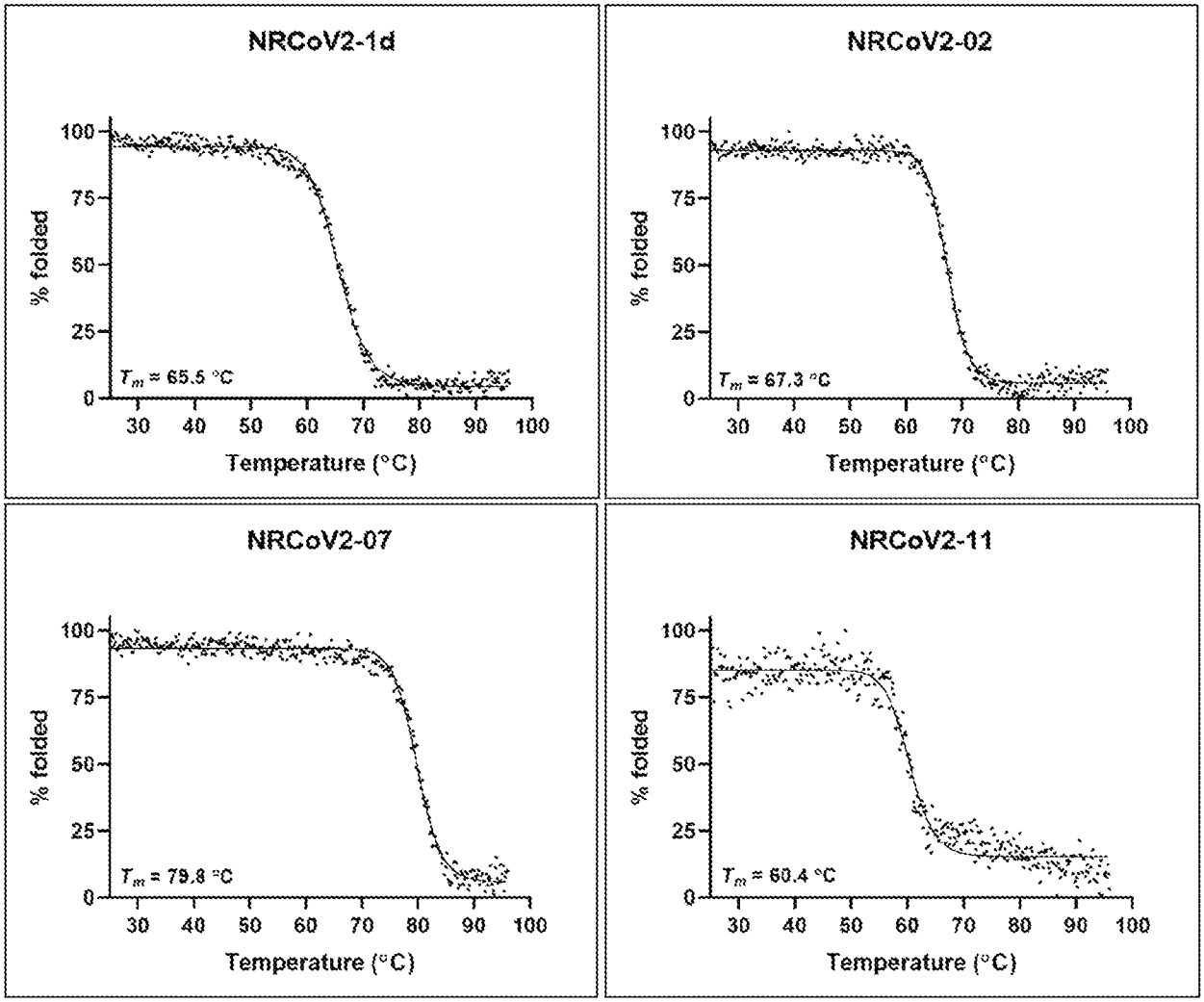
NRCoV2-1d
% folded
100
75
50
25
0
$T_m$ = 65.5 °C
30 40 50 60 70 80 90 100
Temperature (°C)
NRCoV2-02
% folded
100
75
50
25
0
$T_m$ = 67.3 °C
30 40 50 60 70 80 90 100
Temperature (°C)
NRCoV2-07
% folded
100
75
50
25
0
$T_m$ = 79.8 °C
30 40 50 60 70 80 90 100
Temperature (°C)
NRCoV2-11
% folded
100
75
50
25
0
$T_m$ = 60.4 °C
30 40 50 60 70 80 90 100
Temperature (°C)

FIG. 5A

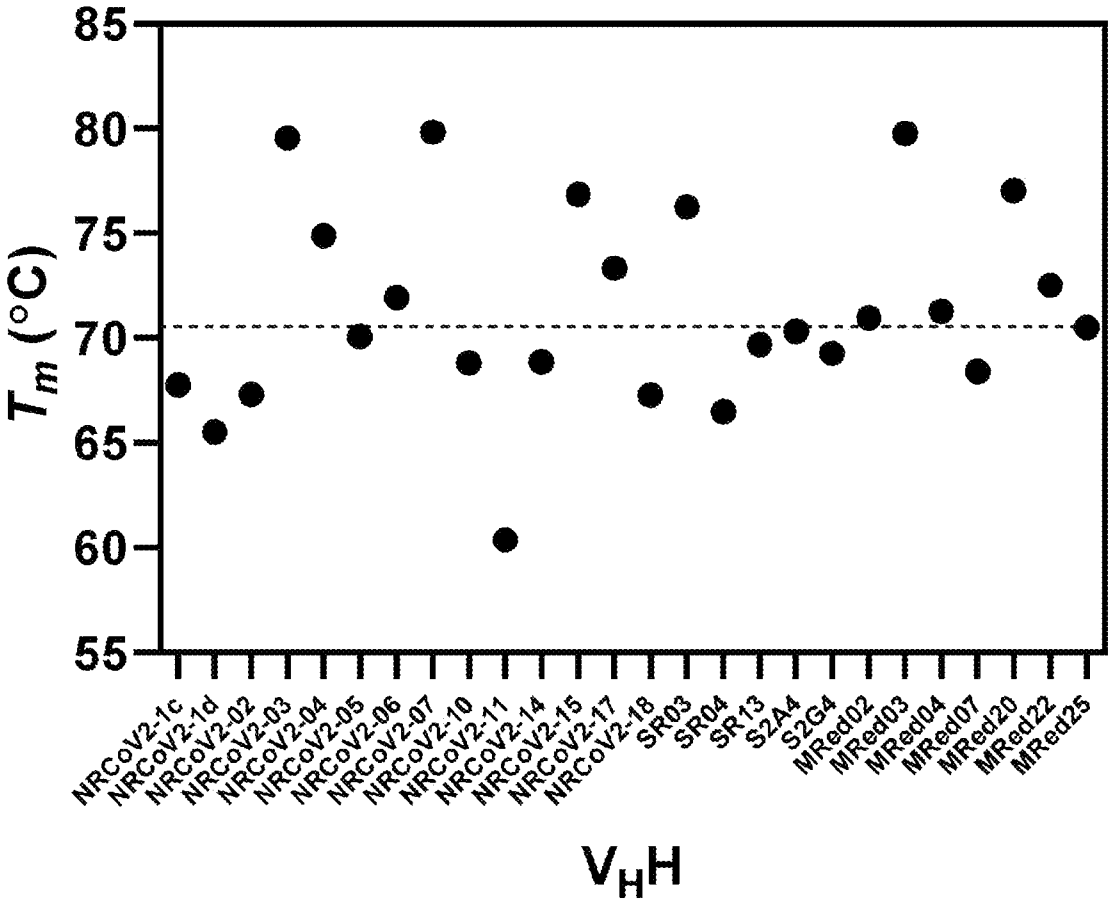
85
80
75
70
65
60
55
$T_m$ (°C)
NRCoV2-1c
NRCoV2-1d
NRCoV2-02
NRCoV2-03
NRCoV2-04
NRCoV2-05
NRCoV2-06
NRCoV2-07
NRCoV2-10
NRCoV2-11
NRCoV2-14
NRCoV2-15
NRCoV2-17
NRCoV2-18
SR03
SR04
SR13
S2A4
S2G4
MRed02
MRed03
MRed04
MRed07
MRed20
MRed22
MRed25
$V_HH$

FIG. 5B

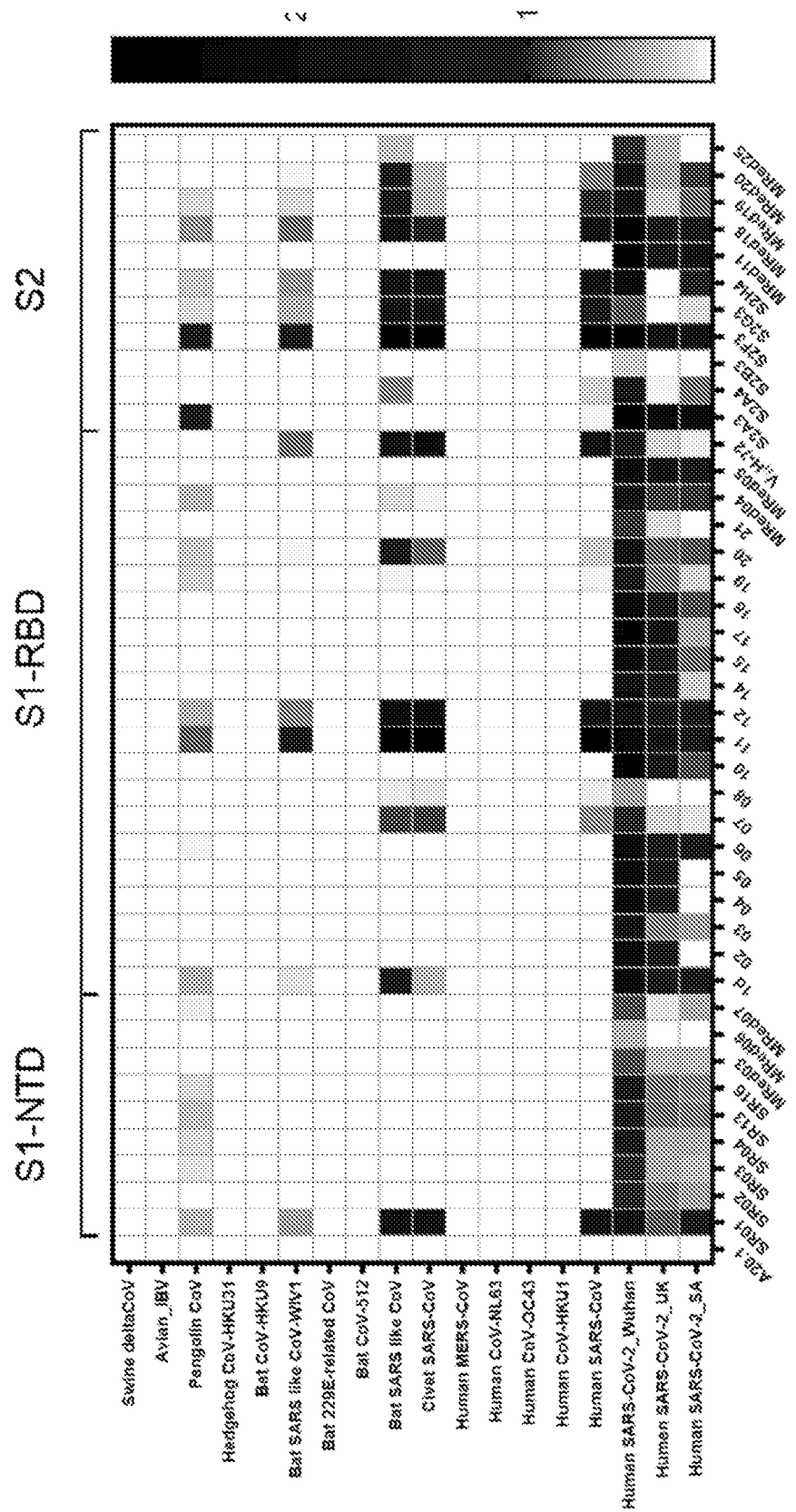
S1-NTD
S1-RBD
S2
Swine deltaCoV
Avian_IBV
Pangolin CoV
Hedgehog CoV-HKU31
Bat CoV-HKU9
Bat SARS like CoV-WIV1
Bat 229E-related CoV
Bat CoV-512
Bat SARS like CoV
Civet SARS-CoV
Human MERS-CoV
Human CoV-NL63
Human CoV-OC43
Human CoV-HKU1
Human SARS-CoV
Human SARS-CoV-2_Wuhan
Human SARS-CoV-2_UK
Human SARS-CoV-2_SA
2
1

FIG. 6A

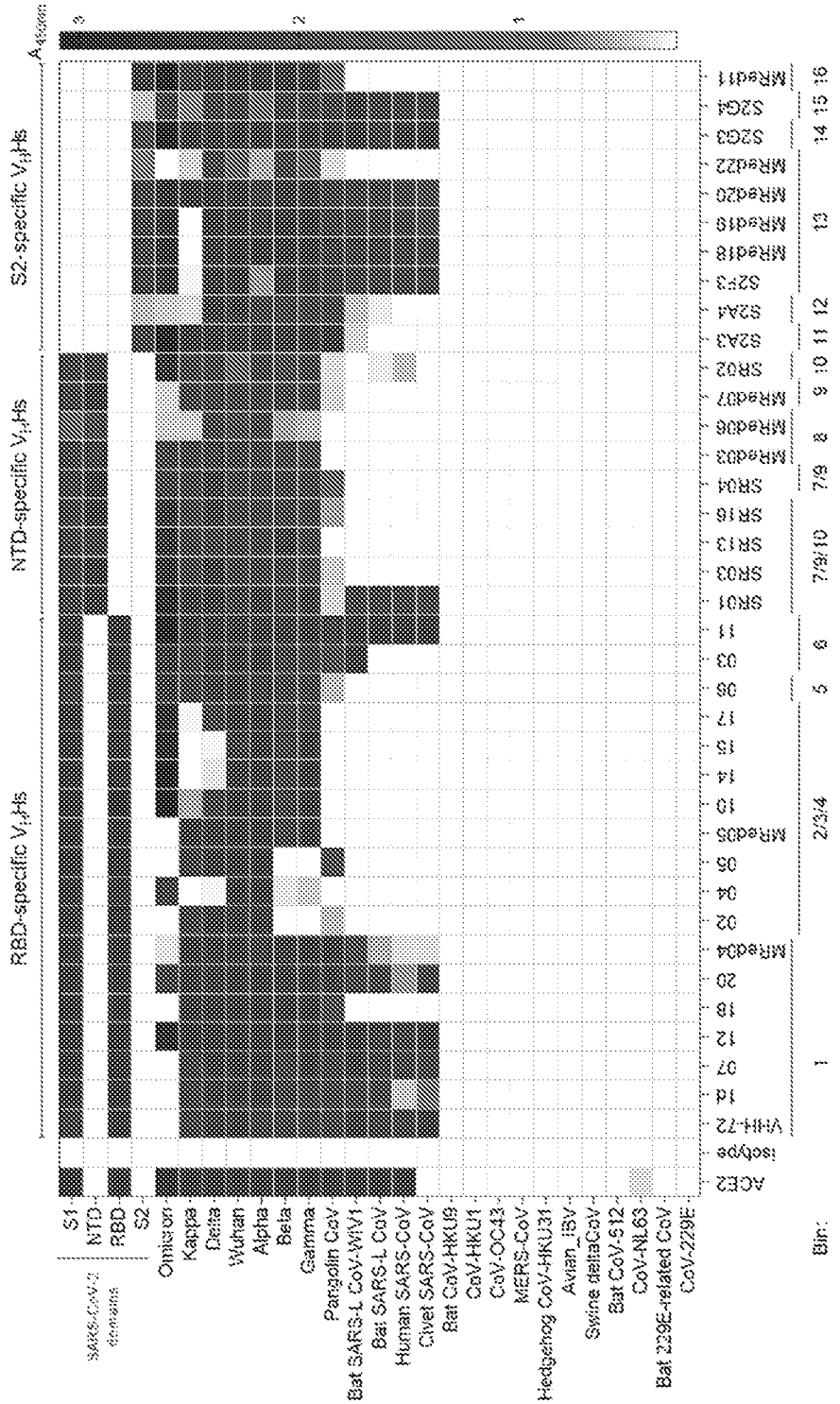
RBD-specific V$_H$Hs
NTD-specific V$_H$Hs
S2-specific V$_H$Hs
A$_{450nm}$
SARS-CoV-2 domains
S1
NTD
RBD
S2
Omicron
Kappa
Delta
Wuhan
Alpha
Beta
Gamma
Pangolin CoV
Bat SARS-L CoV-WIV1
Bat SARS-L CoV
Human SARS-CoV
Civet SARS-CoV
Bat CoV-HKU9
CoV-HKU1
CoV-OC43
MERS-CoV
Hedgehog CoV-HKU31
Avian_IBV
Swine deltaCoV
Bat CoV-512
CoV-NL63
Bat 229E-related CoV
CoV-229E
ACE2
isotype
VHH-72
1d
07
12
18
20
MRad04
02
04
05
MRad05
10
14
15
17
06
03
11
SR01
SR03
SR13
SR16
SR04
MRad03
MRad06
MRad07
SR02
S2A3
S2A4
S2F3
MRad18
MRad19
MRad20
MRad22
S2G3
S2G4
MRad11
Bin:
1
2/3/4
5
6
7/9/10
7/9
8
9
10
11
12
13
14
15
16

FIG. 6B

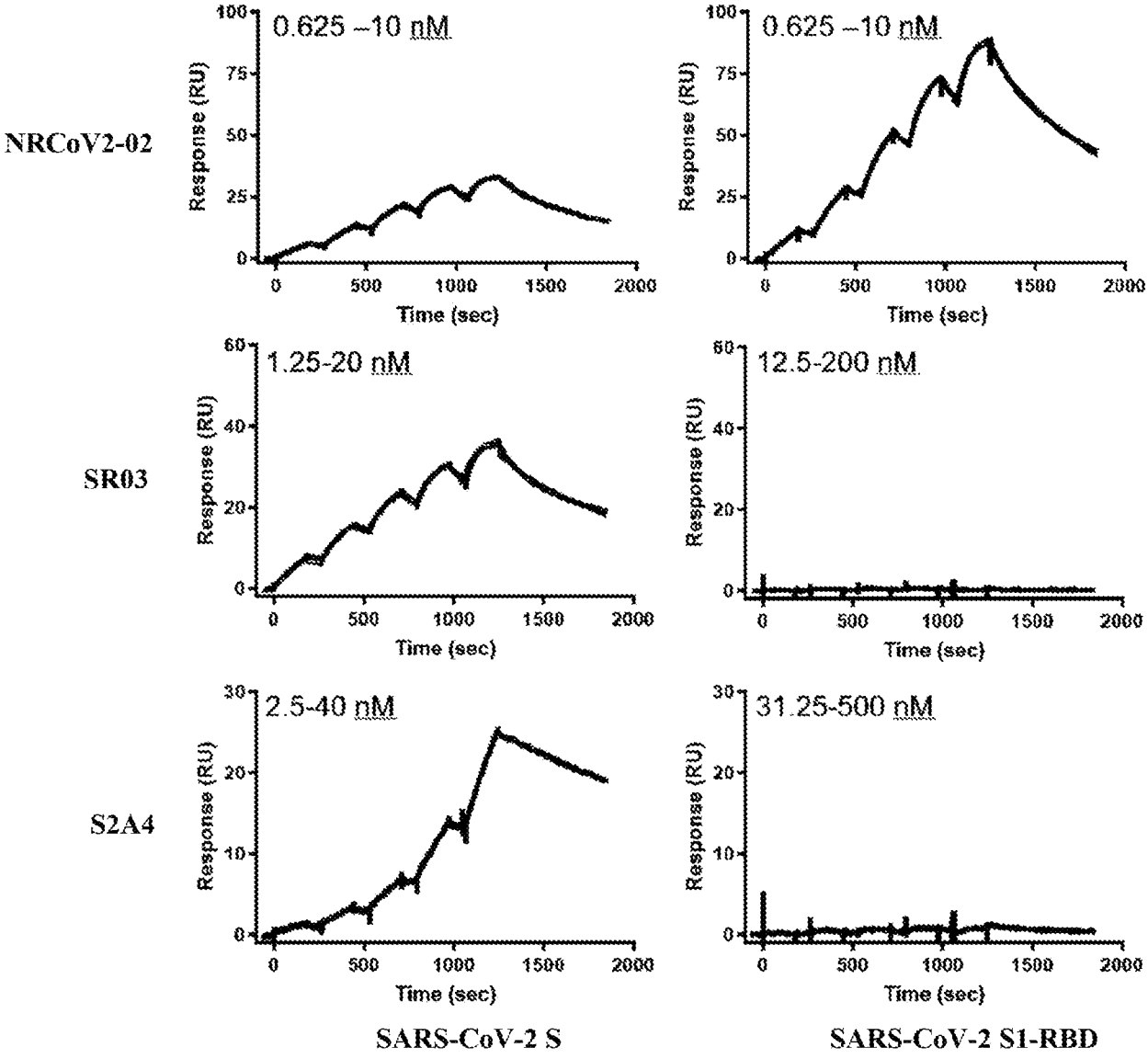
NRCoV2-02
SR03
S2A4
0.625 –10 nM
1.25-20 nM
2.5-40 nM
12.5-200 nM
31.25-500 nM
Response (RU)
Time (sec)
SARS-CoV-2 S
SARS-CoV-2 S1-RBD

FIG. 6C

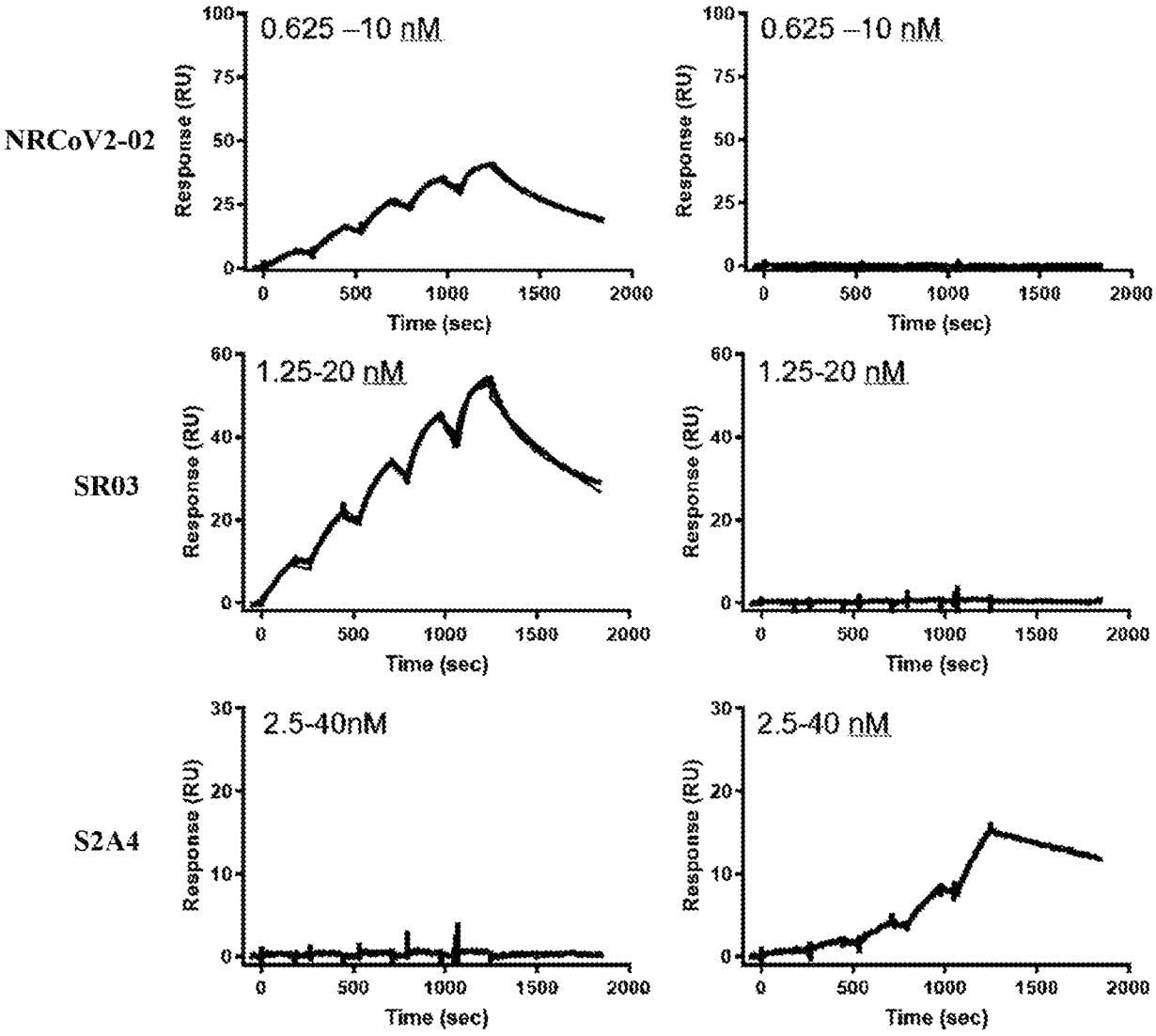
NRCoV2-02
SR03
S2A4
0.625 –10 nM
1.25-20 nM
2.5-40nM
2.5-40 nM
Response (RU)
Time (sec)
SARS-CoV-2 S1
SARS-CoV-2 S2

FIG. 6C (cont.)

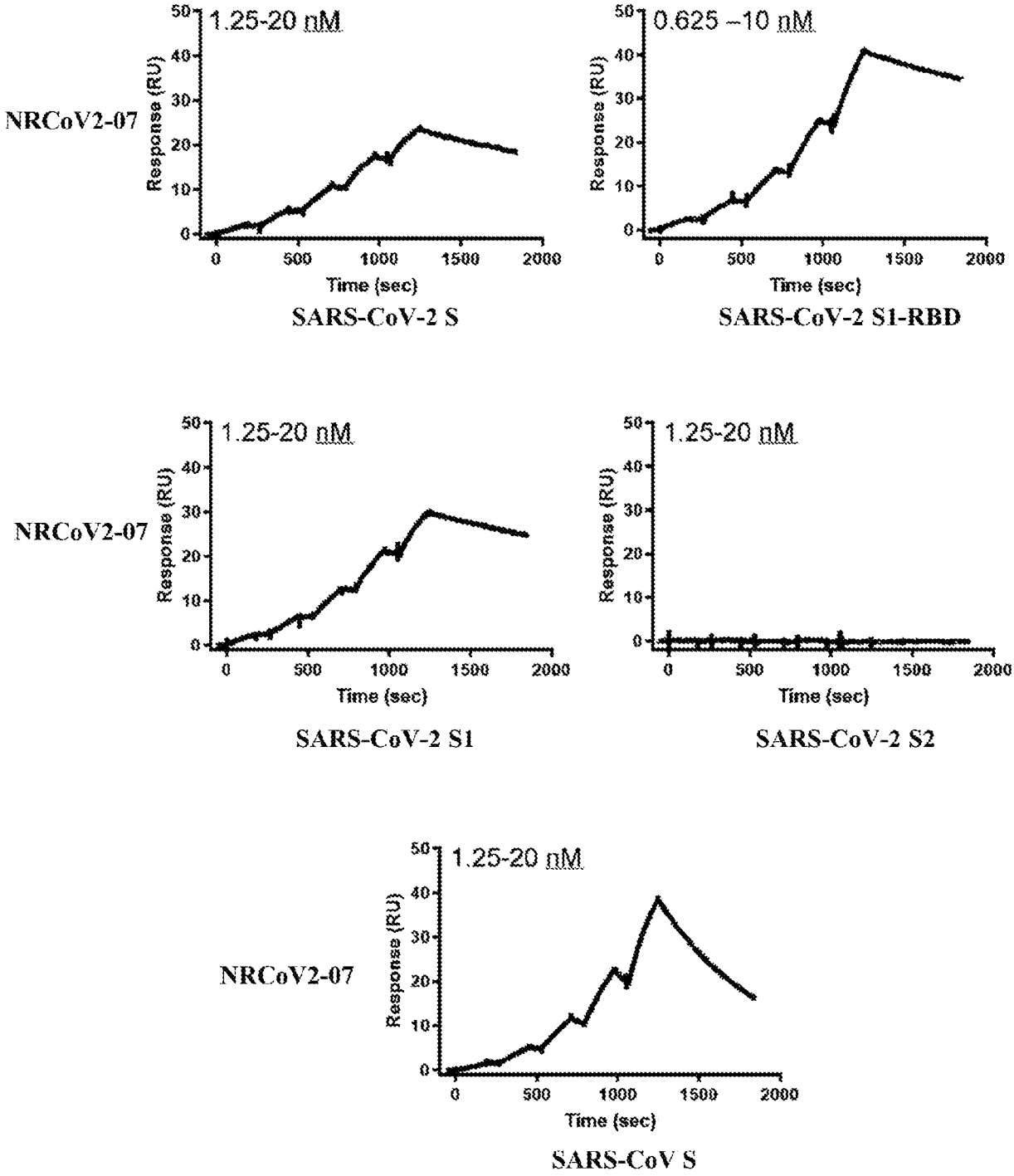
NRCoV2-07
1.25-20 nM
0.625 –10 nM
Response (RU)
Time (sec)
SARS-CoV-2 S
SARS-CoV-2 S1-RBD
SARS-CoV-2 S1
SARS-CoV-2 S2
SARS-CoV S

FIG. 6C (cont.)

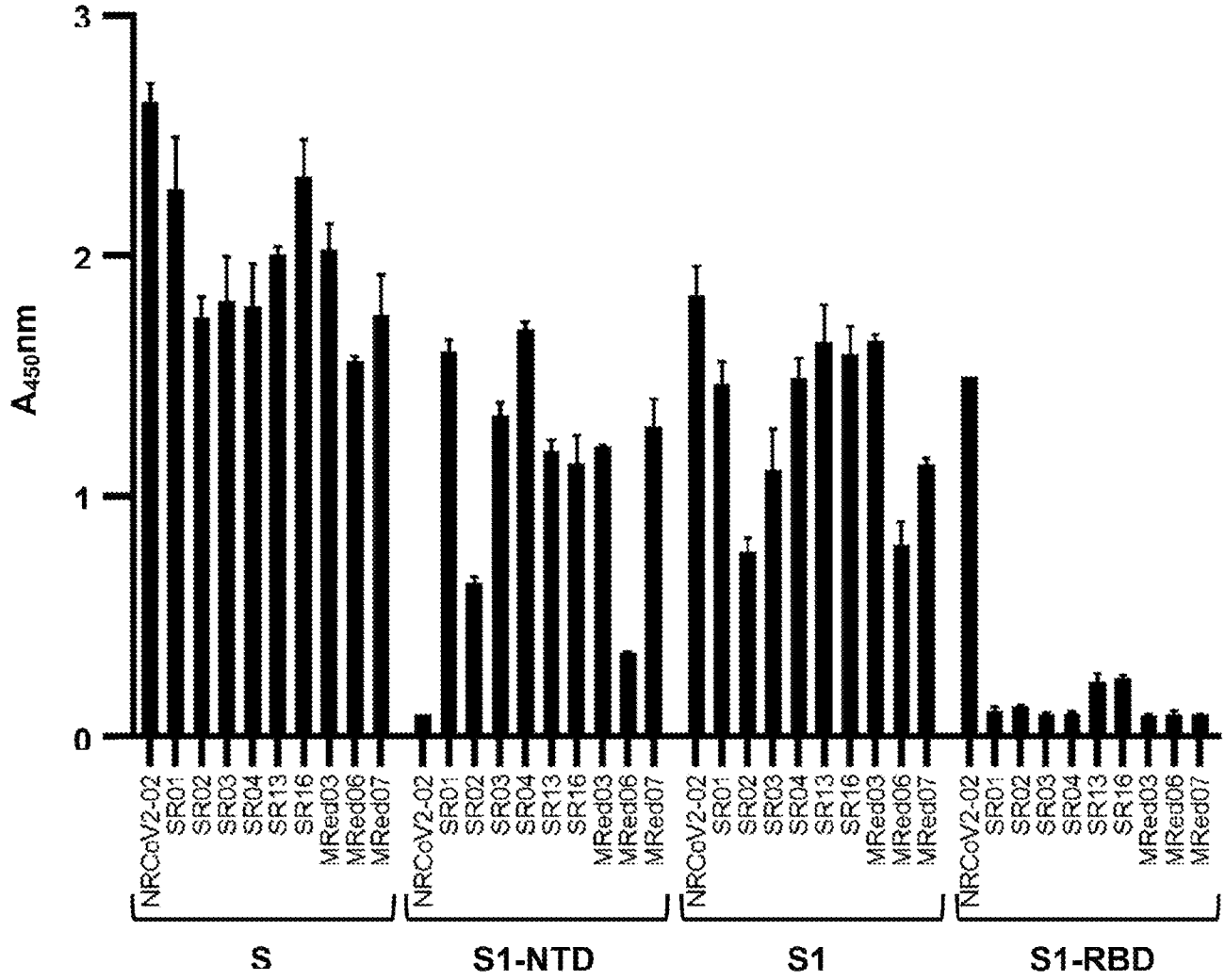
3
2
1
0
A450nm
NRCoV2-02
SR01
SR02
SR03
SR04
SR13
SR16
MRed03
MRed06
MRed07
S
S1-NTD
S1
S1-RBD

FIG 6D

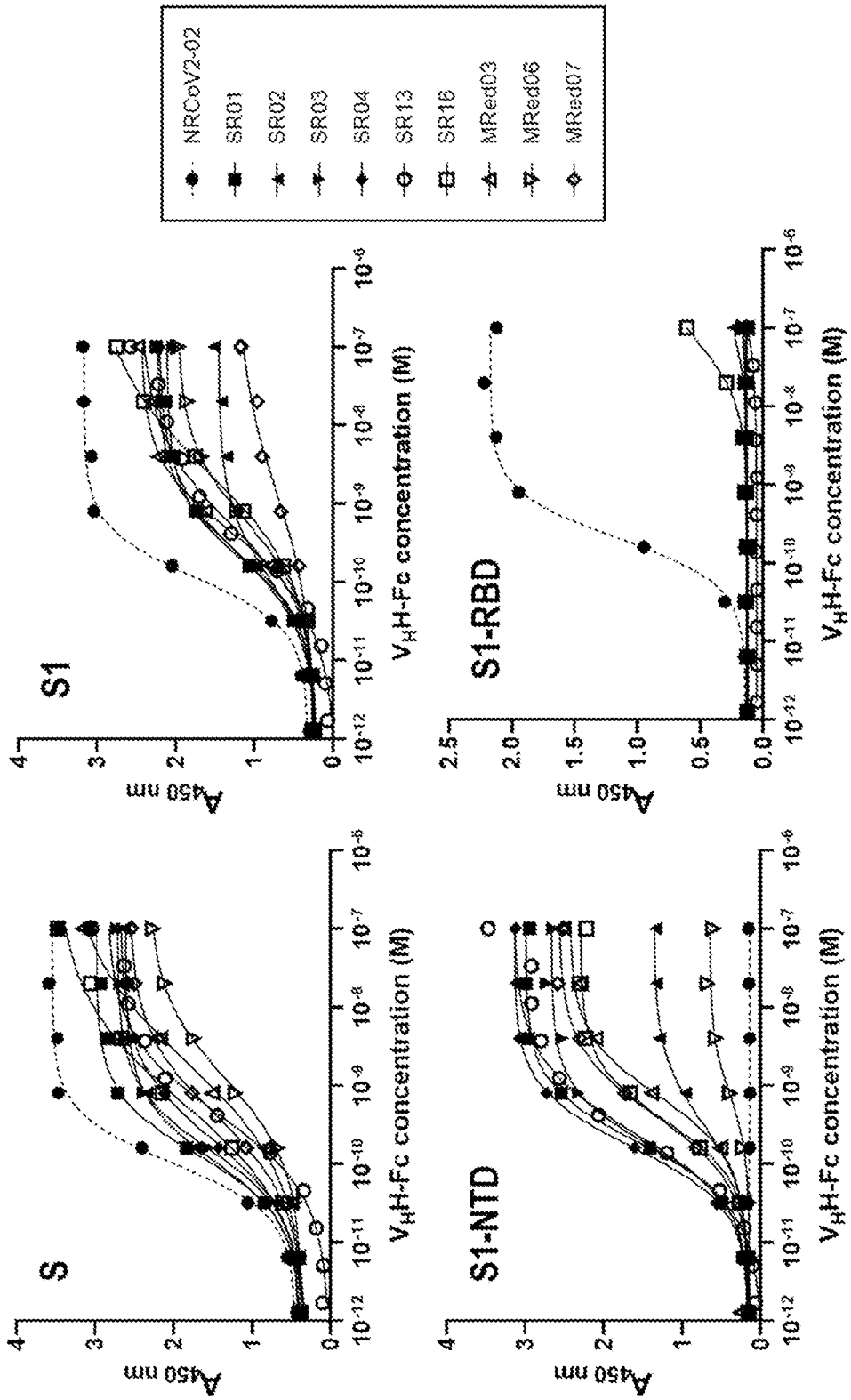
NRCoV2-02
SR01
SR02
SR03
SR04
SR13
SR16
MRed03
MRed06
MRed07
S1
S1-RBD
S
S1-NTD
A450 nm
VHH-Fc concentration (M)

FIG. 6E

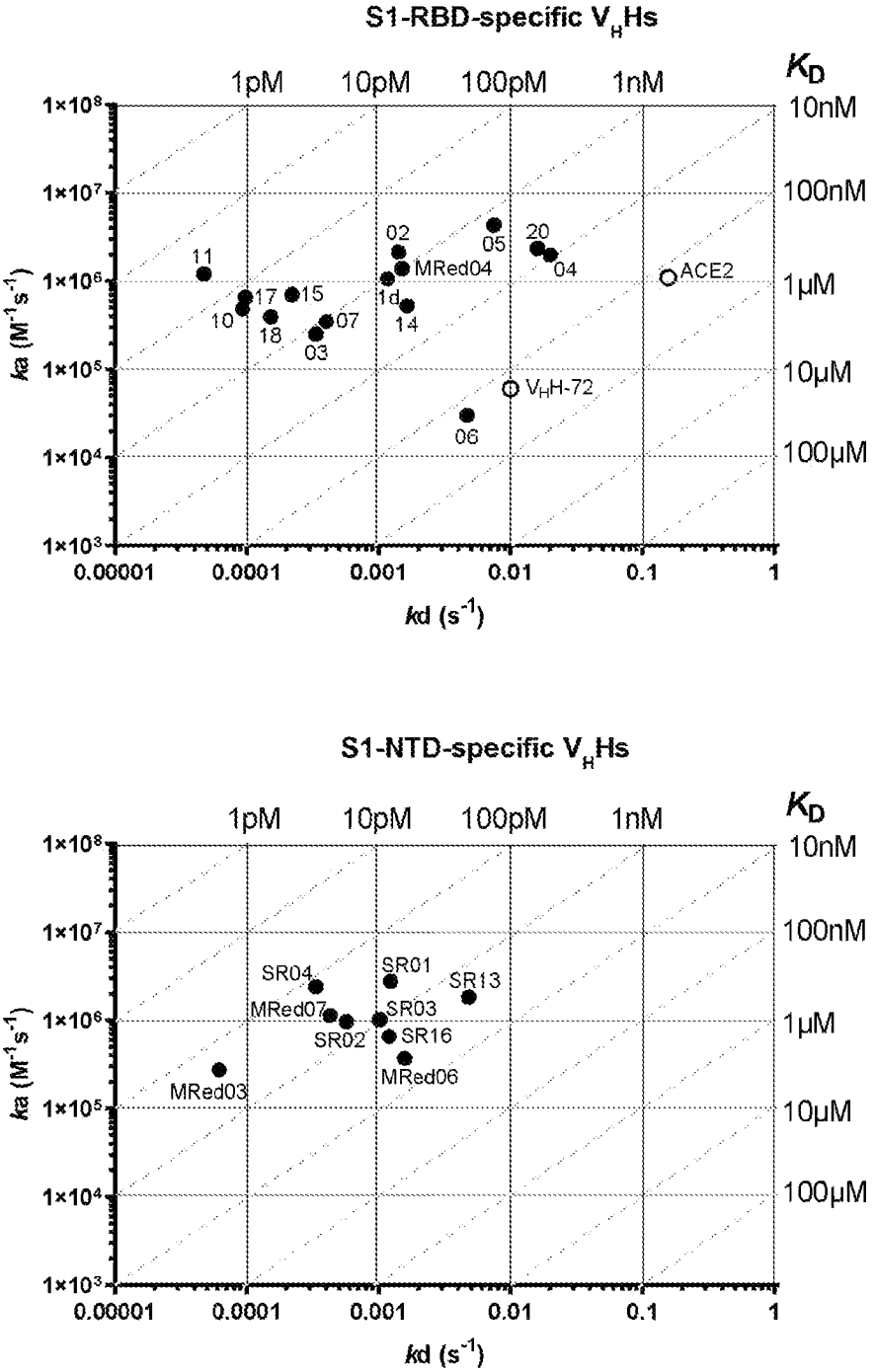
S1-RBD-specific V_HHs
1pM
10pM
100pM
1nM
K_D
10nM
100nM
1µM
10µM
100µM
1×10^8
1×10^7
1×10^6
1×10^5
1×10^4
1×10^3
ka (M^-1s^-1)
0.00001
0.0001
0.001
0.01
0.1
1
kd (s^-1)
11
17
15
10
18
07
03
02
MRed04
1d
14
05
20
04
ACE2
V_HH-72
06
S1-NTD-specific V_HHs
SR04
SR01
SR13
MRed07
SR03
SR02
SR16
MRed06
MRed03

FIG. 7A

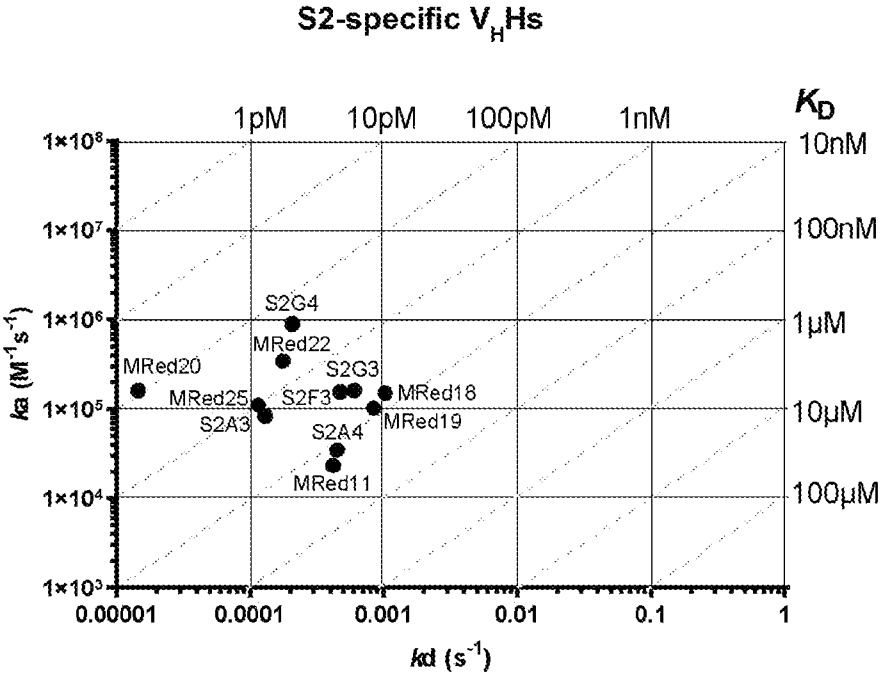


FIG. 7A (cont.)

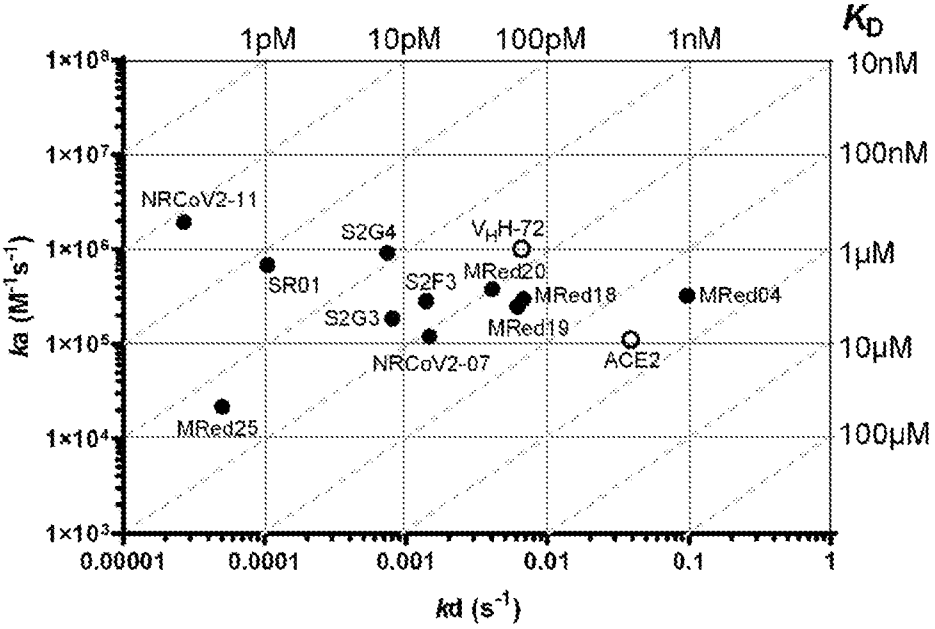


FIG. 7B

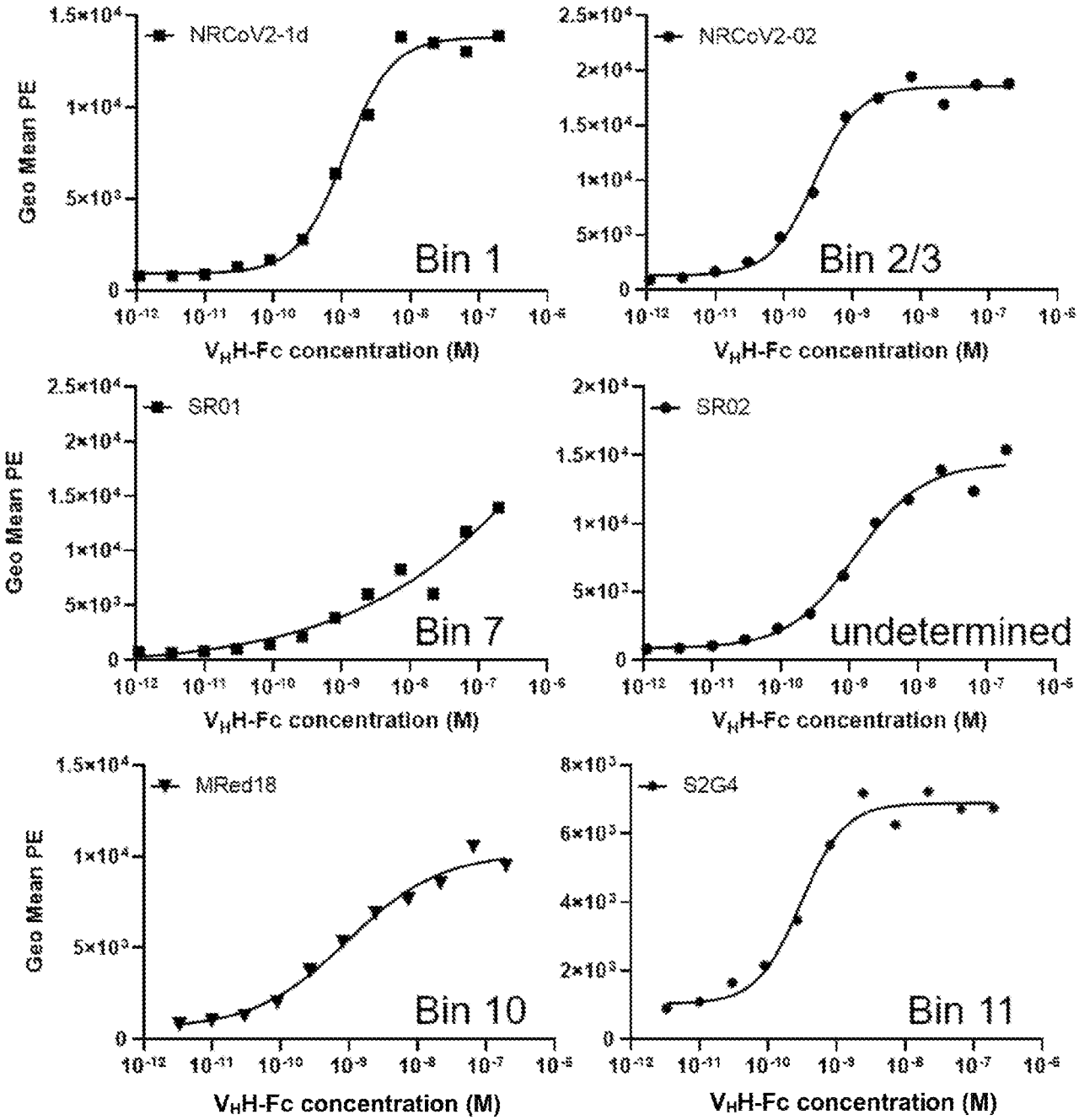
NRCoV2-1d
Bin 1
NRCoV2-02
Bin 2/3
SR01
Bin 7
SR02
undetermined
MRed18
Bin 10
S2G4
Bin 11
Geo Mean PE
VHH-Fc concentration (M)

FIG. 8A

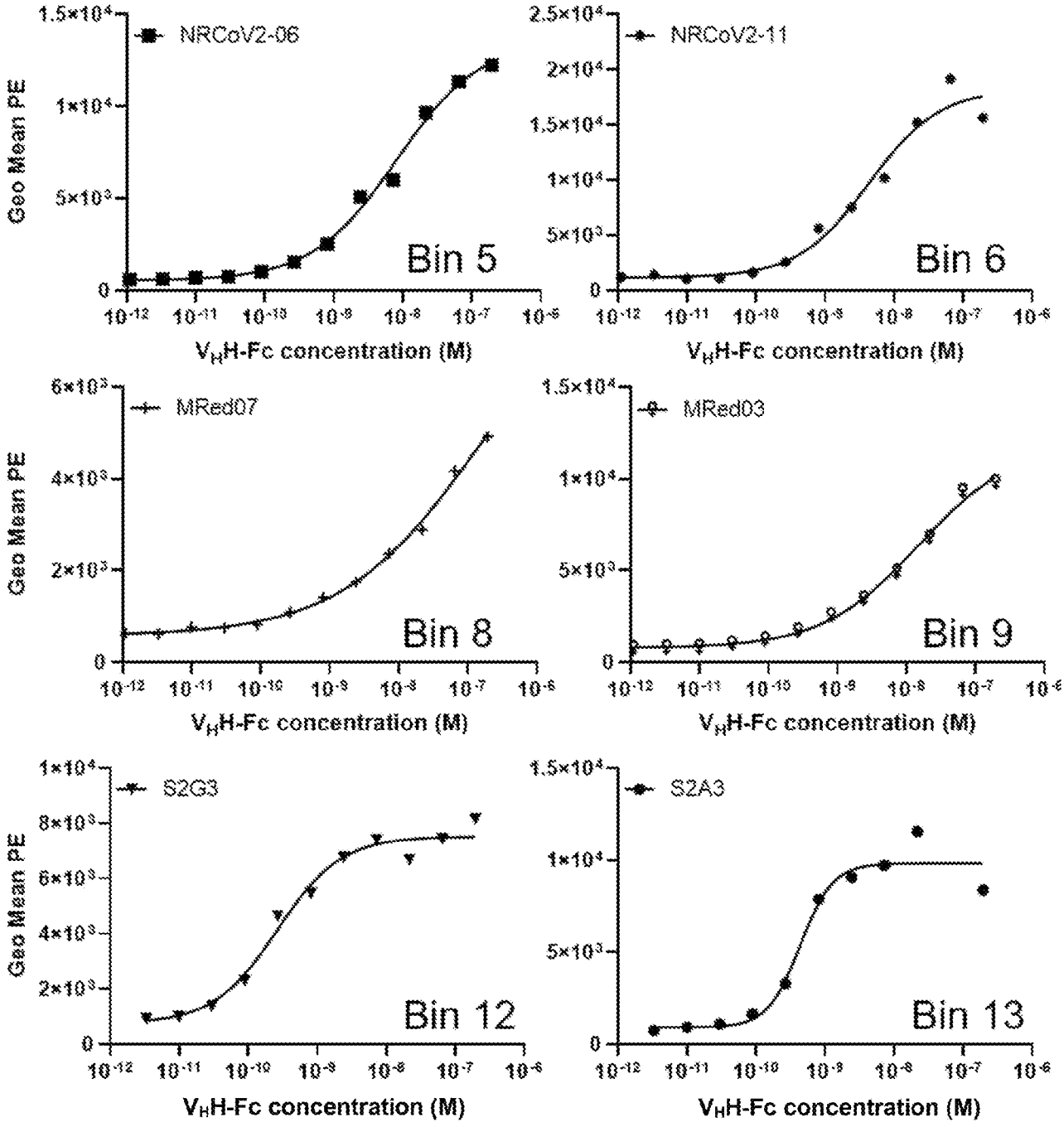
NRCoV2-06
Bin 5
NRCoV2-11
Bin 6
MRed07
Bin 8
MRed03
Bin 9
S2G3
Bin 12
S2A3
Bin 13
Geo Mean PE
VHH-Fc concentration (M)

FIG. 8A (cont.)

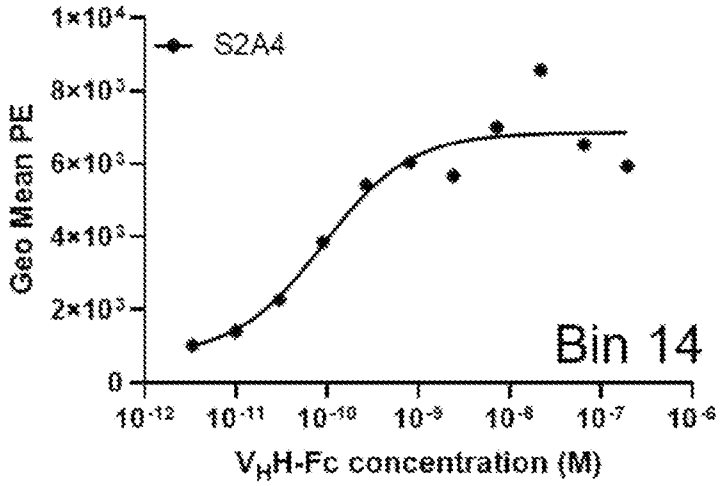


FIG. 8A (cont.)

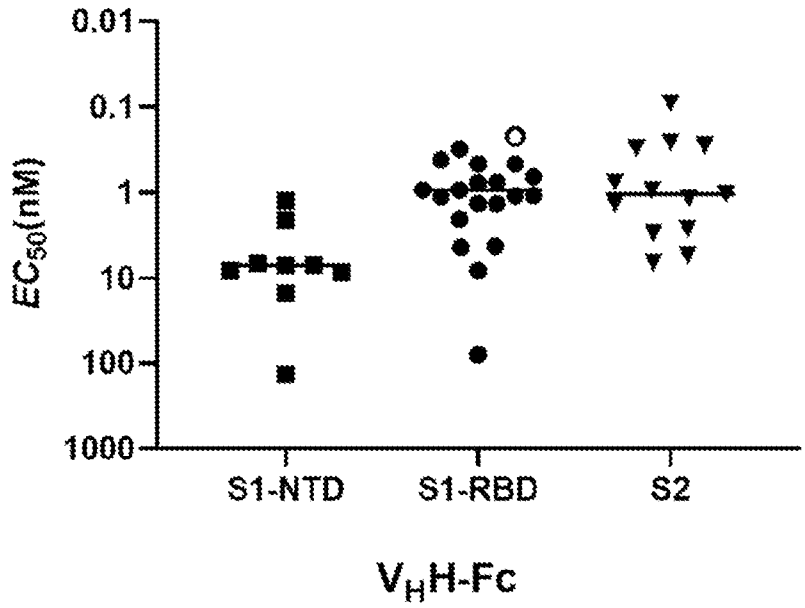


FIG. 8B

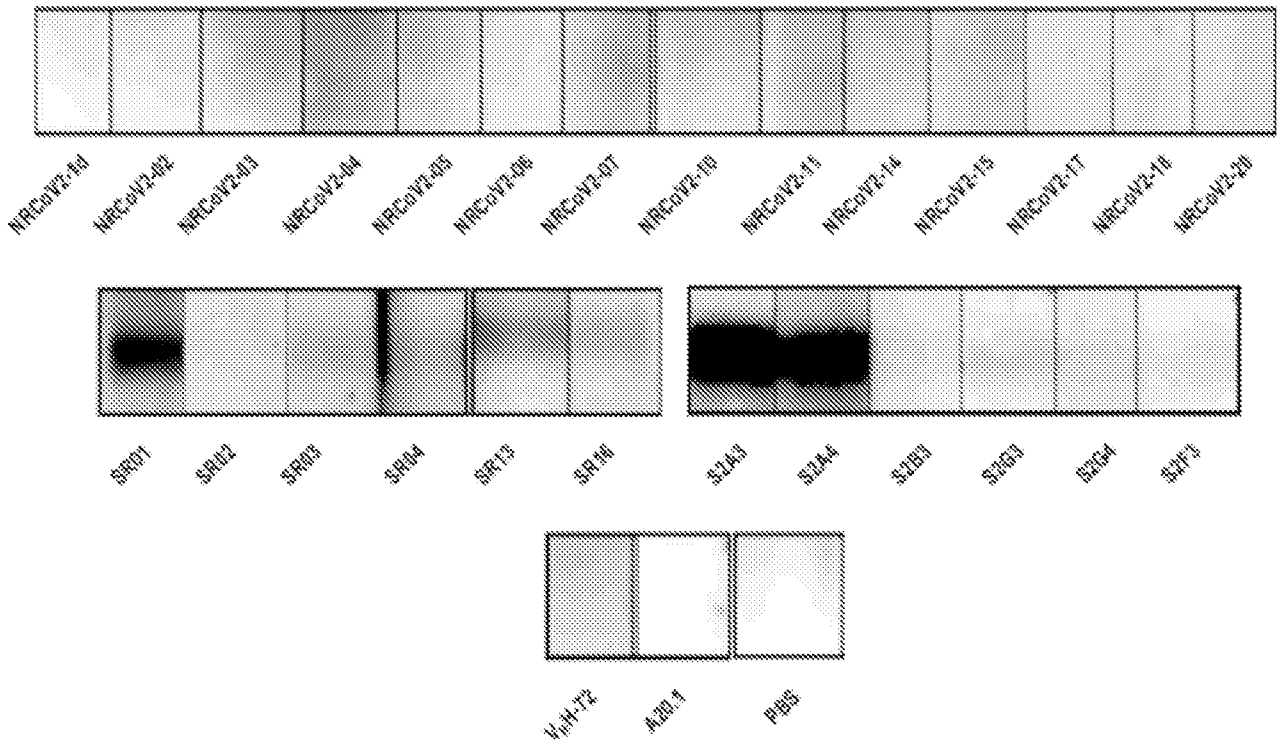
NRCoV2-01
NRCoV2-02
NRCoV2-03
NRCoV2-04
NRCoV2-05
NRCoV2-06
NRCoV2-07
NRCoV2-10
NRCoV2-11
NRCoV2-14
NRCoV2-15
NRCoV2-17
NRCoV2-18
NRCoV2-20
SR01
SR02
SR03
SR04
SR13
SR16
S2A3
S2A4
S2B3
S2E3
G2G4
SHF5
VHH-72
ab20.1
PBS

FIG. 9A

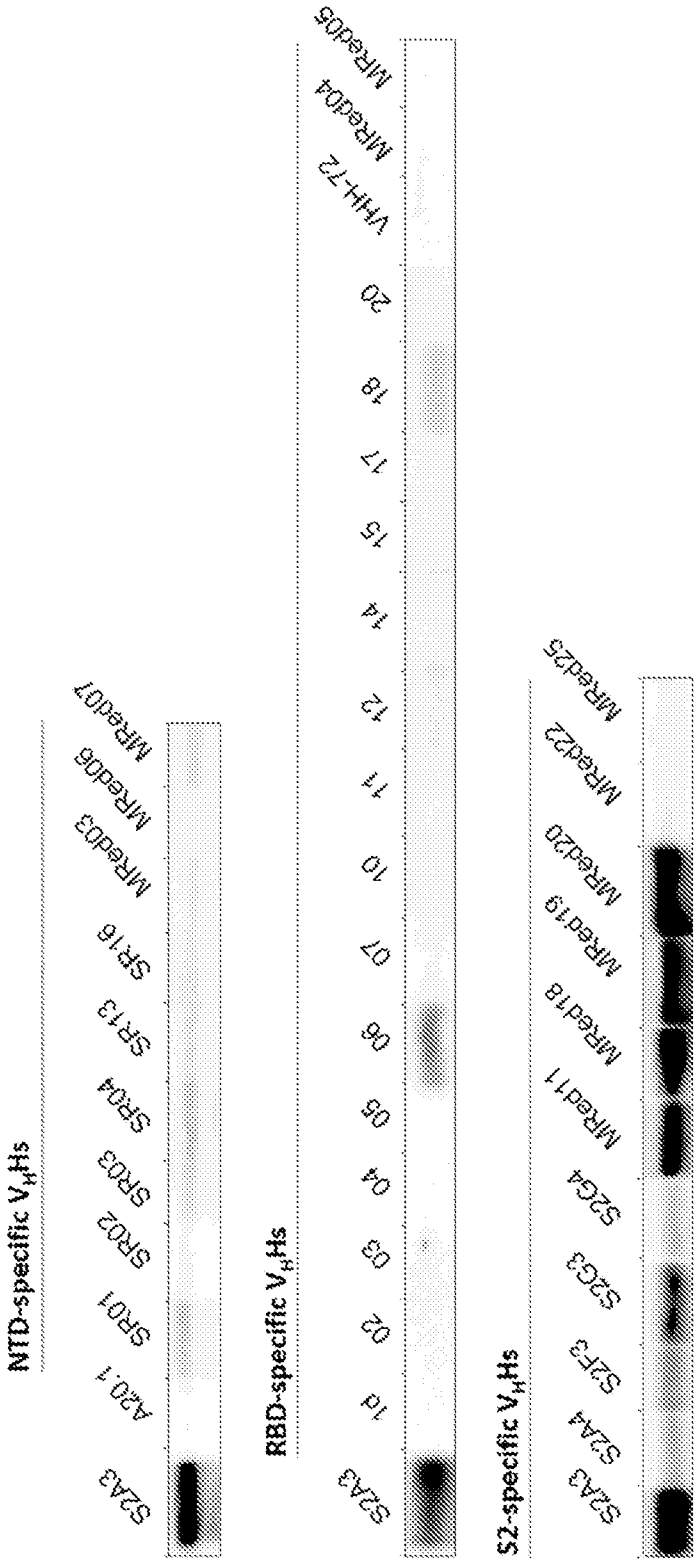
NTD-specific $V_HHs$
S2A3
A20.1
SR01
SR02
SR03
SR04
SR13
SR16
MRed03
MRed06
MRed07
RBD-specific $V_HHs$
S2A3
10
02
03
04
05
06
07
10
11
12
14
15
17
18
20
VHH-72
MRed04
MRed05
S2-specific $V_HHs$
S2A3
S2A4
S2F3
S2G3
S2G4
MRed11
MRed18
MRed19
MRed20
MRed22
MRed25

FIG. 9B

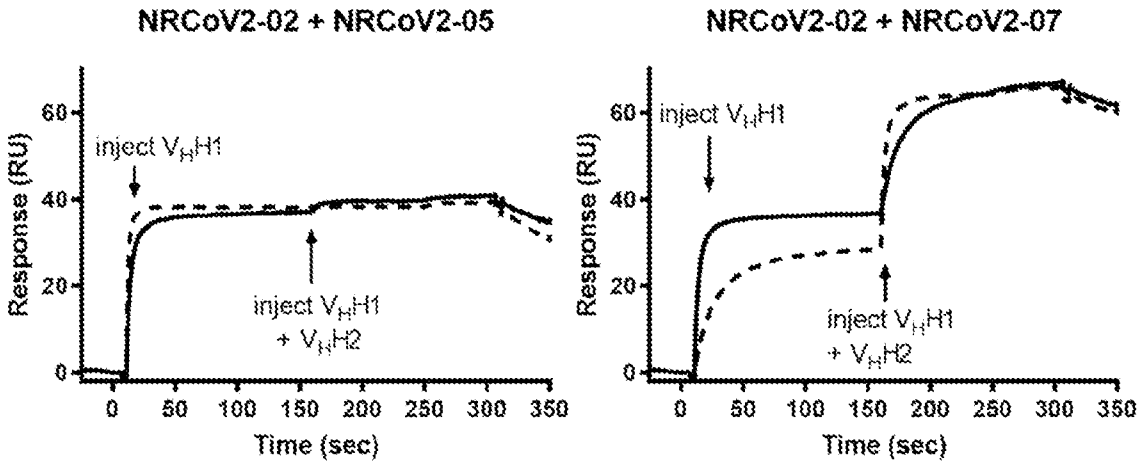
NRCoV2-02 + NRCoV2-05
NRCoV2-02 + NRCoV2-07
Response (RU)
Time (sec)
inject $V_HH1$
inject $V_HH1$ + $V_HH2$
0
20
40
60
0
50
100
150
200
250
300
350

FIG. 9C

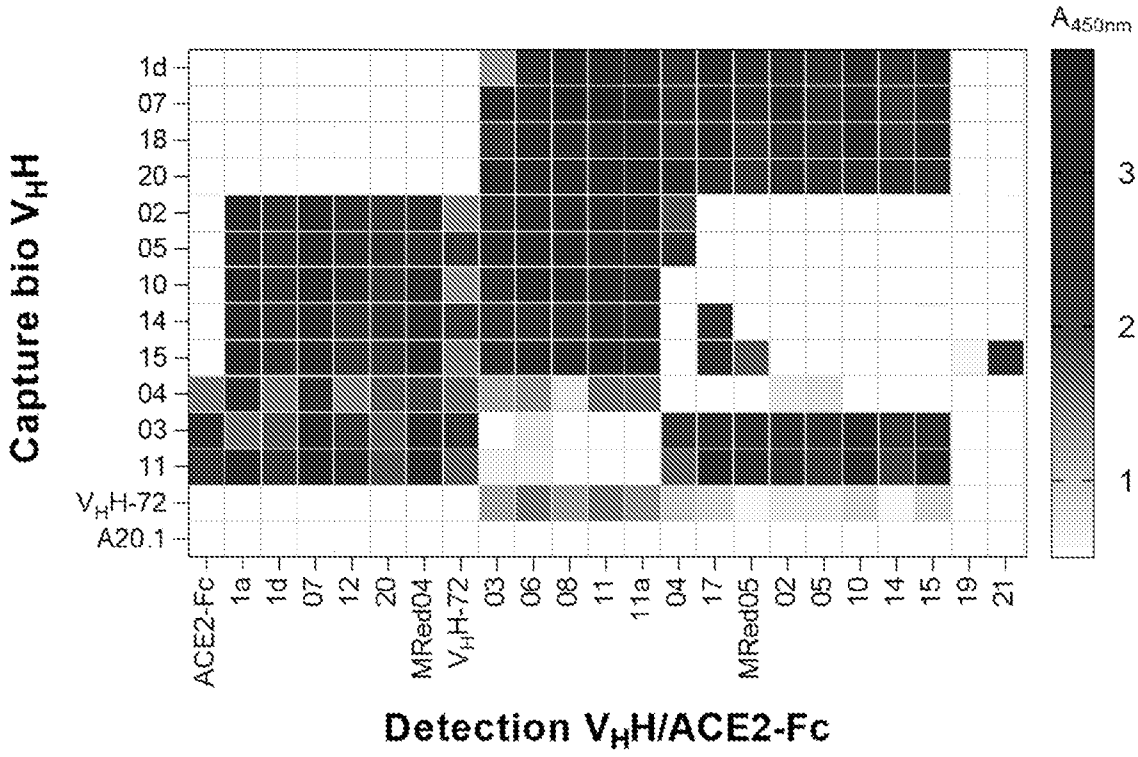
Capture bio $V_HH$
Detection $V_HH$/ACE2-Fc
$A_{450nm}$
1d
07
18
20
02
05
10
14
15
04
03
11
$V_HH$-72
A20.1
ACE2-Fc
1a
1d
07
12
20
MRed04
$V_HH$-72
03
06
08
11
11a
04
17
MRed05
02
05
10
14
15
19
21
1
2
3

FIG. 9D

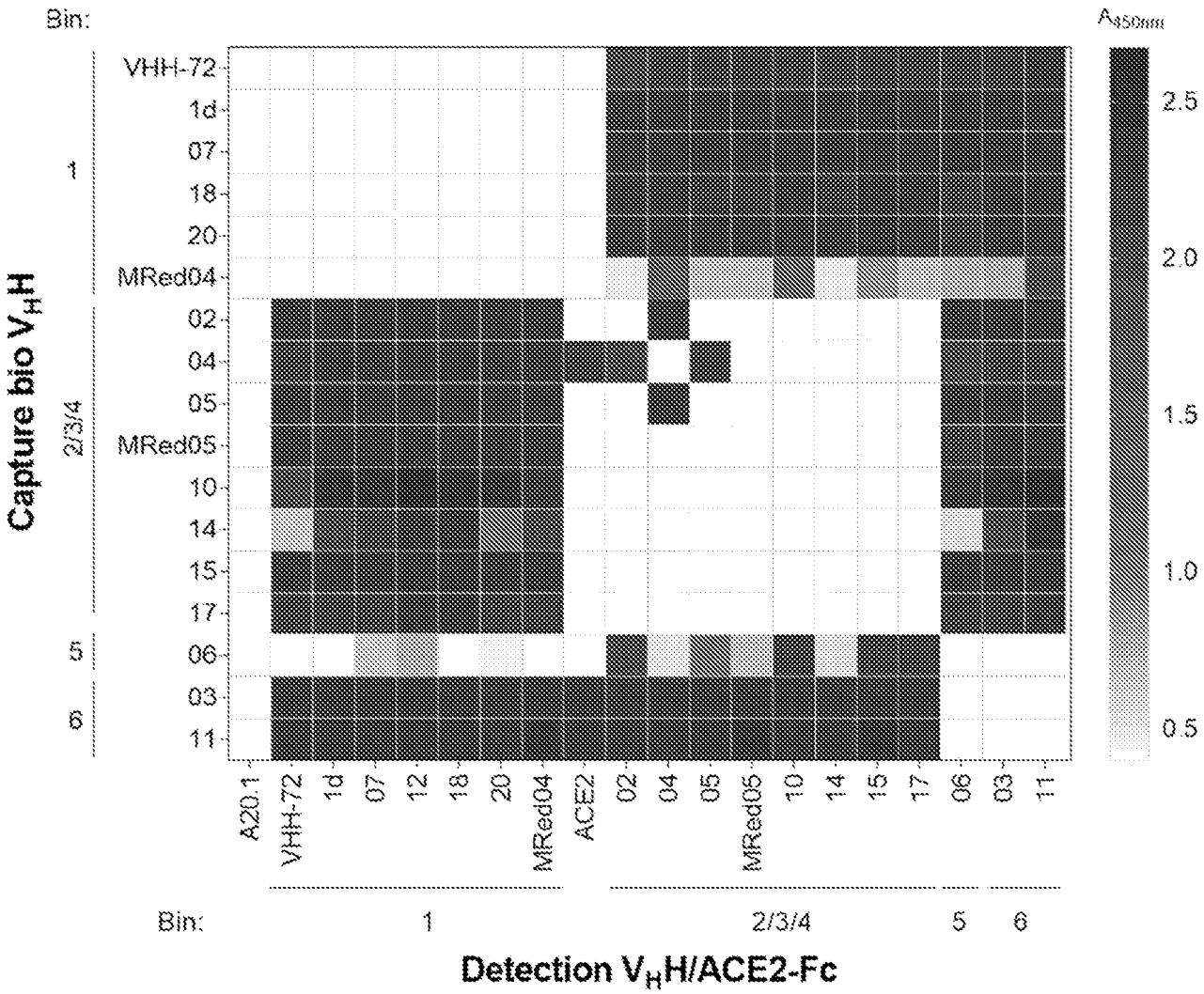
Bin:
A450nm
2.5
2.0
1.5
1.0
0.5
Capture bio VHH
VHH-72
1d
07
18
20
MRed04
02
04
05
MRed05
10
14
15
17
06
03
11
1
2/3/4
5
6
A20.1
VHH-72
1d
07
12
18
20
MRed04
ACE2
02
04
05
MRed05
10
14
15
17
06
03
11
Bin:
1
2/3/4
5
6
Detection VHH/ACE2-Fc

FIG. 9E

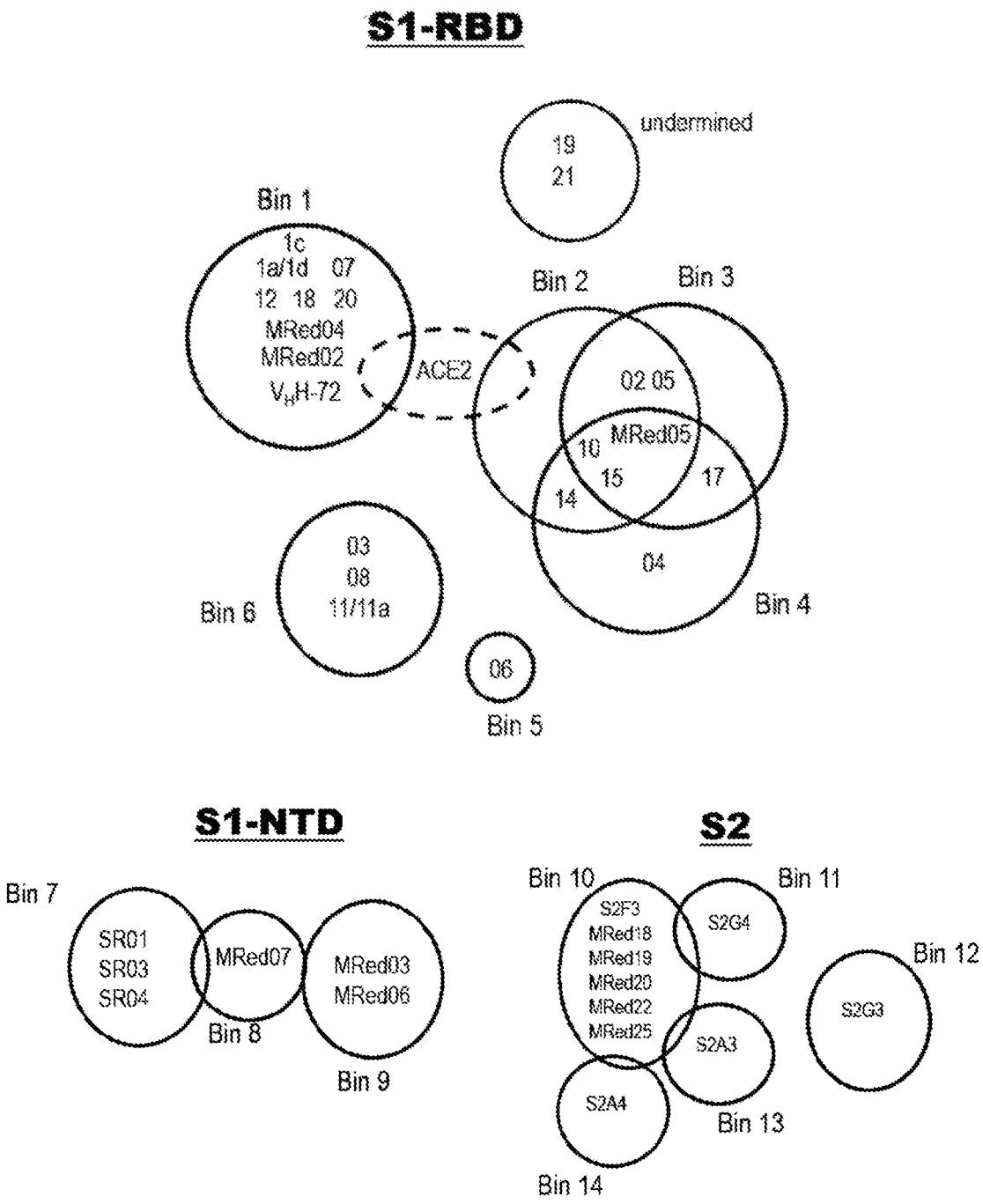
S1-RBD
undermined
19
21
Bin 1
1c
1a/1d 07
12 18 20
MRed04
MRed02
VHH-72
ACE2
Bin 2
Bin 3
02 05
MRed05
10
15
17
14
04
Bin 4
03
08
11/11a
Bin 6
06
Bin 5
S1-NTD
Bin 7
SR01
SR03
SR04
MRed07
Bin 8
MRed03
MRed06
Bin 9
S2
Bin 10
Bin 11
S2F3
MRed18
MRed19
MRed20
MRed22
MRed25
S2G4
Bin 12
S2G3
S2A3
S2A4
Bin 13
Bin 14

FIG. 9F

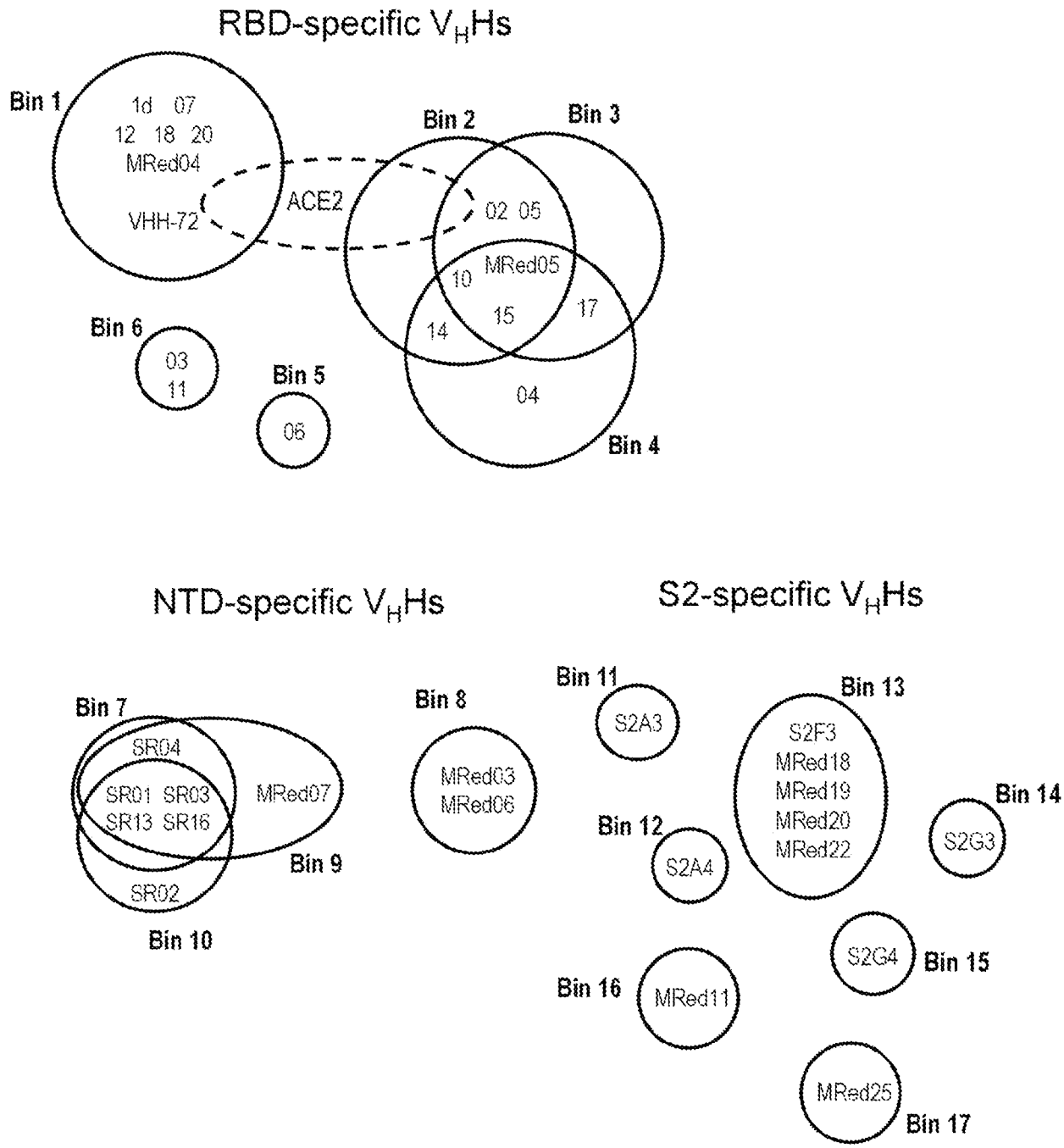
RBD-specific $V_HHs$
Bin 1
1d 07
12 18 20
MRed04
VHH-72
ACE2
Bin 2
Bin 3
02 05
MRed05
10
15
17
14
Bin 6
03
11
Bin 5
06
04
Bin 4
NTD-specific $V_HHs$
S2-specific $V_HHs$
Bin 7
SR04
SR01 SR03
SR13 SR16
MRed07
Bin 9
SR02
Bin 10
Bin 8
MRed03
MRed06
Bin 11
S2A3
Bin 13
S2F3
MRed18
MRed19
MRed20
MRed22
Bin 14
S2G3
Bin 12
S2A4
S2G4
Bin 15
Bin 16
MRed11
MRed25
Bin 17

FIG. 9G

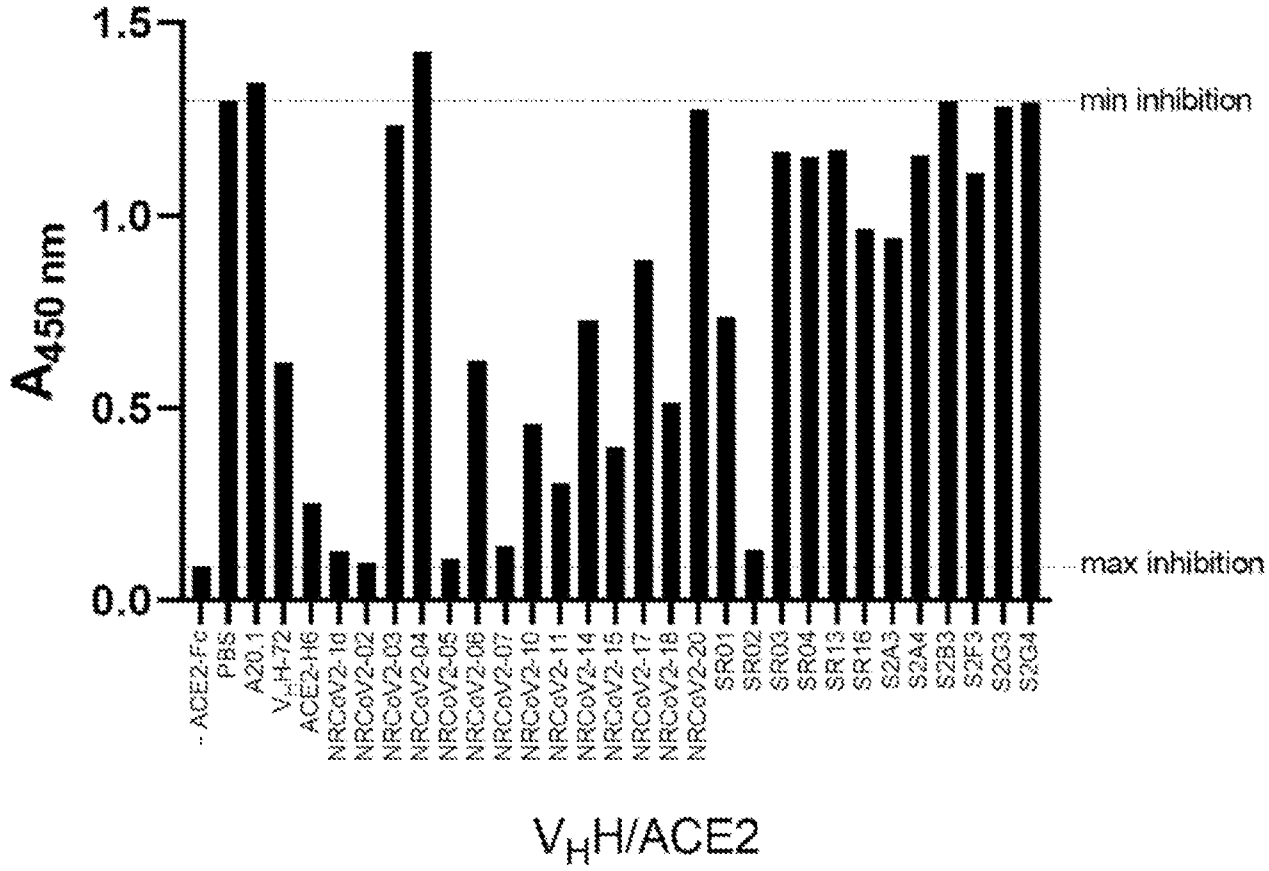
1.5
1.0
0.5
0.0
A450 nm
min inhibition
max inhibition
- ACE2-Fc
PBS
A20.1
VHH-72
ACE2-H6
NRCoV2-01
NRCoV2-02
NRCoV2-03
NRCoV2-04
NRCoV2-05
NRCoV2-06
NRCoV2-07
NRCoV2-10
NRCoV2-11
NRCoV2-14
NRCoV2-15
NRCoV2-17
NRCoV2-18
NRCoV2-20
SR01
SR02
SR03
SR04
SR13
SR15
S2A3
S2A4
S2B3
S2F3
S2G3
S2G4
VHH/ACE2

FIG. 10

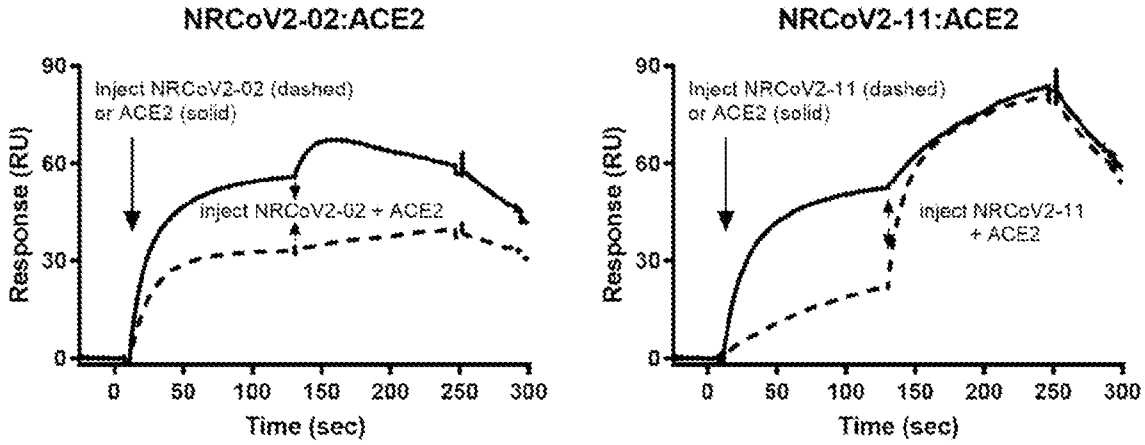
NRCoV2-02:ACE2
Inject NRCoV2-02 (dashed) or ACE2 (solid)
Inject NRCoV2-02 + ACE2
Response (RU)
Time (sec)
NRCoV2-11:ACE2
Inject NRCoV2-11 (dashed) or ACE2 (solid)
Inject NRCoV2-11 + ACE2
Response (RU)
Time (sec)

FIG. 11

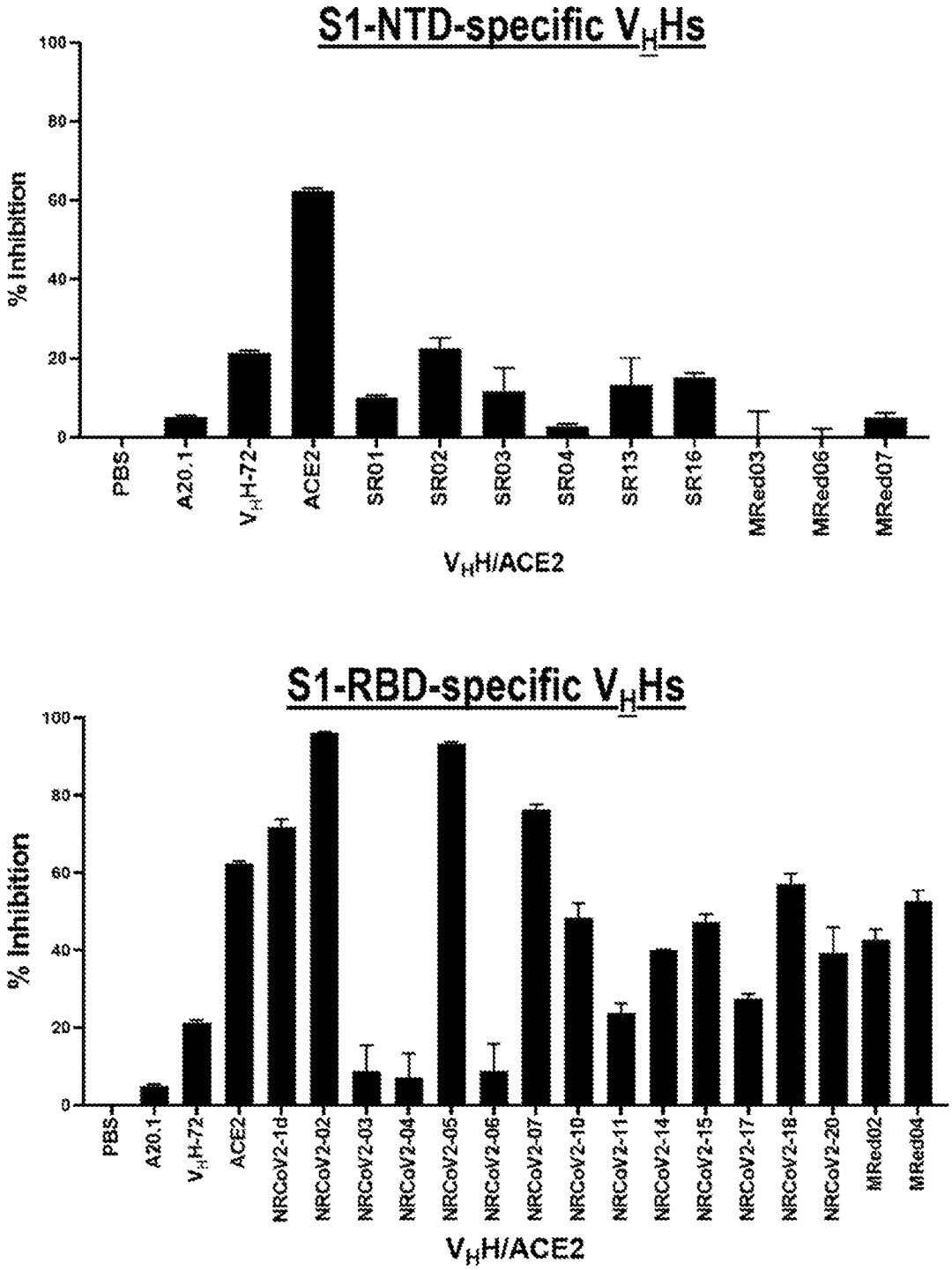
S1-NTD-specific VHHs
% Inhibition
100
80
60
40
20
0
PBS
A20.1
VHH-72
ACE2
SR01
SR02
SR03
SR04
SR13
SR16
MRed03
MRed06
MRed07
VHH/ACE2
S1-RBD-specific VHHs
% Inhibition
100
80
60
40
20
0
PBS
A20.1
VHH-72
ACE2
NRCoV2-1d
NRCoV2-02
NRCoV2-03
NRCoV2-04
NRCoV2-05
NRCoV2-06
NRCoV2-07
NRCoV2-10
NRCoV2-11
NRCoV2-14
NRCoV2-15
NRCoV2-17
NRCoV2-18
NRCoV2-20
MRed02
MRed04
VHH/ACE2

FIG. 12A

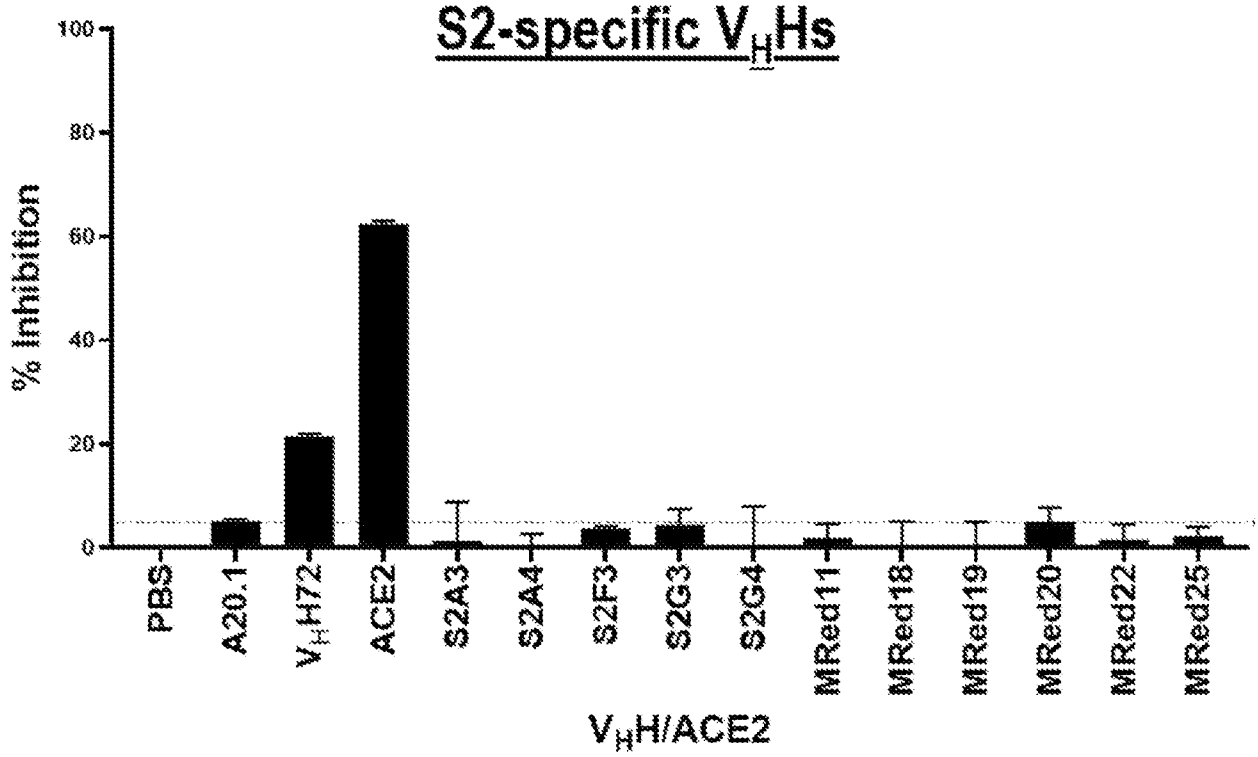
S2-specific VHHs
% Inhibition
100
80
60
40
20
0
PBS
A20.1
VHH72
ACE2
S2A3
S2A4
S2F3
S2G3
S2G4
MRed11
MRed18
MRed19
MRed20
MRed22
MRed25
VHH/ACE2

FIG. 12A (cont.)

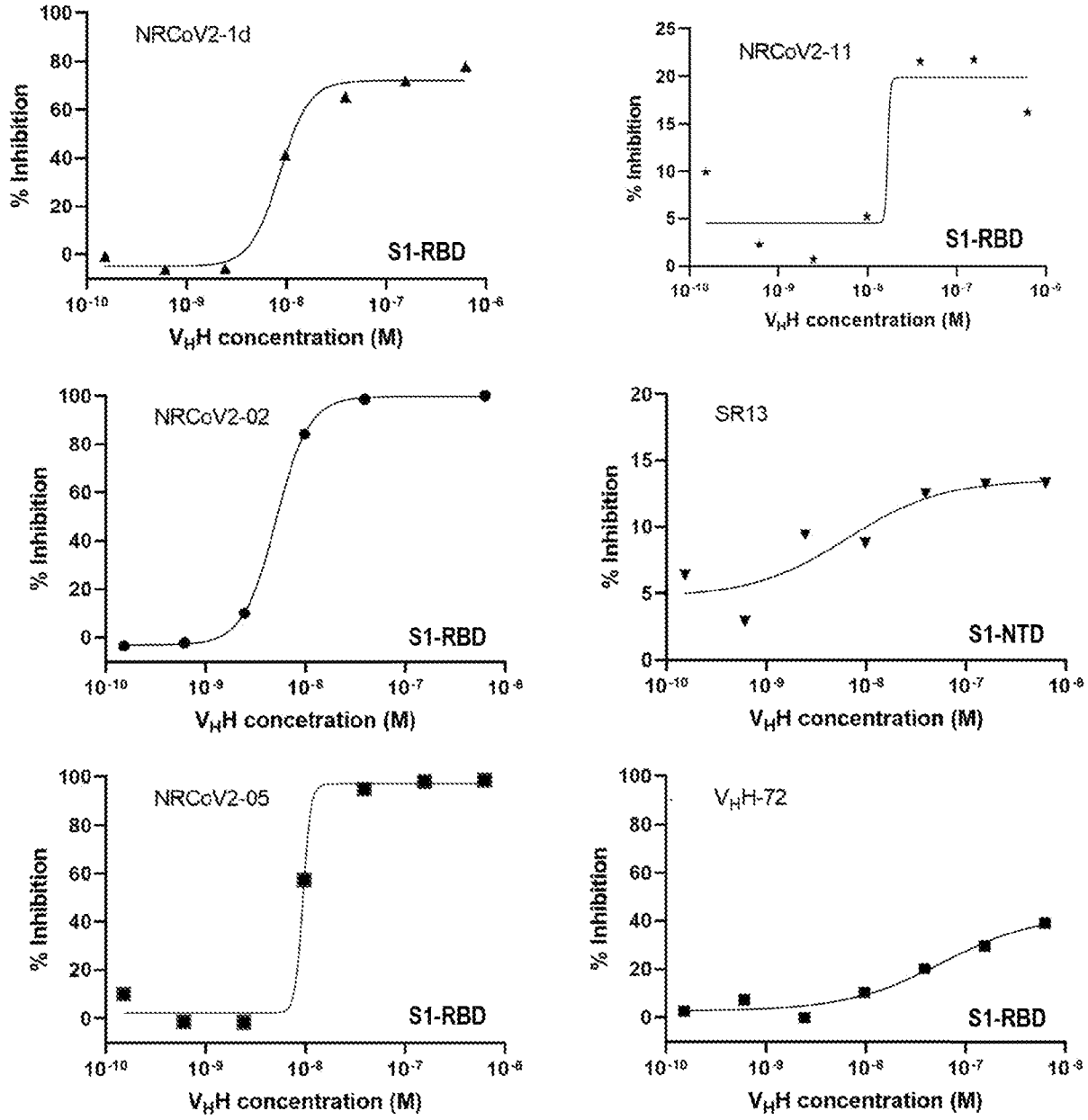
NRCoV2-1d
% Inhibition
S1-RBD
VHH concentration (M)
NRCoV2-11
% Inhibition
S1-RBD
VHH concentration (M)
NRCoV2-02
% Inhibition
S1-RBD
VHH concetration (M)
SR13
% Inhibition
S1-NTD
VHH concentration (M)
NRCoV2-05
% Inhibition
S1-RBD
VHH concentration (M)
VHH-72
% Inhibition
S1-RBD
VHH concentration (M)

FIG. 12B

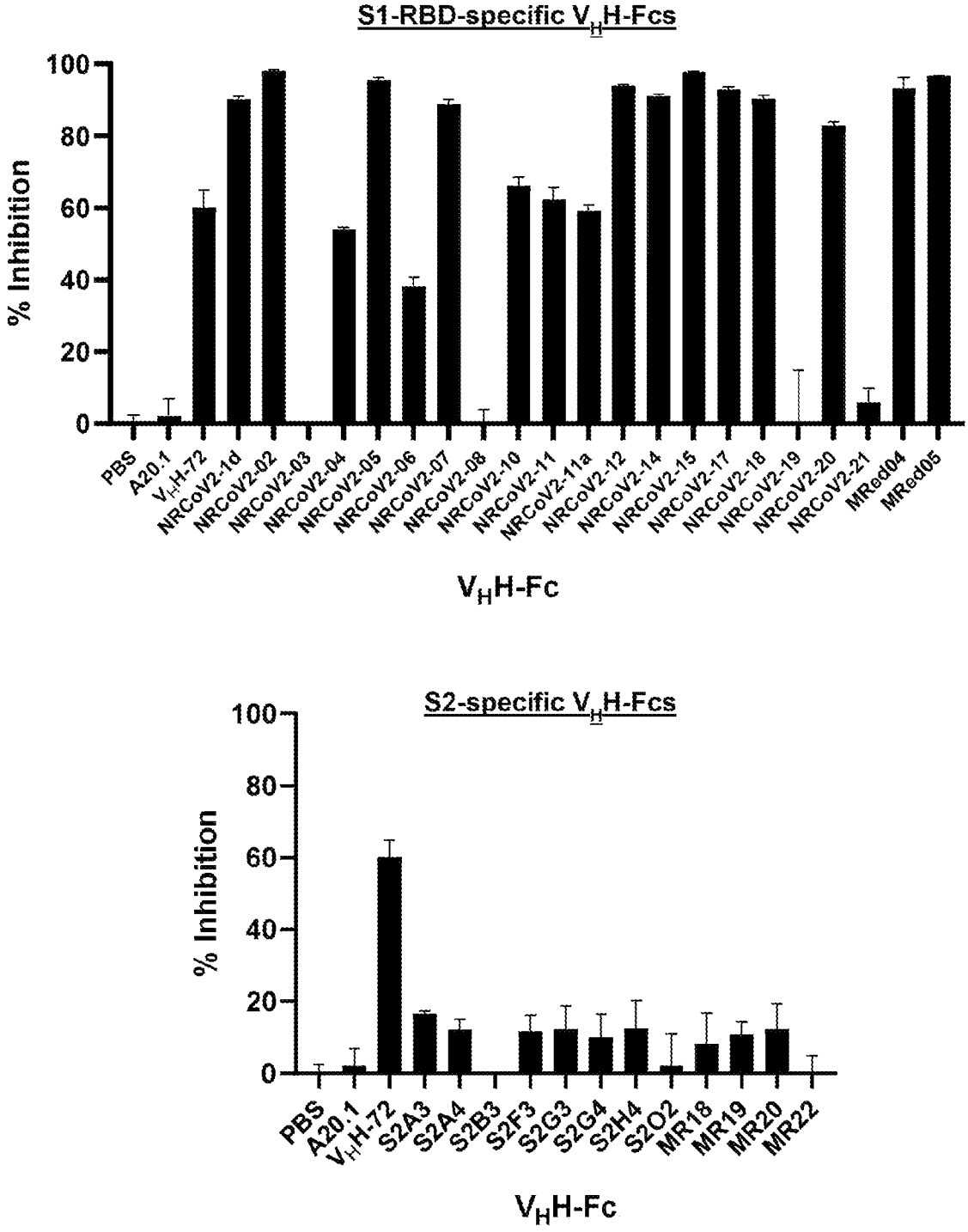
S1-RBD-specific VHH-Fcs
% Inhibition
100
80
60
40
20
0
PBS
A20.1
VHH-72
NRCoV2-1d
NRCoV2-02
NRCoV2-03
NRCoV2-04
NRCoV2-05
NRCoV2-06
NRCoV2-07
NRCoV2-08
NRCoV2-10
NRCoV2-11
NRCoV2-11a
NRCoV2-12
NRCoV2-14
NRCoV2-15
NRCoV2-17
NRCoV2-18
NRCoV2-19
NRCoV2-20
NRCoV2-21
MRed04
MRed05
VHH-Fc
S2-specific VHH-Fcs
% Inhibition
100
80
60
40
20
0
PBS
A20.1
VHH-72
S2A3
S2A4
S2B3
S2F3
S2G3
S2G4
S2H4
S2O2
MR18
MR19
MR20
MR22
VHH-Fc

FIG. 13A

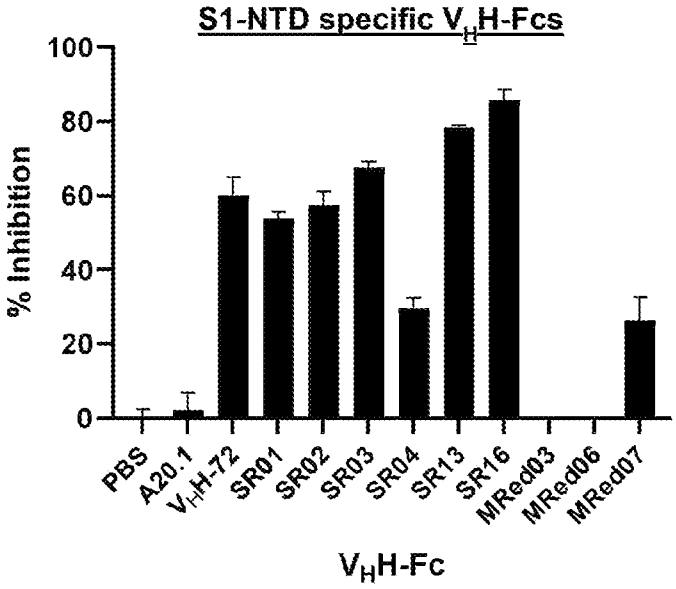
S1-NTD specific VHH-Fcs
% Inhibition
100
80
60
40
20
0
PBS
A20.1
VHH-72
SR01
SR02
SR03
SR04
SR13
SR16
MRed03
MRed06
MRed07
VHH-Fc

FIG. 13A (cont.)

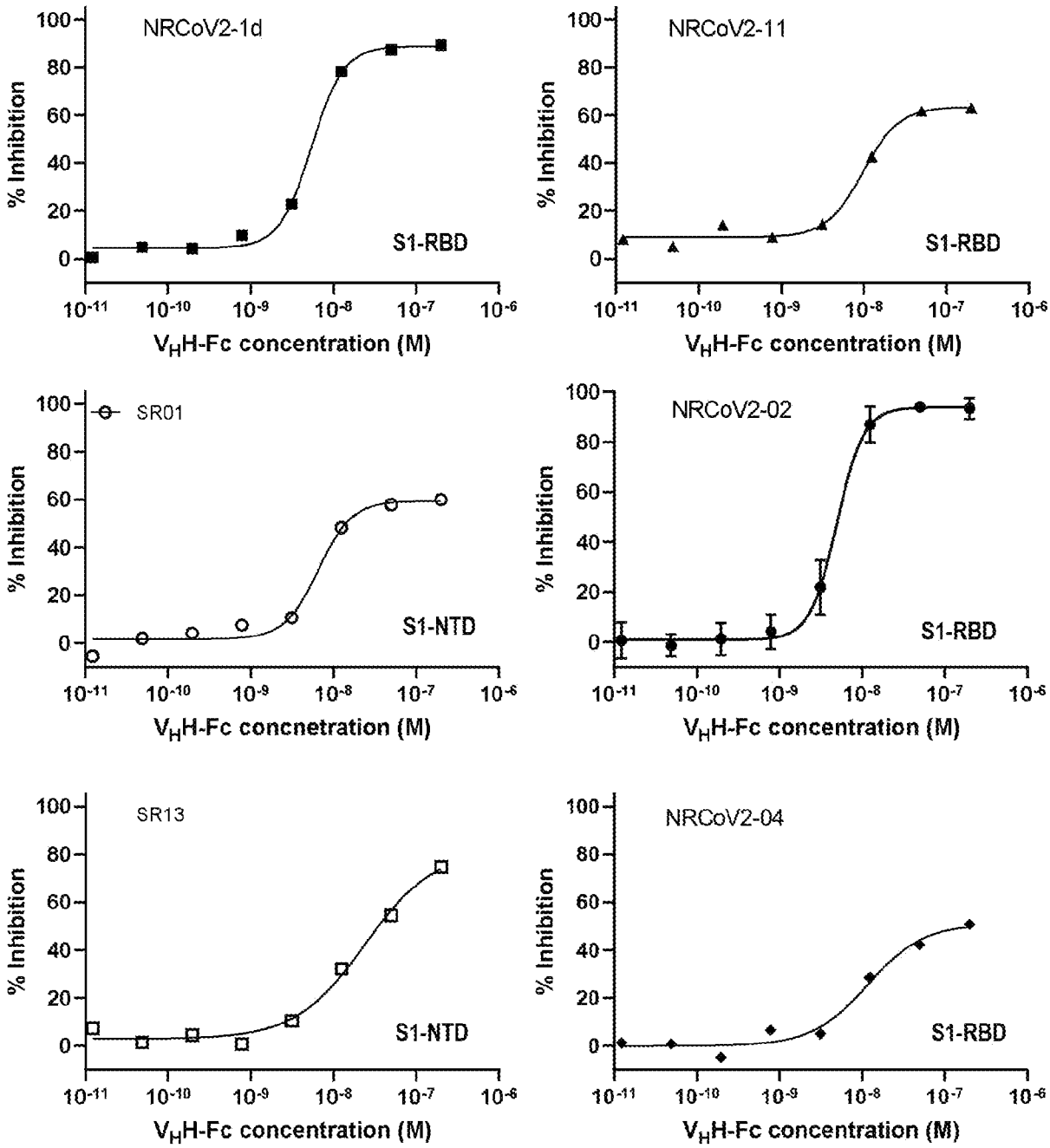
NRCoV2-1d
S1-RBD
% Inhibition
VHH-Fc concentration (M)
NRCoV2-11
S1-RBD
% Inhibition
VHH-Fc concentration (M)
SR01
S1-NTD
% Inhibition
VHH-Fc concnetration (M)
NRCoV2-02
S1-RBD
% Inhibition
VHH-Fc concentration (M)
SR13
S1-NTD
% Inhibition
VHH-Fc concentration (M)
NRCoV2-04
S1-RBD
% Inhibition
VHH-Fc concentration (M)

FIG. 13B

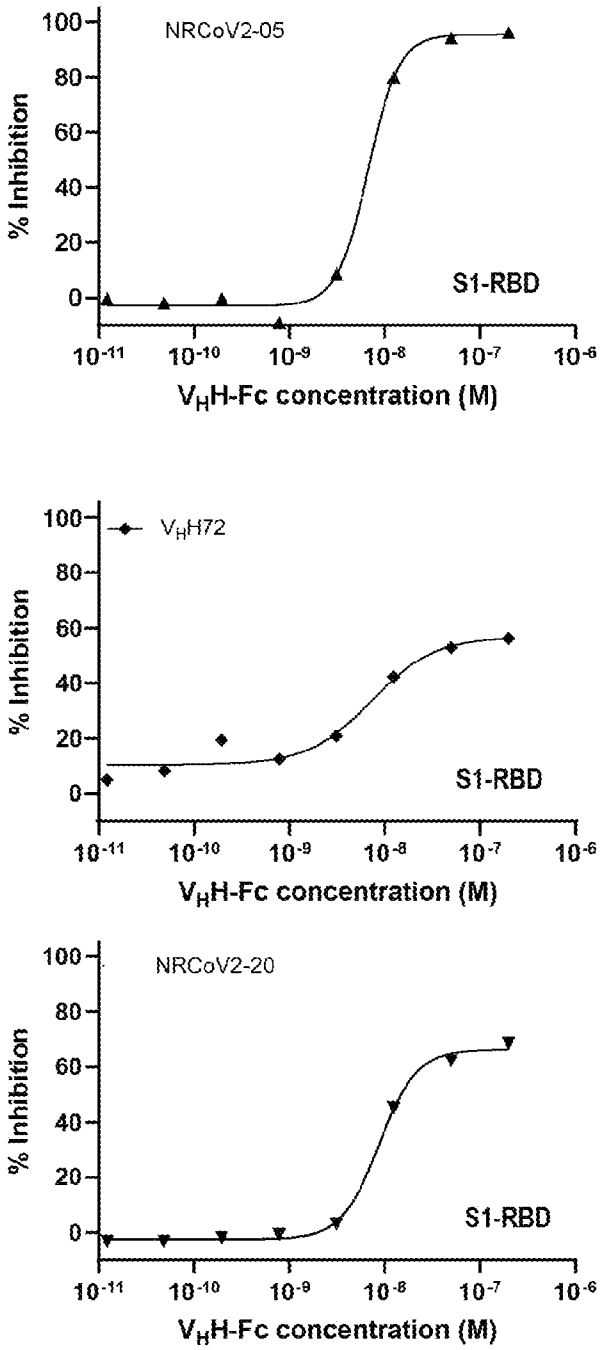
NRCoV2-05
% Inhibition
100
80
60
40
20
0
S1-RBD
10-11
10-10
10-9
10-8
10-7
10-6
VHH-Fc concentration (M)
VHH72
% Inhibition
S1-RBD
VHH-Fc concentration (M)
NRCoV2-20
% Inhibition
S1-RBD
VHH-Fc concentration (M)

FIG. 13B (cont.)

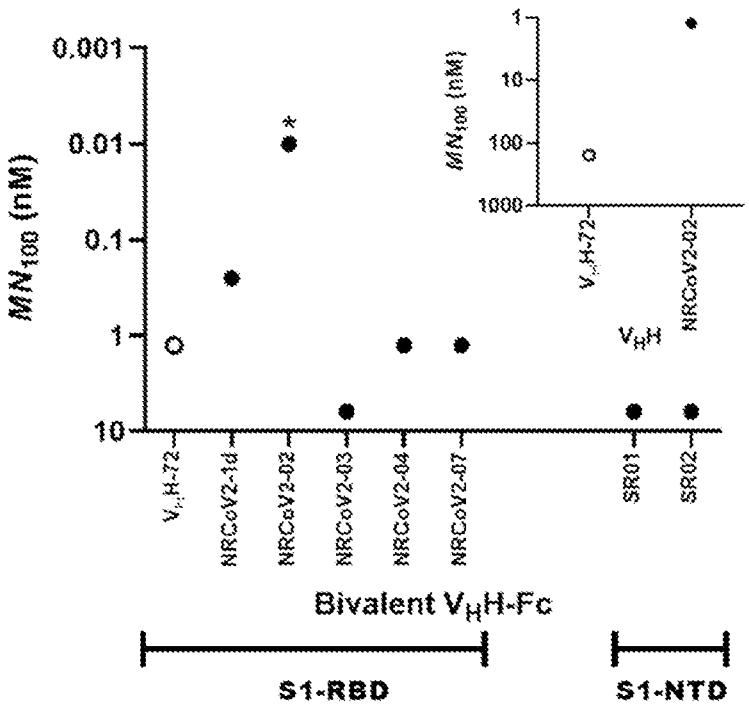


FIG. 14A

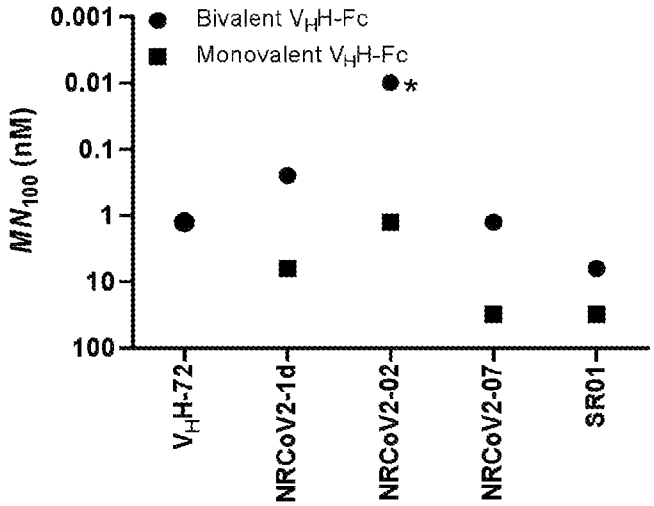


FIG. 14B

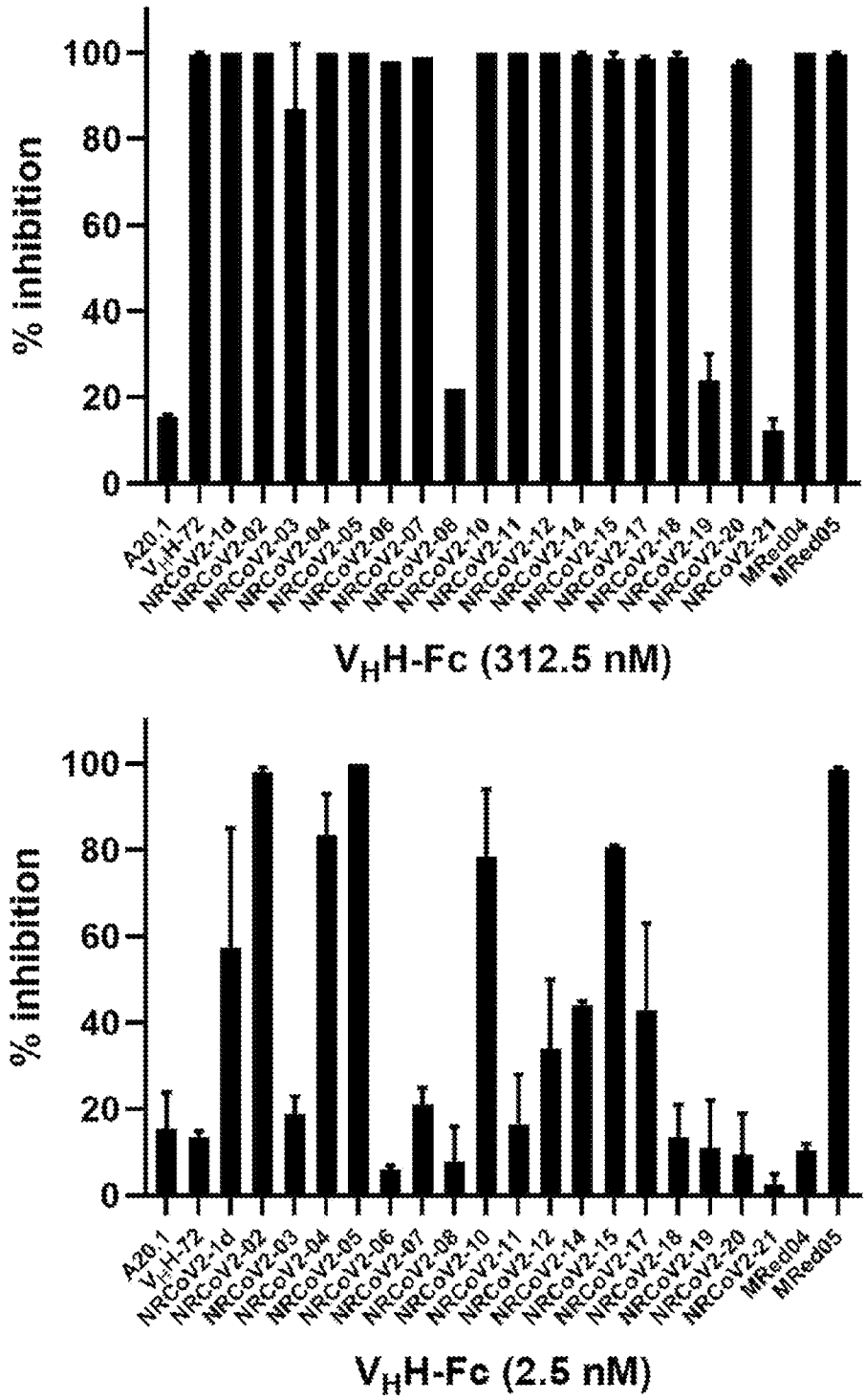
% inhibition
100
80
60
40
20
0
A20.1
VHH-72
NRCoV2-1d
NRCoV2-02
NRCoV2-03
NRCoV2-04
NRCoV2-05
NRCoV2-06
NRCoV2-07
NRCoV2-08
NRCoV2-10
NRCoV2-11
NRCoV2-12
NRCoV2-14
NRCoV2-15
NRCoV2-17
NRCoV2-18
NRCoV2-19
NRCoV2-20
NRCoV2-21
MRed04
MRed05
VHH-Fc (312.5 nM)
% inhibition
100
80
60
40
20
0
A20.1
VHH-72
NRCoV2-1d
NRCoV2-02
NRCoV2-03
NRCoV2-04
NRCoV2-05
NRCoV2-06
NRCoV2-07
NRCoV2-08
NRCoV2-10
NRCoV2-11
NRCoV2-12
NRCoV2-14
NRCoV2-15
NRCoV2-17
NRCoV2-18
NRCoV2-19
NRCoV2-20
NRCoV2-21
MRed04
MRed05
VHH-Fc (2.5 nM)

FIG. 15A

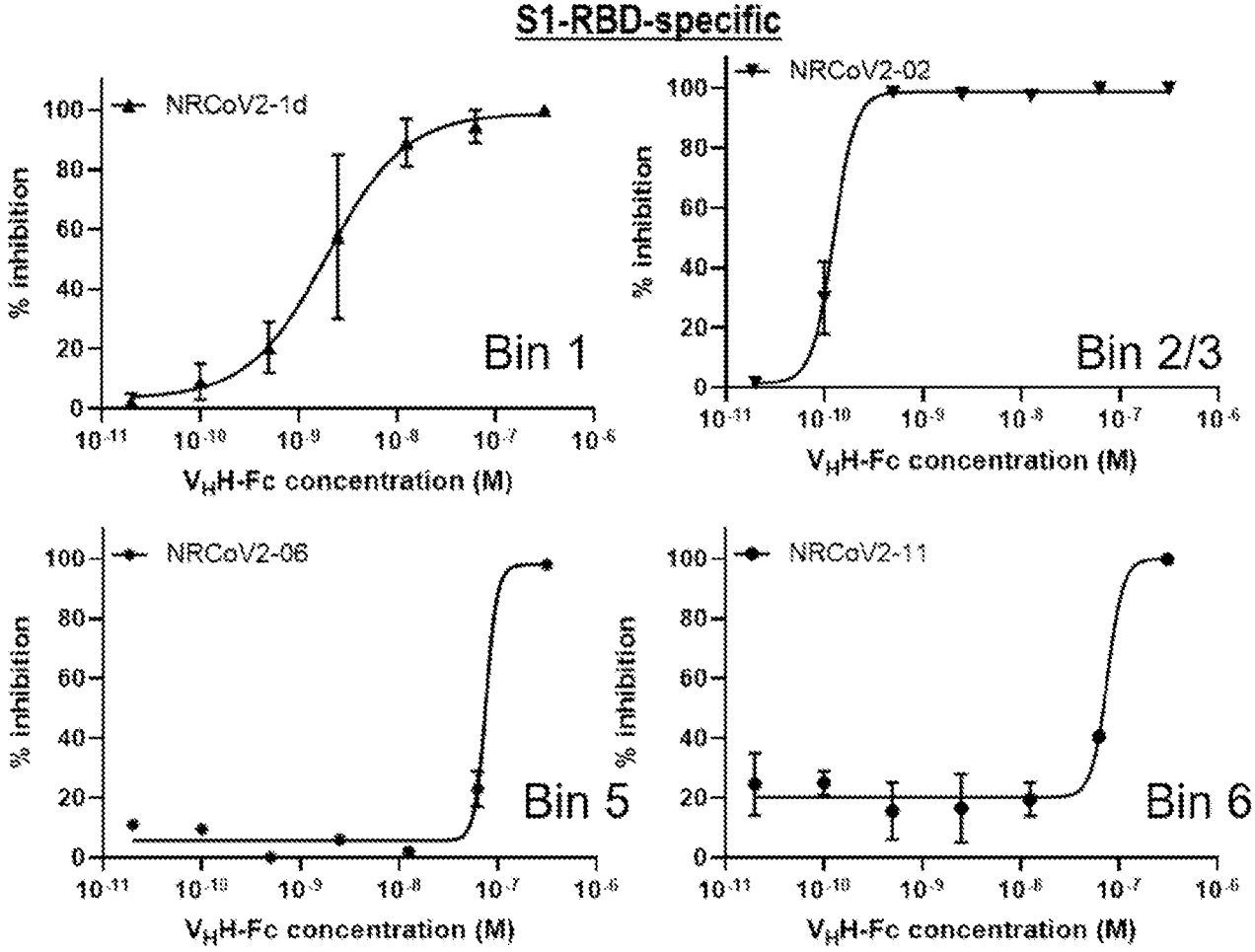
S1-RBD-specific
NRCoV2-1d
% inhibition
Bin 1
VHH-Fc concentration (M)
NRCoV2-02
% inhibition
Bin 2/3
VHH-Fc concentration (M)
NRCoV2-06
% inhibition
Bin 5
VHH-Fc concentration (M)
NRCoV2-11
% inhibition
Bin 6
VHH-Fc concentration (M)

FIG. 15B

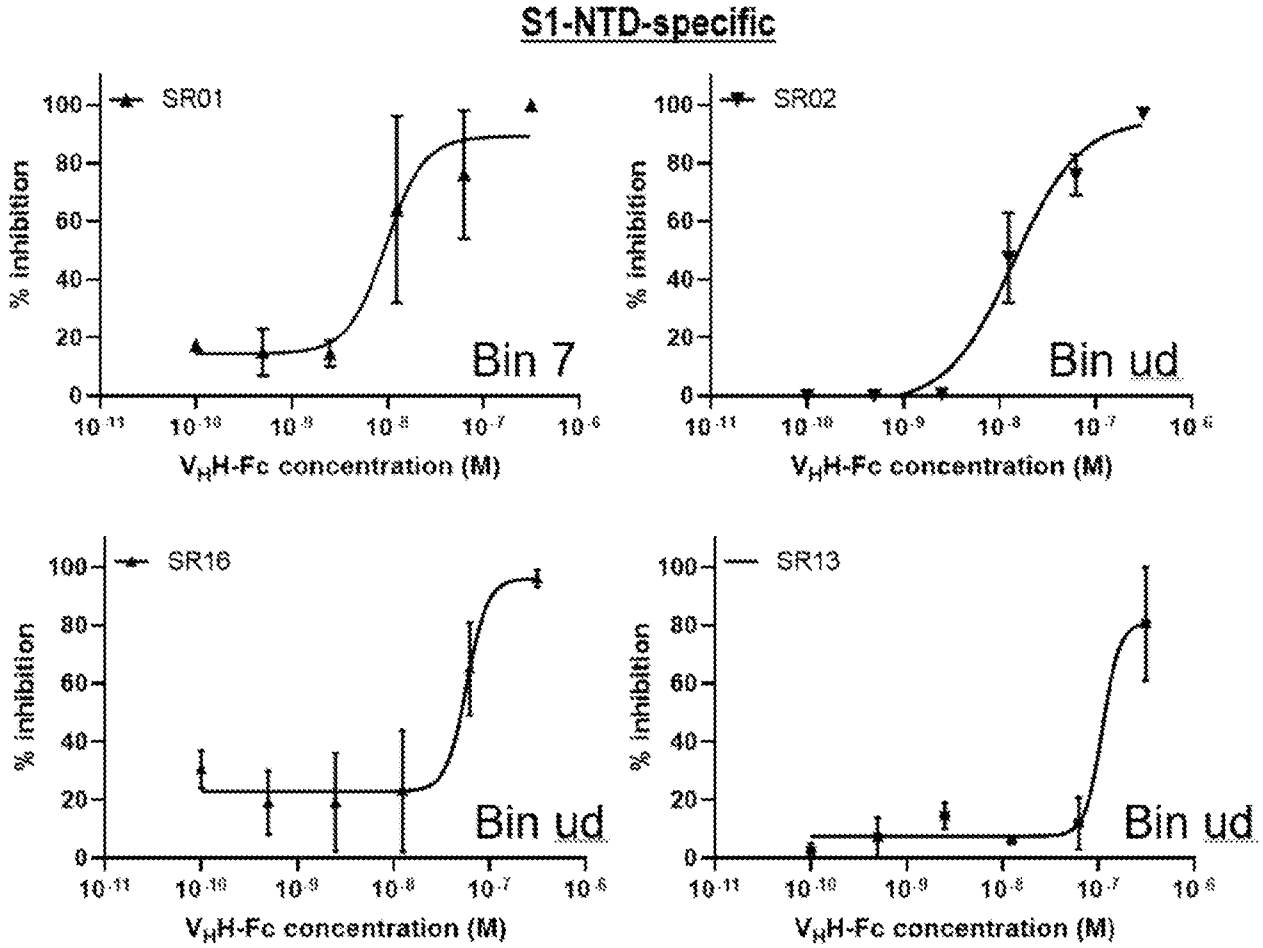
S1-NTD-specific
SR01
Bin 7
SR02
Bin ud
SR16
Bin ud
SR13
Bin ud
% inhibition
VHH-Fc concentration (M)

FIG. 15C

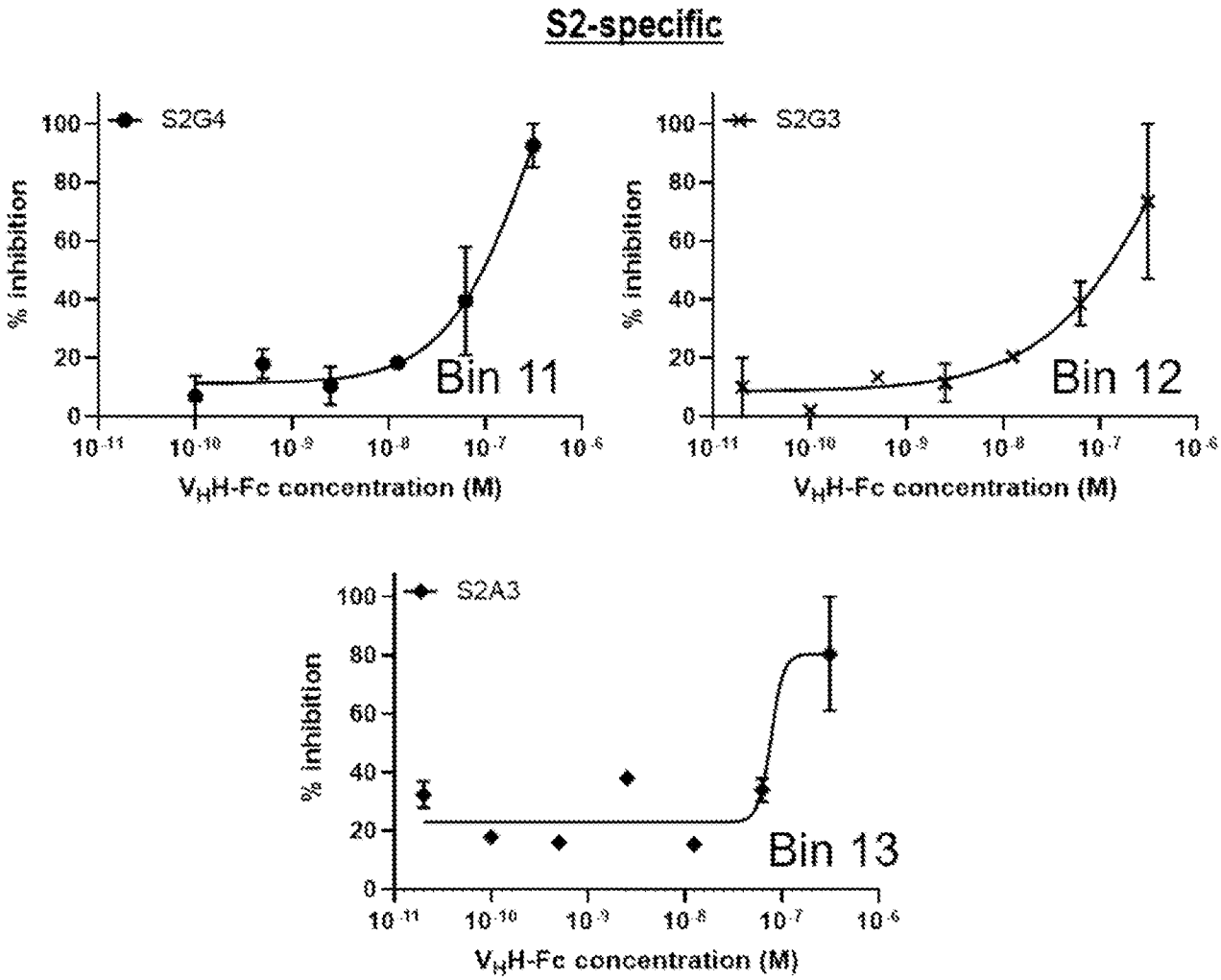
S2-specific
S2G4
% inhibition
Bin 11
$V_HH$-Fc concentration (M)
S2G3
% inhibition
Bin 12
$V_HH$-Fc concentration (M)
S2A3
% inhibition
Bin 13
$V_HH$-Fc concentration (M)

FIG. 15D

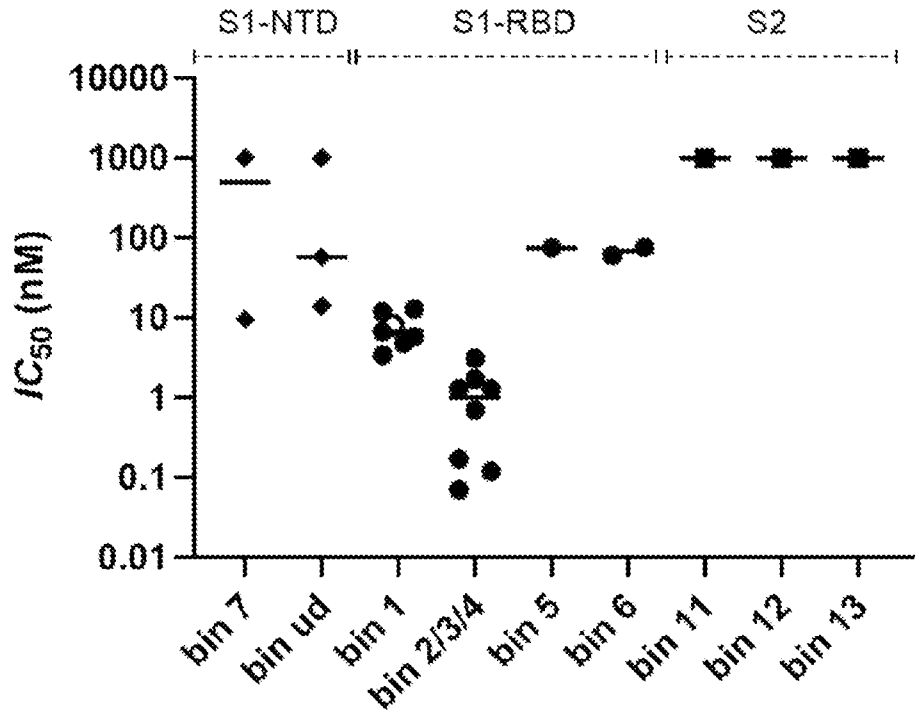
S1-NTD
S1-RBD
S2
10000
1000
100
10
1
0.1
0.01
IC50 (nM)
bin 7
bin ud
bin 1
bin 2/3/4
bin 5
bin 6
bin 11
bin 12
bin 13

FIG. 15E

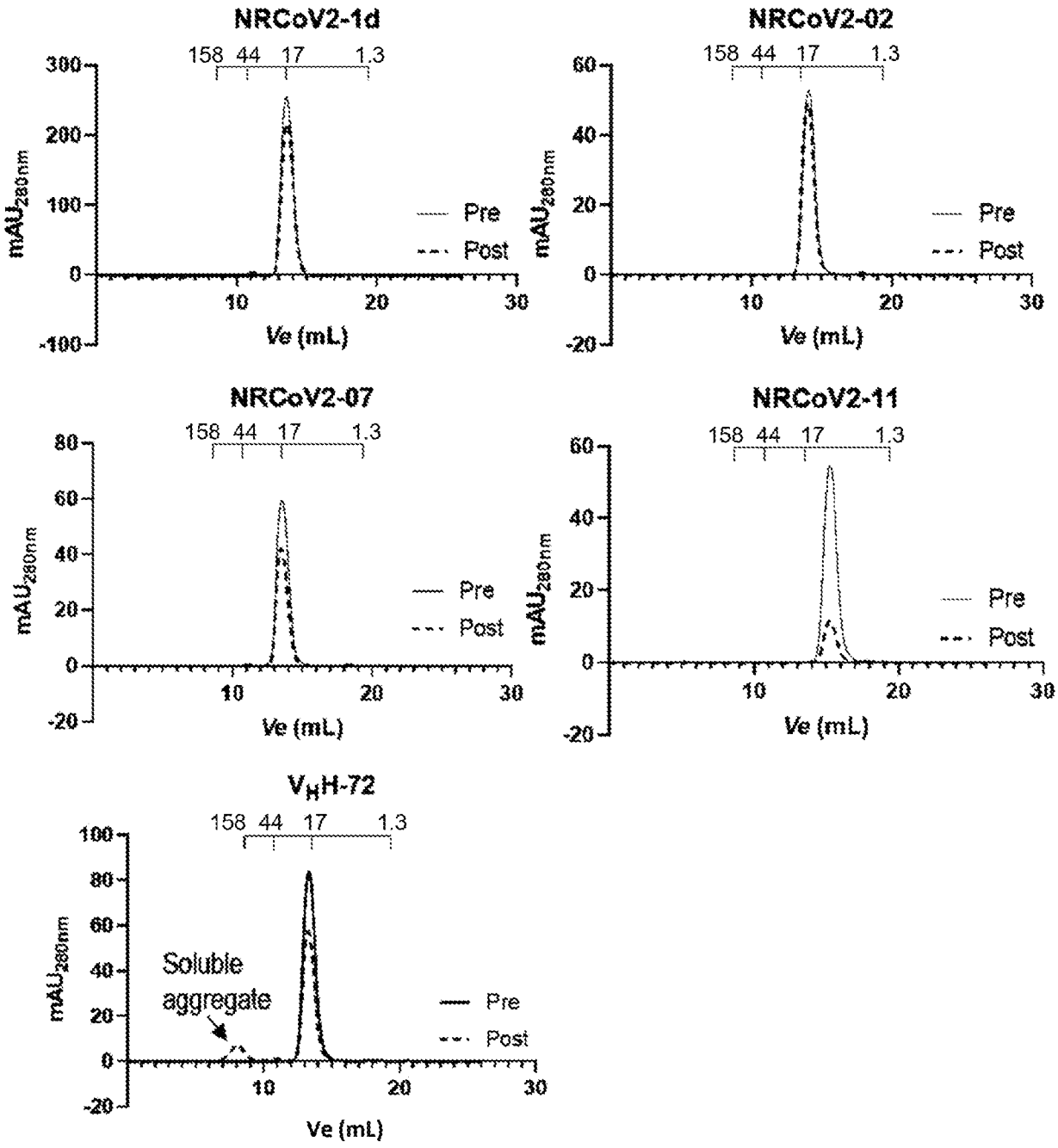
NRCoV2-1d
158 44 17 1.3
mAU280nm
Ve (mL)
Pre
Post
NRCoV2-02
158 44 17 1.3
mAU280nm
Ve (mL)
Pre
Post
NRCoV2-07
158 44 17 1.3
mAU280nm
Ve (mL)
Pre
Post
NRCoV2-11
158 44 17 1.3
mAU280nm
Ve (mL)
Pre
Post
VHH-72
158 44 17 1.3
Soluble aggregate
mAU280nm
Ve (mL)
Pre
Post

FIG. 16A

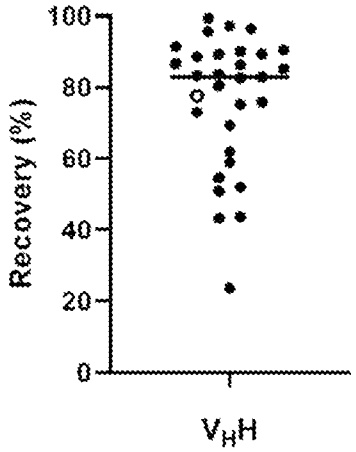


FIG. 16B

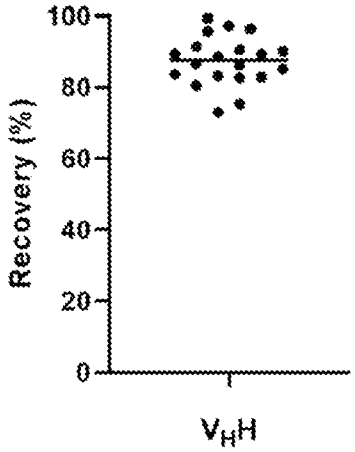


FIG 16C

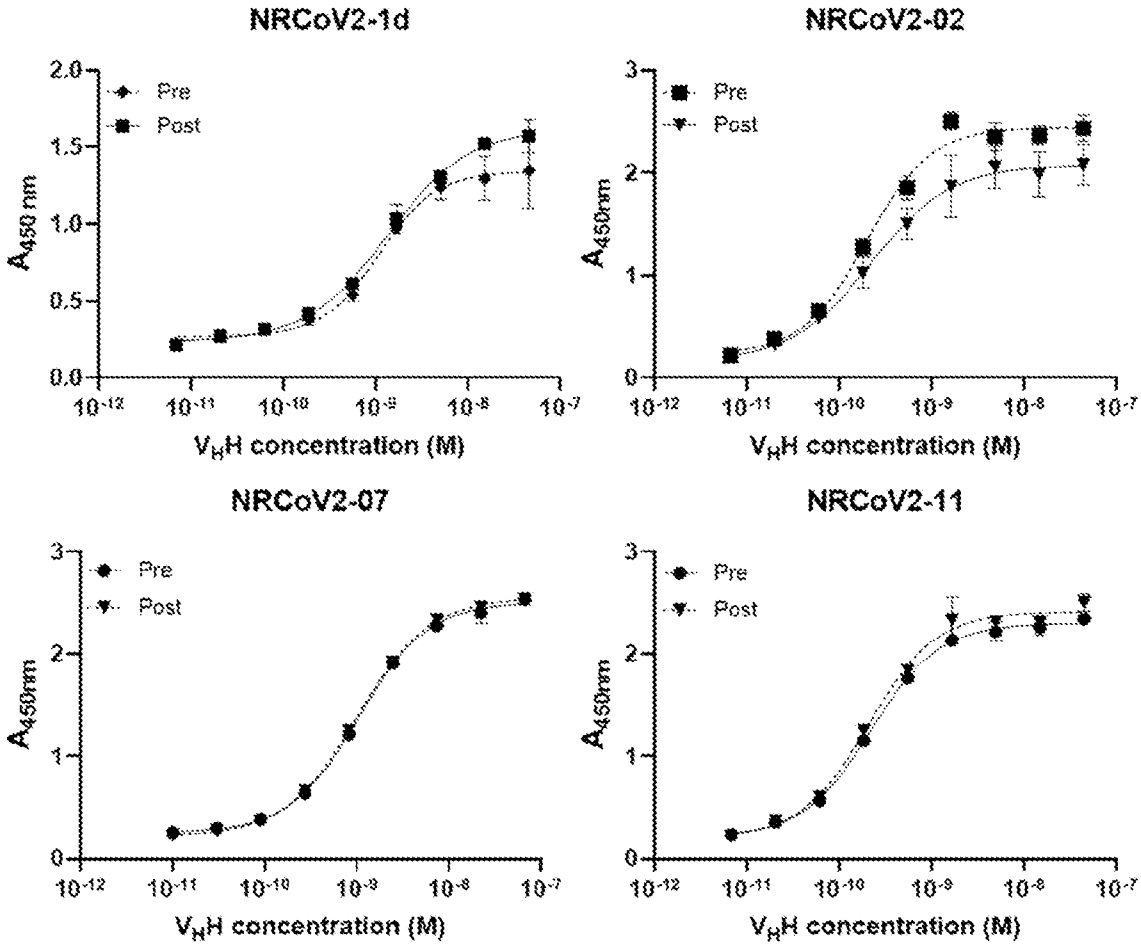


FIG. 16D

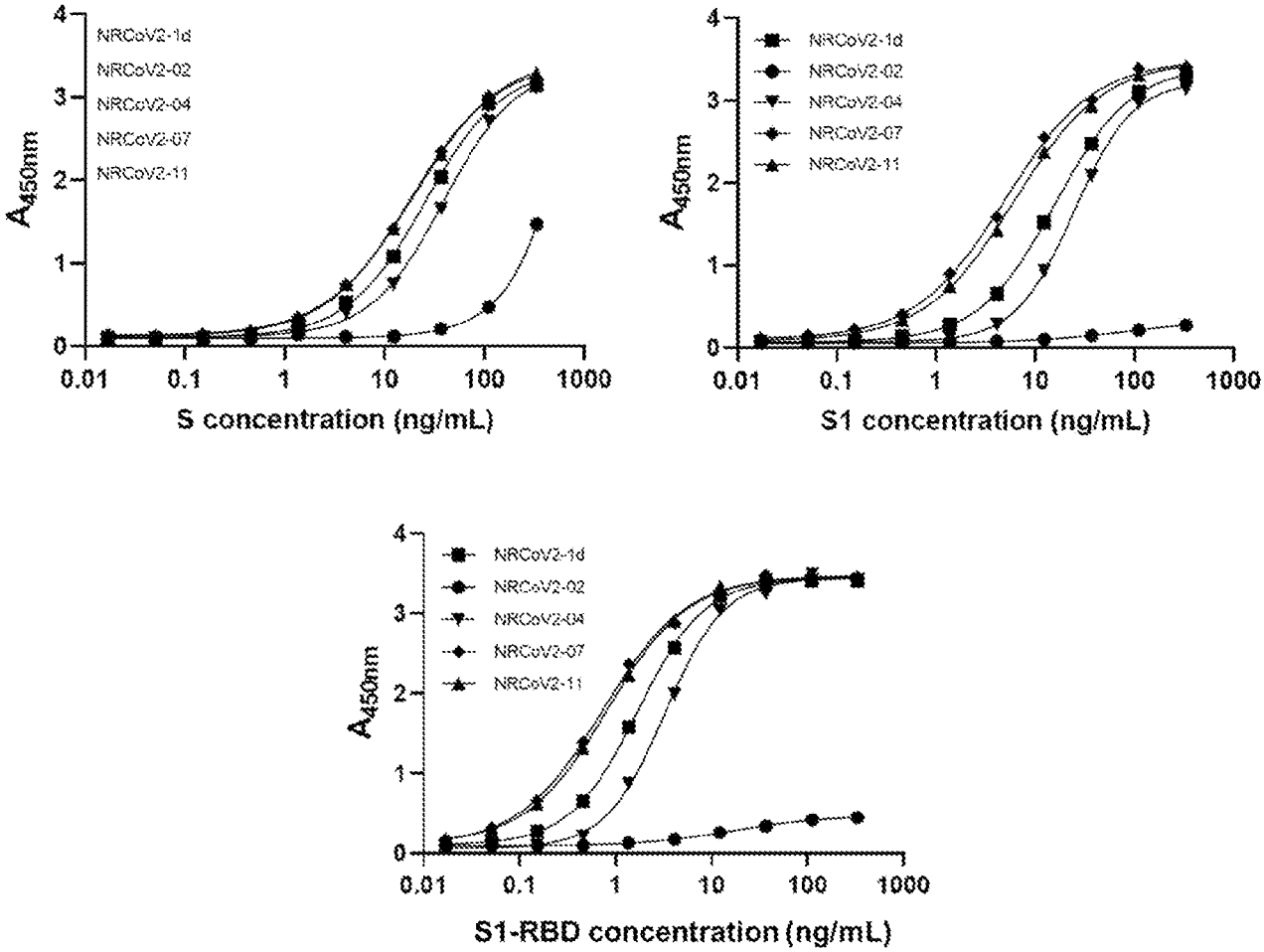
NRCoV2-1d
NRCoV2-02
NRCoV2-04
NRCoV2-07
NRCoV2-11
A450nm
S concentration (ng/mL)
S1 concentration (ng/mL)
S1-RBD concentration (ng/mL)
0.01
0.1
1
10
100
1000
0
1
2
3
4

FIG. 17

```
SEQ_ID_152      EVQLQQSGGGLVQTGGSLRLSCAAAGSPFSQLAMSWYRQI----SGKE----------RAWVA
SEQ_ID_153      EVQLVESGGGLVQAGGSLRLSCVASGITISGYNMAWWRQT---RGKQ---------TERVA
SEQ_ID_171      EVQLVESGGGLVQPGGSLRLSCAASGNIFSINSMGWFRQA---PGKE---------RDVVA
SEQ_ID_173      EVQLVESGGGLVQPGRSLRLSCAASGNSFSISTMGWFRQA---PGKE---------RELVA
SEQ_ID_179      EVQLVESGGGLVQPGGSLRLSCAASTIIFKGQTMGWFRQA----PGNE---------RELVA
SEQ_ID_163      EVQLQQSGGGLVQAGGSLRLSCAASGRPYSNYAMAWYRQA---PGKQHELVAGKQRELVA
SEQ_ID_140      EVQLVSSGGGLVQAGGSLRLSCTASGITFSYYAMGWYRQA---PGQP---------RELVA
SEQ_ID_150      EVQLVSSGGGLVQAGGSLRLSCEASGTTFSHYAVGWYRQA----PGKQ----------REWVA
SEQ_ID_164      QVQLVQSGGGLVQAGGSLRLSCAVSGSPFRSNVMEWYRQA---PGKQ---------RELVA
SEQ_ID_146      QLQLQESGGGLVQPGGSLTLSCAASGNTFSRSNMHWYRQA---PGAQ---------REWVA
SEQ_ID_162      QVQLVQSAGGLVQAGGSLRLSCVVSGTTFSRYHMGWHRQA---PGKQ---------RDFVA
SEQ_ID_176      EVQLVESGGGLVQPGGSLTLSCAASGSIGPFNTMGWYRQA----PGNQ---------REPAA
SEQ_ID_161      EVQLVESGGGLVTTGGSLRLSCATSGSRFGSKHMAWYRQA---PGKQ---------RDLVA
SEQ_ID_151      EVQLVSSGGGLVEAGGSLRLSCIASGSTSGRNTMGWFRQA---PGKQ---------REWVA
SEQ_ID_141      AVQLVDSGGGLVQPGGSLRLSCAASGSPFSNVVMAWYRQA----PGKQ----------RERVA
SEQ_ID_159      AVQLVDSGGGLVQAGGSLRLSCAASGSIFSNNHMGWYRQA---PGKQ---------RELVA
SEQ_ID_168      QVQLVQSGGGSVQAGGSLRLSCAASGSTFGIFLMGWRRQA---PGKQ---------RELVA
SEQ_ID_143      EVQLVQSGGGLVQAGESLRLSCAASVSTFSSYAMGWYRQA----PGKQ----------RELVA
SEQ_ID_169      QVQLVQSGGGLVQAGGSLTLSCAPSGSTFSGYATNWYRQA---PGKQ---------RELVA
SEQ_ID_181      EVQLVESGGGLVQPGGSLRLSCAASGSVFASNAMGWYRQA---PGKQ---------RELVA
SEQ_ID_165      QVQLVDSGGGLVQAGGSLRLSCAASASTFGDSAMGYYRQA---PGKQ---------RELVA
SEQ_ID_178      EVQLVESGGGLVQPGGSLRLSCAASTTVFGRNAMGWYRQA----PGKE---------RELVA
SEQ_ID_166      QVQLVQSGGGLVQAGGSLRLSCAASGFTFNLYSIAWFRQA---PGKE---------REGVS
SEQ_ID_160      QVQLVESGGGLVQAGGSLRLSCAASGRTFSSHTVGWYRQA---PGKQ---------RDLVA
SEQ_ID_167      EVQLVQSGGGLVQAGGSLRLSCATSVRILSVPAMGWYRQA---PGKE---------REMVA
SEQ_ID_170      QVQLVQSGGGLVQAGGSLRLSCAASGITVSRIGMGWYRQA----PGKQ----------RDMVA
SEQ_ID_149      EVQLQQSGGGLVQAGGSLRLSCAASGRTFRNYVMGWFRQAPQAPGKD----------HEFVA
SEQ_ID_155      EVQLQQSGGGLVQPGGSLRLSCAASGRTFSNYVVGWFRQAPQAPGKD---------HEFVA
SEQ_ID_180      EVQLVESGGGSVQAGGSLRLSCAASGLSFSSYDMGWFRQA----PGKE----------REFVA
SEQ_ID_182      EVQLVESGGGLVQAGGSLRLSCAASGHTFSRYGMGWFRQA---PGKE---------REFVA
SEQ_ID_147      EVQLVSSGGGLVQPGGSLRLSCAASGSSLDSYSVSWFRQA---PGKE---------REWIS
SEQ_ID_148      EVQLQQSGGGLVQPGGSLRLSCAASGFTLDSYNIAWFRQA----PGKE----------REWIS
SEQ_ID_177      EVQLVESGGGLVQAGGSLRLSCAASGFTFSSYAMSWHRQA---PGKG---------LEWVS
SEQ_ID_139      EVQLVESGGGLVQAGGSLRLSCAASGFTFSNYAMNWVRQA---PGKG----------LEWVS
SEQ_ID_142      EVKLVQSGGGLVQPGGSLRLSCAASGFIFSNYAMNWVRQA---PGKG---------LEWVS
SEQ_ID_154      EVQLLESGGGLVLPGGSLRLSCAVSGLTLNSYAIGWFRQA----PGKE----------REGLS
SEQ_ID_144      QVQLVQSGGGLVQPGGSLRLSCAASGVTLDYYAIGWFRQA---PGKE----------REAVS
SEQ_ID_145      EVQLQQSGGGLVQPGGSLRLSCAASGFTLDDYAIGWFRQS---PGKE---------REWVT
SEQ_ID_158      EVQLVDSGGGLVQAGGSLRLSCTASEFTLNYYSIGWFRQS----PGKE----------REGVS
SEQ_ID_156      EVQLVESGGGLVQPGGSLRLSCATSGFTLDYYAIGWFRQA---PGKE---------REWVS
SEQ_ID_137      EVQLVESGGGSVQPGGSLRLSCAASGSILDYYAVGWFRQA---PGKE----------REWVS
SEQ_ID_136      EVKLVQSGGGSVQPGGSLRLSCAASGSTLDYYAIGWFRQA---PGKE---------REWVS
SEQ_ID_138      EVQLVESGGGSVQPGGSLRLSCAASGSTLDYYAIGWFRQA---PGKE---------REWVS
SEQ_ID_157      EVQLVQSGGGSVQAGGSLRLSCVASGFTFDNYAIGWFRQA---PGKE----------REGVS
SEQ_ID_172      EVQLVESGGGLVQPGGSLRLSCAAIGFTLDYYAIGWFRQA---PGKE---------REGVS
SEQ_ID_174      EVQLVESGGGLVQPGGSLRLSCAASGFTLDYYAIGWFRQA----PGKE----------REGVS
SEQ_ID_175      EVQLVESGGGLVQAGGSLRLSCAASGFTLAYYAIGWFRQA---PGKE---------REGVS
                 ::* .*.** *  * ** ***           : **     *             :
```

FIG. 18

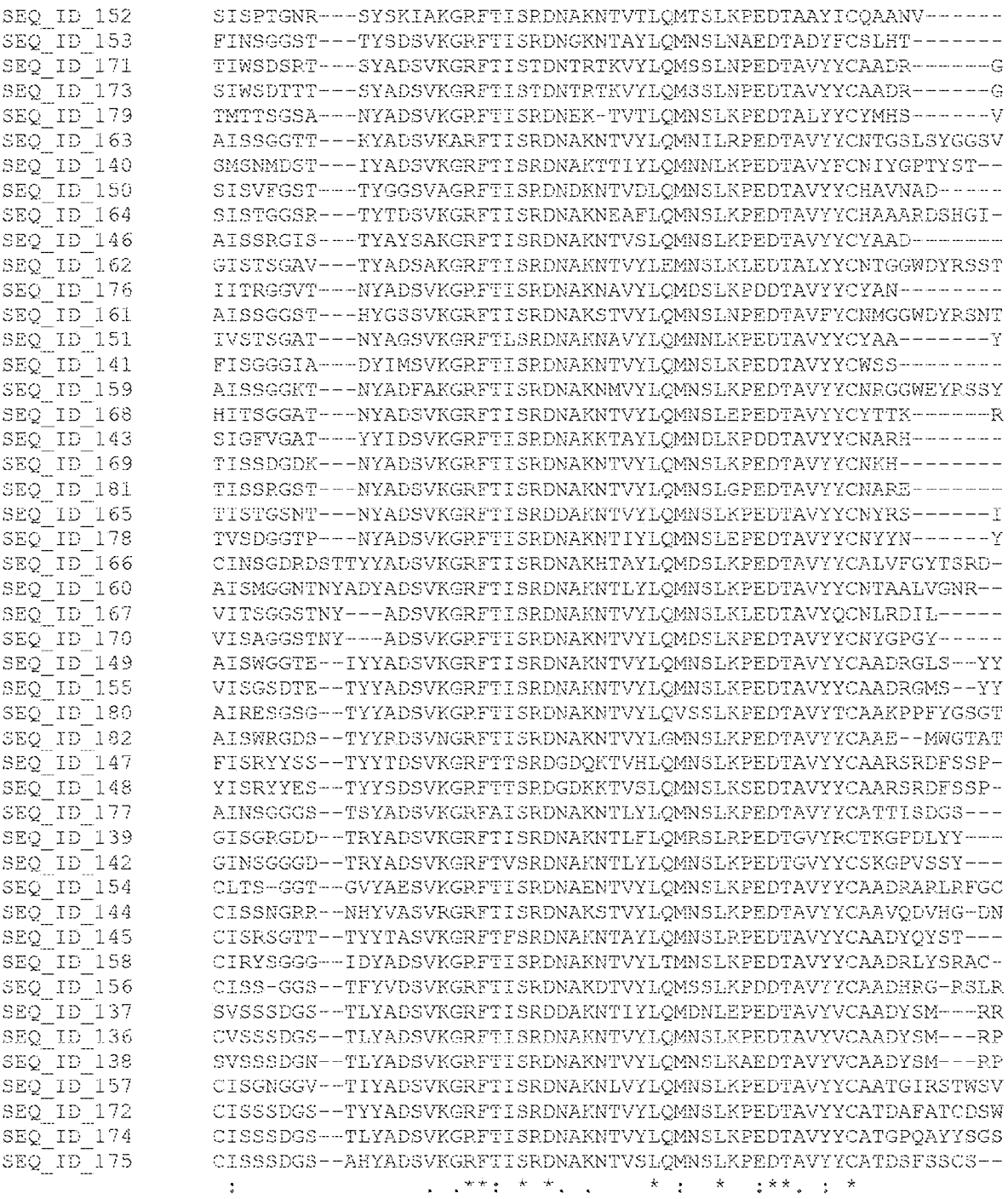
SEQ_ID_152 SISPTGNR---SYSKIAKGRFTISRDNAKNTVTLQMTSLKPEDTAAYICQAANV------
SEQ_ID_153 FINSGGST---TYSDSVKGRFTISRDNGKNTAYLQMNSLNAEDTADYFCSLHT-------
SEQ_ID_171 TIWSDSRT---SYADSVKGRFTISTDNTRTKVYLQMSSLNPEDTAVYYCAADR-------G
SEQ_ID_173 SIWSDTTT---SYADSVKGRFTISTDNTRTKVYLQMSSLNPEDTAVYYCAADR------G
SEQ_ID_179 TMTTSGSA---NYADSVKGRFTISRDNEK-TVTLQMNSLKPEDTALYYCYMHS------V
SEQ_ID_163 AISSGGTT---KYADSVKARFTISRDNAKNTVYLQMNILRPEDTAVYYCNTGSLSYGGSV
SEQ_ID_140 SMSNMDST---IYADSVKGRFTISRDNAKTTIYLQMNNLKPEDTAVYFCNIYGPTYST--
SEQ_ID_150 SISVFGST---TYGGSVAGRFTISRDNDKNTVDLQMNSLKPEDTAVYYCHAVNAD------
SEQ_ID_164 SISTGGSR---TYTDSVKGRFTISRDNAKNEAFLQMNSLKPEDTAVYYCHAAARDSHGI-
SEQ_ID_146 AISSRGIS---TYAYSAKGRFTISRDNAKNTVSLQMNSLKPEDTAVYYCYAAD--------
SEQ_ID_162 GISTSGAV---TYADSAKGRFTISRDNAKNTVYLEMNSLKLEDTALYYCNTGGWDYRSST
SEQ_ID_176 IITRGGVT---NYADSVKGRFTISRDNAKNAVYLQMDSLKPDDTAVYYCYAN--------
SEQ_ID_161 AISSGGST---HYGSSVKGRFTISRDNAKSTVYLQMNSLNPEDTAVFYCNMGGWDYRSNT
SEQ_ID_151 IVSTSGAT---NYAGSVKGRFTLSRDNAKNAVYLQMNNLKPEDTAVYYCYAA-------Y
SEQ_ID_141 FISGGGIA---DYIMSVKGRFTISRDNAKNTVYLQMNSLKPEDTAVYYCWSS---------
SEQ_ID_159 AISSGGKT---NYADFAKGRFTISRDNAKNMVYLQMNSLKPEDTAVYYCNRGGWEYRSSY
SEQ_ID_168 HITSGGAT---NYADSVKGRFTISRDNAKNTVYLQMNSLEPEDTAVYYCYTTK-------R
SEQ_ID_143 SIGFVGAT---YYIDSVKGRFTISRDNAKKTAYLQMNDLKPDDTAVYYCNARH--------
SEQ_ID_169 TISSDGDK---NYADSVKGRFTISRDNAKNTVYLQMNSLKPEDTAVYYCNKH--------
SEQ_ID_181 TISSRGST---NYADSVKGRFTISRDNAKNTVYLQMNSLGPEDTAVYYCNARE-------
SEQ_ID_165 TISTGSNT---NYADSVKGRFTISRDDAKNTVYLQMNSLKPEDTAVYYCNYRS------I
SEQ_ID_178 TVSDGGTP---NYADSVKGRFTISRDNAKNTIYLQMNSLEPEDTAVYYCNYYN------Y
SEQ_ID_166 CINSGDRDSTTYYADSVKGRFTISRDNAKHTAYLQMDSLKPEDTAVYYCALVFGYTSRD-
SEQ_ID_160 AISMGGNTNYADYADSVKGRFTISRDNAKNTLYLQMNSLKPEDTAVYYCNTAALVGNR--
SEQ_ID_167 VITSGGSTNY---ADSVKGRFTISRDNAKNTVYLQMNSLKLEDTAVYQCNLRDIL-----
SEQ_ID_170 VISAGGSTNY---ADSVKGRFTISRDNAKNTVYLQMDSLKPEDTAVYYCNYGPGY------
SEQ_ID_149 AISWGGTE--IYYADSVKGRFTISRDNAKNTVYLQMNSLKPEDTAVYYCAADRGLS--YY
SEQ_ID_155 VISGSDTE--TYYADSVKGRFTISRDNAKNTVYLQMNSLKPEDTAVYYCAADRGMS--YY
SEQ_ID_180 AIRESGSG--TYYADSVKGRFTISRDNAKNTVYLQVSSLKPEDTAVYTCAAKPPFYGSGT
SEQ_ID_182 AISWRGDS--TYYRDSVNGRFTISRDNAKNTVYLQMNSLKPEDTAVYYCAAE--MWGTAT
SEQ_ID_147 FISRYYSS--TYYTDSVKGRFTTSRDGDQKTVHLQMNSLKPEDTAVYYCAARSRDFSSP-
SEQ_ID_148 YISRYYES--TYYSDSVKGRFTTSRDGDKKTVSLQMNSLKSEDTAVYYCAARSRDFSSP-
SEQ_ID_177 AINSGGGS--TSYADSVKGRFAISRDNAKNTLYLQMNSLKPEDTAVYYCATTISDGS---
SEQ_ID_139 GISGRGDD--TRYADSVKGRFTISRDNAKNTLFLQMRSLRPEDTGVYRCTKGPDLYY----
SEQ_ID_142 GINSGGGD--TRYADSVKGRFTVSRDNAKNTLYLQMNSLKPEDTGVYYCSKGPVSSY---
SEQ_ID_154 CLTS-GGT--GVYAESVKGRFTISRDNAENTVYLQMNSLKPEDTAVYYCAADRARLRFGC
SEQ_ID_144 CISSNGRR--NHYVASVRGRFTISRDNAKSTVYLQMNSLKPEDTAVYYCAAVQDVHG-DN
SEQ_ID_145 CISRSGTT--TYYTASVKGRFTFSRDNAKNTAYLQMNSLRPEDTAVYYCAADYQYST---
SEQ_ID_158 CIRYSGGG--IDYADSVKGRFTISRDNAKNTVYLTMNSLKPEDTAVYYCAADRLYSRAC-
SEQ_ID_156 CISS-GGS--TFYVDSVKGRFTISRDNAKDTVYLQMSSLKPDDTAVYYCAADHRG-RSLR
SEQ_ID_137 SVSSSDGS--TLYADSVKGRFTISRDDAKNTIYLQMDNLEPEDTAVYVCAADYSM---RR
SEQ_ID_136 CVSSSDGS--TLYADSVKGRFTISRDNAKNTVYLQMNSLKPEDTAVYVCAADYSM---RP
SEQ_ID_138 SVSSSDGN--TLYADSVKGRFTISRDNAKNTVYLQMNSLKAEDTAVYVCAADYSM---RP
SEQ_ID_157 CISGNGGV--TIYADSVKGRFTISRDNAKNLVYLQMNSLKPEDTAVYYCAATGIRSTWSV
SEQ_ID_172 CISSSDGS--TYYADSVKGRFTISRDNAKNTVYLQMNSLKPEDTAVYYCATDAFATCDSW
SEQ_ID_174 CISSSDGS--TLYADSVKGRFTISRDNAKNTVYLQMNSLKPEDTAVYYCATGPQAYYSGS
SEQ_ID_175 CISSSDGS--AHYADSVKGRFTISRDNAKNTVSLQMNSLKPEDTAVYYCATDSFSSCS--

FIG. 18 (cont.)

```
SEQ_ID_152      --------NGGDYWGQGTQVTVSS
SEQ_ID_153      ---------SHDYWGQGTQVTVSS
SEQ_ID_171      FV---VRGQYDYWGQGTQVTVSS
SEQ_ID_173      FV---VRGQYDYWGQGTQVTVSS
SEQ_ID_179      YY---G---IDYWGKGTQVTVSS
SEQ_ID_163      YY---PS--YDNWGQGTQVTVSS
SEQ_ID_140      -------RRNEYWGQGTQVTVSS
SEQ_ID_150      -------IGGDYWGQGTQVTVSS
SEQ_ID_164      ..............YLLDTWGQGTQVTVSS
SEQ_ID_146      -------DLGDYWGQGTQVTVSS
SEQ_ID_162      FI---M---GLNWGQGTQVTVSS
SEQ_ID_176      -----YGWAIPYWGNGTQVTVSS
SEQ_ID_161      YI---PGSRSDYWGQGTQVTVSS
SEQ_ID_151      GG---G---GDYWGQGTQVTVSS
SEQ_ID_141      -----Y---ESTWGQGTQVTVSS
SEQ_ID_159      YI---M---GPHWGQGTQVTVSS
SEQ_ID_168      DD---A---SVYWGQGTQVTVSS
SEQ_ID_143      YG---G---SEYWGQGTQVTVSS
SEQ_ID_169      WW---T---GDWWGQGTQVTVSS
SEQ_ID_181      FT---G---FDYWGQGTQVTVSS
SEQ_ID_165      YY---G---QNFWGQGTQVTVSS
SEQ_ID_178      YY---G---RNFWGQGTQVTVSS
SEQ_ID_166      -YCL-TPKRGNYWGQGTQVTVSS
SEQ_ID_160      ---L-LPMATITWGQGTQVTVSS
SEQ_ID_167      ---------SQPFWGQGTQVTVSS
SEQ_ID_170      ----------RKAAWGQGTQVTVSS
SEQ_ID_149      ---YTRTTEYNYWGQGTQVTVSS
SEQ_ID_155      ---YTRATEYYYWGQGTQVTVSS
SEQ_ID_180      ---YSTPRAYLYWGQGTQVTVSS
SEQ_ID_182      ---I-VASRYTYWGQGTQVTVSS
SEQ_ID_147      ---FSATDTYTSWGQGTQVTVSS
SEQ_ID_148      ---ISATDKYGSWGQGTQVTVSS
SEQ_ID_177      ------SWSTKSYRGQGTQVTVSS
SEQ_ID_139      -----FGSGYSDRGQGTQVTVSS
SEQ_ID_142      ------YGSGYDYRGQGTQVTVSS
SEQ_ID_154      SLNFRREVAYDYWGQGTQVTVSS
SEQ_ID_144      YYC-TSPNEYNVWGQGTQVTVSS
SEQ_ID_145      -YCLGYDAHYEYWGQGTQVTVSS
SEQ_ID_158      ----PTAGGRNYWGQGTQVTVSS
SEQ_ID_156      FGCSSSTTDYLYWGQGTQVTVSS
SEQ_ID_137      FAVGRWHRDYEYWGQGTQVTVSS
SEQ_ID_136      LWVSRWHRDYEYWGQGTQVTVSS
SEQ_ID_138      FAVGRWHRDYEYWGQGTQVTVSS
SEQ_ID_157      YGCSRLAGPYDYWGQGTQVTVSS
SEQ_ID_172      Y---AQIAQYDFRGQGTQVTVSS
SEQ_ID_174      YYFQCPQAGMDYWGKGTQVTVSS
SEQ_ID_175      ----DYESGMDFWGKGTQVTVSS
                              *:********
```

FIG. 18 (cont.)

```
SEQ_ID_158      EVQLVDSGGGLVQAGGSLRLSCTASEFTLNYYSIGWFRQSPGKEREGVSCIRYSGGGIDY
SEQ_ID_157      EVQLVQSGGGSVQAGGSLRLSCVASGFTFDNYAIGWFRQAPGKEREGVSCISGNGGVTIY
SEQ_ID_172      EVQLVESGGGLVQPGGSLRLSCAAIGFTLDYYAIGWFRQAPGKEREGVSCISSSDGSTYY
SEQ_ID_175      EVQLVESGGGLVQAGGSLRLSCAASGFTLAYYAIGWFRQAPGKEREGVSCISSSDGSAHY
SEQ_ID_176      EVQLVESGGGLVQPGGSLTLSCAASGSIGPFNTMGWYRQAPGNQREPAAIITRG-GVTNY
SEQ_ID_160      QVQLVESGGGLVQAGGSLRLSCAASGRTFSSHTVGWYRQAPGKQRDLVAAISMG-GNTNY
SEQ_ID_161      EVQLVESGGGLVTTGGSLRLSCATSGSRFGSKHMAWYRQAPGKQRDLVAAISSG-GSTHY
SEQ_ID_159      AVQLVDSGGGLVQAGGSLRLSCAASGSIFSNNHMGWYRQAPGKQRELVAAISSG-GKTNY
SEQ_ID_162      QVQLVQSAGGLVQAGGSLRLSCVVSGTTFSRYHMGWHRQAPGKQRDFVAGISTS-GAVTY
                 ****:*.** *  **** ***..         :.*.**:**::*: .: *  . *   *

SEQ_ID_158      ---ADSVKGRFTISRDNAKNTVYLTMNSLKPEDTAVYYCAADRLYSR-----ACPTAGGR
SEQ_ID_157      ---ADSVKGRFTISRDNAKNLVYLQMNSLKPEDTAVYYCAATGIRSTWSVYGCSRLAGPY
SEQ_ID_172      ---ADSVKGRFTISRDNAKNTVYLQMNSLKPEDTAVYYCATDAFATCDSWY---AQIAQY
SEQ_ID_175      ---ADSVKGRFTISRDNAKNTVSLQMNSLKPEDTAVYYCATDSFSSCSDYE---S---GM
SEQ_ID_176      A---DSVKGRFTISRDNAKNAVYLQMDSLKPDDTAVYYCYAN-------------YGWAI
SEQ_ID_160      ADYADSVKGRFTISRDNAKNTLYLQMNSLKPEDTAVYYCNTAALVGN---R---LLPMAT
SEQ_ID_161      G---SSVKGRFTISRDNAKSTVYLQMNSLNPEDTAVFYCNMGGWDYRSNTY---IPGSRS
SEQ_ID_159      A---DFAKGRFTISRDNAKNMVYLQMNSLKPEDTAVYYCNRGGWEYRSSYY---IMGP--
SEQ_ID_162      A---DSAKGRFTISRDNAKNTVYLEMNSLKLEDTALYYCNTGGWDYRSSTF---IMGL--
                    . .************. : * *:**: :***::**

SEQ_ID_158      NYWGQGTQVTVSS
SEQ_ID_157      DYWGQGTQVTVSS
SEQ_ID_172      DFRGQGTQVTVSS
SEQ_ID_175      DFWGKGTQVTVSS
SEQ_ID_176      FYWGNGTQVTVSS
SEQ_ID_160      ITWGQGTQVTVSS
SEQ_ID_161      DYWGQGTQVTVSS
SEQ_ID_159      -HWGQGTQVTVSS
SEQ_ID_162      -NWGQGTQVTVSS
                   *:********
```

FIG. 19

```
SEQ_ID_180      EVQLVESGGGSVQAGGSLRLSCAASGLSFSSYDMGWFRQAPGKE--------REFVAAIR
SEQ_ID_182      EVQLVESGGGLVQAGGSLRLSCAASGHTFSRYGMGWFRQAPGKE--------REFVAAIS
SEQ_ID_166      QVQLVQSGGGLVQAGGSLRLSCAASGFTFNLYSIAWFRQAPGKE--------REGVSCIN
SEQ_ID_177      EVQLVESGGGLVQAGGSLRLSCAASGFTFSSYAMSWHRQAPGKGL--------EWVSAIN
SEQ_ID_179      EVQLVESGGGLVQPGGSLRLSCAASTIIFKGQTMGWFRQAPGNE--------RELVATM-
SEQ_ID_163      EVQLQQSGGGLVQAGGSLRLSCAASGRPYSNYAMAWYRQAPGKQHELVAGKQRELVAAI-
SEQ_ID_164      QVQLVQSGGGLVQAGGSLRLSCAVSGSPFRSNVMEWYRQAPGKQ--------RELVASI-
SEQ_ID_167      EVQLVQSGGGLVQAGGSLRLSCATSVRILSVPAMGWYRQAPGKE--------REMVAVI-
SEQ_ID_170      QVQLVQSGGGLVQAGGSLRLSCAASGITVSRIGMGWYRQAPGKQ--------RDMVAVI-
SEQ_ID_168      QVQLVQSGGGSVQAGGSLRLSCAASGSTFGIFLMGWRRQAPGKQ--------RELVAHI-
SEQ_ID_169      QVQLVQSGGGLVQAGGSLTLSCAPSGSTFSGYATNWYRQAPGKQ--------RELVATI-
SEQ_ID_181      EVQLVESGGGLVQPGGSLRLSCAASGSVFASNAMGWYRQAPGKQ--------RELVATI-
SEQ_ID_165      QVQLVDSGGGLVQAGGSLRLSCAASASTFGDSAMGYYRQAPGKQ--------RELVATI-
SEQ_ID_178      EVQLVESGGGLVQPGGSLRLSCAASTTVFGRNAMGWYRQAPGKE--------RELVATV-
                :*** :**** ** **** **** *          : *****:          : *: :

SEQ_ID_180      ES--GSGTYYADSVKGRFTISRDNAKNTVYLQVSSLKPEDTAVYTCAAKPPFYGSGTYST
SEQ_ID_182      WR--GDSTYYRDSVNGRFTISRDNAKNTVYLGMNSLKPEDTAVYYCAAE--MWGTATI-V
SEQ_ID_166      SGDRDSTTYYADSVKGRFTISRDNAKHTAYLQMDSLKPEDTAVYYCALVFGYTSRDYCLT
SEQ_ID_177      SG--GGSTSYADSVKGRFAISRDNAKNTLYLQMNSLKPEDTAVYYCATTISDG-----SS
SEQ_ID_179      TT--SGSANYADSVKGRFTISRDNEK-TVTLQMNSLKPEDTALYYCYMHSV---------
SEQ_ID_163      SS--GGTTKYADSVKARFTISRDNAKNTVYLQMNILRPEDTAVYYCNTGSLSYGG--SVY
SEQ_ID_164      ST--GGSRTYTDSVKGRFTISRDNAKNEAFLQMNSLKPEDTAVYYCHAAARDSHG-----
SEQ_ID_167      TS--GGSTNYADSVKGRFTISRDNAKNTVYLQMNSLKLEDTAVYQCNLRDI---------
SEQ_ID_170      SA--GGSTNYADSVKGRFTISRDNAKNTVYLQMDSLKPEDTAVYYCNYGPG---------
SEQ_ID_168      TS--GGATNYADSVKGRFTISRDNAKNTVYLQMNSLEPEDTAVYYCYTTKR---------
SEQ_ID_169      SS--DGDKNYADSVKGRFTISRDNAKNTVYLQMNSLKPEDTAVYYCNKH-----------
SEQ_ID_181      SS--RGSTNYADSVKGRFTISRDNAKNTVYLQMNSLGPEDTAVYYCNARE----------
SEQ_ID_165      ST--GSNTNYADSVKGRFTISRDDAKNTVYLQMNSLKPEDTAVYYCNYRSI---------
SEQ_ID_178      SD--GGTPNYADSVKGRFTISRDNAKNTIYLQMNSLEPEDTAVYYCNYYNY---------
                     .   * ***:.**:****: *    * :. *  ****:* *

SEQ_ID_180      PRAYLYWGQGTQVTVSS
SEQ_ID_182      ASRYTYWGQGTQVTVSS
SEQ_ID_166      PKRGNYWGQGTQVTVSS
SEQ_ID_177      WSTKSYRGQGTQVTVSS
SEQ_ID_179      YYGIDYWGKGTQVTVSS
SEQ_ID_163      YPSYDNWGQGTQVTVSS
SEQ_ID_164      IYLLDTWGQGTQVTVSS
SEQ_ID_167      -LSQPFWGQGTQVTVSS
SEQ_ID_170      -YRKAAWGQGTQVTVSS
SEQ_ID_168      DDASVYWGQGTQVTVSS
SEQ_ID_169      WWTGDWWGQGTQVTVSS
SEQ_ID_181      FTGFDYWGQGTQVTVSS
SEQ_ID_165      YYGQNFWGQGTQVTVSS
SEQ_ID_178      YYGRNFWGQGTQVTVSS
                      *:********
```

FIG. 20

```
SEQ_ID_171      EVQLVESGGGLVQPGGSLRLSCAASGNIFSINSMGWFRQA---PGKERDVVATIW-SDSR
SEQ_ID_173      EVQLVESGGGLVQPGRSLRLSCAASGNSFSISTMGWFRQA---PGKERELVASIW-SDTT
SEQ_ID_149      EVQLQQSGGGLVQAGGSLRLSCAASGRTFRNYVMGWFRQAPQAPGKDHEFVAAISWGGTE
SEQ_ID_155      EVQLQQSGGGLVQPGGSLRLSCAASGRTFSNYVVGWFRQAPQAPGKDHEFVAVISGSDTE
SEQ_ID_147      EVQLVSSGGGLVQPGGSLRLSCAASGSSLDSYSVSWFRQA---PGKEREWISFISRYYSS
SEQ_ID_148      EVQLQQSGGGLVQPGGSLRLSCAASGFTLDSYNIAWFRQA---PGKEREWISYISRYYES
SEQ_ID_139      EVQLVESGGGLVQAGGSLRLSCAASGFTFSNYAMNWVRQA---PGKGLEWVSGISGRGDD
SEQ_ID_142      EVKLVQSGGGLVQPGGSLRLSCAASGFIFSNYAMNWVRQA---PGKGLEWVSGINSGGGD
SEQ_ID_154      EVQLLESGGGLVLPGGSLRLSCAVSGLTLNSYAIGWFRQA---PGKEREGLSCLTS-GGT
SEQ_ID_144      QVQLVQSGGGLVQPGGSLRLSCAASGVTLDYYAIGWFRQA---PGKEREAVSCISSNGRR
SEQ_ID_145      EVQLQQSGGGLVQPGGSLRLSCAASGFTLDDYAIGWFRQS---PGKEREWVTCISRSGTT
SEQ_ID_156      EVQLVESGGGLVQPGGSLRLSCATSGFTLDYYAIGWFRQA---PGKEREWVSCISS-GGS
SEQ_ID_174      EVQLVESGGGLVQPGGSLRLSCAASGFTLDYYAIGWFRQA---PGKEREGVSCISSSDGS
SEQ_ID_137      EVQLVESGGGSVQPGGSLRLSCAASGSILDYYAVGWFRQA---PGKEREWVSSVSSSDGS
SEQ_ID_136      EVKLVQSGGGSVQPGGSLRLSCAASGSTLDYYAIGWFRQA---PGKEREWVSCVSSSDGS
SEQ_ID_138      EVQLVESGGGSVQPGGSLRLSCAASGSTLDYYAIGWFRQA---PGKEREWVSSVSSSDGN
SEQ_ID_152      EVQLQQSGGGLVQTGGSLRLSCAAAGSPFSQLAMSWYRQI---SGKERAWVASISP-TGN
SEQ_ID_153      EVQLVESGGGLVQAGGSLRLSCVASGITISGYNMAWWRQT---RGKQTERVAFINS-GGS
SEQ_ID_140      EVQLVSSGGGLVQAGGSLRLSCTASGITFSYYAMGWYRQA---PGQPRELVASMSN-MDS
SEQ_ID_143      EVQLVQSGGGLVQAGESLRLSCAASVSTFSSYAMGWYRQA---PGKQRELVASIGF-VGA
SEQ_ID_141      AVQLVDSGGGLVQPGGSLRLSCAASGSPFSNVVMAWYRQA---PGKQRERVAFISG-GGI
SEQ_ID_146      QLQLQESGGGLVQPGGSLTLSCAASGNTFSRSNMHWYRQA---PGAQREWVAAISS-RGI
SEQ_ID_150      EVQLVSSGGGLVQAGGSLRLSCEASGTTFSHYAVGWYRQA---PGKQREWVASISV-FGS
SEQ_ID_151      EVQLVSSGGGLVEAGGSLRLSCIASGSTSGRNTMGWFRQA---PGKQREWVAIVST-SGA
                 ::* .**** *  * ** *** .:       : * **     *     :: :

SEQ_ID_171      TSYADSVKGRFTISTDNTRTKVYLQMSSLNPEDTAVYYCAADRGFVV---------RGQY
SEQ_ID_173      TSYADSVKGRFTISTDNTRTKVYLQMSSLNPEDTAVYYCAADRGFVV---------RGQY
SEQ_ID_149      IYYADSVKGRFTISRDNAKNTVYLQMNSLKPEDTAVYYCAADRGLSY-----YYTRTTEY
SEQ_ID_155      TYYADSVKGRFTISRDNAKNTVYLQMNSLKPEDTAVYYCAADRGMSY-----YYTRATEY
SEQ_ID_147      TYYTDSVKGRFTTSRDGDQKTVHLQMNSLKPEDTAVYYCAARSRDFSS----PFSATDTY
SEQ_ID_148      TYYSDSVKGRFTTSRDGDKKTVSLQMNSLKSEDTAVYYCAARSRDFSS----PISATDKY
SEQ_ID_139      TRYADSVKGRFTISRDNAKNTLFLQMRSLRPEDTGVYRCTKGPDLYYF--------GSGY
SEQ_ID_142      TRYADSVKGRFTVSRDNAKNTLYLQMNSLKPEDTGVYYCSKGPVSSYY--------GSGY
SEQ_ID_154      GVYAESVKGRFTISRDNAENTVYLQMNSLKPEDTAVYYCAADRARLRFGCSLNFRREVAY
SEQ_ID_144      NHYVASVRGRFTISRDNAKSTVYLQMNSLKPEDTAVYYCAAVQDVH-GDNYYC-TSPNEY
SEQ_ID_145      TYYTASVKGRFTFSRDNAKNTAYLQMNSLRPEDTAVYYCAADYQY----STYCLGYDAHY
SEQ_ID_156      TFYVDSVKGRFTISRDNAKDTVYLQMSSLKPDDTAVYYCAADHRGRSL-RFGCSSSTTDY
SEQ_ID_174      TLYADSVKGRFTISRDNAKNTVYLQMNSLKPEDTAVYYCATGPQAYYSGSYYFQCPQAGM
SEQ_ID_137      TLYADSVKGRFTISRDDAKNTIYLQMDNLEPEDTAVYVCAADY---SMRRFAVGRWHRDY
SEQ_ID_136      TLYADSVKGRFTISRDNAKNTVYLQMNSLKPEDTAVYVCAADY---SMRPLWVSRWHRDY
SEQ_ID_138      TLYADSVKGRFTISRDNAKNTVYLQMNSLKAEDTAVYVCAADY---SMRPFAVGRWHRDY
SEQ_ID_152      RSYSKIAKGRFTISRDNAKNTVTLQMTSLKPEDTAAYICQAAN----------VNGG
SEQ_ID_153      TTYSDSVKGRFTISRDNGKNTAYLQMNSLNAEDTADYFCSLH----------TSH
SEQ_ID_140      TIYADSVKGRFTISRDNAKTTIYLQMNNLKPEDTAVYFCNIYGPTYS---------TRRN
SEQ_ID_143      TYYIDSVKGRFTISRDNAKKTAYLQMNDLKPDDTAVYYCNARH----------YGGS
SEQ_ID_141      ADYIMSVKGRFTISRDNAKNTVYLQMNSLKPEDTAVYYCWSS---YE----------
SEQ_ID_146      STYAYSAKGRFTISRDNAKNTVSLQMNSLKPEDTAVYYCYAA----------DDLG
SEQ_ID_150      TTYGGSVAGRFTISRDNDKNTVDLQMNSLKPEDTAVYYCHAV---NA---------DIGG
SEQ_ID_151      TNYAGSVKGRFTLSRDNAKNAVYLQMNNLKPEDTAVYYCYAA---Y----------GGGG
                  *   . **** * *. .    *** .*. :**. * *
```

FIG. 21

```
SEQ_ID_171      DYWGQGTQVTVSS
SEQ_ID_173      DYWGQGTQVTVSS
SEQ_ID_149      NYWGQGTQVTVSS
SEQ_ID_155      YYWGQGTQVTVSS
SEQ_ID_147      TSWGQGTQVTVSS
SEQ_ID_148      GSWGQGTQVTVSS
SEQ_ID_139      SDRGQGTQVTVSS
SEQ_ID_142      DYRGQGTQVTVSS
SEQ_ID_154      DYWGQGTQVTVSS
SEQ_ID_144      NVWGQGTQVTVSS
SEQ_ID_145      EYWGQGTQVTVSS
SEQ_ID_156      LYWGQGTQVTVSS
SEQ_ID_174      DYWGKGTQVTVSS
SEQ_ID_137      EYWGQGTQVTVSS
SEQ_ID_136      EYWGQGTQVTVSS
SEQ_ID_138      EYWGQGTQVTVSS
SEQ_ID_152      DYWGQGTQVTVSS
SEQ_ID_153      DYWGQGTQVTVSS
SEQ_ID_140      EYWGQGTQVTVSS
SEQ_ID_143      EYWGQGTQVTVSS
SEQ_ID_141      STWGQGTQVTVSS
SEQ_ID_146      DYWGQGTQVTVSS
SEQ_ID_150      DYWGQGTQVTVSS
SEQ_ID_151      DYWGQGTQVTVSS
                   *:********
```

FIG. 21 (cont.)

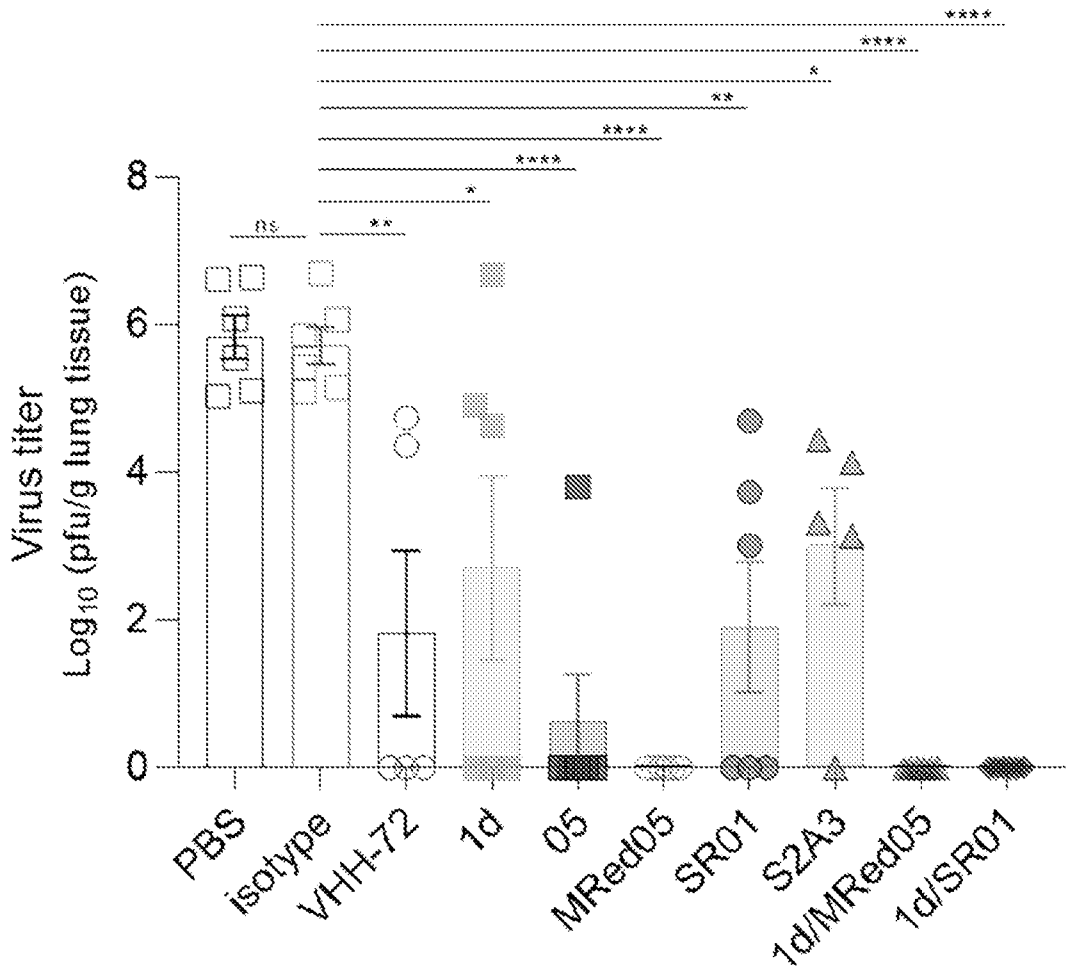
Virus titer
Log10 (pfu/g lung tissue)
0
2
4
6
8
ns
**
*
****
****
**
*
****
****
PBS
isotype
VHH-72
1d
05
MRed05
SR01
S2A3
1d/MRed05
1d/SR01

FIG. 22A

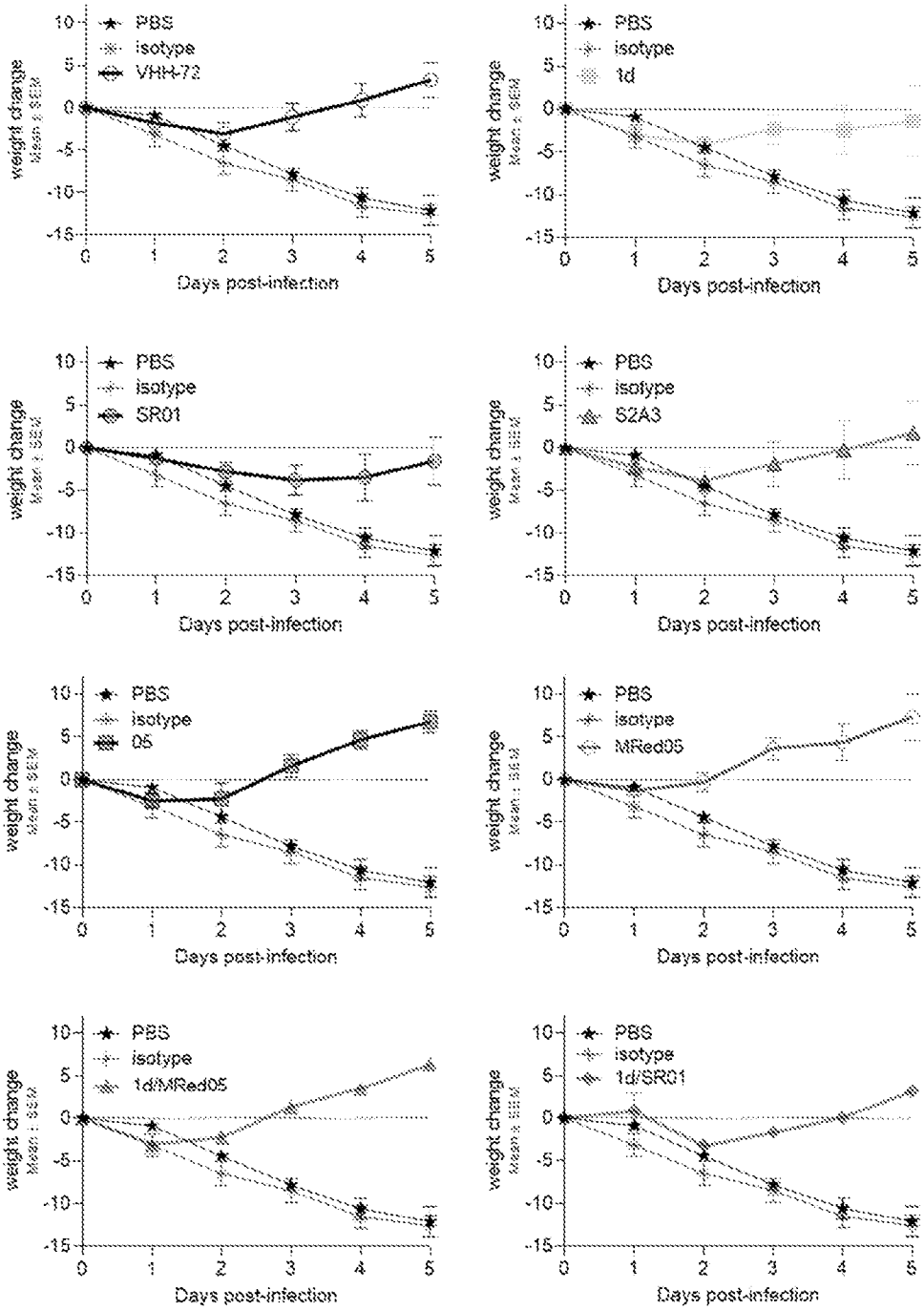
PBS
isotype
VHH-72
1d
SR01
S2A3
05
MRed05
1d/MRed05
1d/SR01
weight change
Days post-infection

FIG. 22B

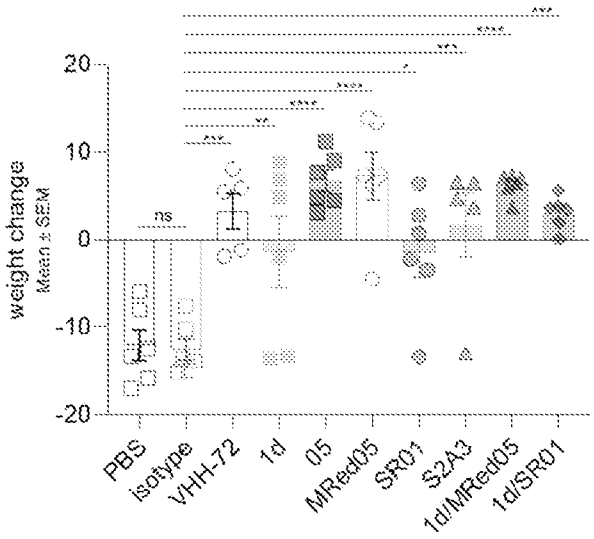


FIG. 22C

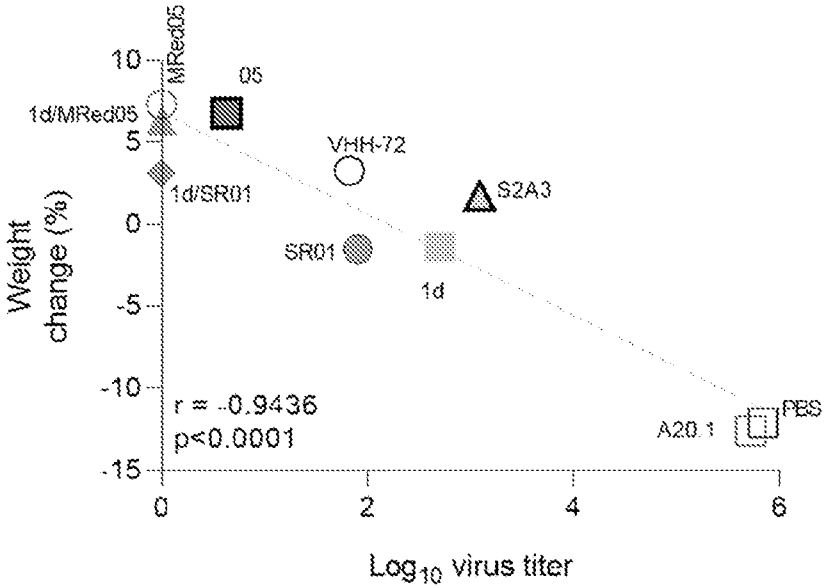


FIG. 22D

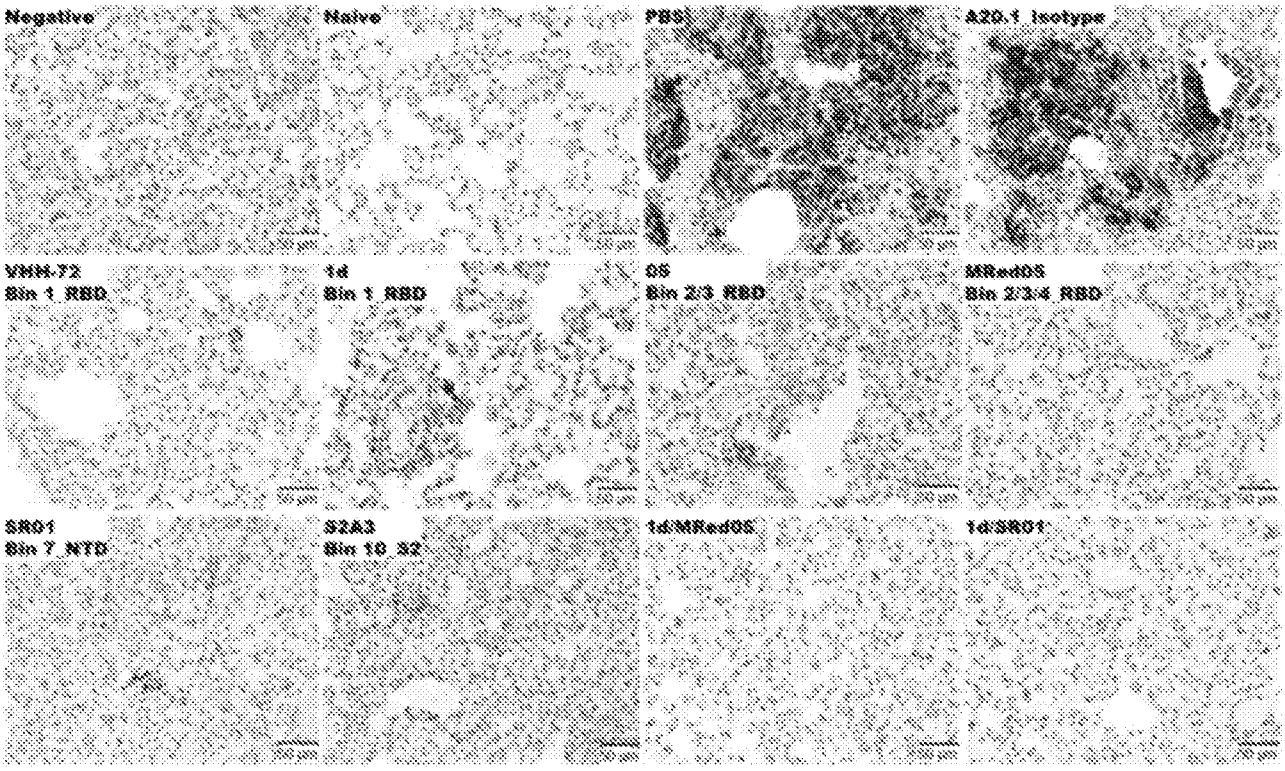
Negative
Naive
PBS
A20.1 Isotype
VHH-72
Bin 1_RBD
1d
Bin 1_RBD
CR
Bin 2/3_RBD
MRad05
Bin 2/3/4_RBD
SR01
Bin 7_NTD
S2A3
Bin 10_S2
1d/MRad05
1d/SR01

FIG. 23

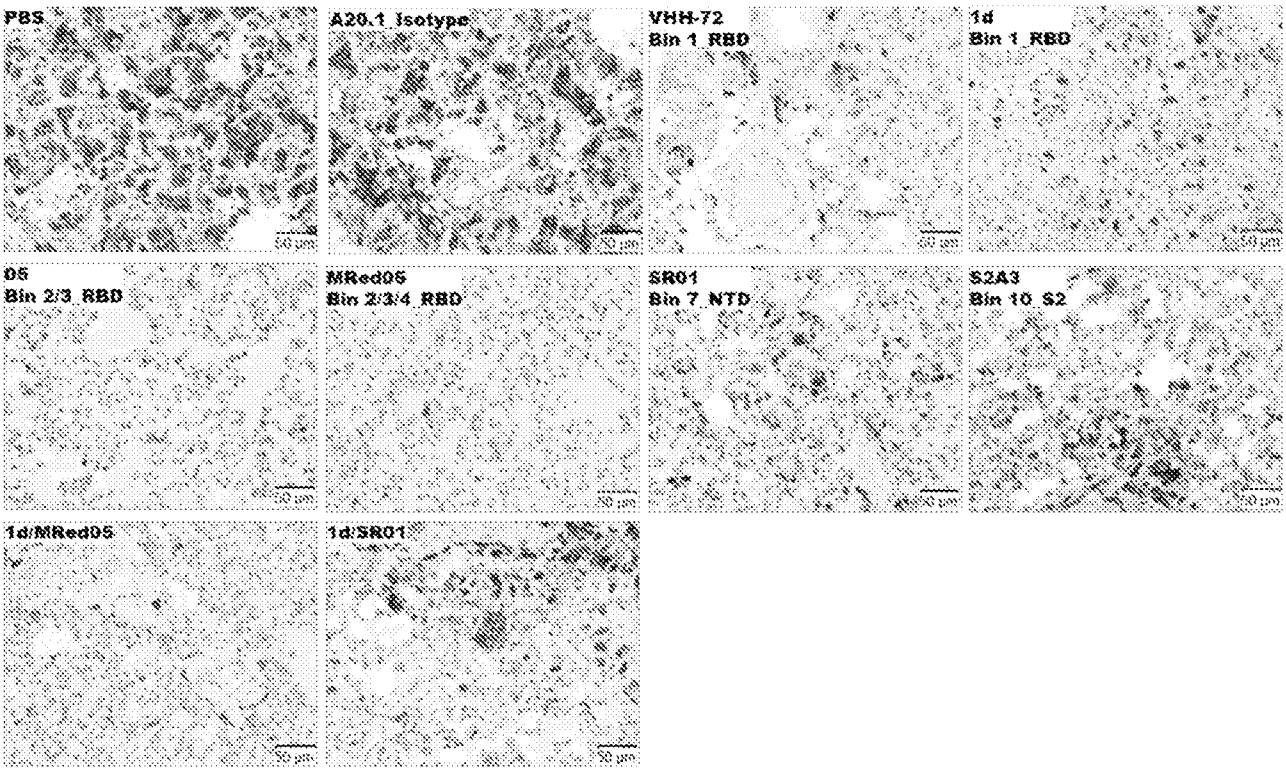
PBS
A20.1_Isotype
VHH-72
Bin 1_RBD
1d
Bin 1_RBD
05
Bin 2/3_RBD
MRed05
Bin 2/3/4_RBD
SR01
Bin 7_NTD
S2A3
Bin 10_S2
1d/MRed05
1d/SR01

FIG. 24

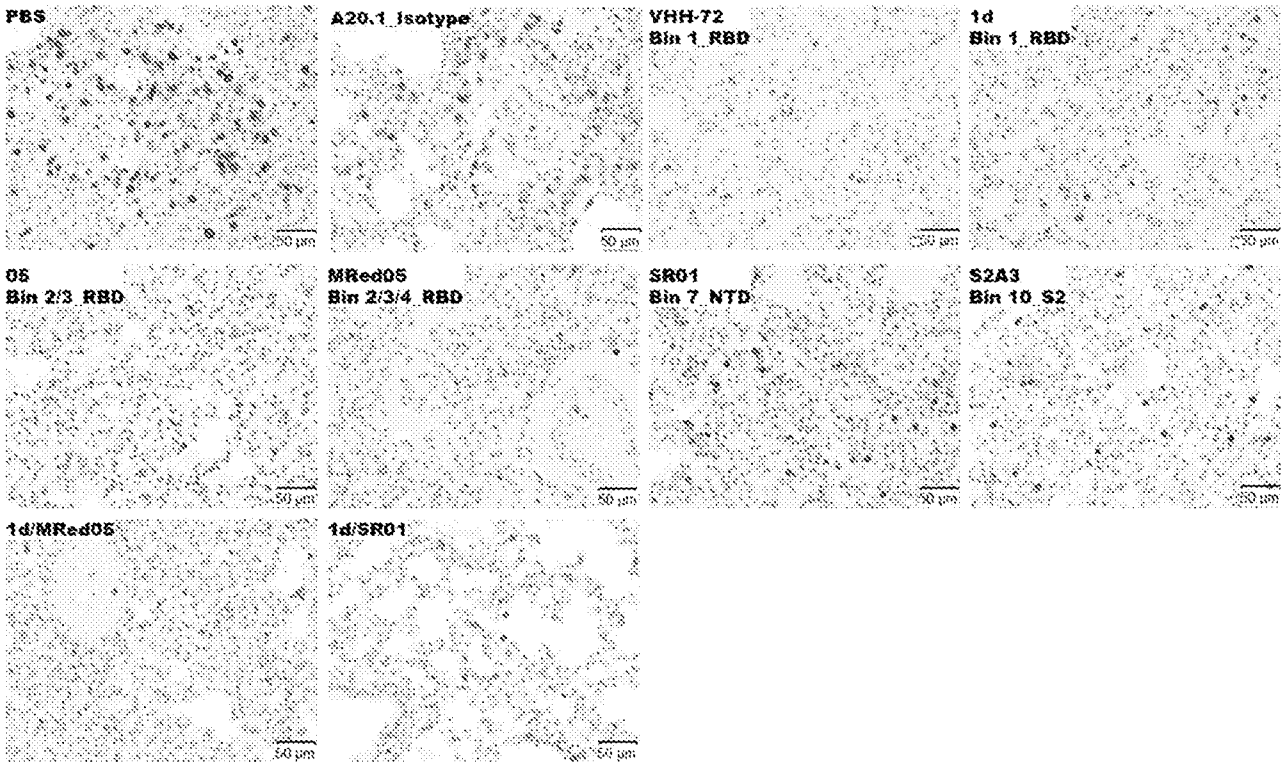
PBS
A20.1_Isotype
VHH-72
Bin 1_RBD
1d
Bin 1_RBD
05
Bin 2/3_RBD
MRed05
Bin 2/3/4_RBD
SR01
Bin 7_NTD
S2A3
Bin 10_S2
1d/MRed05
1d/SR01

FIG. 25

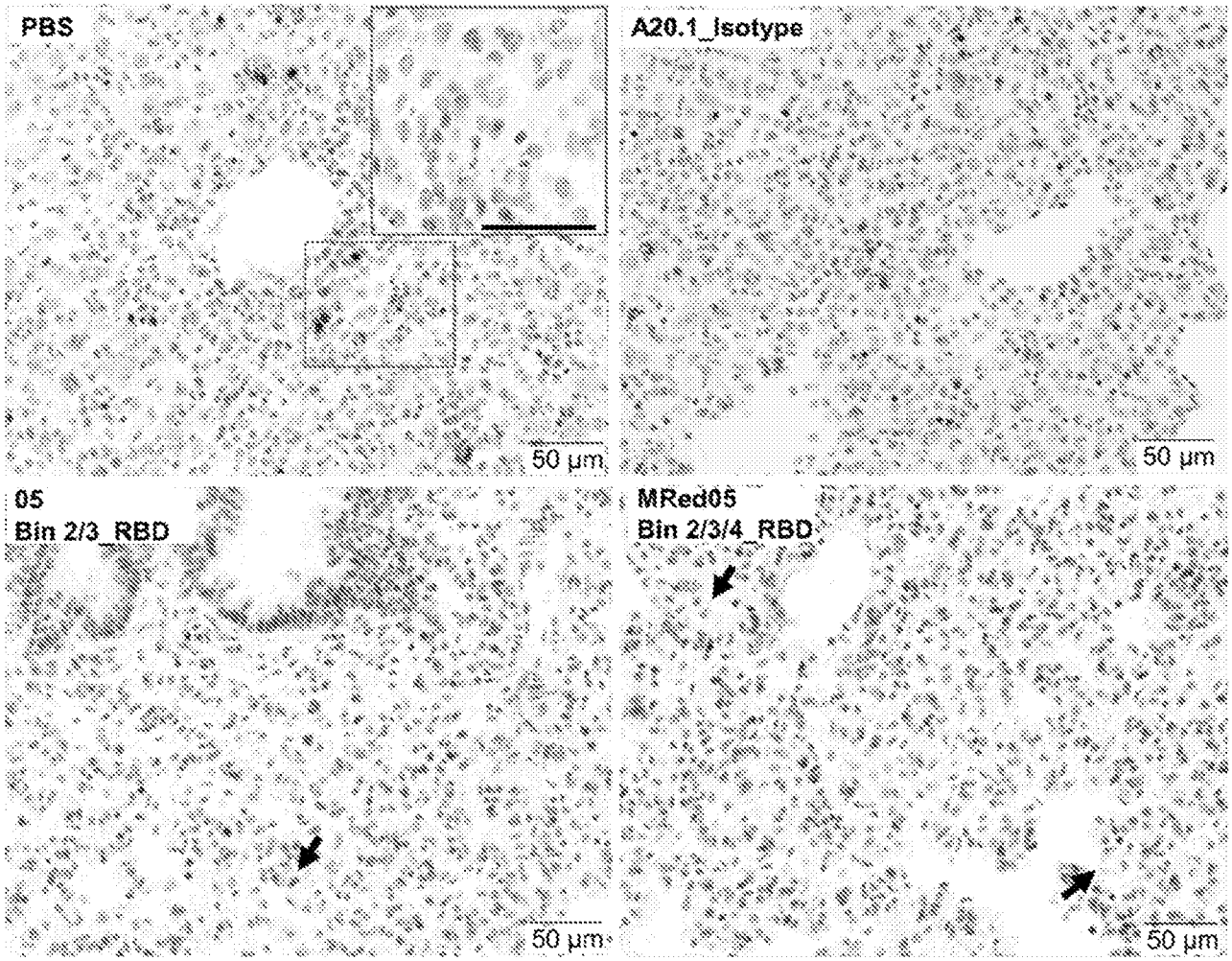
PBS
50 µm
A20.1_Isotype
50 µm
05
Bin 2/3_RBD
50 µm
MRed05
Bin 2/3/4_RBD
50 µm

FIG. 26

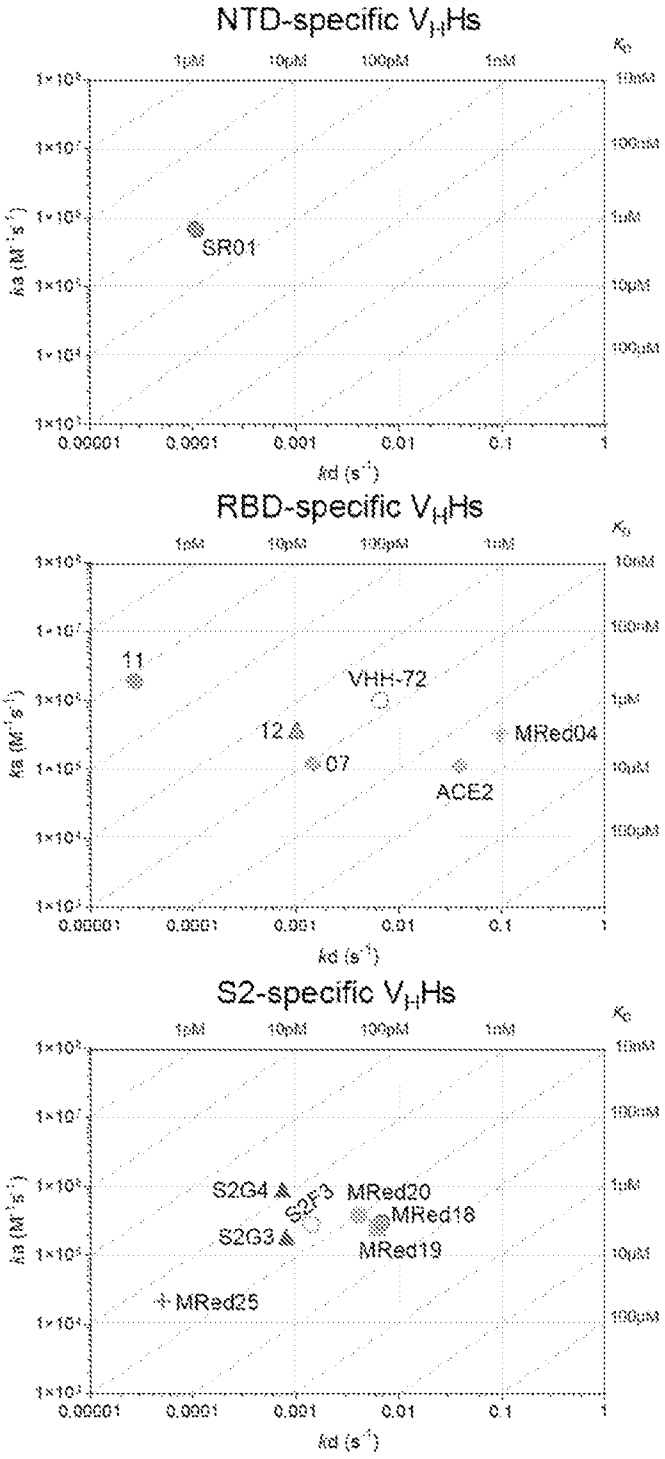
NTD-specific VHHs
SR01
RBD-specific VHHs
11
VHH-72
12
07
MRed04
ACE2
S2-specific VHHs
S2G4
S2F3
MRed20
MRed18
S2G3
MRed19
MRed25
ka (M-1s-1)
kd (s-1)
KD

FIG. 27

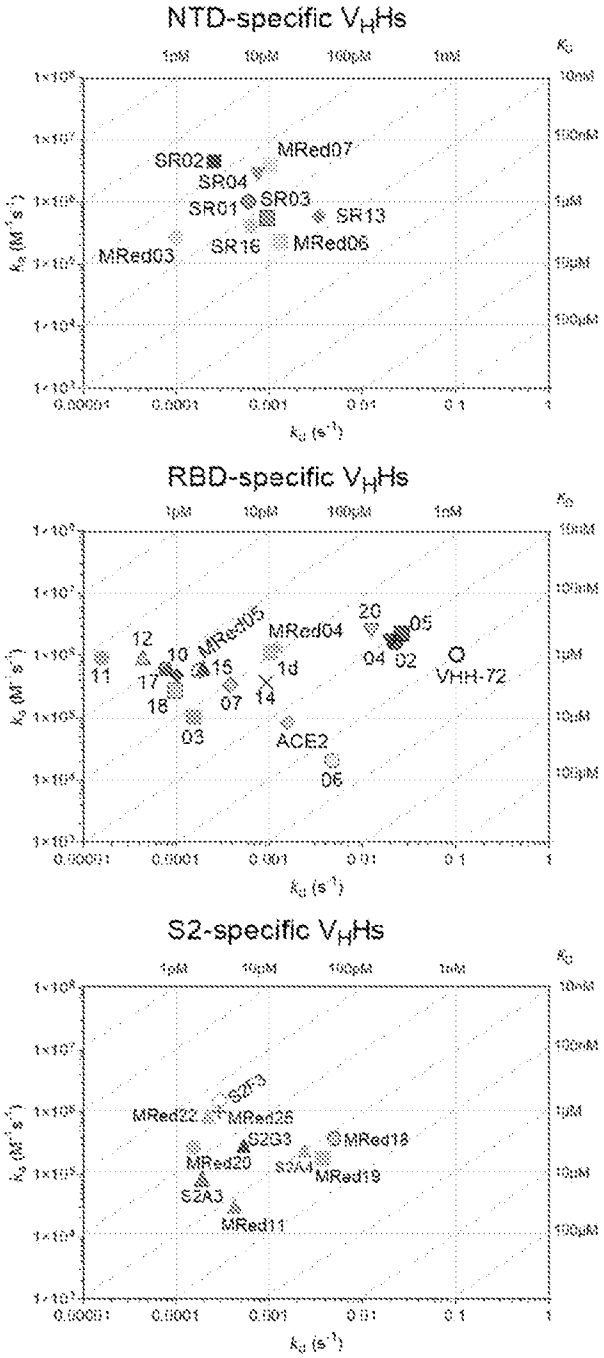
NTD-specific VHHs
RBD-specific VHHs
S2-specific VHHs
SR02
MRed07
SR04
SR01
SR03
SR13
SR16
MRed06
MRed03
MRed05
MRed04
VHH-72
ACE2
MRed22
MRed25
MRed18
MRed20
MRed19
MRed11

FIG. 28A

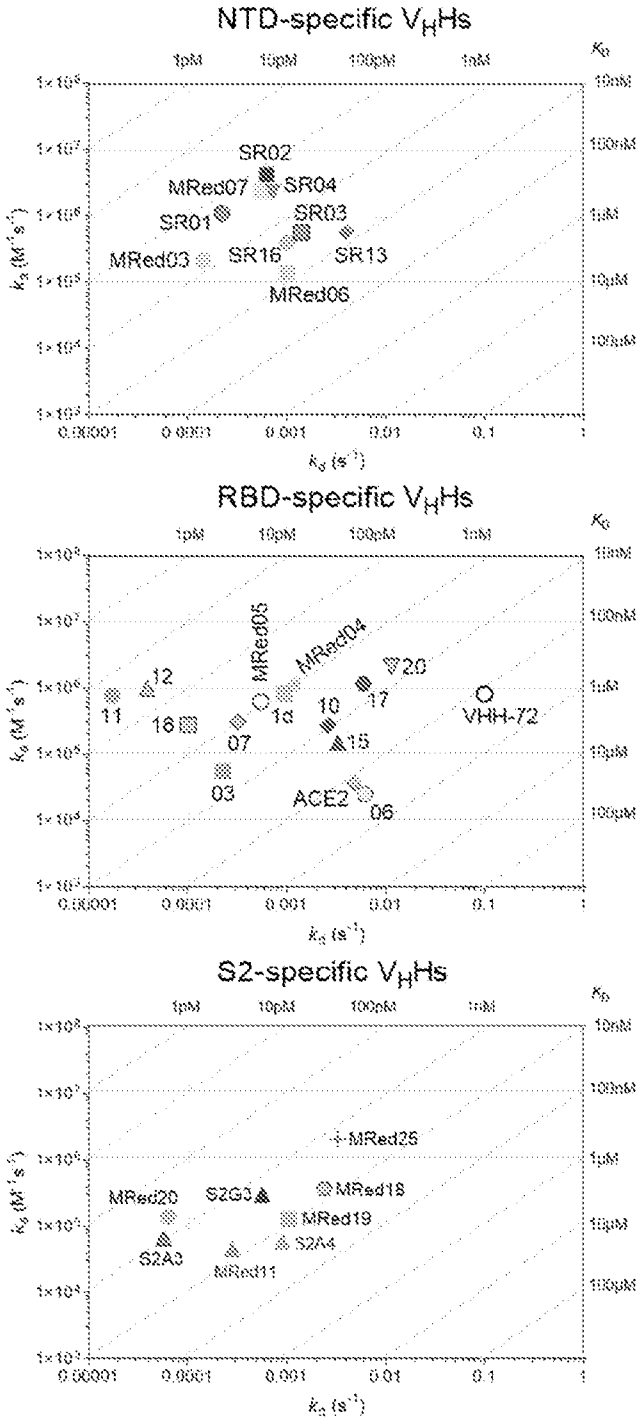
NTD-specific VHHs
RBD-specific VHHs
S2-specific VHHs
SR02
MRed07
SR04
SR01
SR03
MRed03
SR16
SR13
MRed06
MRed05
MRed04
12
20
11
16
1a
10
17
VHH-72
07
15
03
ACE2
06
MRed25
MRed20
S2G3
MRed18
MRed19
S2A4
S2A3
MRed11

FIG. 28B

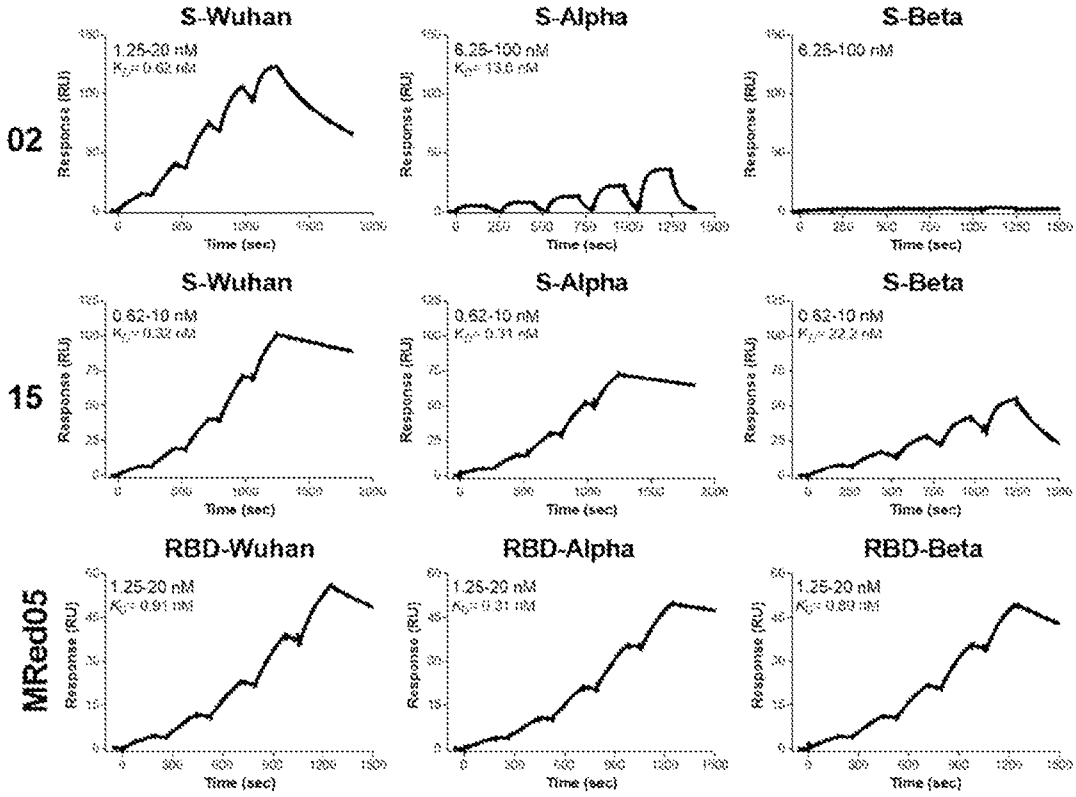
S-Wuhan
S-Alpha
S-Beta
02
1.25-20 nM
6.25-100 nM
6.25-100 nM
15
0.62-10 nM
0.62-10 nM
0.62-10 nM
MRed05
RBD-Wuhan
RBD-Alpha
RBD-Beta
1.25-20 nM
1.25-20 nM
1.25-20 nM
Response (RU)
Time (sec)

FIG. 29

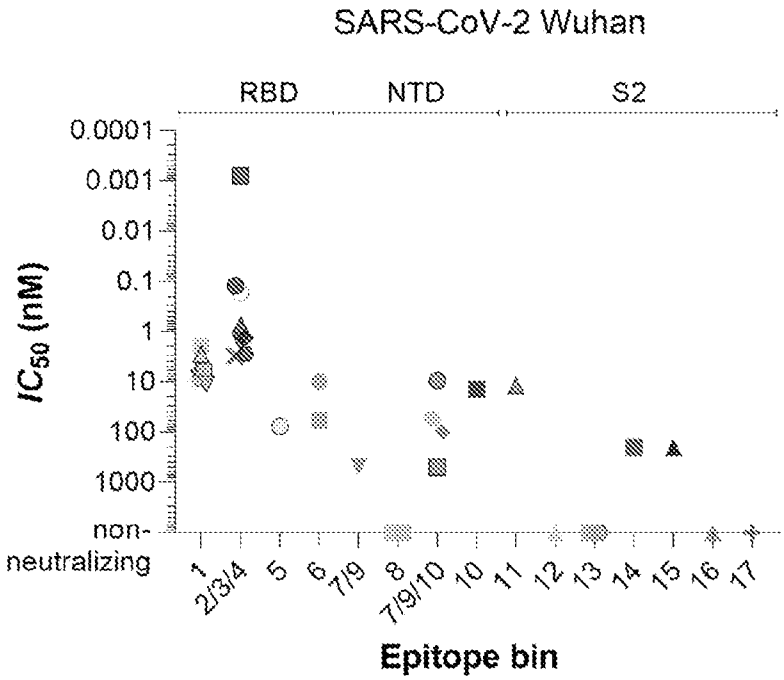
SARS-CoV-2 Wuhan
RBD
NTD
S2
0.0001
0.001
0.01
0.1
1
10
100
1000
non-neutralizing
IC50 (nM)
1
2/3/4
5
6
7/9
8
7/9/10
10
11
12
13
14
15
16
17
Epitope bin

FIG. 30

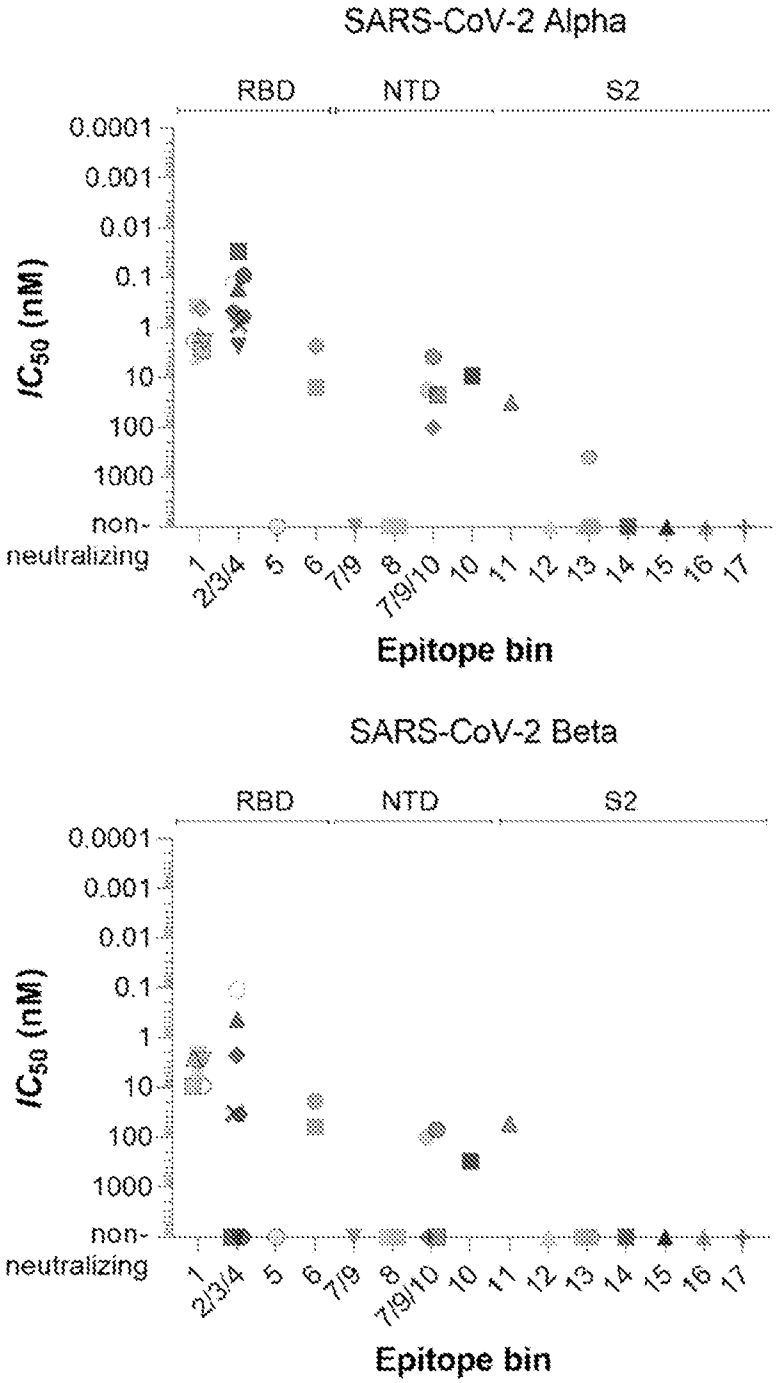
SARS-CoV-2 Alpha
RBD
NTD
S2
0.0001
0.001
0.01
0.1
1
10
100
1000
non-neutralizing
IC50 (nM)
1
2/3/4
5
6
7/9
8
7/9/10
10
11
12
13
14
15
16
17
Epitope bin
SARS-CoV-2 Beta
RBD
NTD
S2
0.0001
0.001
0.01
0.1
1
10
100
1000
non-neutralizing
IC50 (nM)
1
2/3/4
5
6
7/9
8
7/9/10
10
11
12
13
14
15
16
17
Epitope bin

FIG. 30 (cont.)

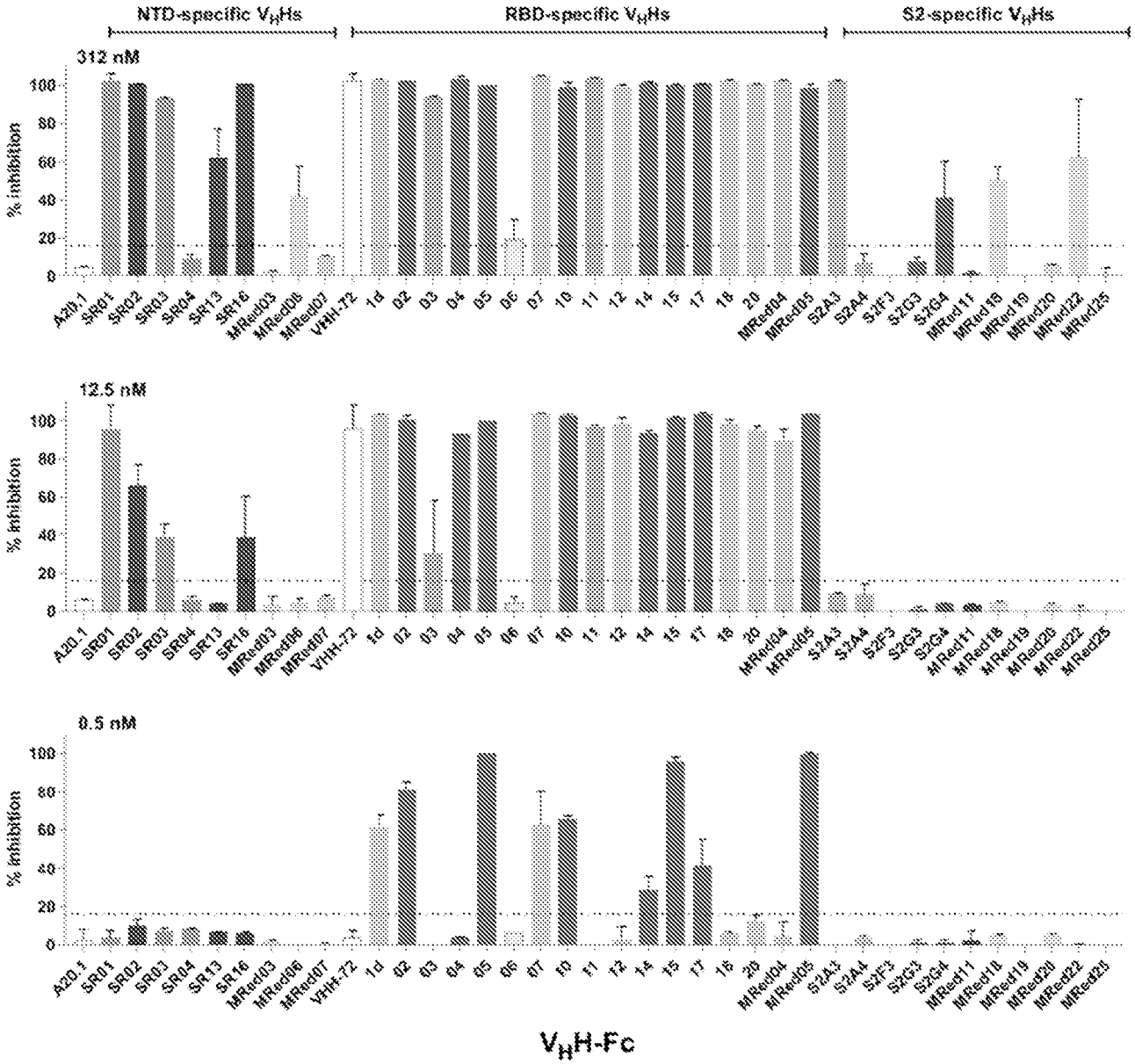
NTD-specific VHHs
RBD-specific VHHs
S2-specific VHHs
312 nM
12.5 nM
8.5 nM
% inhibition
A20.1
SR01
SR02
SR03
SR04
SR13
SR16
MRed03
MRed06
MRed07
VHH-72
1d
02
03
04
05
06
07
10
11
12
14
15
17
18
20
MRed04
MRed05
S2A3
S2A4
S2F3
S2G3
S2G4
MRed11
MRed18
MRed19
MRed20
MRed22
MRed25
VHH-Fc

FIG. 31A

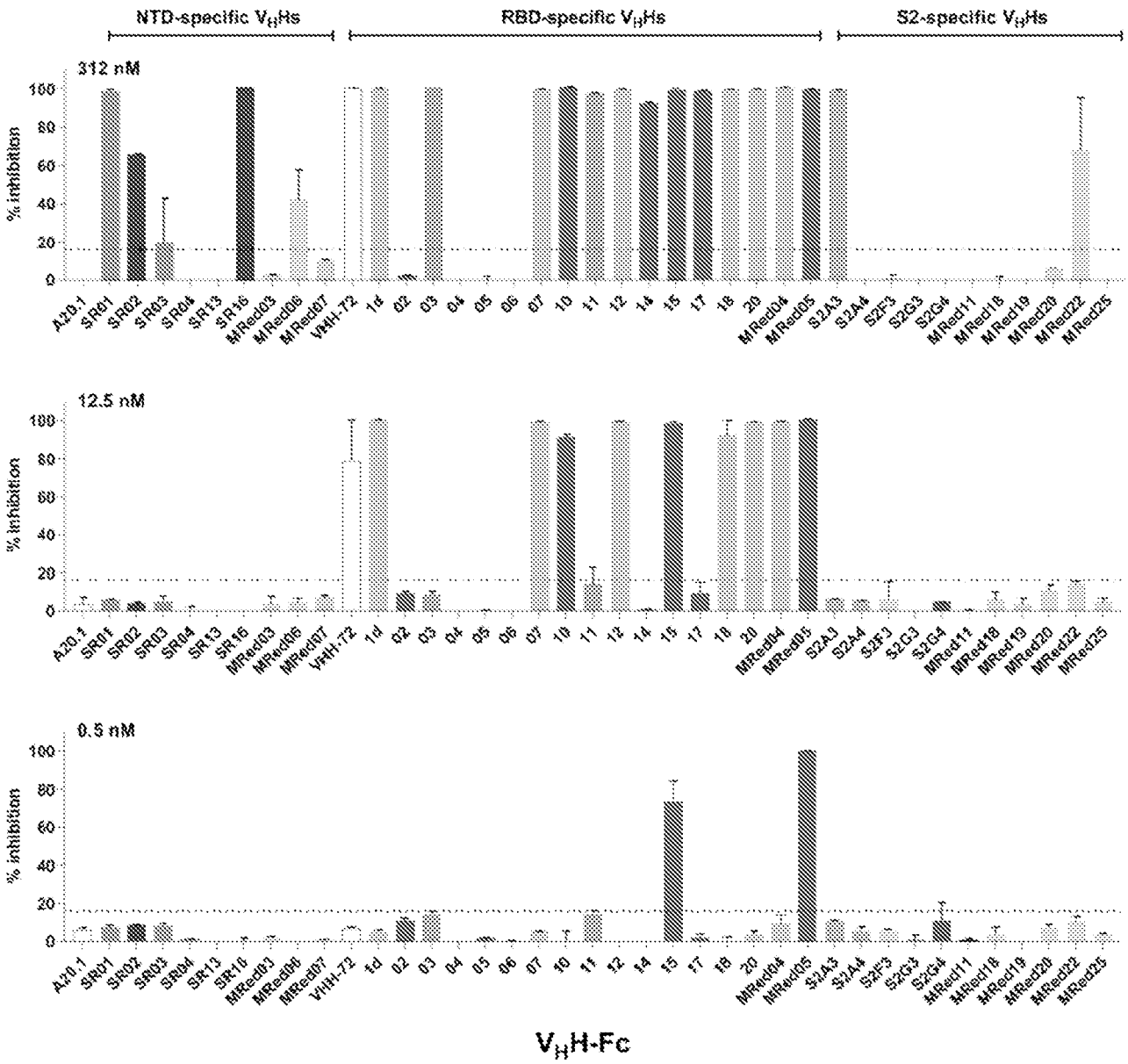
NTD-specific VHHs
RBD-specific VHHs
S2-specific VHHs
312 nM
12.5 nM
0.5 nM
% inhibition
A20.1
SR01
SR02
SR03
SR04
SR13
SR16
MRed03
MRed06
MRed07
VHH-72
1d
02
03
04
05
06
07
10
11
12
14
15
17
18
20
MRed04
MRed05
S2A3
S2A4
S2F3
S2G3
S2G4
MRed11
MRed18
MRed19
MRed20
MRed22
MRed25
VHH-Fc

FIG. 31B

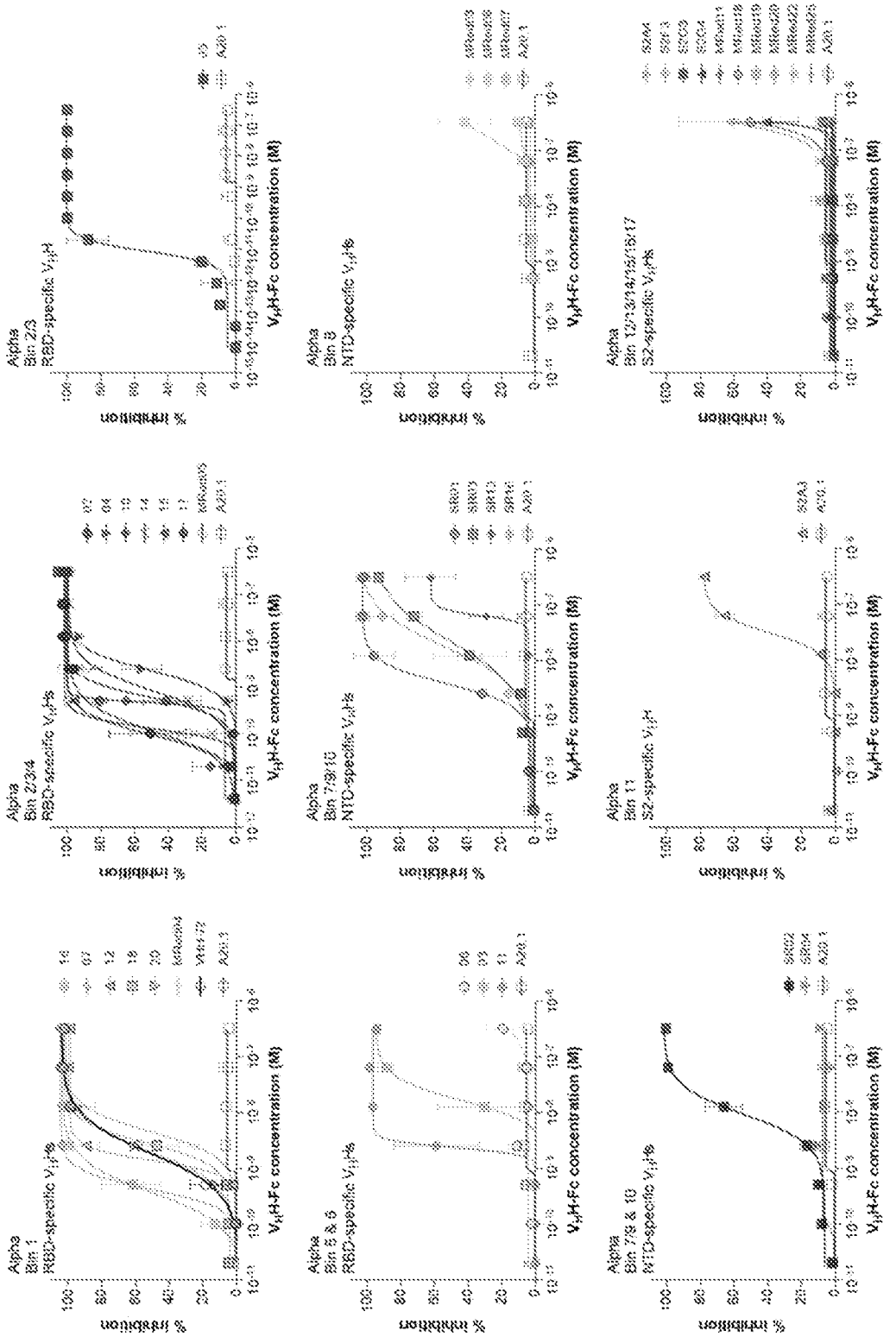
Alpha
Bin 1
RBD-specific $V_HH$
Alpha
Bin 2/3/4
RBD-specific $V_HH$s
Alpha
Bin 2/3
RBD-specific $V_HH$
Alpha
Bin 5 & 6
RBD-specific $V_HH$s
Alpha
Bin 7/8/10
NTD-specific $V_HH$s
Alpha
Bin 8
NTD-specific $V_HH$s
Alpha
Bin 7/8 & 10
NTD-specific $V_HH$s
Alpha
Bin 11
S2-specific $V_HH$
Alpha
Bin 12/13/14/15/16/17
S2-specific $V_HH$s
% inhibition
$V_HH$-Fc concentration (M)

FIG. 31C

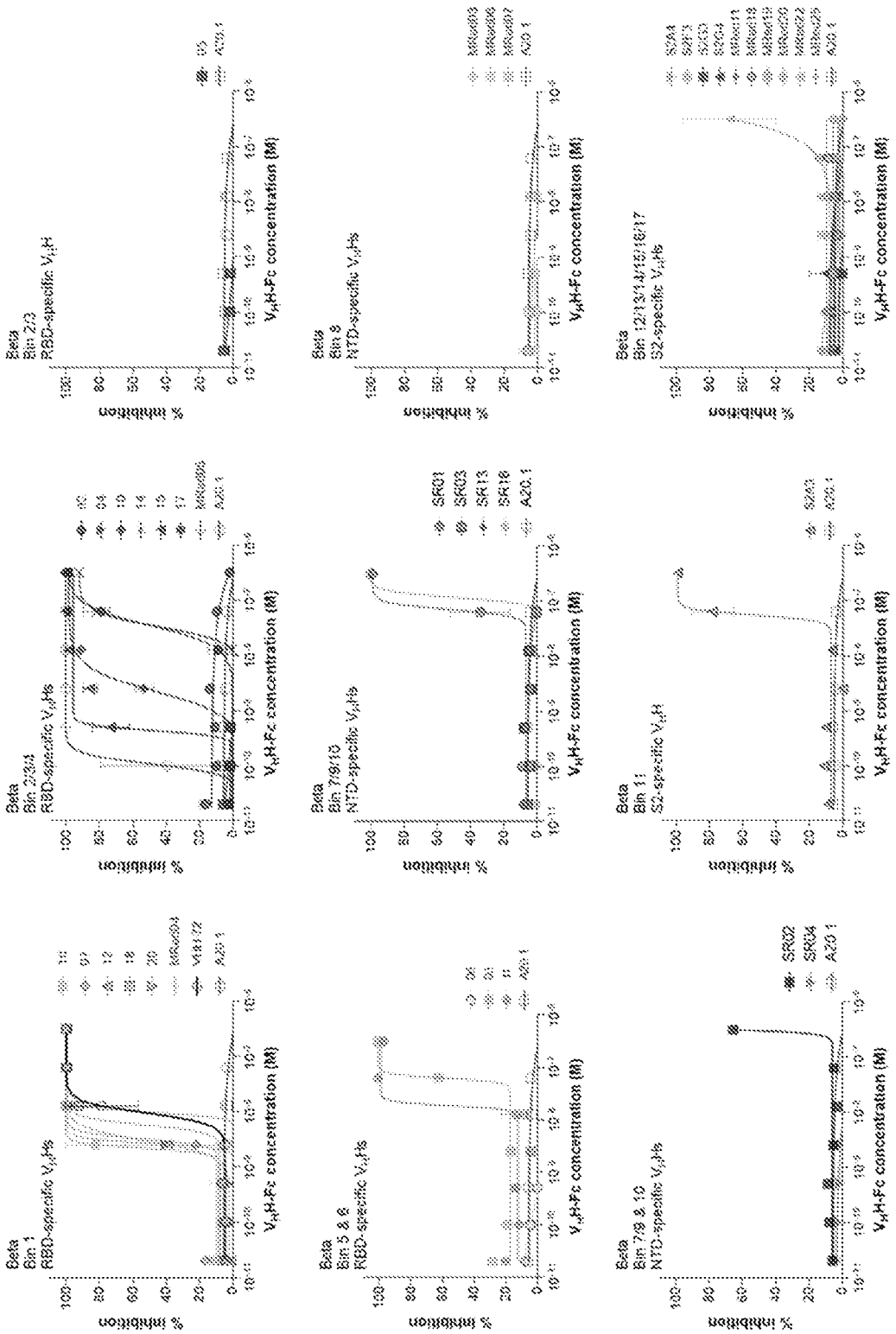
Beta
Bin 1
RBD-specific VHH
% inhibition
VHH concentration (M)
Beta
Bin 2/3/4
RBD-specific VHH
Beta
Bin 2/3
RBD-specific VHH
Beta
Bin 5 & 6
RBD-specific VHH
Beta
Bin 7/8/10
NTD-specific VHH
Beta
Bin 8
NTD-specific VHH
Beta
Bin 7/8 & 10
NTD-specific VHH
Beta
Bin 11
S2-specific VHH
Beta
Bin 12/13/14/15/16/17
S2-specific VHH
SR02
SR04
A20.1

FIG. 31D

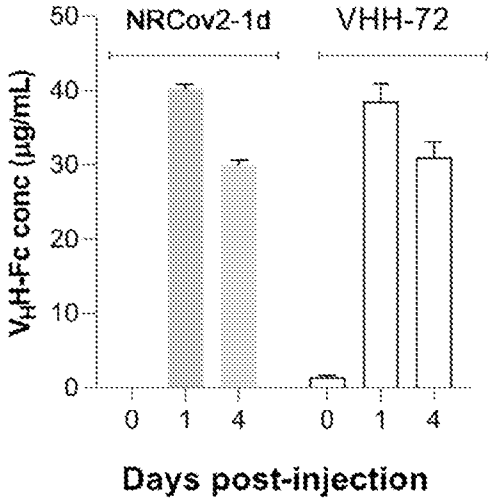
NRCov2-1d
VHH-72
$V_HH$-Fc conc (µg/mL)
50
40
30
20
10
0
0 1 4 0 1 4
Days post-injection

FIG. 32

**INTERNATIONAL SEARCH REPORT**

International application No.
**PCT/IB2022/053756**

A. CLASSIFICATION OF SUBJECT MATTER

IPC: ***C07K 16/10*** (2006.01), ***A61K 9/72*** (2006.01), ***A61K 39/42*** (2006.01), ***A61K 39/44*** (2006.01), ***A61K 47/68*** (2017.01), ***A61K 49/00*** (2006.01) (more IPCs on the last page)

CPC: , A61K 9/007 (2020.01), A61K 39/42 (2020.01), A61K 39/44 (2020.01), A61K 47/68 (2020.01), A61K 49/00 (2020.01) (more CPCs on the last page)

According to International Patent Classification (IPC) or to both national classification and IPC

B. FIELDS SEARCHED

Minimum documentation searched (classification system followed by classification symbols)

IPC: ***C07K 16/10*** (2006.01), ***A61K 9/72*** (2006.01), ***A61K 39/42*** (2006.01), ***A61K 39/44*** (2006.01), ***A61K 47/68*** (2017.01), ***A61K 49/00*** (2006.01), ***A61P 31/14*** (2006.01), ***C12N 15/13*** (2006.01), ***G01N 33/569*** (2006.01) CPC: A61K 9/007 (2020.01), A61K 39/42 (2020.01), A61K 39/44 (2020.01), A61K 47/68 (2020.01), A61K 49/00 (2020.01), A61P 31/14 (2020.01), C07K 16/10 (2020.01), C12N 15/10 (2022.05), G01N 33/56983 (2020.01), C07K 2317/565 (2020.01)

Documentation searched other than minimum documentation to the extent that such documents are included in the fields searched

Electronic database(s) consulted during the international search (name of database(s) and, where practicable, search terms used)

**Database(s):** STN (CAplus, Biosis, Biotechabs, canpatfull, Embase, Genbank, Medline, Registry, USgene); GenomeQuest (GQ-Pat GoldPlus Protein, GQ-Pat Platinum Protein, Protein Data Bank, Genpept); SCOPUS; Questel Orbit
**Keyword(s):** Coronavirus, COVID-19, Spike, antibody
**Sequence(s):** SEQ ID NOs: 1, 45 and 90

C. DOCUMENTS CONSIDERED TO BE RELEVANT

| Category* | Citation of document, with indication, where appropriate, of the relevant passages | Relevant to claim No. |
|---|---|---|
| A | WRAPP et al., "*Structural Basis for Potent Neutralization of Betacoronaviruses by Single-Domain Camelid Antibodies*". Cell, 28 May 2020 (28-05-2020), Vol. 181, pp. 1004-1015, Retrieved from the Internet: <doi: 10.1016/j.cell.2020.04.031> | |

☐ Further documents are listed in the continuation of Box C. ☐ See patent family annex.

| | | | |
|---|---|---|---|
| * | Special categories of cited documents: | "T" | later document published after the international filing date or priority date and not in conflict with the application but cited to understand the principle or theory underlying the invention |
| "A" | document defining the general state of the art which is not considered to be of particular relevance | "X" | document of particular relevance; the claimed invention cannot be considered novel or cannot be considered to involve an inventive step when the document is taken alone |
| "D" | document cited by the applicant in the international application | "Y" | document of particular relevance; the claimed invention cannot be considered to involve an inventive step when the document is combined with one or more other such documents, such combination being obvious to a person skilled in the art |
| "E" | earlier application or patent but published on or after the international filing date | "&" | document member of the same patent family |
| "L" | document which may throw doubts on priority claim(s) or which is cited to establish the publication date of another citation or other special reason (as specified) | | |
| "O" | document referring to an oral disclosure, use, exhibition or other means | | |
| "P" | document published prior to the international filing date but later than the priority date claimed | | |

| | |
|---|---|
| Date of the actual completion of the international search<br>4 July 2022 (05-07-2022) | Date of mailing of the international search report<br>04 August 2022 (04-08-2022) |
| Name and mailing address of the ISA/CA<br>Canadian Intellectual Property Office<br>Place du Portage I, C114 - 1st Floor, Box PCT<br>50 Victoria Street<br>Gatineau, Quebec K1A 0C9<br>Facsimile No.: 819-953-2476 | Authorized officer<br>Madiha Khan (819) 360-9148 |

**INTERNATIONAL SEARCH REPORT**

International application No.
**PCT/IB2022/053756**

**Box No. I** **Nucleotide and/or amino acid sequence(s) (Continuation of item 1.c of the first sheet)**

1. With regard to any nucleotide and/or amino acid sequence disclosed in the international application, the international search was carried out on the basis of a sequence listing:

a. ☒ forming part of the international application as filed:

☒ in the form of an Annex C/ST.25 text file.

☐ on paper or in the form of an image file.

b. ☐ furnished together with the international application under PCT Rule 13*ter*.1(a) for the purposes of international search only in the form of an Annex C/ST.25 text file.

c. ☐ furnished subsequent to the international filing date for the purposes of international search only:

☐ in the form of an Annex C/ST.25 text file (Rule 13*ter*.1(a)).

☐ on paper or in the form of an image file (Rule 13*ter*.1(b) and Administrative Instructions, Section 713).

2. ☐ In addition, in the case that more than one version or copy of a sequence listing has been filed or furnished, the required statements that the information in the subsequent or additional copies is identical to that in the application as filed or does not go beyond the application as filed, as appropriate, were furnished.

3. Additional comments:

**INTERNATIONAL SEARCH REPORT**

International application No.
**PCT/IB2022/053756**

**Box No. II Observations where certain claims were found unsearchable (Continuation of item 2 of the first sheet)**

This international search report has not been established in respect of certain claims under Article 17(2)(a) for the following reasons:

1. ☐ Claim Nos.:
because they relate to subject matter not required to be searched by this Authority, namely:

2. ☐ Claim Nos.:
because they relate to parts of the international application that do not comply with the prescribed requirements to such an extent that no meaningful international search can be carried out, specifically:

3. ☐ Claim Nos.:
because they are dependent claims and are not drafted in accordance with the second and third sentences of Rule 6.4(a).

**Box No. III Observations where unity of invention is lacking (Continuation of item 3 of first sheet)**

This International Searching Authority found multiple inventions in this international application, as follows:
**See extra sheet**

1. ☐ As all required additional search fees were timely paid by the applicant, this international search report covers all searchable claims.

2. ☐ As all searchable claims could be searched without effort justifying additional fees, this Authority did not invite payment of additional fees.

3. ☐ As only some of the required additional search fees were timely paid by the applicant, this international search report covers only those claims for which fees were paid, specifically claim Nos.:

4. ☒ No required additional search fees were timely paid by the applicant. Consequently, this international search report is restricted to the invention first mentioned in the claims; it is covered by claim Nos.:

1 and 3-45 (partially) as relating to Group 1a: antibody NRCoV2-1a (SEQ ID NO: 1, 45 and 90)

**Remark on Protest**

☐ The additional search fees were accompanied by the applicant's protest and, where applicable, the payment of a protest fee.

☐ The additional search fees were accompanied by the applicant's protest but the applicable protest fee was not paid within the time limit specified in the invitation.

☐ No protest accompanied the payment of additional search fees.

**Continuation of Box III from page 3**

WRAPP et al., *"Structural Basis for Potent Neutralization of Betacoronaviruses by Single-Domain Camelid Antibodies".* Cell, 28 May 2020 (28-05-2020), Vol. 181(5), pp. 1004-1015, [online] [retrieved on 20 May 2022 (20-05-2022)]. Retrieved from the Internet: <doi: 10.1016/j.cell.2020.04.031 >

**Unity Groupings:**
The claims are directed to a plurality of inventive concepts as follows:

Group I(a-i): Claims 1-45 (partially)
The claims are directed to isolated or purified antibodies that bind to epitopes in BIN 1 (see Figure 9F, 9G and Table 14) and their compositions and uses. Groups I(a-i) are divided by VHH as follows: a) NRCoV2-Ia; b) NRCoV2-Ic; c) NRCoV2-Id; d) NRCoV2-07; e) NRCoV2-12; f) NRCoV2-18; g) NRCoV2-20; h) NRCoV2-MRed02; and i) NRCoV2-MRed04.
Group 2: Claim 1, 3-45 (partially)
The claims are directed to isolated or purified antibodies that bind to epitopes in BIN 2,3 (see Figure 9F, 9G and Table 14) and their compositions and uses.
Group 3: Claim 1, 3-45 (partially)
The claims are directed to isolated or purified antibodies that bind to epitopes in BIN 2, 3, 4 (see Figure 9F, 9G and Table 14) and their compositions and uses.
Group 4: Claim 1, 3-45 (partially)
The claims are directed to isolated or purified antibodies that bind to epitopes in BIN 2, 4 (see Figure 9F, 9G and Table 14) and their compositions and uses.
Group 5: Claim 1, 3-45 (partially)
The claims are directed to isolated or purified antibodies that bind to epitopes in BIN 3, 4 (see Figure 9F, 9G and Table 14) and their compositions and uses.
Group 6: Claim 1, 3-45 (partially)
The claims are directed to isolated or purified antibodies that bind to epitopes in BIN 4 (see Figure 9F, 9G and Table 14) and their compositions and uses.
Group 7: Claim 1, 3-45 (partially)
The claims are directed to isolated or purified antibodies that bind to epitopes in BIN 5 (see Figure 9F, 9G and Table 14) and their compositions and uses.
Group 8: Claim 1-45 (partially)
The claims are directed to isolated or purified antibodies that bind to epitopes in BIN 6 (see Figure 9F, 9G and Table 14) and their compositions and uses.
Group 9: Claim 1, 3-45 (partially)
The claims are directed to isolated or purified antibodies that bind to epitopes in BIN 7, 9 (see Figure 9F, 9G and Table 14) and their compositions and uses.
Group 10: Claim 1-45 (partially)
The claims are directed to isolated or purified antibodies that bind to epitopes in BIN 7, 9, 10 (see Figure 9F, 9G and Table 14) and their compositions and uses.
Group 11: Claim 1, 3-45 (partially)
The claims are directed to isolated or purified antibodies that bind to epitopes in BIN 8 (see Figure 9F, 9G and Table 14) and their compositions and uses.
Group 12: Claim 1, 3-45 (partially)
The claims are directed to isolated or purified antibodies that bind to epitopes in BIN 9 (see Figure 9F, 9G and Table 14) and their compositions and uses.
Group 13: Claim 1, 3-45 (partially)
The claims are directed to isolated or purified antibodies that bind to epitopes in BIN 10 (see Figure 9F, 9G and Table 14) and their compositions and uses.
Group 14: Claim 1, 3-45 (partially)
The claims are directed to isolated or purified antibodies that bind to epitopes in BIN 11 (see Figure 9F, 9G and Table 14) and their compositions and uses.
Group 15: Claim 1, 3-45 (partially)
The claims are directed to isolated or purified antibodies that bind to epitopes in BIN 12 (see Figure 9F, 9G and Table 14) and their compositions and uses.
Group 16: Claim 1, 3-45 (partially)
The claims are directed to isolated or purified antibodies that bind to epitopes in BIN 13 (see Figure 9F, 9G and Table 14) and their compositions and uses.
Group 17: Claim 1, 3-45 (partially)
The claims are directed to isolated or purified antibodies that bind to epitopes in BIN 14 (see Figure 9F, 9G and Table 14) and their compositions and uses.

Group 18: Claim 1, 3-45 (partially)
The claims are directed to isolated or purified antibodies that bind to epitopes in BIN 15 (see Figure 9F, 9G and Table 14) and their compositions and uses.
Group 19: Claim 1, 3-45 (partially)
The claims are directed to isolated or purified antibodies that bind to epitopes in BIN 16 (see Figure 9F, 9G and Table 14) and their compositions and uses.
Group 20: Claim 1, 3-45 (partially)
The claims are directed to isolated or purified antibodies that bind to epitopes in BIN 17 (see Figure 9F, 9G and Table 14) and their compositions and uses.
Group 21: Claim 1, 3-45 (partially)
The claims are directed to VHH NRCoV-19 (see Table 14) and their compositions and uses.
Group 22: Claim 1, 3-45 (partially)
The claims are directed to VHH NRCoV-21 (see Table 14) and their compositions and uses.
Group 23: Claim 1, 3-45 (partially)
The claims are directed to VHH NRCoV-S2B3 (see Table 14) and their compositions and uses.
Group 24: Claim 1, 3-45 (partially)
The claims are directed to VHH NRCoV-S2H4 (see Table 14) and their compositions and uses.
Group 25: Claim 1, 3-45 (partially)
The claims are directed to VHH NRCoV-S202 (see Table 14) and their compositions and uses.

Unity of invention is only fulfilled when there is at least a single general inventive concept present in the claims that both, provides a common set of elements among all the claims, and the common set of elements are new and inventive over the prior art. The groups of inventions listed above lack shared elements and thus, there is *a priori* lack of unity. The antibodies in each group identified above bind to separate or undetermined epitopes as taught in the specification (see paragraph [00219], Figure 9F and 9G; Table 14).

Furthermore, there is *a posteriori* lack of unity since VHH to the coronavirus spike polypeptide are known in the prior art (Wrapp et al., 2020). Although VHH in BIN 1 bind to the same epitope, they do not provide a single general inventive feature as it does not make a contribution over the prior art in view of Wrapp et al., 2020. Wrapp et al., 2020 identified VHH-72 which binds to the same epitope as the antibodies of the instant application in BIN 1 (see paragraphs [0067] and [00219], as well as Figures 9F and 9G of the instant application). Thus, each VHH in BIN 1 is a separate invention.

The claims must be limited to one inventive concept as set out in PCT Rule 13.

**INTERNATIONAL SEARCH REPORT**

International application No.
**PCT/IB2022/053756**

IPC:
***A61P 31/14*** (2006.01) , ***C12N 15/13*** (2006.01) , ***G01N 33/569*** (2006.01)

CPC:
A61P 31/14 (2020.01) , C07K 16/10 (2020.01) , C12N 15/10 (2022.05) , G01N 33/56983 (2020.01) , C07K 2317/565 (2020.01)